Proceedings of the 3rd International

TRIGO (Wheat) Yield Potential

WORKSHOP 2017

CENEB, CIMMYT, Cd. Obregón, Sonora, México
March 22-23rd, 2017

Matthew Reynolds, Gemma Molero and Alma McNab (Editors)

USAID FROM THE AMERICAN PEOPLE
CIMMYT International Maize and Wheat Improvement Center
MasAgro Modernización Sustentable de la Agricultura Tradicional
SAGARPA SECRETARÍA DE AGRICULTURA, GANADERÍA, DESARROLLO RURAL, PESCA Y ALIMENTACIÓN
CONACYT

Proceedings of the 3rd International

TRIGO (Wheat) Yield Potential

WORKSHOP 2017

CENEB, CIMMYT, Cd. Obregón, Sonora, Mexico

(March 22-23rd, 2017)

Matthew Reynolds, Gemma Molero and Alma McNab

(Editors)

Sponsored by:

USAID FROM THE AMERICAN PEOPLE

CIMMYT

MasAgro Modernización Sustentable de la Agricultura Tradicional

SAGARPA SECRETARÍA DE AGRICULTURA, GANADERÍA, DESARROLLO RURAL PESCA Y ALIMENTACIÓN

CONACYT

CIMMYT - The International Maize and Wheat Improvement Center - is the global leader in publicly-funded maize and wheat research and related farming systems. Headquartered near Mexico City, CIMMYT works with hundreds of partners throughout the developing world to sustainably increase the productivity of maize and wheat cropping systems, thus improving global food security and reducing poverty. CIMMYT is a member of the CGIAR System Organization and leads the CGIAR Research Programs on Maize and Wheat. The Center receives support from national governments, foundations, development banks and other public and private agencies.

Correct citation: Reynolds M, et al, (2017). Proceedings of the 3rd International TRIGO (Wheat) Yield Potential Workshop 2017. CENEB, CIMMYT, Cd. Obregón, Sonora, Mexico, 22-23rd March 2017. Mexico, CDMX: CIMMYT.

Abstract: The abstracts herein are of presentations by crop experts for the "TRIGO (Wheat) Yield Potential Workshop". Sponsored by SAGARPA's international strategic component for increasing wheat performance, under the Sustainable Modernization of Traditional Agriculture Program (MasAgro); and CRP WHEAT.

The event covers innovative methods to significantly raise wheat yield potential, including making photosynthesis more efficient, improving adaptation of flowering to diverse environments, addressing the physical processes involved in lodging, and physiological and molecular breeding. The workshop represents the current research of the MasAgro TRIGO project and CRP WHEAT that involves scientists working on all continents to strategically integrate research components in a common breeding platform, thereby speeding the delivery to farmers of new wheat genotypes.

Table of Contents

3rd International TRIGO (Wheat) Yield Potential Workshop Program

March 22- 23, 2017

Wednesday, 22 March

Field Presentations, Global Wheat Program, CENEB Field Station

07:45	**Departure from hotels by bus to CENEB (Campo Experimental Norman E. Borlaug)**
08:15 – 08:25	**Welcome to CENEB-CIMMYT Operation** Hans J. Braun, Director Global Wheat Program Rodrigo Rascón, CIMMYT-CENEB Superintendent
08:30 – 09:00	**Spring Bread Wheat Improvement and rust resistance** Ravi Singh, Julio Huerta, Suchismita Mondal, Caxia Lan, Leonardo Crespo, Mandeep Randhawa Singh
09:00 – 09:10	**Wheat Bio Fortification – Harvest Plus** Velu Govindan
09:15 – 09:55	**Physiological Approaches to Wheat Improvement for Climate Change** Matthew Reynolds, Gemma Molero, Francisco Pinto, Jacinta Gimeno, Siva Sukumaran, Francisco Piñera, Carolina Rivera
10:00 – 10:20	**Global Improvement of Durum Wheat** Karim Ammar
10:20 – 10:40	**Wheat Industrial Quality Improvement** Carlos Guzman
10:50 – 11:20	**Conservation Agriculture-Based Cropping Systems** Bram Govaerts, Nele Verhulst
11:20 – 11:30	**Precision Agriculture & Nutrient Use Efficiency** Ivan Ortiz-Monasterio
11:35 – 11:55	**Seeds of Discovery** Carolina Saint Pierre, Prashant Vikram, Sukhwinder Singh
12:00 – 13:00	**Lunch**

1:00-5:00 PM: Field Presentations, International Wheat Yield Partnership Hub, CENEB

Wednesday 22nd March Afternoon IWYP Field Day	**Lead**	**Time approx**
· **General introduction to IWP-Hub**	Jeff Gwyn Matt Reynolds	13:00 – 13:15
· ***Experimental Treatments*** *Station: Source-Sink Trial* o Density, light, source:sink	Matt Reynolds Sam Knapp	13:15-13:30
· ***Panels, Traits, Genotypes*** *Station: Bread Wheat Diversity Panel* o Genotyping o Lodging	Anthony Hall Francisco Pinera	13:40-14:00
Station: Mapping Populations	Simon Griffiths	14:10-14:40

o NAM o Bacanora/Weebil o WAMI	Daniel Calderini Marta Lopes	
Station: High Biomass Panel (HiBAP) o RUE & canopy architecture o Respiration o Partitioning of assimilates	Gemma Molero Barry Pogson John Foulkes	14:50-15:20
· ***Pre-Breeding*** *Station: Prebreeding: Products (4th WYCYT)* o Use of PT lines	Matt Reynolds GP Singh	15:30-15:45
Station: Prebreeding: Methods (F2, F4, PYT) o Plant Selection o Marker assisted selection o Genomic selection	Siva Sukumaran Sue Dresigacker Jose Crossa	15:45-16:15
· ***Hub Facilities*** *Station: Remote sensing* o Water Index o Wheat Physiology Predictor o Practical challenges o HUB support to research o Regional "hotspot"platforms	Ali Babar John Evans Francisco Pinto Jacinta Gimeno Carolina Saint Pierre	16:20-16:50
· ***Exotic Genetic Resources*** *Station: Primary synthetic hexaploids* o Rubsico screening o Tapping untapped genetic resources	Eliz. Carmo Silva Ian King	17:00-17:20
Group Dinner at CIMMYT Research Station (in conjunction with CIMMYT Visitors Day)	All	17:30-20:00
Depart for Hotel		20:00

Thursday 23 March 2017

Topic	Lead	Time
· 62nd Farmers' Day (Dia del Agricultor),	NIFAP, PIEAES A. C. and Fundacion PIEAES de Sonora Mexico, A. C, CENEB Station	8:00-11:30
Lunch Quality Inn		12:00-13:00
MasAgro-TRIGO Oral Presentations **Session 1: PLANT SELECTION & BREEDING**	**Chair**: Gemma Molero	
Aerial measurements of NDVI and canopy temperature for prediction of biomass at different phenological stages.	Francisco Pinto	13:00-13:15
Evaluation of heat shock tolerance in different wheat genotypes under contrasting environmental conditions	Rut Sanchez-Bragado	13:15-13:30
Genomics and pedigree based prediction of grain yield in international environments	Jose Crossa	13:30-13:45

Genetic diversity of IWYP-HUB panels and TGW loci in WAMI	Sivakumar Sukumaran	13:45-14:00
Strategic research for developing improved wheat germplasm for Mexico	Franciso Piñera-Chavez; Jorge Valenzuela-Antelo	14:00-14:15
Evaluation Of The 3rd Wheat Yield Consortium Yield Trial Under Irrigated Growing Conditions In Mexico During The 2015-2016 Cycle	Javier Ireta Moreno)	14:15-14:30
Evaluation of the 1st stress adaptive trait yield trial (1st SATYT) and 5th stress adaptive trait yield nursery (5th. SATYN) under irrigated conditions in Mexico during the 2015-2016 growing season	Miguel A. Camacho-Casas	14:30-14:45
Genetic gains in wheat under high yield and heat stressed conditions resulting from physiological breeding. (Matthew Reynolds)	Matthew Reynolds	14:45-15:00
3:00-3:30 COFFEE BREAK		15:00-15:30
Session 2: PARTITIONING TO GRAIN YIELD	**Chair**: Matthew Reynolds	
Natural variation and genetic analysis of wheat spike-ethylene under heat stress conditions	Ravi Vallaru	15:30-15:45
Physiological traits to increase grain partitioning in high biomass cultivars in wheat	Aleyda Sierra-Gonzalez	15:45-16:00
Identifying avenues for increases in harvest index in high biomass wheat cultivars whilst maintaining post-anthesis photosynthetic capacity	Carolina Rivera-Amado	16:00-16:15
The trade-off between grain weight and grain number is affected by environmental conditioning: Wheat breeding strategies to increase yield potential	Daniel Calderini	16:15-16:30
Phenotypic characterization of the International Wheat Yield Partnership-Hub (IWYP-HUB) panels	Gemma Molero	16:30-16:45
Lignin, structural and non-structural carbohydrates and their association with stem strength components of irrigated spring wheat	Francisco J. Piñera-Chavez	16:45-17:00
DISCUSSION CLOSE		17:00-17:30

List of Participants:

Sawsen Ayadi
Tunisia
sawsen.ayadi@gmail.com

Kebere Bezaweletaw
Ethiopia
Kebeze1968@gmail.com

Hans Braun
CIMMYT, Mexico
h.j.braun@cgiar.org

Daniel Calderini
Universidad Austral de Chile, Chile
danielcalderine@uach.cl

Miguel A. Camacho-Casas
INIFAP, Mexico
Camacho.miguel@inifap.gob.mx

Huitzimengari Campos García
CIMMYT, Mexico
hcamposg@colpos.mx

Elizabete Carmo-Silba
Lancaster University, UK
e.carmosilva@lancaster.ac.uk

Jose Crossa
CIMMYT, Mexico
j.crossa@cgiar.org

Huizar Leonardo Diaz Ceniceros
INIFAP, Mexico
Hldc19@gmail.com

Emily Delorean
USA
Emily.delorean@gmail.com

Sherzod Dilmurodov
Uzbekistan
s.dilmurodov@mail.ru

Susanne Dreisigacker
CIMMYT, Mexico
s.dreisigacker@cgiar.org

John Evans
Australian National University, Australia
John.evans@anu.edu.au

Pedro Figueroa Lopez
INIFAP, Mexico
Figuero.pedro@inifap.gob.mx

John Foulkes
University of Nottingham, UK
John.foulkes@nottingham.ac.uk

Jacinta Gimeno Romeu
CIMMYT, Mexico
j.gimeno@cgiar.org

Francisco Gnocato
Brazil
Francisico.saccolgnocato@gmail.com

Gopalreddy
India
gopalgpb@cgiar.org

Artem Gorelov
Russia
Artem.gorelob@syngenta.com

Bram Govaerts
CIMMYT, Mexico
b.govaerts@cgiar.org

Simon Griffiths
John Innes Center, UK simon.griffiths@jiv.ac.uk

Carlos Guzman
CIMMYT, Mexico
c.guzman@cgiar.org

Anthony Hall
Earlham Institute, UK
Anthony.hall@earlham.ac.uk

Xinguo Mao
Institute of Crop Sciences, CAAS, China
maoxinguo@caas.cn

Javier Ireta Moreno
INIFAP, México
Ireta.javier@inifap.org

Ryan Joynson
Earlham Institute, UK
Ryan.joynson@earlham.ac.uk

Mehmet Karaman
Turkey
Karaman2178@hotmail.com

Wang Ke
CAAS, China
Wangkey03@caas.cn

Victor Kommerell
CIMMYT, Mexico
v.kommerell@cgiar.org

Harikrishna Krishnappa
India
Harikrishna.agri@gmail.com

Marta Lopes
CIMMYT, Turkey
m.dasilva@cgiar.org

Dennis Nicuh Lozada
USA
dblozada@email.uark.edu

Marufqul Mahkamov
Tajikistan
Mmaruf85@gmail.com

Asghar Mehreban
Iran
Mk_moedano@hotmail.com

Gemma Molero
CIMMYT, Mexico
g.molero@cgiar.org

Jennifer Nelson
CIMMYT, Mexico
j.nelson@cgiar.org

Martin Parry
Lancaster University, UK
m.parry@lancaster.ac.uk

Francisco Pinto
CIMMYT, Mexico
f.pinto@cgiar.org

Francisco Javier Piñera
CIMMYT, Mexico
f.pinera@cgiar.org

Matthew Reynolds
CIMMYT, Mexico
m.reynolds@cgiar.org

Alma Carolina Rivera Amado
CIMMYT, Mexico
c.rivera@cgiar.org

Carlos Alfredo Robles Zazueta
CIMMYT, Mexico
carlosarb12@gmail.com

Carolina Saint Pierre
CIMMYT, Mexico
c.saintpierre@cgiar.org

Rut Sanchez Bragado
CIMMYT, Mexico
r.s.bragado@cgiar.org

Boureima Seyni
Niger
boureimaseyani@yahoo.fr

Aleyda Sierra
Nottingham University, UK
stxaasi@nottingham.ac.uk

Pawan Singh
CIMMYT, Mexico
Pk.singh@cgiar.org

Ravi Singh
CIMMYT, Mexico
r.singh@cgiar.org

Ernesto Solis Moya
INIFAP, Mexico
Solis.ernesto@inifiap.gob.mx

Tafesse Solomon
Ethiopia
tafesse@ymail.com

Sivakumar Sukamaran
CIMMYT, Mexico
s.sukamaran@cgiar.org

Daniyar Tajibayev
Kazakhstan
Dan.bass.tad@gmail.com

Animut Tarik Bogale
Ethiopia
Animuttarik2001@gmail.com

Jorge L. Valenzuela- Antelo
CIMMYT, Mexico
Jorgeluisva13@hotmail.com

Ravi Valluru
CIMMYT, Mexico
r.valluru@cgiar.org

Chang Xiaoping
Institute of Crop Sciences, CAAS, China
jingruilian@caas.cn

Xuexin Xu
China Agricultural University, China
xuxuexin2008@126.com

Amor Yahyaoui
CIMMYT, Mexico
a.yahyaoui@cgiar.org

Hao Zhuanfang
Institute of Crop Sciences, CAAS, China
haozhuanfang@caas.cn

PLANT SELECTION AND BREEDING

Aerial measurements of NDVI and canopy temperature for predicting biomass at different phenological stages

Francisco Pinto and Matthew Reynolds
CIMMYT, México

Abstract
Estimating plant biomass under field conditions is a labor intensive and expensive activity that limits the capability to screen for this important trait in large wheat germplasm populations. Remote sensing represents a potential alternative to derive biomass and other relevant traits from spectral reflectance and thermal measurements. Using an unmanned aerial vehicle, we explored the capacity of aerial measurements of NDVI and canopy temperature (CT) to predict genetic variation for biomass in two spring wheat populations under yield potential conditions: the 2nd Wheat Yield Collaboration Yield Trial (2 WYCYT; 50 genotypes) and the High Biomass Association Panel (HiBAP; 150 genotypes). In each population the biomass was sampled at three different phenological stages: 40 days after emergence (E+40), 7 days after anthesis (A+7) and at physiological maturity (PM). Aerial data were collected six times during the growing season, covering the vegetative and grain filling stages of spring wheat. A correlation analysis was performed comparing aerial NDVI data with biomass estimated at the three phenological stages. A positive correlation was observed between NDVI and biomass during the vegetative period. No significant correlation was found at A+7 in both populations. At PM, only 2WYCYT showed a positive, but weak, correlation with final biomass. The relationship between cumulative CT and biomass was studied. In most cases, CT correlated negatively with biomass at a particular phenological stage. The biomass accumulated at A+7 and PM showed a strong negative relationship with CT measurements taken during grain filling. In general, no relationship was observed with CT measurements during the vegetative stage.

Introduction
Ultimately wheat yield is determined by biomass production and the harvest index (i.e., the proportion of the biomass that is allocated to the grains; Reynolds et al., 2005). Since the harvest index has a theoretical maximum of 0.6 (Austin et al., 1980), the genetic gain for yield will basically depend on breeding for genotypes with high biomass capacity. Direct measurement of plant biomass is labor intensive and costly, which makes it almost impracticable in situations where thousands of genotypes need to be screened. Alternatively, remote sensing approaches have been suggested as potential tools for making indirect biomass estimations based on spectral reflectance properties of the vegetation (Aparicio et al., 2000; Babar et al., 2006).

Remote sensing tools provide an excellent opportunity for improving the capacity to phenotype under field conditions. In particular, unmanned aerial vehicles (UAVs) have become the preferred platforms since they have shown to be versatile and effective for remotely measuring plant traits at suitable spatial and temporal resolutions (Tattaris et al., 2016). Furthermore, the latest advances in UAVs and sensors make it easy to implement these measurements at a relatively low cost. Two commonly used remote sensing parameters are the normalized difference vegetation index (NDVI) and canopy temperature using thermography. NDVI is one of the most widely used spectral reflectance indices. By comparing the spectral reflectance of the vegetation in the red and in the near-infrared part of the spectrum, the NDVI relates to the amount of green photosynthetic active material. On the other hand, canopy temperature (CT) is a relevant trait related to stomatal conductance and water status of the vegetation. A previous study carried out by Babar et al. (2006) found significant correlations between ground-based measurements of NDVI and biomass during heading and grain filling. Further, they observed a close relationship between CT and water reflectance indices, which in turn showed the best correlations with final biomass.

The objective of the present study was to explore the capacity of aerial measurements of NDVI and CT to predict biomass variability at discrete phenological stages in two spring wheat populations grown under yield potential conditions. The relationship between NDVI and biomass was studied at 40 days after emergence, 7 days after anthesis and at physiological maturity. On the other hand, aerial thermography was used to evaluate the impact of cumulative CT on biomass production at each of these phenological stages.

Methods

Measurements were made at the CIMMYT experiment station close to Ciudad Obregon, northwestern Mexico (27◦20′N; 109◦54′ W; and 38 m above sea level). Environmental and management details of this area are given in Sayre et al. (1997). Two spring wheat populations were studied under yield potential conditions: the 2nd Wheat Yield Collaboration Yield Trial (2 WYCYT; 50 genotypes) and the High Biomass Association Panel (HiBAP; 150 genotypes). Both trials had an alpha-lattice design with 2 replicates in case of 2WYCYT and 4 replicates in HiBAP. Biomass was directly estimated in each plot at 40 days after emergence (E+40), 7 days after anthesis (A+7) and at physiological maturity (PM). Alpha-lattice analyses were performed for biomass, NDVI and CT using META-R (2015) Version 5.0 ©. The prediction capacity of NDVI was estimated through correlation analyses between the biomass estimated at each of the three phenological stages and the closest measurement of NDVI. On the other hand, PCA bipolar plots were used to test biomass prediction through cumulative CT measured prior to each cut of biomass.

Aerial measurements of NDVI and canopy temperature (CT) were performed using the fixed wing UAV eBee (SenseFly, Switzerland). Six measurements took place between day 43 until day 100 after emergence (DAE), covering the trials' vegetative and grain filling stages. During the vegetative period (between 40 to 80 DAE), aerial data were collected approximately on a weekly basis. However, during grain filling, weather conditions and technical issues limited the number of measuring days. NDVI images were taken at an altitude of 100 m, while thermal images were taken at 75 m. Pixel resolution was ca. 10 cm/pixel and 14 cm/pixel, respectively. The area was covered by several pictures (80% overlap) which were later stitched together into a mosaic using the software Pix4D (Pix4D SA, Switzerland). A georeferenced map of the trials was used to identify the pixels belonging to each plot and extract their NDVI values. Soil and outlier pixels were discarded using supervised classification methods. The capacity of NDVI and CT to predict biomass at different stages was finally tested by performing a genotypic correlation analysis.

Results/Discussion

Table 1 shows the yield and biomass production of both study populations. The 2WYCYT population had a higher yield than HiBAP and also higher biomass during the vegetative period and at A+7. Nevertheless, at physiological maturity, the biomass of both populations was similar. The 2WYCYT population showed higher variability than HiBAP.

Table 1. Average values of final yield and biomass measured at three key phenological stages: 40 days after emergence (E+40), 7 days after anthesis (A+7) and at physiological maturity (PM). All values are expressed in g/m^2.

	Yield	Biomass E+40	Biomass A+7	Biomass PM
HiBAP	631.91 ± 4.4**	148.27 ± 1.9**	863.72 ± 7.3**	1472.33 ± 11**
2WYCYT	764.22 ± 19.1**	201.8 ± 4.0	987.13 ± 12.4	1410.13 ± 35.1**

**Significant at *p=0.01*.

Despite the difficulty of collecting data at a higher frequency during grain filling, available aerial data revealed seasonal variations in NDVI and CT, and the changes in their relationship with biomass. In Fig. 1, the average biomass estimated for both populations at different phenological stages is contrasted with the closest NDVI and CT measurements. High NDVI values had already been observed around E+40 in both populations (Fig. 1a). An increase in biomass towards A+7 was reflected in an increase in NDVI. Furthermore, the average NDVI was close to saturation in both trials at this stage. At PM, the further increase of biomass contrasted with the decrease in NDVI. This is a consequence of the progressive senescence of leaves during grain filling, which reduces the reflectance in the near-infrared while the reflectance in the red part of the spectrum increases due to chlorophyll loss (Aparicio et al., 2000; Babar et al., 2006). On the other hand, CT showed a sustained increase towards PM (Fig. 1b). However, the results shown below demonstrate that this is due to the change in daily temperatures throughout the season, rather than a positive correlation of CT with biomass.

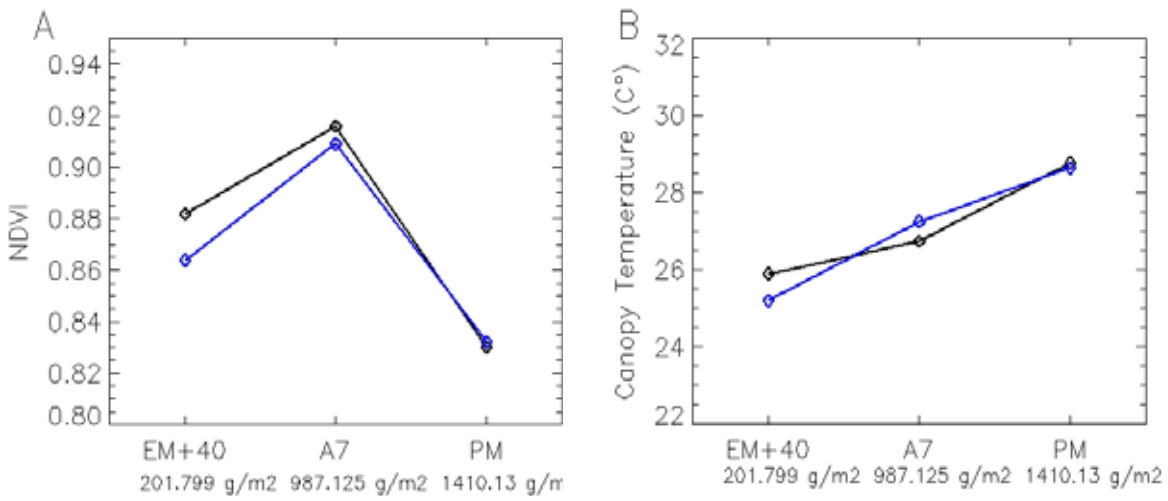

Fig. 1. Changes in NDVI (A) and canopy temperature (B) estimated from aerial measurements during the growing season in HiBAP (black line) and 2WYCYT (blue line). The values correspond to the mean estimated over all plots at the nearest measuring day for a given phenological stage (E+40, A+7 and PM). The day for each phenological stage was estimated when 50% of the plots reached a particular phenology.

The capacity of measured NDVI and CT to predict biomass at different phenological stages is shown in Figs. 2 and 3, respectively. In both populations, the NDVI measured 43 DAE showed a strong correlation with biomass estimated at E+40 (Fig. 2a). In HiBAP, this correlation was r= 0.41 ($p<0.05$), while in 2WYCYT it was r= 0.47 ($p<0.05$). In A+7, NDVI did not show a significant correlation with biomass. This can be explained by the fact that the nearest measurements available for this stage were taken close to heading, where the phenological variability within each population greatly affects the NDVI measurements due to the changes in illumination the emergence of the spike imposes within the canopy. At harvest, only 2WYCYT showed a significant positive correlation with biomass (r=0.246, $p<0.05$). The poor prediction capacity of NDVI for biomass variations at later growth stages has been reported previously in the literature (Aparicio et al., 2000, 2002).

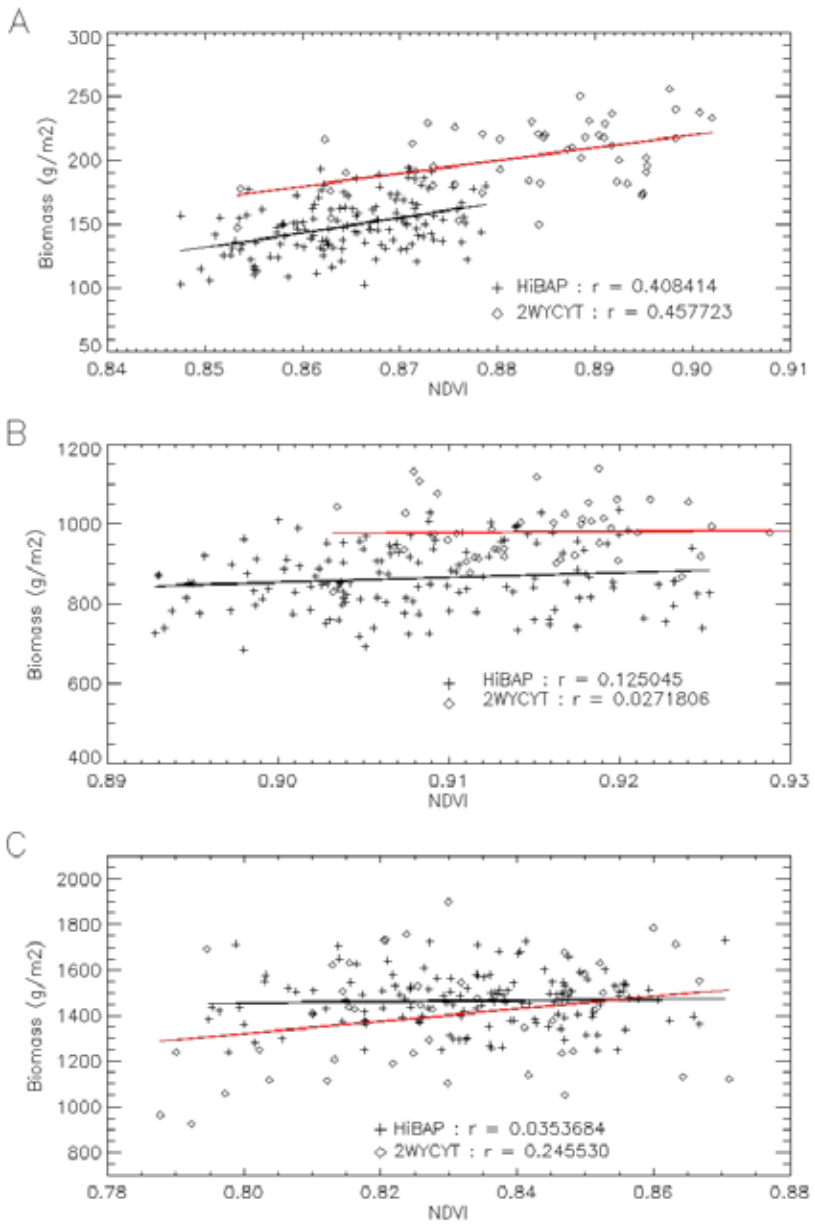

Fig. 2. Seasonal changes in the genetic correlation between NDVI and biomass in HiBAP (cross symbols, black fitting line) and 2WYCYT (open circles, red fitting line) estimated in three phenological stages: 40 days after emergence (E+40, A), 7 days after anthesis (A+7, B) and at physiological maturity (PM, C).

In general, the relationship between CT and biomass tended to be negative for a particular phenological stage. This negative relationship is explained by the larger rates of carbon fixation that cooler plants have due to their greater stomatal conductance (Reynolds et al., 1994; Babar et al., 2006). The relationship between cumulative CT and biomass production was only tested at A+7 and PM. No aerial data were available prior to the cutting of biomass at E+40. In HiBAP, the CT measured on 63 DAE and 70 DAE had a significant negative relationship with the biomass estimated at A+7 (Fig. 3a), while measurements taken before 63 DAE (i.e., before heading) did not have an impact. In contrast, only CT measurements taken 48 DAE showed a correlation with biomass at A+7 in 2WYCYT (Fig. 3c). The biomass estimated at harvest had a stronger negative relationship with CT measurements taken at 70 DAE and 98 DAE in both

populations (Fig. 3b and d). In 2WYCYT, the results also show a strong positive effect of CT at 63 DAE, and to a lesser extent, at 57 DAE on final biomass.

A few factors may affect the strength of the relationship observed between biomass and aerial measurements of NDVI and CT. First, uncertainties could be introduced in the correlation analyses due to the differences in phenology within each population. While biomass was estimated per plot whenever a particular phenological stage was reached, the aerial data were collected for all the population at once and at a lower day frequency, not accounting for these phonological differences. Therefore, it would be necessary to increase the frequency of aerial data collection around those key phenological stages. Another factor that could affect our results is the insensitivity of NDVI at high leaf area index. This problem can be accentuated if the aerial imagery has a coarse spatial resolution. In this study, the pixel resolution was approximately 10 cm to 14 cm, which allowed few pixels per plot. However, this resolution is not enough to account for small variations within the canopy structure, which can directly affect the estimated values of

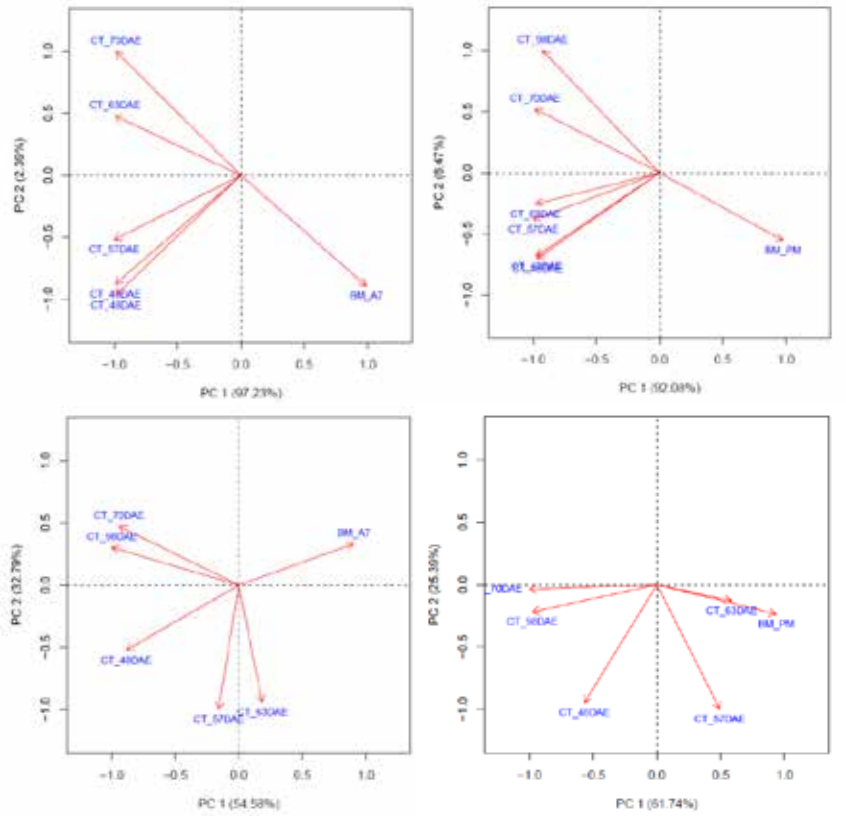

NDVI and CT.

Fig. 3. Biplot of canopy temperature (CT) measured on different dates and biomass measured at 7 days after anthesis and at physiological maturity in HiBAP and 2WYCYT. (A) CT vs biomass of HiBAP at 7 days after anthesis (A+7); (B) CT vs biomass of HiBAP at physiological maturity (PM); (C) CT vs biomass of 2WYCYT at 7 days after anthesis (A+7); and (D) CT vs biomass of 2WYCYT at physiological maturity (PM).

Conclusions

- The relationship between NDVI and biomass changed during the growing season. Only during the vegetative stage was this relationship significant in both populations. No significant correlation was found during A+7 in any of the populations. A significant but weak correlation was found between NDVI and biomass at harvest for 2WYCYTW, whereas in HiBAP the capacity of NDVI to predict biomass at harvest could not be proved.

- Cumulative CT measured during grain filling has a close relationship with biomass estimated at A+7 and PM. Generally, CT correlated negatively with biomass at a particular phenological stage.
- The phenological variability within each population could have an impact in the results. Therefore, higher frequency of aerial data collection should be considered in future measurements.

References

Aparicio, N., D. Villegas, J.L. Araus, J. Casadesus, and C. Royo. 2002. Relationship between growth traits and spectral vegetation indices in durum wheat. Crop Sci. 42(5): 1547–1555.

Aparicio, N., D. Villegas, J. Casadesus, J.L. Araus, and C. Royo. 2000. Spectral vegetation indices as nondestructive tools for determining durum wheat yield. Agron. J. 92(1): 83–91.

Austin, R.B., J. Bingham, R.D. Blackwell, L.T. Evans, M.A. Ford, C.L. Morgan, and M. Taylor. 1980. Genetic improvements in winter wheat yields since 1900 and associated physiological changes. J. Agric. Sci. 94: 675.

Babar, M.A., M.P. Reynolds, M. Van Ginkel, A.R. Klatt, W.R. Raun, and M.L. Stone. 2006. Spectral reflectance to estimate genetic variation for in-season biomass, leaf chlorophyll, and canopy temperature in wheat. Crop Sci. 46(3): 1046–1057.

Reynolds, M.P., M. Balota, M.I.B. Delgado, I. Amani, and R.A. Fischer. 1994. Physiological and morphological traits associated with spring wheat yield under hot, irrigated conditions. Aust. J. Plant Physiol. 21(6): 717–730.

Reynolds, M.P., A. Pellegrineschi, and B. Skovmand. 2005. Sink-limitation to yield and biomass: a summary of some investigations in spring wheat. Ann. Appl. Biol. 146: 39–49.

Sayre, K.D., S. Rajaram, and R.A. Fischer. 1997. Yield potential progress in short bread wheats in northwest Mexico. Crop Sci. 37(1): 36–42.

Tattaris, M., M.P. Reynolds, and S.C. Chapman. 2016. A Direct Comparison of Remote Sensing Approaches for High-Throughput Phenotyping in Plant Breeding. Front. Plant Sci. 7(August): 1131.

Prediction accuracy of high-resolution spectral information for non-destructive phenotyping of epicuticular wax in wheat

Fatima Camarillo-Castillo [1], Maria Tattaris[2], Dirk B. Hays[1]and Matthew P. Reynolds[2]
[1] Texas A&M University, USA; [2] CIMMYT, Mexico

Abstract
The focus of this study is to define the spectral response of the plant to epicuticular wax (EW) accumulation, and evaluate the prediction accuracy of spectral reflectance based indices to estimate EW. As expected, EW has a significant effect on the plant-light interactions. The accumulation of these waxes increases the light reflected by the leaf, and decreases the percentage of light that is absorbed and transmitted. Empirical indices were developed by deriving combinations of spectral bands using eleven mathematical forms of indices. A cross-validation analysis was conducted to select the statistically associated indices with the highest coefficients of determination (R2), and the Root Mean Square Error (RMSE) was calculated from the linear inverse models by bootstrapping a validation data set 1000 times. Sixteen indices were identified as candidate indices by selecting the spectral index (SI) with the highest R2 and lowest RMSE. These indices were evaluated under heat stress and yield potential conditions. Two of these indices were consistently associated with EW across all environments: the broad index $\frac{(\mathrm{Red}^2-\mathrm{Blue})}{(\mathrm{Red}-\mathrm{Blue}^2)}$ and the narrow index 694-625.
Keywords: *Spectral indices; epicuticular wax, wheat.*

Introduction
Wheat is the second most important source of calories in the diets of developing countries (FAO), and the first source of protein for 2.5 billion consumers who live on less than 2 USD per day. To overcome the demand of wheat by 2050, the global wheat production (GWP) will have to increase by 110 percent at a rate of 2.4% per year (Ray et al. 2013). Nonetheless, any substantial increase in grain yield (GY) will be limited by an estimated reduction of 6% by every °C of increase in the global mean temperature (Asseng et al. 2014). Wheat is particularly sensitive to heat stress. Plants respond to this genotype by environment interaction by modifying stress-adaptive traits for light interception, water-uptake and use-efficiency, and harvest index (Reynolds et al. 2007). As photo-protective traits, reflective hair and waxes increase albedo, reflecting the excess photosynthetic (Johnson 1975) and infrared radiation, regulating the plant temperature (Mondal et al. 2014) and unnecessary evaporative cooling (i.e. water loss) (Shepherd and Wynne Griffiths 2006). Optimizing this cuticle in plants can reduce as much as 31,000 liters/acre, or 1/3 inch of rain/irrigation water per day (Richards et al. 1986). However, the current slow and inefficient chemical method use for quantification has limited the phenotyping of this trait in large breeding populations and its introgression into elite backgrounds. The development of an indirect method for phenotyping these waxes will provide clarity and direction for breeders to select and combine this adaptive trait into new drought and heat tolerant wheat cultivars that work synergically to enhance grain yield. The main objective of this study is to estimate the accuracy of spectral indices to estimate the phenotypic variations of EW in wheat.

Methods
Twenty-four recombinant inbreed lines (RIL) derived from the cross of the heat tolerant cultivar 'Helberd' and the heat susceptible 'Len' were established in a plant growth chamber as a completely randomized design with four replications. For the acquisition of the data, the population was separated in two groups at 10 days after pollination (DAP). Each group contained only fifty percent of the plants, from now on will be referred as EW-change and EW-content. For the lines in the EW-change group; light reflected, absorbed and transmitted through the leaf was recorded for the abaxial and adaxial side using a CI-710 Miniature Leaf Spectrometer from CID Bio-Science before and after EW was removed with HPL chloroform. Only light reflectance was measured for the lines in the group EW-content, and samples of flag leaves were simultaneously collected to quantify EW via the colorimetric technique described by (Ebercon et al. 1977). The spectral signatures in the EW-change group were filtered by the Savitzy-Golay method (Bromba and Ziegler 1981) to estimate the first and second derivative. All pairwise combinations for eleven mathematical forms of indices were calculated using the spectral bands from the 4.0 to 9.5µm of the light reflectance obtained in the EW-content data set. A leave-one-out cross-validation (LOOCV) analysis was conducted to define the significance of the linear and non-linear models and estimate the coefficient of

determination (R2) for every spectral index. The R2 values of the models were grouped using a K-means cluster analysis, and the number of clusters was defined with the elbow method. Only the spectral indices included in the cluster with the highest R2 values were considered for further analysis. For a defined training set (66% of the observations), linear models to estimate the spectral index (SI) response based on EW values were fitted ($SI = a+\beta(EW)$). The statistically significant models were inverted, $EW = \frac{SI-a}{\beta}$, and an estimator for the Root Mean Square Error (RMSE) was calculated by bootstrapping the validation data set (34% of the individuals) 1000 times. Spectral indices with the lowest RMSE values were selected as candidates to be evaluated under field conditions.

Seven spring wheat populations were established during 2013, 2014 and 2015 at the Norman E. Borlaug Experimental Station (CENEB), Ciudad Obregon, Sonora in Northwest Mexico (27.20°N, 109.54°W, 38 masl). These trials were set ups as an alpha-lattice design in 2013, 2014 and 2015 under the raised bed system with two rows per bed, an inter-row spacing within each bed of 10 centimeters (cm), and a space between beds of 80 cm. The planting date was delayed about 80 days from the normal plating date in the Yaqui Valley, Mexico to expose plants to average daily temperatures of 28°C and maximum temperatures of 39°C during heading and anthesis. A second population, AMPSY, composed of 296 synthetic winter wheat genotypes was established in College Station, Chillicothe, and Bushland, TX in 2016 under non-irrigated conditions. These lines were sown in a randomized complete block design with two replications per line. Canopy reflectance was recorded between 11 AM and 1 PM using a spectroradiometer FieldSpec 4 Hi-Res for the populations established in the CENEB, and a Hand-held 2 spectroradiometer for the AMPSY population. This light reflectance was obtained by placing the fiber optic 40 cm above the top of the canopy. Both spectroradiometers was calibrated to 100% of reflectance with a white BaSO4 reference card and to 0% of reflectance by blocking any light intercepted by the optic fiber. Non-destructive hyperspectral imagery was acquired for the AMPSY population at College Station, Texas with an airborne hyperspectral imagining system mounted on a Cessna 206 single-engine aircraft. The system was configurated to capture 12-bit imagery with 120 bands over a spectral range from 392 nm to1009 nm at ~5 nm intervals, and a spatial resolution of 0.25 meters (m). The images were rectified in the software ERDAS IMAGE (Leica Geosystems Geospatial Imaging, LLC, Norcross, Georgia). For the radiometric calibration of the images, four tarpaulins with reflectance values of 8, 16, 32 and 48% were laid out in the field when images were captured. The exact reflectance values from the tarpaulins were measured using a Field HandHeld spectroradiometer with the previously described characteristics. The average digital counts (DCs) per tarpaulins and plots captured with the hyperspectral camera were extracted in ENVY version 4.8 (Exelis Visual Information Solutions, Boulder, Colorado). The DCs of the four tarps were associated with the percentage of light reflectance to derive 120 calibration equations, one per every spectral band. These regression equations were applied to estimate the reflectance values for every plot in the images. Flag-leaf samples were collected for all the locations in Texas and Obregon to quantify EW as previously described. Pearson correlation analysis was conducted for the sixteen candidate indices calculated with the canopy reflectance and the EW content.

Results and Discussion

3.1. Effect of epicuticular waxes on plant-light interactions

Variations in light reflectance, transmittance and absorbance derived by the presence and absence of EW in the surface of the leaves are summarized in Figure 1. These changes are represented as the difference between the reflectance collected with EW in place minus the reflectance after EW was removed with chloroform ($CHCl_3$). Comparing the response of all three plant-light interactions for the abaxial (A) and adaxial (B) surface, we find larger differences for the abaxial side, suggesting EW is mainly accumulated on the abaxial surface of flag leaves. The decrease in the percentage of light that is reflected with EW in place at the photosynthetically active radiation region enhances the importance of these waxes as a photo protective trait for high light intensity environments. A minimum change in reflectance is observed for the red-edge region, but there is a significant increase in transmittance and absorbance after the EW was removed.

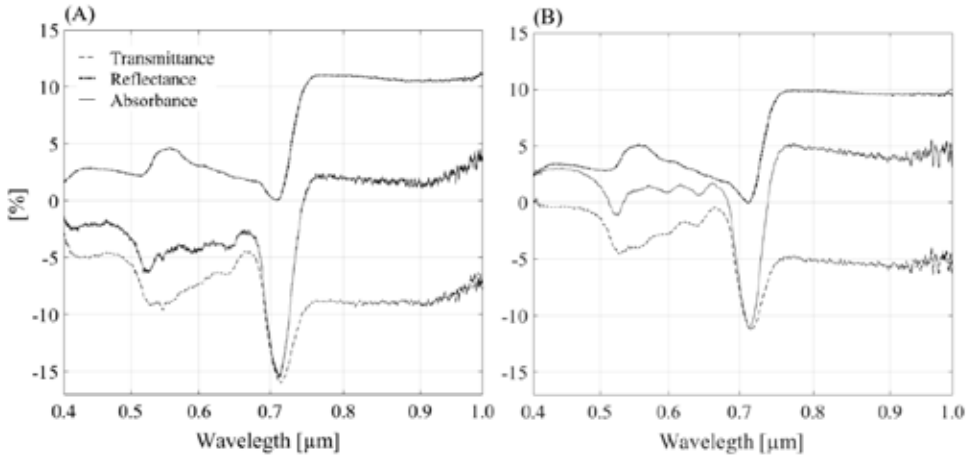

Fig. 1 Associated changes in light reflected, absorbed and transmitted with the presence and absence of EW on the leaf surfaces. It is represented as the difference of the response with EW in place minus the response after EW was removed with HPTS chloroform for the (A) abaxial and (B) adaxial surface of the leaf.

The first and second derivative of light reflectance enhanced specific changes in the spectral signature, separating the peaks from the overlapping of bands (Figure 2.0). For the first derivative (A), three main distinct peaks were detected at the 514, 570 and 700 nm. Another five peaks were identified with the second derivative (B). One of the peaks was centered at 510 nm and a second peak was found at 532 nm, where the reflectance reached the maximum absorption for the green color. The other two peaks were detected at 640 and 670 nm, and are directly associated with the absorption of chlorophyll b and a. The last peak at the 730 nm corresponds to the spectral change where the reflectance starts to increase to the NIR region.

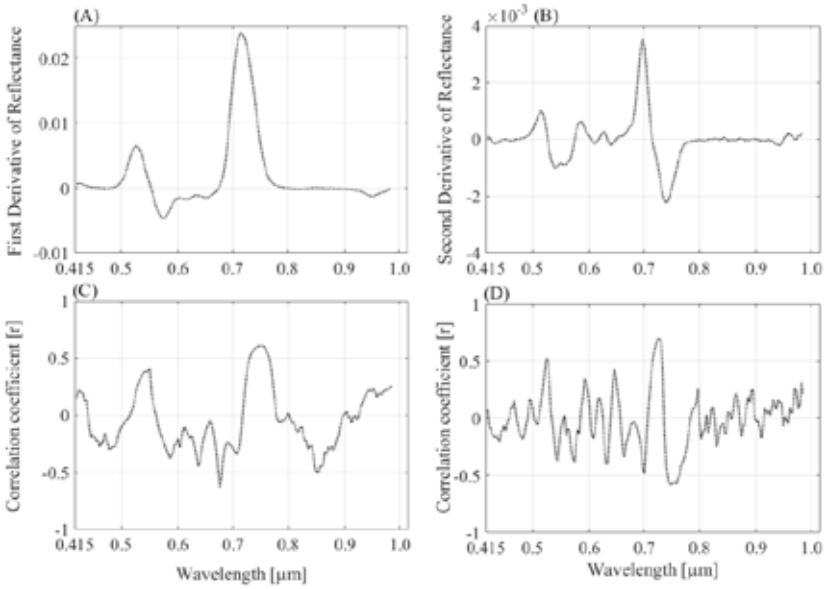

Fig. 2 Average response of the first (A) and second (B) derivative of the spectral signatures, and Pearson correlation coefficients of the first (C) and second (D) derivative with EW content.

Derivative changes at the visible region of the spectrum were highly associated with the phenotypic variation of EW. Several spectral bands in these regions (664 to 712, 487 to 550 and 712 to 775) have already been related to wax concentration in Pistacia species (Kozhoride et al. 2016). According to the results in Figure 1 and 2, EW can be indirectly monitored by detecting variations on the percentage of light reflected by the leaf. These waxes modify the reflectance of major absorption bands for vegetation, as chlorophyll and carotenoids, and by combining these sensitive bands an index can be developed to facilitate the screening of EW. Derivative vegetation indices have several advantages over the use of simple

reflectance based indices. The detected derivative peaks can be integrated to define the area under the curve, associate this response with the EW content, and develop derivative based indices. These derivative based indices can potentially increase the prediction accuracy of the empirical band indices proposed in this manuscript, particularly for the characterization of waxes under field conditions.

3.2. Narrow and broad band indices to estimate EW load in leaves

Approximately 65% of the EW variation can be estimated with empirical spectral indices. All sixteen narrow band indices reported in Table 3 were selected as candidate indices to estimate EW content based on their RMSE and R2 values. These indices involved combinations of spectral bands located around the 650, 700 and 830 nm. Most of these bands were previously correlated to EW in the derivative analysis. Thus, the first and second derivative can be an effective approach to eliminate unassociated spectral information for a response variable. Two indices combining the spectral bands at the 625, 736 and 832 nm were identified as best predictors for EW. Incorporating the blue and red bands, broad indices estimate as much as 44% of the EW variation. The NIR region is also significant predicting EW, but an index that involves this spectral band will be highly sensitive to differences in LAI when applied for canopy reflectance.

Table 3. Narrow and broad band indices selected based on their higher R2 values from the LOOCV and lowest RMSE in the validation data set.

	Bests fitted model parameters					
Index	**a**	**B**	**R^2**	**RMSE (mg/dm^2)**	**95% CI**	**p-value**
Broad indices involving two RGB and NIR spectral bands						
$EWI-1\ \frac{Blue}{Red}$	0.213	0.04	0.44	1.19	1.037-2.17	<0.0001
$EWI-2\ \frac{Blue}{NIR}$	0.07	0.13	0.39	1.18	0.98-1.98	<0.0001
$EWI-3\ \frac{(NIR-Red)}{Blue}$	-0.93	0.01	0.31	1.19	1.04-1.97	<0.0001
$EWI-4\ \frac{(Red^2-Blue)}{(Red-Blue^2)}$	-0.09	-0.03	0.32	1.19	1.09-2.55	<0.0001
Narrow indices involving one and two spectral bands						
$EWI-5\ _{676}$	0.019	0.005	0.45	0.84	0.62-1.25	<0.0001
$EWI-6\ \frac{658}{712}$	0.12	0.03	0.52	0.83	0.78-1.06	<0.0001
$EWI-7\ \frac{625}{706}$	0.22	0.05	0.50	0.81	0.65-1.25	<0.0001
$EWI-8_{694-625}$	-0.006	-0.002	0.42	1.08	0.96-1.55	<0.0001
$EWI-9\ \frac{670-718}{670+718}$	-0.85	0.03	0.51	0.61	0.55-0.81	<0.0001
$EWI-10\ \frac{691-661}{(691+661)^2}$	4.92	-1.03	0.51	0.92	0.79-1.09	<0.0001
$EWI-11\ \left(\frac{1}{661}\right)-\left(\frac{1}{694}\right)$	29.13	-5.73	0.48	0.72	0.48-0.86	<0.0001
$EWI-12\ \frac{622}{(724)^2}$	0.45	0.07	0.48	0.69	0.57-0.95	<0.0001
$EWI-13\ \left(\frac{622}{718}\right)^{-1}$	0.62	0.12	0.51	0.77	0.51-0.92	<0.0001
$EWI-14\ \frac{700^2-625}{700-625^2}$	-0.15	-0.05	0.52	0.77	0.68-0.81	<0.0001
Narrow indices involving three spectral bands						

$EWI-15_{625\left[\frac{1}{736}-\frac{1}{832}\right]}$	0.008	0.004	0.65	0.53	0.49-0.86	<0.0001
$EWI-16_{\frac{(625-736)}{832}}$	0.02	0.007	0.62	0.47	0.36-0.79	<0.0001

The Figure 3 shows the relationship of three narrow and one broad band index with EW. The narrow index $\frac{(625-733)}{832}$ (A) and the index $625\left(\frac{1}{736}-\frac{1}{832}\right)$ (B) were selected when light reflectance was captured with an active sensor, and non-additional factors as canopy architecture or light scattering were considered. The narrow band index 694-625 (C) was consistently associated to EW across all environments (Table 4), as well as the broad index $\frac{(\text{Red}^2-\text{Blue})}{(\text{Red}-\text{Blue}^2)}$ (D). When both indices were calculated in the validation data set, the values of the index D simultaneously decrease with the increase of EW, and the values of the narrow index C decreased from positive to negative as the EW content rises.

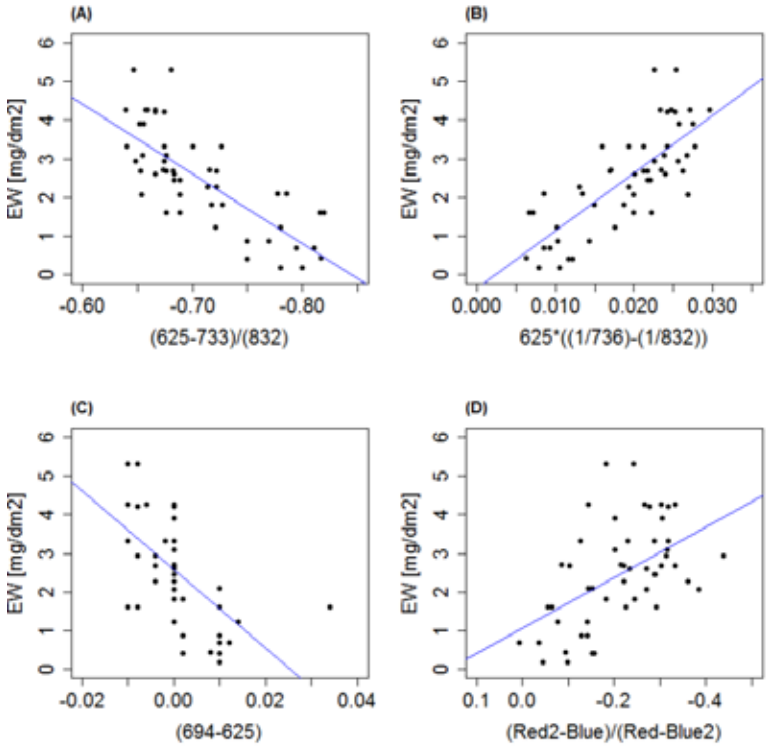

Fig. 3 Relationship between EW and EWI-16 (A), EWI-15 (B), EWI-8 (C) and EWI-4 (D). The solid line indicates the best fitted line in the validation data set.

The spectral bands at the 733 and 832 nm are highly sensitive to changes in the characteristics of the canopy. This sensitivity is associated with the response of the index A and B under field conditions. For both indices, high correlation coefficients were determined under yield potential, with full canopy cover, but no significant association was determined under heat stress conditions, where the canopy is scarce. When correlations were calculated for the subsets of high and low EW content (mg/md2), most of the indices were insensitive to estimate any variation for high values of EW, but they estimate a large proportion of the variation of low wax values. The application of these indices for airborne sensor is limited. Additional adjustment for factors as canopy cover and bidirectional reflectance might provide a more precise estimation of these waxes when monitored with airborne sensors.

Table 4. Pearson correlation coefficients of the indices detected with the leaf-clip reflectance evaluated under field conditions.

	HS/ASD			YP/ASD			YP/HI		
	MV	HV	LV	MV	HV	LV	MV	HV	LV
$EWI-1\ \frac{Blue}{Red}$	0.41**	0.05^{ns}	0.36**	0.21**	0.04^{ns}	0.26**	0.13**	-0.01^{ns}	0.19**
$EWI-2\ \frac{Blue}{NIR}$	0.13**	-0.09^{ns}	0.26**	-0.41**	-0.11^{ns}	-0.45**	-0.02^{ns}	0.001^{ns}	-0.01^{ns}
$EWI-3\ \frac{(NIR-Red)}{Blue}$	-0.13**	0.07^{ns}	-0.25**	0.35**	0.09^{ns}	0.41**	0.03^{ns}	-0.001^{ns}	0.02^{ns}
$EWI-4\ \frac{(Red^2-Blue)}{(Red-Blue^2)}$	-0.64**	-0.26**	-0.56**	-0.29**	-0.06^{ns}	-0.36**	-0.14**	0.003^{ns}	-0.21**
$EWI-5\ _{676}$	-0.35**	-0.26**	-0.12**	-0.36**	-0.13*	-0.41**	-0.20**	-0.011^{ns}	-0.23**
$EWI-6\ \frac{658}{712}$	0.03^{ns}	-0.15**	0.22**	-0.02^{ns}	-0.03^{ns}	0.003^{ns}	-0.02^{ns}	0.004^{ns}	0.002^{ns}
$EWI-7\ \frac{625}{706}$	0.09**	-0.14^{ns}	0.25**	-0.11**	-0.07^{ns}	-0.08**	-0.09*	-0.007^{ns}	-0.009^{ns}
$EWI-8_{694-625}$	-0.52**	-0.27**	-0.31**	0.41**	0.14*	0.45**	-0.23**	0.02^{ns}	-0.28**
$EWI-9\ \frac{670-718}{670+718}$	0.02^{ns}	-0.13^{ns}	0.21**	0.27**	0.02^{ns}	0.37**	-0.08^{ns}	0.001^{ns}	-0.05^{ns}
$EWI-10\ \frac{691-661}{(691+661)^2}$	0.66**	0.26**	0.58**	-0.18**	-0.04^{ns}	-0.25**	0.05^{ns}	0.09^{ns}	-0.002^{ns}
$EWI-11\ \left(\frac{1}{661}\right)-\left(\frac{1}{694}\right)$	0.19**	0.19**	-0.05^{ns}	-0.13**	-0.03^{ns}	-0.21**	0.02^{ns}	0.08^{ns}	-0.11*
$EWI-12\ \frac{622}{(724)^2}$	0.38**	0.07^{ns}	0.42**	0.41**	0.18**	0.48**	-0.008^{ns}	-0.006^{ns}	0.02^{ns}
$EWI-13\ \left(\frac{622}{718}\right)^{-1}$	0.03^{ns}	-0.12^{ns}	0.21**	0.14**	-0.01^{ns}	0.26**	-0.07^{ns}	-0.003^{ns}	-0.06^{ns}
$EWI-14\ \frac{700^2-625}{700-625^2}$	0.36**	0.28**	0.12**	0.19**	0.06^{ns}	0.18**	-0.002^{ns}	0.024^{ns}	-0.03^{ns}
$EWI-15_{625\left[\frac{1}{736}-\frac{1}{832}\right]}$	-0.09^{ns}	-0.16**	0.07^{ns}	0.46**	0.08^{ns}	0.51**	-0.07^{ns}	0.007^{ns}	-0.07^{ns}
$EWI-16_{\frac{(625-736)}{832}}$	-0.04^{ns}	-0.19**	0.14**	0.23**	0.13*	0.27**	0.07^{ns}	0.03^{ns}	0.11*

** P-values<0.001 * P-value<0.05
HS/ASD- Heat stress conditions for the reflectance data collected with an ASD spectroradiometer
YP/ASD- Yield potential conditions for the reflectance data collected with an ASD spectroradiometer
YP/HI- Yield potential conditions for the reflectance data collected with a hyperspectral camera
MV-mixed values of EW (mg/dm^2): HS/ASD= 0.5 to 12.6 mg, YP/ASD= 0.3 to 8.9, and YP/HI= 0.5 to 6.2
HV- high values of EW(mg/dm^2): HS/ASD=0.5 to 5.0, YP/ASD=0.3 to 5.0, and YP/HI=0.5 to 5.0
LV- low values of EW (mg/dm^2): HS/ASD=5.1 to 12.6, YP/ASD=5.1 to 8.9, and YP/HI=5.0 to 6.2

Conclusions

The spectral bands in the visible region of the spectrum are highly associated to EW content, and variations on these specific bands provide a reliable estimation of EW. Two novel empirical based indices are proposed for phenotyping EW under field conditions: the broad index $\frac{(\mathrm{Red}^2-\mathrm{Blue})}{(\mathrm{Red}-\mathrm{Blue}^2)}$ and the narrow index 694-625. The sensitivity of the candidate indices to changes in canopy cover suggests an additional adjustment is needed to mitigate this effect. A radiative transfer model approach to estimate the bidirectional reflectance under field conditions is necessary to increase the prediction accuracy of the proposed indices to estimate EW, particularly for airborne applications.

References

Asseng, S., Ewert, F., Martre, P., Rötter, R.P., Lobell, D.B., Cammarano, D., Kimball, B.A., Ottman, M.J., Wall, G.W., White, J.W., Reynolds, M.P., Alderman, P.D., Prasad, P.V.V., Aggarwal, P.K., Anothai, J., Basso, B., Biernath, C., Challinor, A.J., De Sanctis, G., Doltra, J., Fereres, E., Garcia-Vila, M., Gayler, S., Hoogenboom, G., Hunt, L.A., Izaurralde, R.C., Jabloun, M., Jones, C.D., Kersebaum, K.C., Koehler, A.K., Müller, C., Naresh Kumar, S., Nendel, C., O'Leary, G., Olesen, J.E., Palosuo, T., Priesack, E., Eyshi Rezaei, E., Ruane, A.C., Semenov, M.A., Shcherbak, I., Stöckle, C., Stratonovitch, P., Streck, T., Supit, I., Tao, F., Thorburn, P.J., Waha, K., Wang, E., Wallach, D., Wolf, J., Zhao, Z., & Zhu, Y. (2014). Rising temperatures reduce global wheat production. *Nature Climate Change, 5*, 143-147

Bromba, M.U.A., & Ziegler, H. (1981). Application hints for Savitzky-Golay digital smoothing filters. *Analytical Chemistry, 53*, 1583-1586

Ebercon, A., Blum, A., & Jordan., W.R. (1977). A rapid colorimetric method for epicuticular wax contest of sorghum leaves. *Crop Science, 17(1)*, 179-180

Johnson, H.B. (1975). Plant pubescence: an ecological perspective. *Botanical Reviews, 41*, 233-258

Kozhoride, G., Orlovsky, N., Prlovsky, L., Blumberg, D.G., & Golan-Goldhirsh, A. (2016). Remote sensing models of structure-related biochemical ana pigments for calssification tress. *Remote Sensing of Environment*, 184-195

Mondal, S., Mason, R.E., Huggins, T., & Hays, D.B. (2014). QTL on wheat (Triticum aestivum L.) chromosomes 1B, 3D and 5A are associated with constitutive production of leaf cuticular wax and may contribute to lower leaf temperatures under heat stress. *Euphytica, 201*, 123-130

Ray, D.K., Mueller, N.D., West, P.C., & Foley, J.A. (2013). Yield Trends Are Insufficient to Double Global Crop Production by 2050. *PLoS One, 8*, e66428

Reynolds, M.P., Pierre, C.S., Saad, A.S.I., Vargas, M., & Condon, A.G. (2007). Evaluating Potential Genetic Gains in Wheat Associated with Stress-Adaptive Trait Expression in Elite Genetic Resources under Drought and Heat Stress. *Crop Science, 47*, S-172

Richards, R.A., Rawson, H.M., & Johnson, D.A. (1986). Glacousness in wheat: Development and effect on water-use efficiency, gas exchange and photosynthetic tissue temperatures. *Plant Physiol, 13*, 465-473

Shepherd, T., & Wynne Griffiths, D. (2006). The effects of stress on plant cuticular waxes. *New Phytol, 171*, 469-499

Evaluation of heat shock tolerance in different wheat genotypes under contrasting environmental conditions

Fadia Chairi[1], Rut Sanchez-Bragado[1], Gemma Molero[2], Matthew P. Reynolds[2] and Jose Luis Araus[1]
[1] Universitat de Barcelona, Spain; [2] CIMMYT, Mexico

Abstract
Wheat is one of the world's most important food crops. While wheat yield is severely limited by the impact of environmental stresses such as drought and heat, forecasts for the next decades indicate increases in temperature as a result of climate change. Therefore, studying wheat's adaptation to heat waves can be vital for developing wheat varieties that are better adapted to climate change. It is also important to develop methodologies to help assess genotypic variability in heat shock tolerance. The present research aims to establish a methodology to select, under field conditions, genotypes that are more heat tolerant. We used portable plastic houses to induce transient increases in air temperature at different key phenological stages (heading, anthesis and mid grain filling) together with different planting (normal versus late) times to assess different temperatures during the whole cycle. Under good agronomic conditions (fully irrigated crop, planted at the right time), the effect of transient heat stress (i.e., heat waves) on grain yield directly affected grain number per spike, particularly when stress occurred at heading; TKW was less affected and the effect did not appear to be mediated primarily by a decrease in leaf photosynthesis. The effect of transient heat on late planting was more severe, with stress occurring at heading being the one that most affected grain yield. Moreover, in the late planting, photosynthesis was severely affected by heat. Genotypic differences were detected for HI and kernel weight/spike, particularly in the late planting.

Introduction
Wheat is the main source of food for the human population (www: //fao.org/). Over the past decades, wheat breeding efforts have focused primarily on disease resistance and abiotic stress tolerance, along with increased yield potential (Araus et al., 2002; Reynolds and Borlaug, 2006). However, there is a need to develop more efficient wheat improvement methodologies that complement existing traditional techniques (Araus et al., 2008). This is more challenging in the context of climate change, since mean temperature increases ranging from 1.0 to 3.7ºC are expected for 2050, together with higher likelihood of heat waves, frequently of greater intensity and duration than today, and variability in precipitation patterns (Tebaldi et al., 2006). Therefore, the most direct solution to this challenge would be to increase yield potential and improve wheat's adaptation to the increasing incidence of abiotic stresses by selecting genotypes better adapted to heat waves (Parry et al., 2011).

However, effects of heat shock associated with high temperatures and low humidity are still scarce (Yang et al., 2002). For example, during grain filling, a decrease in photosynthesis associated with an increase in temperature may limit the amount of assimilates assigned to the grains, implying a decrease in their growth and final weight (Reynolds et al., 1994b). If the heat shock takes place before the fertility of the flowers decreases, this may reduce the number of grains in the spike. Therefore, the development of "phenotypic" capacity evaluation protocols to assess the effect of heat waves on photosynthetic capacity and grain setting will make it possible to develop wheat with better adaptation to climate change.

The main focus of this study was to establish a methodology for estimating the physiological mechanisms associated with wheat tolerance to heat waves. To that end, we evaluated grain yield and its agronomic components, together with gas exchange performance of the flag leaves, in response to transient increases in air temperature during specific key stages of the crop's reproductive phase. Higher temperatures were induced by the temporary installment of mobile plastic houses above the canopies of fully irrigated crops. Moreover, diverse planting dates were assayed, thereby ensuring different temperatures throughout the entire crop growth cycle.

Methods
Durum wheat (*Triticum turgidum* L. ssp. *durum* (Desf.) Husn.) cultivar Movas was selected for developing a specific methodology aimed at determining the genetic variability in tolerance to heat waves. In addition, a subset of 6 durum wheat genotypes from the High Biomass Association Mapping Panel (HiBAP, 150 lines) was also tested. All the evaluations were performed under fully irrigated field conditions during the 2016 spring growing season at MEXPLAT (Mexican Phenotyping Platform) located at CIMMYT's

Experiment Station, Norman E. Borlaug (CENEB) in the Yaqui Valley, near Ciudad Obregon, Sonora, Mexico (27º24′N, 109º56′W, 38 m above sea level). Diverse planting dates were assayed to ensure different temperatures during the entire crop cycle, including a late planting date to test the effect of continuous heat. Transient increases in heat (herein also referred to as heat shock or heat waves) were generated with the use of plastic greenhouses, which allowed near 100% light transmission (Fig. 1).

Fig. 1. Portable plastic greenhouses installed in the field under yield potential (fully irrigated normal planted; left image) and heat (late planting; right image) conditions.

The heat wave (consisting of an increase in temperature from 2 ºC to 4 ºC, Fig. 2) was generated by installing a portable plastic greenhouse during: a) two and four days at heading; b) two days at anthesis; and c) two and four days at ten days after anthesis.

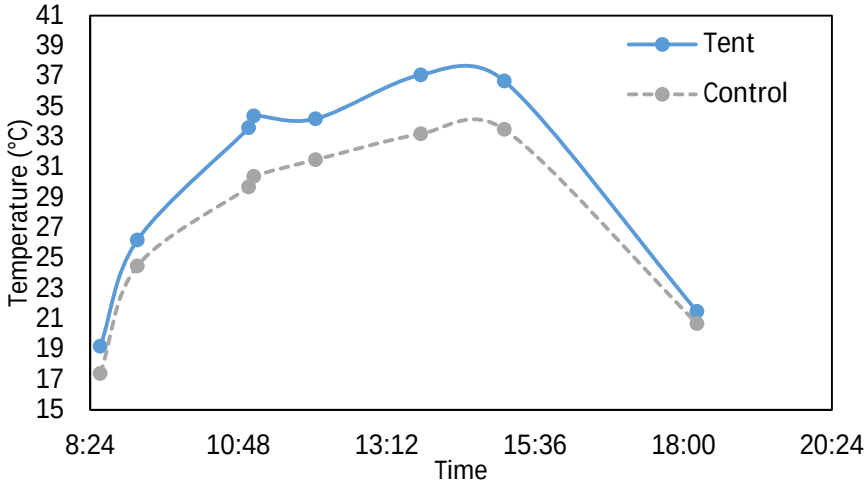

Fig. 2. Air temperature inside the plastic tents compared with control plants throughout a daily cycle.

The effects of these heat treatments were tested under yield potential (normal planting) and heat conditions (late planting) in: a) the genotype Movas (3-4 replicates per treatment) and once the methodology settled down; and b) in the subset of 6 genotypes. Photosynthetic rates of the flag leaf blade (Sanchez-Bragado et al., 2014) in the control and heat-shock treated plants were measured during the heat treatments and the days following the removal of the plastic house. Canopy temperature of the plot was taken with an infrared thermometer. Heading, flowering and maturity dates were also recorded. Grain yield, harvest index and agronomic components (spikes/m^2, grains/spike, thousand-kernel weight, kernel weight/spike and harvest index) were recorded at maturity. The decrease in the agronomical components of the heat treatments relative to the control (Maydup et al., 2010) was calculated as follows in equation 1:

$$Decrease\ (\%) = \left[\frac{Control\ plants - treated\ plants}{Control\ plants}\right] x\ 100 \qquad (1)$$

Results and Discussion

Heat treatment decreased the grain weight per spike (GWSP) and the harvest index (HI), particularly when the stress occurred at heading (Table 1). Plants growing under high temperature (i.e. late planting) were more affected by a transient increase in temperature than those coming from the yield potential (i.e. normal planting) trial. Heat stress at heading mainly affected number of grains per spike (GSP) whereas thousand kernel weight (TKW) was unaffected or even slightly increased. When the heat wave occurred during grain filling TKW decreased, whereas GSP did not change.

Table 1. Decrease in grain weight per spike (GWSP), harvest index (HI), thousand-kernel weight (TKW) and number of grains per spike (GSP) calculated as mentioned in eq. 1. Trt duration indicates the number of days the heat shock treatment was applied. Evaluation was performed in genotype Movas

Treatment	**Trt duration**	**Movas YP**				**Movas Late planting**	
	(days)	GWSP (%)	HI (%)	TKW (%)	GSP (%)	GWSP (%)	HI (%)
Heat heading	4	6.2a	10.0a	-5.5b	9.1a	19.8a	18.3a
Heat heading	2	4.6ab	1.4a	1.0ab	0.9a	32.3a	21.3a
Heat anthesis	4	-0.2ab	6.0a	-3.3b	0.6a	-	-
Heat anthesis+10	2	-8.2b	2.5a	10.8a	0-0a	9.7a	7.0a
Heat anthesis+10	4	0.4ab	7.4a	-0.7ab	-1.1a	8.4a	5.5a

When the subset of 6 genotypes was assessed (Table 2), the heat shock treatments at anthesis and 10 days after also decreased GWSP, HI and GSP in the normal planting (yield potential) experiment, whereas TKW was not significantly affected. However, in the late planting experiment, heat shock applied during grain filling did not negatively affect GWSP and HI. The genotypic effect was significant for GWSP and HI in the late planting and marginally significant ($p<0.1$) in the normal planting. Genotypic differences were also observed for GSP.

Table 2. Mean values of grain weight per spike (GWSP), harvest index (HI), thousand-kernel weight (TKW) and number of grains per spike (GSP) of six genotypes from the HiBAP population (2 replicates per treatment). Trt duration, indicates the number of days the heat shock treatment was applied.

Treatment	**HiBAP YP**				**HiBAP Heat**	
	GWSP (g)	HI	TKW (g)	GSP (#)	GWSP (g)	HI
Anthesis	1.94b	0.45b	40.1a	48.6ab	-	-
Anthesis+10	1.82b	0.45b	41.3a	44.1b	1.15a	0.30a
Control	2.31a	0.49a	42.8a	54.4a	1.16a	0.23a
Level of significance						
Treatment	0.006	0.004	0.347	0.011	0.922	0.992
Genotype	0.076	0.088	0.119	0.06	0.002	0.003
TxG	0.615	0.471	0.63	0.531	0.945	0.783

The negative effect of increased temperature on grain yield is illustrated by the negative linear relationship between canopy temperature and total kernel weight per spike (Fig. 3). This also helps to explain not only the negative effect of the late planting versus the normal one but also the effect of transient increases in heat.

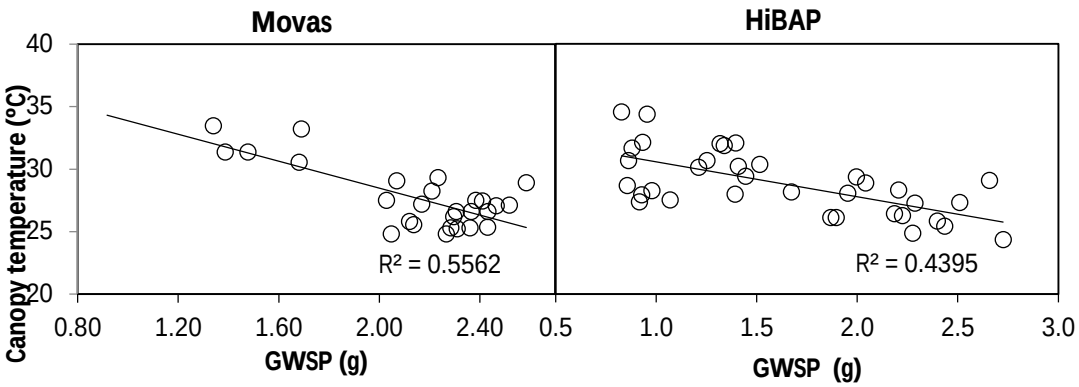

Fig. 3. Linear regression of the relationship between grain weight per spike (GWSP) and canopy temperature (ºC), of one genotype Movas (3 replicates per treatment) (left panel) and six genotypes from the HiBAP population (2 replicates per treatment) (right panel). For each figure, all the individual values for each treatment and planting date were plotted together. Level of significance: ***P<0.001.

Photosynthetic rates were mostly unaffected (or even increased) by heat treatments in the normal planting trial, whereas in the late planting trial, some of the heat treatments negatively affected photosynthesis (Table 3). The Fv'/Fm' ratio was not affected by the heat shock in the normal planting, whereas in the late planting, regardless of the treatment, the values were lower and the heat shock negatively affected the ratio. The heat shock treatments induced an increase in stomatal conductance and transpiration in the normal planting, while in the late planting, these gas exchange traits tended to decrease. Canopy temperature was lower in the normal planting compared with the late planting, whereas the values increased in response to the heat shock treatments, particularly in the normal planting.

When the set of six genotypes was assessed, transient high temperature again did not affect photosynthetic rates of the flag leaf blade in the high yield (i.e., normal planting) crop (Table 4). Stomatal conductance, transpiration and the Fv'/Fm' ratio were also unaffected, as was the canopy temperature. There were no genotypic differences for any of these photosynthetic traits. In the late planting, the photosynthetic rate decreased in response to transient heat, apparently associated with a tendency to lower stomatal conductance, whereas the Fv'/Fm' ratio did not change. In this case, genotypic variability was only marginally significant for the net photosynthetic rate and the Fv'/Fm' ratio.

Table 3. Mean values of flag leaf lamina photosynthetic rates (μmol $CO_2 \cdot m^{-2} \cdot s \cdot^{-1}$), chlorophyll florescence (relative quantum yield of photosystem II), canopy temperature (CT; ºC), stomatal conductance (g_s) and transpiration (Tr) (both in mmol $H_2O \cdot m^{-2} \cdot s \cdot^{-1}$) of six genotypes from the HiBAP population (2 replicates per treatment).

	Treatment	Trt days	Photosynthesis	CT	g_s	Tr	Fv'/Fm'
MOVAS Yield Potential	Heat heading	4	26.8a	27.8a	0.35bc	6.4c	0.52a
	Heat heading	2	35.5a	25.8bc	0.72a	10.2a	0.56a
	Heat anthesis	4	-	27.1ab	-	-	-
	Heat anthesis+10	2	22.2a	28.a	0.49b	8.7ab	0.52a
	Heat anthesis+10	4	20.7a	27.9a	0.33bc	7.4bc	0.51a
	Control		23.7a	25.8c	0.27c	5.6c	0.51a
MOVAS Late Planting	Heat heading	2	20.4a	-	0.22a	5.8a	0.48a
	Heat heading	4	18.7a	-	0.18ab	4.4a	0.45b
	Heat anthesis+10	2	13.6b	32.4a	0.13b	4.1a	0.41c
	Heat anthesis+10	3	-	33.2a	-		
	Control		22.6a	30.9a	0.24a	6.1a	0.48a

Table 4. Absolute mean values of flag leaf lamina photosynthetic rates (μmol $CO_2 \cdot m^{-2} \cdot s \cdot^{-1}$), chlorophyll florescence (relative quantum yield of photosystem II), canopy temperature (CT; ºC), stomatal conductance (g_s) and transpiration Tr (both in mmol $H_2O \cdot m^{-2} \cdot s \cdot^{-1}$) of six genotypes from the HiBAP population (2 replicates per treatment).

	Treatment	Trt days	Photosynthesis	Fv'/Fm'	CT	g_s	Tr
HiBAP Yield Potential	Anthesis	4	30.3a	0.56ab	28.2b	0.50a	6.49a
	Control (ant)	4	32.2a	0.58a	26.0b	0.54a	6.63a
	Anthesis+10	2	22.3b	0.54b	28.3b	0.27b	1.87b
	Control (A+10)	4	21.9b	0.54b	27.6b	0.23b	1.78b
	Level of significance						
	Treatment		0.002	0.079	0.001	0	0
	Genotype		0.88	0.622	0.895	0.944	0.782
	TxG		0.858	0.786	0.137	0.73	0.822
HiBAP Late Planting	Anthesis	4	-	-	-	-	-
	Anthesis+10	2	14.6a	0.46a	30.3a	0.16a	4.67a
	Control	4	18.6b	0.46a	46.6a	0.18a	4.66a
	Level of significance						
	Treatment		0.006	0.917	0.467	0.187	0.956
	Genotype		0.084	0.073	0.633	0.184	0.358
	TxG		0.244	0.923	0.711	0.337	0.927

Extreme heat reduces seed number by directly affecting the flowering processes, and can reduce GW perhaps through its effect on photosynthesis and green area senescence. Both responses reduce HI. Heat shock reduces the amount of photosynthetic pigments (Todorov et al., 2003), soluble proteins, rubisco binding proteins (RBP) and large (LS) and small subunits (SS) of rubisco in darkness, but increases them in light, indicating their roles as chaperones and HSPs (Demirevska-Kepova et al., 2005). However, in our results, at least under the fully irrigated normal planting, the effect of transient heat on grain yield did not appear to be associated with a decrease in photosynthesis.
In addition to chronic high temperature during grain filling, heat waves or hot spells (periods of 1–3 days of Tmax above ~34 °C) may affect wheat yield. The reported effect is markedly reduced grain size (Reynolds et al., 1994; Asseng et al., 2011), possibly attributed to widely observed loss of green leaf area reducing grain growth rate. Hot spell effects appear to be largely avoided in irrigated wheat crops because the canopies and spikes can be cooled up to 5 °C or more below air temperature, depending on prevailing vapor pressure deficit (VPD). However, in rainfed crops there is usually some water stress during grain filling, little or no canopy cooling, and increased damage from hot spells with increased water stress (Asseng et al., 2011).

However, in our study, the late planting, even when fully irrigated, was far more affected by transient increases in temperature. Moreover, photosynthesis appeared to be affected by these treatments, probably because the plant was already growing under high temperature, closer to the metabolic limit for normal functioning of photosynthesis, moreover to exacerbate photorespiratory losses. An additional factor to consider may be the increases in VPD due to the heat waves. Whereas in the normal planting, stomatal conductance and transpiration increased in response to the transient increases in heat, in the late planting, stomatal conductance and transpiration decreased, probably due to excessive VPD, which induces water deficit and stomatal closure.

Conclusions
The present study highlights the feasibility of using removable plastic houses together with the study of agronomic yield components of single spikes to assess the genotypic variability to tolerate heat waves during the reproductive phase. Under good agronomic conditions (fully irrigated crop, planted at the right

time), the effect of transient heat stress (i.e., heat waves) on grain yield directly affected grain number per spike, particularly when stress occurred at heading; TKW was less affected and the effect did not appear to be mediated primarily by a decrease in leaf photosynthesis. The effect of transient heat on late planting was more severe, with the stress occurring at heading being again the one that most affected grain yield. Moreover, in the late planting, photosynthesis was severely affected by heat. Genotypic differences were detected for HI and kernel weight/spike, particularly in the late planting. The present study illustrates and highlights the existence of genotypic variability in wheat for tolerance to transient heat stress, particularly when agronomic conditions are not optimal.

References

Araus JL, Slafer GA, Reynolds MP, Royo C. 2002. Plant breeding and drought in C-3 cereals: What should we breed for? Annals of Botany 89, 925–940.

Araus JL, Slafer GA, Royo C, Serret MD. 2008. Breeding for Yield Potential and Stress Adaptation in Cereals. Critical Reviews in Plant Sciences 27, 377–412.

Asseng S, Foster I, Turner NC. 2011. The impact of temperature variability on wheat yields. Global Change Biology 17, 997–1012.

Demirevska-Kepova K, Holzer R, Simova-Stoilova L, Feller U. 2005. Heat stress effects on ribulose-1,5-bisphosphate carboxylase/oxygenase, Rubisco binding protein and Rubisco activase in wheat leaves. Biologia Plantarum 49, 521–525.

Parry M a J, Reynolds MP, Salvucci ME, Raines C, Andralojc PJ, Zhu X-G, Price GD, Condon AG, Furbank RT. 2011. Raising yield potential of wheat. II. Increasing photosynthetic capacity and efficiency. Journal of experimental botany 62, 453–67.

Reynolds M, Balota M, Delgado M, Amani I, Fischer R. 1994*a*. Physiological and morphological traits associated with spring wheat yield under hot, irrigated conditions. australian journal of plant physiology 21, 717.

Reynolds MP, Borlaug NE. 2006. Impacts of breeding on international collaborative wheat improvement. The Journal of Agricultural Science 144, 3.

Tebaldi C, Hayhoe K, Arblaster JM, Meehl GA. 2006. Going to the Extremes. Climatic Change 79, 185–211.

Todorov DT, Karanov EN, Smith AR, Hall MA. 2003. Chlorophyllase Activity and Chlorophyll Content in Wild Type and eti 5 Mutant of Arabidopsis thaliana Subjected to Low and High Temperatures. Biologia Plantarum 46, 633–636.

Yang J, Sears RG, Gill BS, Paulsen GM. 2002. Genotypic differences in utilization of assimilate sources during maturation of wheat under chronic heat and heat shock stresses. Euphytica 125, 179–188.

Genome wide association mapping for grain weight in spring wheat across multiple environments

Sivakumar Sukumaran[1], Marta Lopes[2], Susanne Dreisigacker[1] and Matthew Reynolds[1]
[1] CIMMYT, Mexico; [2] CIMMYT, Turkey

Abstract
In the present study, 287 elite spring bread wheat lines were phenotyped for thousand grain weight (TGW) in 16 environments across different wheat growing regions in Mexico, South Asia and North Africa. The population was genotyped with the 90K Illumina Infinitum SNP array, and 11K SNPs were used for conducting a genome-wide association study (GWAS). Statistical analysis of multi-environment data revealed an estimated heritability (h^2) of 0.80 for TGW. A GWAS applied for each single environment, for clusters of environments defined by growing region, and for all environments combined. It identified several genomic regions associated with TGW (2A (130cM), 3B at 51cM and 134cM, 5A at 60cM and 98cM, 6A at 109 to 113cM and at 77 to 85cM), among them a locus on chromosome 6A at 79 to 85 cM that was associated with gene *TaGW2* previously identified to affect TGW. The average allelic substitution effect was 1.6 g for TGW across 16 environments. The haplotype *TaGW2-6A-G* was observed to be the superior allele.

Introduction
Grain weight and grain number per unit area of land are important yield components determining grain yield (Griffiths et al., 2015). Most of the genetic advances in grain yield are based on increasing the number of grains per unit area, but grain weight is also an important trait. The genetic basis of high grain weight is not fully understood in spring wheat. Several studies have identified QTL related to TGW (Simmonds et al., 2014; Ain et al., 2015; Griffiths et al., 2015; Zanke et al., 2015). The most studied gene affecting TKW in wheat is gene *TaGW2*, an orthologue of the *OsGW2* gene in rice that influences grain width and weight (Su et al., 2011). This gene is located on 6A chromosome and has two SNPs in the promotor region forming two haplotypes: Hap-6A-A (-593A and -739G) and Hap-6A-G (-593G and -739A). Among them Hap-6A-A was initially associated with wider grain and higher TGW (Su et al., 2011). A second study, however, found that Hap-6A-G was associated with higher grain weight and that Hap-6A-A reduced grain weight (Zhang et al., 2013). A third study reported that the homologous gene *TaGW2-6B* has an even stronger influence on TGW than *TaGW2-6A* (Qin et al., 2014). Differences in the effect of *TaGW2-6A* were observed depending on the geographical distribution of investigated cultivars, the *TaGW-6A-A* haplotype being favored in Chinese, Australian, and Russian cultivars and the *TaGW2-6A-G* haplotype being preferred in European, American, and CIMMYT cultivars (Qin et al., 2014).

Genetic mapping through association analysis is the state-of-the-art method for the genetic dissection of complex traits. However, in wheat there are few studies that pinpoint genes responsible for traits of interests. One recent example is the identification of “earliness per se” in spring wheat through GWAS and a candidate gene study (Sukumaran et al., 2016). In the present paper, we identified the genomic region responsible for TKW through GWAS and validated a *TaGW2* gene through a candidate gene approach in a spring wheat population grown in multiple environments.

Methods
The germplasm used in the study was the wheat association mapping initiative (WAMI) panel of 287 spring bread wheat lines assembled from the Elite Spring Wheat Yield Trial (ESWYT), Semiarid Wheat Yield Trial (SAWYT), and High Temperature Wheat Yield Trial (HTWYT), which are CIMMYT international nurseries distributed to developing countries around the world (Lopes et al., 2012). The population structure of the panel is based on the 1B.1R translocation as well as the pedigree of the lines. This population has a low range of phenology: 9 days and 35 cm variation for days to heading and plant height, respectively, when grown under temperate irrigated conditions in Mexico (Lopes et al., 2015; Sukumaran et al., 2015).

The WAMI population was phenotyped in major wheat growing areas in India, Pakistan, Nepal, Bangladesh, Iran, Egypt, and Mexico in the 2009-2010 and 2010-2011 growing seasons. These environments were diverse in terms of rainfall, heat stress, drought stress and solar radiation patterns. Minimum and maximum temperatures and coordinates of the environments were described in earlier publications. The experimental design was an alpha lattice with two replications (Sukumaran et al., 2016,

2017). Phenotyped traits included grain yield, thousand grain weight (TGW), grain number/m^2, and plant height; here we focus on TGW.

Statistical analysis

Single environment means were estimated using the META-R package and broad-sense heritability was estimated. To understand the genetic variance and estimate variance components, an analysis of variance was conducted in SAS using the PROC MIXED commands. META-R software (Vargas et al., 2013) was used to estimate Best Linear Unbiased Estimates (BLUEs) by considering genotypes, environments, and genotype-by-environment interaction (GEI) as random factors in the model and days to heading as a covariate. The locations with heritability (h^2) estimates <0.05 were not included in the cluster based and combined analysis.

1. Single environment analysis

Analysis was performed using an alpha lattice design adjusted with days to heading as a covariate using the following model:

$$Y_{ijk} = \mu + R_i + B_j(R_i) + G_k + Cov + \varepsilon_{ijk}$$

where *Y* is the trait of interest, μ is the mean effect, R*i* is the effect of the *i*th replicate, B*j*(R*i*) is the effect of the *j*th incomplete block within the *i*th replicate, G*k* is the effect of the *k*th genotype, Cov is the effect of the covariate, and ε*ijk* is the error associated with the *i*th replication, *j*th incomplete block, and *k*th genotype, which is assumed to be normally and independently distributed, with mean zero and variance σ^2.

Broad-sense heritability was estimated as

$$h^2 = \frac{\sigma_g^2}{\sigma_g^2 + \sigma_e^2/r}$$

where σ_g^2 and σ_e^2 are the genotype and error variance, respectively, and r is the number of replications.

2. Cluster based and combined analysis

Ward's minimum variance clustering (Ward, 1963) was incorporated in the META-R software for each trait to group environments into different clusters to avoid high G × E interaction. Once the clusters were formed, BLUEs and h^2 were estimated for each cluster. Combined BLUEs were also estimated in the META-R software.

The following model was used for the cluster based and combined analysis:

$$Y_{ijk} = \mu + L_i + R_j(L_i) + B_k(L_iR_j) + G_l + L_i \times G_l + Cov + \varepsilon_{ijk}$$

where the new terms L_i and $L_i \times G_l$ are the effects of the *i*th environment and the G × E interaction, respectively. For the combined analysis the heritability was estimated as

$$h^2 = \frac{\sigma_g^2}{\sigma_g^2 + \sigma_{ge}^2/l + \sigma_e^2/rl}$$

where σ_{ge}^2 is the genotype by environment interaction variance and *l* is the number of environments.

When BLUEs were calculated, genotype was considered as a random effect and all other terms as fixed effects. For calculating broad-sense heritability (h^2), all effects except the covariate were treated as random.

Genome-wide association analysis

A GWAS was performed with the BLUEs of each single environment, each cluster, and with the BLUEs of the combined analyses for each trait. We followed the mixed model approach (Yu et al., 2006) in the TASSEL 5.0 software to test for marker-trait associations (Bradbury et al., 2007). To account for population structure principal components (PC) from the principal component analysis of the genotypic data, the Q matrix from the STRUCTURE software using the model based clustering method (Pritchard et

al., 2000; Falush et al., 2003, 2007), and non-metric multi-dimensional scaling (nMDS) (Zhu and Yu, 2009) were used. In addition, kinship matrix (K) was calculated using SPARGeDi (Hardy and Vekemans, 2002) and a coefficient of parentage matrix (COP) was used. Different models accounting for population structure and family relatedness were fitted using the mixed model framework in TASSEL. Model fitting was performed using the quantile-quantile plots, and the threshold to call significant marker-trait associations was based on the deviation of the expected *p*-values from the observed *p*-values.

Results and Discussion

Across all environments, TGW ranged from 27.71 g (Ind H10) to 43.58 g (Mex I10) with a mean value of 32.91g (Table 1). Heritability estimates were medium to high with highest h^2 value of 0.95 in Mex I10.

Table 1. Descriptive statistics for TGW on the WAMI panel in multiple environments.

Country	Place	Abbreviation	Year	Thousand grain weight (g)		
				Mean	SD	H^2
Bangladesh	Joydebpur	BGLD J10	2010	30.97	4.14	0.70
Bangladesh	Joydebpur	BGLD J11	2011	31.14	4.08	0.84
India	Dharwad	Ind H10	2010	27.71	3.51	0.71
India	Indore	Ind I11	2011	32.84	3.60	0.80
India	Karnal	Ind K11	2011	38.40	4.59	0.73
India	Ludhiana	Ind L11	2011	38.31	2.89	0.50
Mexico	Cd. Obregon Drought	Mex D10	2010	37.86	4.63	0.92
Mexico	Cd. Obregon Heat	Mex H10	2010	30.65	3.49	0.90
Mexico	Cd. Obregon Heat + drought	Mex HD10	2010	29.36	4.21	0.93
Mexico	Cd. Obregon Yield potential	Mex I10	2010	43.58	4.68	0.95
Nepal	Bhairahawa	Nepal B10	2010	32.06	4.33	0.83
Nepal	Bhairahawa	Nepal B11	2011	33.06	4.32	0.76
Pakistan	Islamabad	Pak I10	2010	29.83	3.09	0.70
Sudan	Wad Madani	Sudan W10	2010	34.78	3.73	0.72
	Mean Yield			**32.91**	**4.58**	

SD, standard deviation, H^2 broad-sense heritability

The environments were divided into two clusters based on Ward's clustering approach for TGW (Table 2). Cluster 1 consisted of environments in India, Nepal and Pakistan, and cluster 2 included environments mainly in Mexico. Ward's clustering of grain yield, plant height and grain number/m^2 indicated three clusters (data not shown). The heritability estimate was 0.80 for the combined analysis. The cluster analysis and heritability estimates did not show a drastic increase in the estimated H^2, indicating BLUEs from the combined analysis are good enough for the GWAS.

Table 2. Combined and cluster based variance components and heritability estimates for TGW measured in the WAMI population under different environments.

Trait	**Env**	σ^2_{Env}	σ^2_G	$\sigma^2_{G \times Env}$	σ^2_e	**Mean**	**CV**	H^2
Cluster 1	7	2.67	10.41	2.88	3.83	34.10	5.74	0.80
Cluster 2	6	9.70	9.60	3.20	7.40	32.20	8.40	0.70
Combined	13	8.56	9.77	3.26	5.51	33.24	7.06	0.80

Env: environments; σ^2**:** variance; σ^2_{Env}**:** genetic variance; $\sigma^2_{G \times Env:}$ genotype by environment variance; $\sigma^2_{e:}$ residual variance; CV: coefficient of variation; H^2: broad-sense heritability.

Marker-trait associations

Association analysis for TGW showed several significant marker-trait associations. For cluster 1, 49 SNPs in 10 regions—2A (130cM), 2B (16cM), 3B (51 and 134cM), 4B (74 to 75cM), 5A (60 and 98cM), 6A (77 to 85cM), 6B (112 to 113cM) and 7B (46 and 55cM)—were associated with TGW with *p*-values lower than 10^{-04}. For cluster 2, 48 SNPs in 11 genomic regions—1B (128cM), 2A (130cM), 3B (51cM, 67 to 69cM,

and 134cM), 4B (95cM, 100 to 103cM), 5A (60 and 98cM), 6A (78 and 85cM), 6B (109 and 113cM), and 7B (46cM)—were significantly associated with TGW. Combined GWA analysis showed the association of 52 SNPs in 12 genomic regions; 2A (130cM), 3B (30, 51 and 134cM), 4A (95 and 100 to 102), 4B (74cM), 5A (60, 66, 98cM), 6A (77 and 85cM), 6B (112 to 113cM), and 7B (46cM).

A comparison of the cluster based GWAS and combined GWAS indicated several genomic regions consistently detected for TGW: 2A (130cM), 3B at 51cM and 134cM, 5A at 60cM and at 98cM, and 6A at 109 to 113cM and 77 to 85cM with low *p*-values (**Fig. 1**). The locus on 5A is 8cM away from the *Vrn* locus at 90cM affecting flowering time in the population. The locus on chromosome 6A is a pleotropic loci affecting grain yield, TGW, grain number and plant height (Sukumaran et al., 2015).

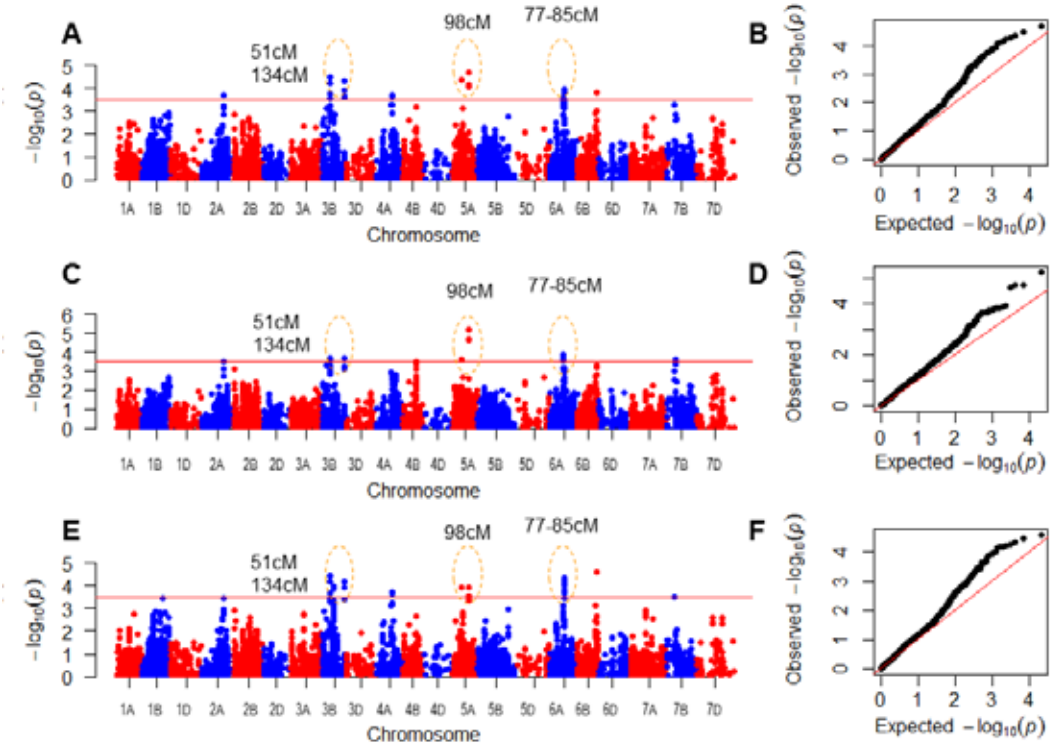

Fig. 1. GWAS results for grain weight based on (A) combined analysis and (C) cluster 1 and (E) cluster 2 based analyses. Q-Q plots for the (B) combined analysis, (D) cluster 1 and (F) cluster 2 are also shown.

Using the marker score of *TaGW2* as a phenotypic score to locate the position of the gene indicated the position as 79cM on chromosome 6A. To determine if marker loci in the region between 79cM and 85cM are segregating, we estimated the linkage disequilibrium between the loci (Fig. 2). High LD in the region indicated that the *TaGW2* gene haplotype is associated with the variation in TGW.

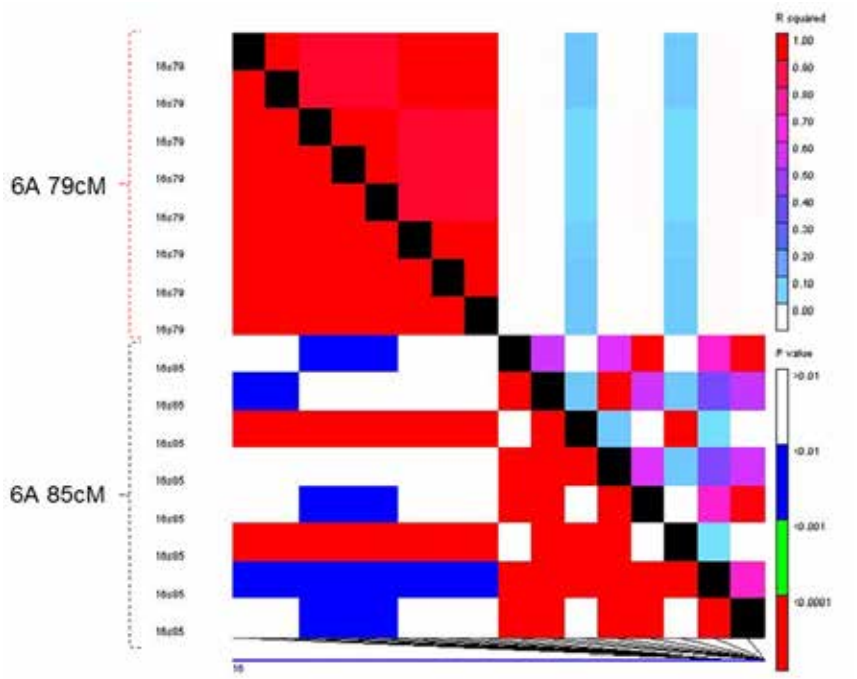

Fig. 2. Linkage disequilibrium on chromosome 6A at 79cM (denoted by 16s79) and 85cM (denoted by16s85).

The effect of the two haplotypes, Hap-6A-A and Hap-6A-A-G, of the *TaGW2* gene was measured and found to be significantly associated with grain yield, TGW, grain number/m^2 and plant height similar to an earlier study (Zhang et al., 2013). Significant differences between the alleles for grain yield and TGW in several environments indicated that this region is a constitutive region affecting yield and yield components (data not shown). Our study agreed with the study on *TaGW2* that concluded that *Hap-6A-G* is the superior allele in CIMMYT germplasm (Zhang et al., 2013). The loci on chromosomes 2A (130cM), 3B at 51cM and 134cM, 5A at 60cM and at 98cM, and 6A at 109 to 113cM need to be further explored.

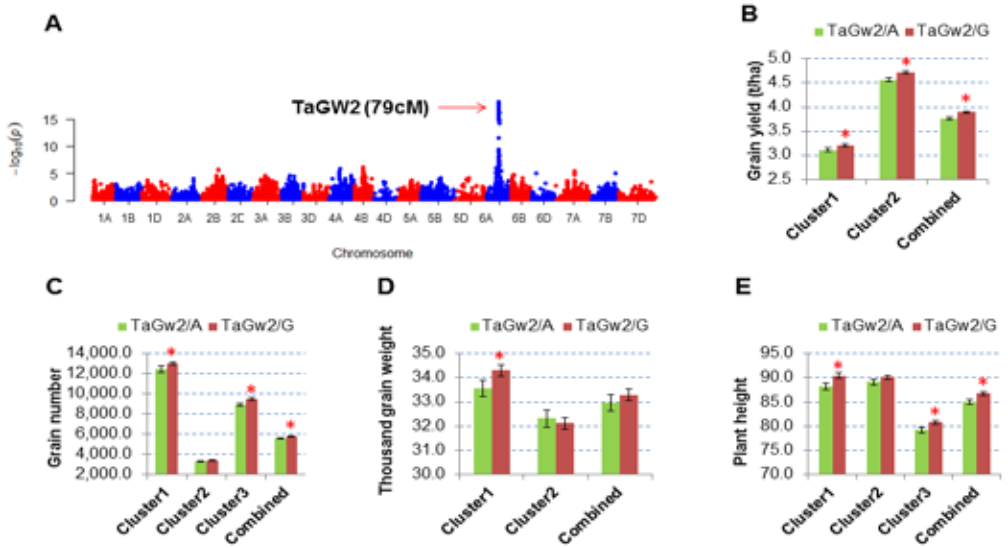

Fig. 3. Location of the *TaGW2* gene on (A) chromosome 6A and the effect of the *TaGW2* gene on the measured traits: (B) grain yield (C) grain number m^{-2}, (D) thousand grain weight and (E) plant height. Error bars indicate the standard error and * denotes the significance of means at $\alpha = 0.05$ in the t-test.

Conclusions

Genome-wide association analyses identified several key genomic regions associated with grain weight in spring wheat in addition to the genomic region harboring gene *TaGW2* on chromosome 6A. The *TaGW2* gene haplotype *Hap-6A-G* showed a positive effect on thousand grain weight, confirming previous reports.

Acknowledgments

We are grateful to the staff at the research stations for their help in collecting data and managing the trials. Financial support from ARCADIA Biosciences, International Wheat Yield Partnership (IWYP), USAID, and SAGARPA is acknowledged.

References

Ain, Q.-U., A. Rasheed, A. Anwar, T. Mahmood, M. Imtiaz, X. Xia, Z. He, and U.M. Quraishi. 2015. Genome-wide association for grain yield under rainfed conditions in historical wheat cultivars from Pakistan. Front. Plant Sci. 6(September): 743Available at http://www.pubmedcentral.nih.gov/articlerender.fcgi?artid=4585131&tool=pmcentrez&rendertype=abstract.

Bradbury, P.J., Z. Zhang, D.E. Kroon, T.M. Casstevens, Y. Ramdoss, and E.S. Buckler. 2007. TASSEL: software for association mapping of complex traits in diverse samples. Bioinformatics 23(19): 2633–2635Available at http://www.ncbi.nlm.nih.gov/pubmed/17586829 (verified 12 July 2014).

Falush, D., M. Stephens, and J.K. Pritchard. 2003. Inference of population structure using multilocus genotype data: linked loci and correlated allele frequencies. Genetics 164: 1567–1587.

Falush, D., M. Stephens, and J.K. Pritchard. 2007. Inference of population structure using multilocus genotype data: Dominant markers and null alleles. Mol. Ecol. Notes 7(4): 574–578.

Griffiths, S., L. Wingen, J. Pietragalla, G. Garcia, A. Hasan, D. Miralles, D.F. Calderini, J.B. Ankleshwaria, M.L. Waite, J. Simmonds, J. Snape, and M. Reynolds. 2015. Genetic dissection of grain size and grain number trade-offs in CIMMYT wheat germplasm. PLoS One 10(3): 1–18.

Hardy, O.J., and X. Vekemans. 2002. SPAGeDI: A versatile computer program to analyse spatial genetic structure at the individual or population levels. Mol. Ecol. Notes 2: 618–620Available at http://www.scopus.com/inward/record.url?eid=2-s2.0-0036899010&partnerID=40&md5=ede1e77221338ab9c2b8a5248b59a307.

Lopes, M.S., S. Dreisigacker, R.J. Peña, S. Sukumaran, and Ma.P. Reynolds. 2015. Genetic characterization of the wheat association mapping initiative (WAMI) panel for dissection of complex traits in spring wheat. Theor. Appl. Genet. 128(3): 453–464Available at http://link.springer.com/article/10.1007/s00122-014-2444-2.

Lopes, M.S., M.P. Reynolds, M.R. Jalal-Kamali, M. Moussa, Y. Feltaous, I.S.A. Tahir, N. Barma, M. Vargas, Y. Mannes, and M. Baum. 2012. The yield correlations of selectable physiological traits in a population of advanced spring wheat lines grown in warm and drought environments. F. Crop. Res. 128: 129–136.

Pritchard, J.K., M. Stephens, and P. Donnelly. 2000. Inference of population structure using multilocus genotype data. Genetics 155: 945–959.

Qin, L., C. Hao, J. Hou, Y. Wang, T. Li, L. Wang, Z. Ma, and X. Zhang. 2014. Homoeologous haplotypes, expression, genetic effects and geographic distribution of the wheat yield gene TaGW2. BMC Plant Biol. 14(1): 107Available at http://www.ncbi.nlm.nih.gov/pubmed/24766773.

Simmonds, J., P. Scott, M. Leverington-Waite, A.S. Turner, J. Brinton, V. Korzun, J. Snape, and C. Uauy. 2014. Identification and independent validation of a stable yield and thousand grain weight QTL on chromosome 6A of hexaploid wheat (Triticum aestivum L.). BMC Plant Biol. 14: 191Available at

http://www.pubmedcentral.nih.gov/articlerender.fcgi?artid=4105860&tool=pmcentrez&rendertype=abstract.

Su, Z., C. Hao, L. Wang, Y. Dong, and X. Zhang. 2011. Identification and development of a functional marker of TaGW2 associated with grain weight in bread wheat (Triticum aestivum L.). Theor. Appl. Genet. 122(1): 211–223.

Sukumaran, S., J. Crossa, D. Jarquin, M. Lopes, and M.P. Reynolds. 2017. Genomic Prediction with Pedigree and Genotype 3 Environment Interaction in Spring Wheat Grown in. G3 Genes, Genomes, Genet. 7(February).

Sukumaran, S., S. Dreisigacker, M. Lopes, P. Chavez, and M.P. Reynolds. 2015. Genome-wide association study for grain yield and related traits in an elite spring wheat population grown in temperate irrigated environments. Theor. Appl. Genet. 128(2): 353–363Available at http://link.springer.com/article/10.1007%2Fs00122-014-2435-3 (verified 18 February 2015).

Sukumaran, S., M.S. Lopes, S. Dreisigacker, L.E. Dixon, M. Zikhali, S. Griffiths, B. Zheng, S. Chapman, and M.P. Reynolds. 2016. Identification of earliness per se flowering time locus in spring wheat through a genome-wide association study. Crop Sci. 56(6): 2962–2972.

Vargas, M., E. Combs, G. Alvarado, G. Atlin, K. Mathews, and J. Crossa. 2013. Meta: A suite of sas programs to analyze multienvironment breeding trials. Agron. J. 105(1): 11–19.

Ward, J.H. 1963. Hierarchical grouping to optimize an objective function. J. Am. Stat. Assoc. 58(301): 236–244.

Yu, J., G. Pressoir, W.H. Briggs, I. Vroh Bi, M. Yamasaki, J.F. Doebley, M.D. McMullen, B.S. Gaut, D.M. Nielsen, J.B. Holland, S. Kresovich, and E.S. Buckler. 2006. A unified mixed-model method for association mapping that accounts for multiple levels of relatedness. Nat. Genet. 38: 203–208.

Zanke, C.D., J. Ling, J. Plieske, S. Kollers, E. Ebmeyer, V. Korzun, O. Argillier, G. Stiewe, M. Hinze, F. Neumann, A. Eichhorn, A. Polley, C. Jaenecke, M.W. Ganal, and M.S. Röder. 2015. Analysis of main effect QTL for thousand grain weight in European winter wheat (Triticum aestivum L.) by genome-wide association mapping. Front. Plant Sci. 6(September): 1–14Available at http://journal.frontiersin.org/article/10.3389/fpls.2015.00644.

Zhang, X., J. Chen, C. Shi, J. Chen, F. Zheng, and J. Tian. 2013. Function of TaGW2-6A and its effect on grain weight in wheat (Triticum aestivum L.). Euphytica 192(3): 347–357.

Zhu, C., and J. Yu. 2009. Nonmetric multidimensional scaling corrects for population structure in association mapping with different sample types. Genetics 182(3): 875–888.

Genetic characterization of the International Wheat Yield Partnership-Hub (IWYP-HUB) association mapping populations

Sivakumar Sukumaran[1], Ryan Joynson[2], Laura-Jayne Gardiner[2], Anthony Hall[2], Carolina Sansaloni[3], Gemma Molero[1] and Matthew Reynolds[1]
[1] CIMMYT, Mexico; [2] Earlham Institute, UK; [3] Genetic Resources Program, CIMMYT

Abstract
A total of 905 accessions including synthetics, durums, landraces, elite lines, and gene bank accessions formed into different panels—high biomass association mapping panel (*HiBAP*), bread wheat diversity (*BWDiv*) panel, synthetic panel (*SynPan*), and durum wheat panel—were screened using single nucleotide polymorphism (SNP) markers. These populations were grown at the IWYP-HUB in Cd. Obregon, NW Mexico, for physiological and agronomic characterization. Except for the durum panel, which was genotyped using the DArTseq™ genotyping method, all other populations were genotyped by 35K SNP array. The genetic diversity and population structure of each population were analyzed individually which indicated genetic diversity and subgroups within the population. The *HiBAP* and *BWDiv* panels were divided into subgroups based on the genome of *Weebil 1*, a line highly used in the pre-breeding program at CIMMYT. The synthetic panel was sub-grouped into three groups but the grouping was not based on geographical origin of the *Ae. squarrosa* accessions nor on the most frequent durum parent. The durum panel was grouped into five subpopulations based on the pedigree of the lines.

Introduction
The basis of plant breeding is the creation of genetic variation and selection of useful variation for future generations (Bernardo, 2008). The variation can be created by crossing, mutation, and introducing exotic chromatin, or it may be present as native trait variation due to historical recombination of the alleles. In spring wheat, landraces, wild relatives, and gene banks are sources of natural variation. CIMMYT's Wheat Physiology has screened about 60,000 accessions from the gene bank and created association mapping panels for the physiological and genetic dissection of complex traits. The most common method is genome-wide association mapping (GWAS). Genome-wide association mapping is the state-of-the-art method for dissecting the genetic basis of complex traits in plants. This approach has higher resolution and faster development time when compared to the bi-parental mapping population (Zhu et al., 2008). But the limiting factor is population structure and familial relatedness, which can confound gene/QTL discovery. To account for population structure, statistical methods, mixed linear models (Yu et al., 2006) and phenology controlled populations (Seri/Babax and wheat association mapping initiative [WAMI] population) were developed at CIMMYT (Pinto et al., 2010; Lopes et al., 2015). Here we analyze the association mapping panels developed for IWYP research (*HiBAP*, *BWDiv*, *SynPan*, and durum panels) and describe their population structure.

Materials and Methods

Genetic material

- ***High Biomass Association Mapping Panel (HiBAP, 150 lines).*** Systematic screening of genetic resources from the World Wheat Collection identified genotypes with favorable biomass expression. Approximately 150 spring wheat types, including elite high yielding material, pre-breeding lines crossed and selected for high yield and biomass, synthetic-derived lines, and appropriate checks. The material has a restricted range of maturity to avoid confounding effects associated with extreme phenology.
- ***Primary Synthetics Diversity Panel (SynPan, 160 lines).*** CIMMYT has generated 2,000 so-called 'synthetic wheat' genotypes using novel genetic variation in diploid and tetraploid wheat. These primary synthetics can be crossed easily with elite bread wheat lines, and backcross derivatives are already well represented in new high yielding lines distributed by the International Wheat Improvement Network (IWIN). Wheat Physiology recently screened all 2,000 lines under yield potential conditions as well as under heat and drought stress, and a panel of 160 of the best primary synthetics has been assembled.

- ***Wheat diversity panels***. Association panels of selected wheat genetic resources (370 bread wheat; 225 durum wheat) have been assembled from spring wheat sources after screening approximately 60,000 lines for heat and drought adaptation in the Sonoran Desert. They were derived from the following sources:
  - International nurseries. Every year approximately 1,000 new, high yielding, disease resistant wheat lines with appropriate end-use quality are generated by CIMMYT and delivered via IWIN to most public and private wheat improvement programs worldwide, where they are tested at approximately 200 sites annually.
  - Wheats with ancestral chromosomal introductions. Many elite lines already contain alien introgressions from the *Triticeae* tribe that are linked to improved yield potential and disease resistance (Ortiz et al., 2008). CIMMYT's gene bank holds around 500 accessions with specific translocations (e.g., *7Ag.7DL*, *1B.1R*, *Lr34*, *Lr42*), while thousands of elite lines are derived from crosses with synthetic wheat.
  - Landraces. Approximately 15,000 spring wheat landraces from the World Wheat Collection were recently pre-screened under high temperature stress. Several hundred landraces were selected for superior yield and biomass.
  - Focused Identification of Germplasm Strategy (FIGS) is a panel of landraces that were selected because they originated from regions with abiotic stress (Street et al., 2016).

Genotyping the panels

Genomic DNA was extracted from fresh leaves collected from 5-10 individuals using a modified CTAB (cetyltrimethylammonium bromide) method. DNA quality and concentration were determined by electrophoresis in 1% agarose gel. The *HiBAP*, *BWDiv*, and *SynPan* panels were genotyped through 35K SNP array in the UK. SNP loci were anchored to the TGACv1.0 Chinese Spring reference genome through alignment of up- and downstream sequences of each locus with inference from the established genetic map positions. The durum panel was genotyped using DArTseq™ (http://www.diversityarrays.com/dart-application-dartseq) (Sansaloni et al., 2011) by the Genetic Analysis Service for Agriculture (SAGA) at CIMMYT in Mexico.

Population structure analysis

Population structure estimation for the panel of accessions was done using the Bayesian clustering approach implemented in STRUCTURE (Pritchard et al., 2000). In addition, a neighbor-joining tree was constructed based on the genetic distances calculated between pairs of accessions. Cluster analyses and bootstrap resampling (1000 pseudo replicates) were performed. The evolutionary history was inferred using the Neighbor-Joining method (Saitou and Nei, 1987) conducted in MEGA7 (Kumar et al., 2016). Principal component analyses were performed on the data using TASSEL (Bradbury et al., 2007). These analyses were done on combined populations as well as on individual panels.

Results and Discussion

Molecular markers

A total of 905 accessions were analyzed in the study, of which 639 were genotyped through 35K array and 225 were genotyped through DArTseq™. The *BWDiv*, *SynPan*, and *HiBAP* panels had 13,723 polymorphic SNPs with 2% missing data and 13,622 markers had SNP position information on the chromosome. The durum panel had 34,813 SNPs in total, of which 5,366 SNPs were polymorphic after the missing value cut-off of 10% and minor allele frequency of 5%.

Population structure

The combined analysis of the panels showed more than 11 groups, and the different panels were represented within each group (Fig. 1A). Most of the lines from the synthetic panel were separated from the *HiBAP* and *BWDiv* panels. PCA plots indicated three groups for *SynPan*; some of the synthetic lines were genetically close to the *HiBAP* and *BWDiv* lines, indicating the used of synthetic lines in crosses and the presence of synthetic-derived material in the germplasm used (Fig. 1B).

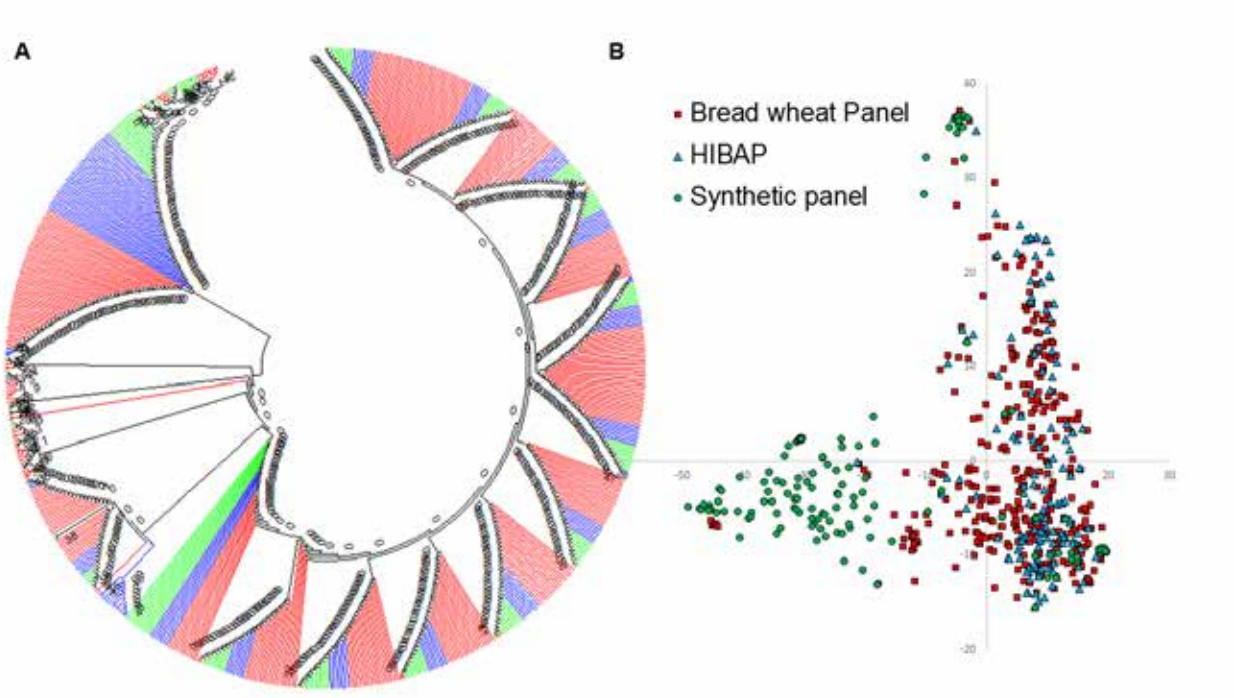

Fig. 1. Population structure of the IWYP-HUB populations (*HiBAP*, *BWDiv*, and *SynPan* panels) in a combined analysis using 13,622 SNPs. Red, blue, and green lines indicate *BWDiv*, *HiBAP*, and *SynPan*, respectively.

The analysis of the *HiBAP* population structure indicated a population structure containing no definite groups; although groups were present, they were genetically close to each other. The separation of the germplasm based on the quadrants of PCA plots indicated mainly four groups, three of which had the Weebil 1 genome and another group had higher amount of synthetic-derived materials with a lower number of lines with Weebil 1 pedigree. Further analysis is needed to show clear grouping patterns, if any. This result indicates the important role that the Weebil line plays in the pre-breeding program. A collection of elite spring wheat lines (WAMI) also showed similar trends (Sukumaran et al., 2015).

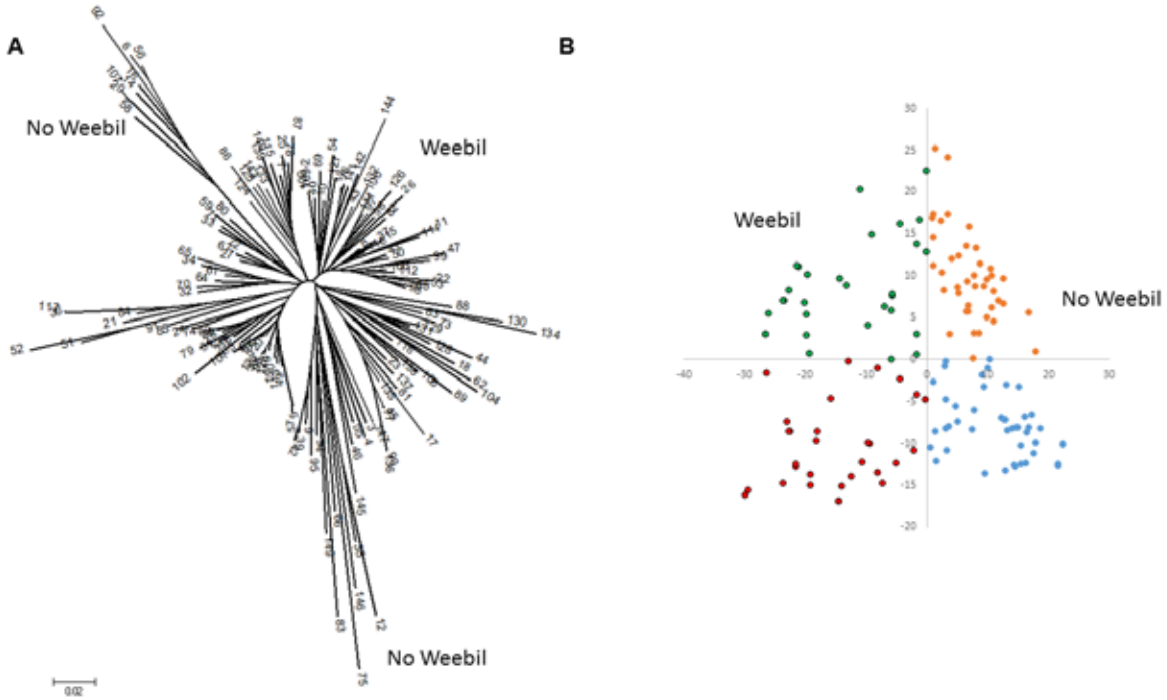

Fig. 2. (A) Genetic diversity and **(B)** population structure of the *HiBAP* panel. The Weebil genome contributes to the population structure of the panel.

For the synthetic panel of 160 lines, the information on the collected site of *Ae. squarrosa* was available. They were mainly from Iran (62), Afghanistan (26), Armenia (3), Azerbaijan (3), Japan (3), Russia (3), China (2), Georgia (2), and Syria (2); there was also one each from Pakistan, Sweden, Turkey, and Uzbekistan. We color coded the NJ tree based on the origin of *Ae. squarrosa* and it did not match the sub-groupings of three in the synthetic panel. However, the PCA analysis and delta K (Evanno et al., 2005) showed three different groupings (Fig. 3B) of the panel. Some of the branches of the NJ tree were clustered and they were based on the durum parents used to create the synthetic wheat. However, the grouping of the panel based on the most common durum parent did not confirm the grouping pattern either.

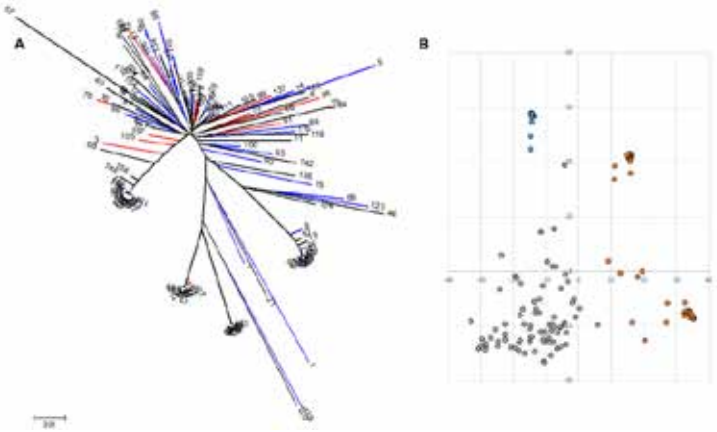

Fig. 3. (A) Genetic diversity and (B) population structure of the synthetic panel. The population was divided into three groups. Geographical origin of the *Ae. squarrosa* genome and durum parent pedigree information did not separate the groups.

Analysis of the bread wheat panel indicated three major groups in the population. Group 1 was comprised of landraces, group 2 had accessions with the Weebil genome, and group 3 had most of the accessions containing the Pastor and/or Sokoll genomes. Sokoll is a synthetic-derived line used as a check in drought

and heat environments. Weebil 1, generated by CIMMYT in northern Mexico, is a non-synthetic wheat with high yield potential and good adaptation to a range of drought stresses. This line was extensively used in CIMMYT's pre-breeding program and a recent study has shown that a major percentage of lines related to CIMMYT's international nursery has Weebil as a parent (Sukumaran et al., 2015). The pedigree of Weebil 1 is Babax/Amadina/Babax. Amadina is a hard spring wheat from CIMMYT that is reported to carry four or five minor genes for leaf rust resistance and has an intermediate level of resistance to stripe rust. Babax is a selection from a Babax cross (BOW/NAC//VEE/3/BJY/COC). Babax is recognized for its drought tolerance and high yield potential (Olivares-Villegas et al., 2007).

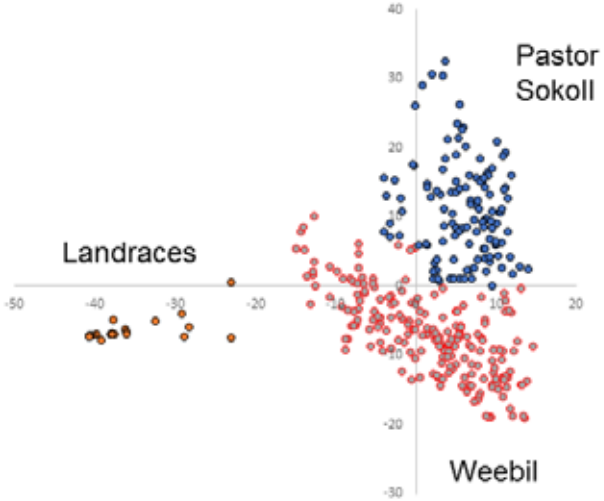

Fig. 4. Population structure of the bread wheat (*BWDiv*) panel. The panel was divided into three groups: (1) landraces; (2) lines with Weebil genome; and (3) lines with the Pastor and/or Sokoll genomes.

The durum wheat panel was formed by screening 60,000 gene bank accessions. The population structure analysis indicated five subgroups based on the delta K values. Among those, three subgroups were genetically closer than two sub-populations (1 and 4). The NJ tree analysis was consistent with the PC analysis and indicated similar patterns. When conducting the association mapping analysis, it is best to avoid distant populations and use the Q matrix to account for population structure (Fig. 5C).

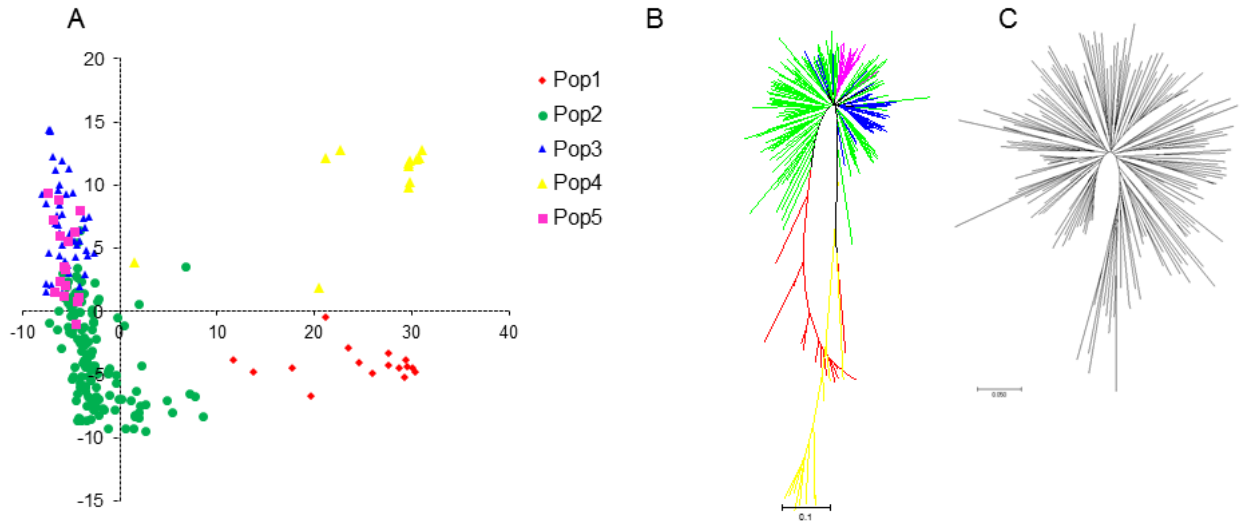

Fig. 5. (A) Genetic diversity and (B) population structure of the durum panel. The population can be divided into five subgroups based on the STRCTURE and delta K methods. An ideal subset of 187 lines for GWAS (C) is indicated after removing the distant clusters.

Conclusions

IWYP-HUB association mapping has good genetic diversity for the dissection of complex traits. These are primarily meant to increase the genetic gains in spring wheat. Genotyping and genetically characterizing these panels are the first steps for using these panels for further yield potential research. Within each population analyzed, there is a population structure that needs to be taken into account for genome-wide association studies. Weebil is the line that appears most frequently in the panels and thus important in accounting for population structure. Both the genotyping by sequencing based SNPs and 35K array based SNPs were efficient in dissecting the population structure of the panels.

Acknowledgments

We acknowledge the staff at the Normal Borlaug Experiment Station at Cd. Obregon, Mexico, for their help in growing the trials. Funding support from the International Wheat Yield Partnership (IWYP) and *Secretaría de Agricultura, Ganadería, Desarrollo Rural, Pesca y Alimentación* (SAGARPA) is acknowledged. DArTseq analysis was supported by the CGIAR research program on WHEAT.

References

Bernardo, R. 2008. Molecular Markers and Selection for Complex Traits in Plants: Learning from the Last 20 Years. Crop Sci. 48(5): 1649Available at https://www.crops.org/publications/cs/abstracts/48/5/1649 (verified 23 February 2017).

Bradbury, P.J., Z. Zhang, D.E. Kroon, T.M. Casstevens, Y. Ramdoss, and E.S. Buckler. 2007. TASSEL: software for association mapping of complex traits in diverse samples. Bioinformatics 23(19): 2633–2635Available at http://www.ncbi.nlm.nih.gov/pubmed/17586829 (verified 12 July 2014).

Evanno, G., S. Regnaut, and J. Goudet. 2005. Detecting the number of clusters of individuals using the software structure: a simulation study. Mol. Ecol. 14(8): 2611–2620Available at http://www.ncbi.nlm.nih.gov/pubmed/15969739 (verified 23 February 2017).

Kumar, S., G. Stecher, and K. Tamura. 2016. MEGA7: Molecular Evolutionary Genetics Analysis Version 7.0 for Bigger Datasets. Mol. Biol. Evol. 33(7): 1870–1874Available at http://www.ncbi.nlm.nih.gov/pubmed/27004904 (verified 23 February 2017).

Lopes, M.S., S. Dreisigacker, R.J. Peña, S. Sukumaran, and Ma.P. Reynolds. 2015. Genetic characterization of the wheat association mapping initiative (WAMI) panel for dissection of complex traits in spring wheat. Theor. Appl. Genet. 128(3): 453–464Available at http://link.springer.com/article/10.1007/s00122-014-2444-2.

Olivares-Villegas, J.J., M.P. Reynolds, and G.K. Mcdonald. 2007. Drought-adaptive attributes in the Seri / Babax hexaploid wheat population. Funct. Plant Biol. 34(3): 189–203Available at http://www.publish.csiro.au/?paper=FP06148.

Ortiz, R., H.-J. Braun, J. Crossa, J.H. Crouch, G. Davenport, J. Dixon, S. Dreisigacker, E. Duveiller, Z. He, J. Huerta, A.K. Joshi, M. Kishii, P. Kosina, Y. Manes, M. Mezzalama, A. Morgounov, J. Murakami, J. Nicol, G. Ortiz Ferrara, J.I. Ortiz-Monasterio, T.S. Payne, R.J. Peña, M.P. Reynolds, K.D. Sayre, R.C. Sharma, R.P. Singh, J. Wang, M. Warburton, H. Wu, and M. Iwanaga. 2008. Wheat genetic resources enhancement by the International Maize and Wheat Improvement Center (CIMMYT). Genet. Resour. Crop Evol. 55(7): 1095–1140Available at http://link.springer.com/10.1007/s10722-008-9372-4 (verified 23 February 2017).

Pinto, R.S., M.P. Reynolds, K.L. Mathews, C.L. McIntyre, J.-J.J. Olivares-Villegas, S.C. Chapman, M. CL, O.-V.J.-J. J, S.C. Chapman, C.L. McIntyre, J.-J.J. Olivares-Villegas, and S.C. Chapman. 2010. Heat and drought adaptive QTL in a wheat population designed to minimize confounding agronomic effects. Theor. Appl. Genet. 121(6): 1001–1021Available at http://dx.doi.org/10.1007/s00122-010-1351-4 (verified 6 March 2013).

Pritchard, J.K., M. Stephens, and P. Donnelly. 2000. Inference of population structure using multilocus genotype data. Genetics 155: 945–959.

Saitou, N., and M. Nei. 1987. The neighbor-joining method: a new method for reconstructing phylogenetic trees. Mol. Biol. Evol. 4: 406–425.

Sansaloni, C., C. Petroli, D. Jaccoud, J. Carling, F. Detering, D. Grattapaglia, and A. Kilian. 2011. Diversity Arrays Technology (DArT) and next-generation sequencing combined: genome-wide, high throughput, highly informative genotyping for molecular breeding of Eucalyptus. BMC Proc. 5(Suppl 7): P54Available at http://bmcproc.biomedcentral.com/articles/10.1186/1753-6561-5-S7-P54 (verified 23 February 2017).

Street, K., A. Bari, M. Mackay, and A. Amri. 2016. How the Focused Identification of Germplasm Strategy (FIGS) is used to mine plant genetic resources collections for adaptive traits. p. 54–63. *In* Enhancing crop genepool use: capturing wild relative and landrace diversity for crop improvement. CABI, Wallingford.

Sukumaran, S., S. Dreisigacker, M. Lopes, P. Chavez, and M.P. Reynolds. 2015. Genome-wide association study for grain yield and related traits in an elite spring wheat population grown in temperate irrigated environments. Theor. Appl. Genet. 128(2): 353–363Available at http://link.springer.com/article/10.1007%2Fs00122-014-2435-3 (verified 18 February 2015).

Yu, J., G. Pressoir, W.H. Briggs, I. Vroh Bi, M. Yamasaki, J.F. Doebley, M.D. McMullen, B.S. Gaut, D.M. Nielsen, J.B. Holland, S. Kresovich, and E.S. Buckler. 2006. A unified mixed-model method for association mapping that accounts for multiple levels of relatedness. Nat. Genet. 38: 203–208.

Zhu, C., M. Gore, E.S. Buckler, and J. Yu. 2008. Status and Prospects of Association Mapping in Plants. Plant Genome J. 1: 5.

Genomics and pedigree-based prediction of grain yield in international environments

Sivakumar Sukumaran[1], Jose Crossa[1], Diego Jarquin[2], Marta Lopes[3], Susanne Dreisigacker[1] and Matthew Reynolds[1]

[1]CIMMYT, Mexico; [2]University of Nebraska, Lincoln, NE, USA; [3]CIMMYT, Turkey

Abstract

Genomic selection (GS) is the new selection tool for plant breeders, especially when the traits are complex and phenotyping is expensive. Our recent studies on developing genomic associated prediction models in wheat based on multi-environmental data have resulted in pedigree-based and genomic-based models that incorporate genotype-by-environment (G×E) interaction terms. However, these models have not yet been widely applied in real breeding programs. Here we report two extensive studies (WAMI phenotyped in 18 environments and International nurseries phenotyped in 136 environments) using pedigree- and marker-based prediction in spring bread wheat and propose using these models in a real breeding program to complement conventional phenotype-based selection.

Introduction

The first to propose predicting breeding values of individual lines for complex traits using genome-wide markers were Meuwissen et al. (2001). This initial study was followed, in plants, by Bernardo and Yu (2007), who demonstrated that whole genome regression predicts complex traits more accurately than using only a few markers. These seminal investigations led to testing of different statistical parametric and non-parametric genomic models with pedigree information in different crops (de los Campos et al., 2009; Crossa et al., 2010; Poland et al., 2012; Jarquín et al., 2014; Pérez-Rodríguez et al., 2015; Saint Pierre et al., 2016). Burgueño et al. (2012) were the first to use marker- and pedigree-based Best Linear Unbiased Predictor (BLUP) models for assessing G×E in genomic prediction that account for correlated environmental structures and thus predict performance of unobserved phenotypes in several environments. Heslot et al. (2015) incorporated crop modelling data for studying genomic G×E and Jarquín et al. (2014) proposed a random effect GBLUP model where the main effect and the G×E interaction effects of markers and environmental covariates are introduced via co-variance structures of markers and environmental co-variables in a reaction norm model. Recently, Saint Pierre et al. (2016) and Jarquin et al. (2014) used the reaction norm model incorporating environmental co-variables to predict the performance of spring bread wheat genotypes in untested environments. Here we report the prediction accuracy of seven models, four of them including G × E interaction terms in two different international trials.

Methods and Statistical Models

Two extensive data sets were used in this study: (1) the Wheat Association Mapping Initiative (WAMI) population grown in 18 international environments (Sukumaran et al., 2015, 2016, 2017); and (2) CIMMYT's wheat international nurseries (Wheat Yield Collaboration Yield Trials [WYCYT] and Stress Adapted Trait Yield Nurseries [SATYN]). The wheat international nurseries were grown altogether in 136 environments. More details about the sites and environments can be found in Sukumaran et al. (2017) and Reynolds et al. (2017). Here we focus on the prediction of grain yield based on genomic and pedigree-based reaction norm models. The WAMI population was genotyped using a 90K SNP array of which 15K SNP data were used for analyses. Only the pedigree-based matrix was used for international nurseries.

The genomic prediction analyses were computed using the BGLR package (de los Campos and Pérez, 2013). All phenotypic data for each environment and trait, as well as the genomic data can be downloaded from the link: http://hdl.handle.net/11529/10714.

Individual environment analyses

Best Linear Unbiased Estimators (BLUEs) were computed using mixed model analysis for each of the traits in each environment. The model used to calculate BLUEs for each environment was

$$y_{jkrm} = \mu + L_j + r_k + b_{m(r)} + e_{ijk}$$

where y_{jrm} is the phenotypic value of grain yield, L_j is a fixed effect of the j^{th} wheat line, r_k is the random effect of the k^{th} replicate assumed independent and identically multivariate normally distributed (IDD) $N(0, \boldsymbol{I}\sigma_r^2)$ (where $\boldsymbol{I}$ is the identity matrix and σ_r^2 the variance between replicates), $b_{m(r)}$ denotes the effect of the m^{th} incomplete block within the r^{th} replicate assumed independent and identically distributed (IDD) with $N(0, \boldsymbol{I}\sigma_{b(r)}^2)$ with $\sigma_{b(r)}^2$ being the variance of the incomplete block within replicate, and e_{jrm} is the random error assumed iid with $N(0, \mathbf{I}\sigma_e^2)$ where σ_e^2 denotes the error variance.

For GS, we used the reaction norm model that is an extension of the random effect Genomic Best Linear Unbiased Predictor (GBLUP) model where the main effect of lines, the main effect of environments, the main effect of markers, the main effect of pedigree, and their interactions with environments are modelled using random covariance structures that are functions of marker or pedigree genotypes and environmental covariates (Jarquín et al., 2014). Brief descriptions of the baseline model as well as the reaction norm models with G×E are given below.

Baseline model

The response of the phenotypes (y_{ij}) random baseline model is described as

$y_{ij} = \mu + E_i + L_j + EL_{ij} + e_{ij}$

where μ is the overall mean, E_i is the random effect of the ith environment, L_j is the random effect of the jth line, EL_{ij} is the interaction between the ith environment and the jth line, and e_{ij} is the random error term. All random effects follow a multivariate normal distribution such that $E_i \overset{iid}{\sim} N(0, \sigma_E^2)$, $L_j \overset{iid}{\sim} N(0, \sigma_L^2)$, $EL_{ij} \overset{iid}{\sim} N(0, \sigma_{EL}^2)$, and $e_{ij} \overset{iid}{\sim} N(0, \sigma_e^2)$.

In the model above, the random effect of the line (L_j) can be replaced by g_j, which is an approximation of the genetic value of the jth line from the genomic relationship matrix. Also the effects of the line (L_j) can be replaced by a_j, which is the additive effect obtained from the pedigree information. Zhang et al. (2014) used extensive maize data with individuals genotyped using highly dimensional dense markers as well as low density markers. In the models described below, we used either g_j or a_j or both g_j and a_j as well as their interactions with environment E_i $(gE_{ij}$, or $aE_{ij})$. Full descriptions of the different reaction norm models can be found, among others, in Jarquin et al. (2014) and Zhang et al. (2015). Below we give a brief description of the different reaction norm models that can be fitted using pedigree and genomic information.

Reaction norm models

We fitted 7 different models (M1-M7) with different components including E=environments, L=line, A=pedigree, G=genomic, AE=pedigree × environment interaction, GE=genomic × environment interaction, and e=residual error.

M1 – Environment and line main effects (Y=E+L+e)

The response of the phenotypes (y_{ij}) from the baseline model but excluding the interaction term, EL_{ij}, is described as

$$y_{ij} = \mu + E_i + L_j + e_{ij} \quad (1)$$

M2 – Environment, line, and pedigree main effects (Y=E+L+A+e)

Adding the random effect that incorporates pedigree information by means of the additive relationship matrix ($\boldsymbol{A}$) to M1 we get model M2 as

$$y_{ij} = \mu + E_i + L_j + a_j + e_{ij} \quad (2)$$

where a_j is a random additive effect of the line, which in this case accounts for pedigree-relationships where $\boldsymbol{a} = (a, \ldots, a_J)'$ contains the pedigree values of all the lines and is assumed to follow a multivariate normal density with zero mean and covariance-matrix $Cov(\boldsymbol{a}) = \boldsymbol{A}\sigma_a^2$, where $\boldsymbol{A}$ is the numerical relationship matrix and σ_a^2 is the additive genetic variance. The random effects $\boldsymbol{a} = (a, \ldots, a_J)'$ are correlated such that model M2 allows borrowing of information across lines based on the numerical relationship matrix ($\boldsymbol{A}$) computed from the pedigree information.

M3 – Environment, line, and genomic main effects (Y=E+L+G+e)
Model M3 is fitted by adding the genomic random effect of the line g_j to M1 which is an approximation of the genetic value of the j^{th} line and is defined by the regression on marker covariates $g_j = \sum_{m=1}^{p} x_{jm} b_m$, where x_{jm} is the genotype of the j^{th} line at the m^{th} marker, and b_m is the effect of the m^{th} marker assuming that $b_m \overset{iid}{\sim} N(0, \sigma_b^2)$ (m=1,…,p) and σ_b^2 is the variance of the marker effects. The vector $\boldsymbol{g} = (g_1, \ldots, g_J)'$ contains the genomic values of all the lines and is assumed to follow a multivariate normal density with zero mean and covariance-matrix $Cov(\boldsymbol{g}) = \boldsymbol{G}\sigma_g^2$, where $\boldsymbol{G}$ is the genomic relationship matrix and $\sigma_g^2 \propto \sigma_b^2$ is the genomic variance. Model M3 is

$$y_{ij} = \mu + E_i + L_j + g_j + e_{ij} \quad (3)$$

with $\boldsymbol{g} \sim N(\boldsymbol{0}, \boldsymbol{G}\sigma_g^2)$. The random effects $\boldsymbol{g} = (g_1, \ldots, g_J)'$ are correlated such that model (3) allows borrowing of information across lines.

M4 - Environment, line, pedigree, and pedigree × environment interaction effects (Y=E+L+A+AE+e)
Adding the interaction between additive relationship matrix and environments (Ea_{ij}) to model M2, model M4 becomes

$$y_{ij} = \mu + E_i + L_j + a_j + Ea_{ij} + e_{ij}, \quad (4)$$

where the term Ea_{ij} is the interaction between the additive value of the i^{th} genotype in the j^{th} environment and $\boldsymbol{Ea} \sim N(\boldsymbol{0}, (\boldsymbol{Z_a G Z_a'}) \circ (\boldsymbol{Z_E Z_E'}) \sigma_{\boldsymbol{Ea}}^2)$. Matrices $\boldsymbol{Z_a}$ and $\boldsymbol{Z_E}$ are the incidence matrices for the effects of the additive genetic values of the genotypes and the environments, respectively, and σ_{Ea}^2 is the variance component of Ea_{ij}.

M5 – Environments, lines, genomic, genomic × environment interaction effect (genomic × environment) (Y=E+L+G+GE+e)
Adding the interaction between markers and environments (Eg_{ij}) to model M3, model M5 becomes

$$y_{ij} = \mu + E_i + L_j + g_j + Eg_{ij} + e_{ij}, \quad (5)$$

where the term Eg_{ij} is the interaction between the genetic value of the i^{th} genotype in the j^{th} environment and then $\boldsymbol{Eg} \sim N(\boldsymbol{0}, (\boldsymbol{Z_g G Z_g'}) \circ (\boldsymbol{Z_E Z_E'}) \sigma_{\boldsymbol{Eg}}^2)$. Matrices $\boldsymbol{Z_g}$ and $\boldsymbol{Z_E}$ are the incidence matrices for the effects of the genetic values of the genotypes and the environments, respectively, and σ_{Eg}^2 is the variance component of Eg_{ij}, and '∘' stands for Hadamart product between two matrices.

M6 – Environment, line, pedigree, and genomic main effects (Y=E+L+A+G+e)
We added to model M1, both the pedigree and genomic effects of the lines (g_j, and a_j), which contain the genomic random vector $\boldsymbol{g} = (g_1, \ldots, g_J)'$ and the pedigree random vector, $\boldsymbol{a} = (a, \ldots, a)'$. Therefore, model M6 is

$$y_{ij} = \mu + E_i + L_j + g_j + a_j + e_{ij}, \quad (6)$$

Model 7 – Environment, line, pedigree, genomic, pedigree × environment interaction and genomic × environment interaction effects (M7=E+L+A+G+AE+GE+e)
Adding to model M6, both the interactions between pedigree and environment (Ea_{ij}), and the interaction between markers (genomic) and environments (Eg_{ij}), then model M7 becomes

$$y_{ij} = \mu + E_i + L_j + g_j + a_j + Eg_{ij} + Ea_{ij} + e_{ij}, \quad (7)$$

All the terms in this model and the following three models were previously defined.

Prediction assessment by cross-validation
Two distinct cross-validation schemes were used. The first cross-validation (CV1) evaluates the prediction ability of models when a set of lines have not been evaluated in any of the environments (Burgueño et al., 2012). The second cross-validation scheme (CV2) evaluates the prediction ability of models when some lines have been evaluated in some environments but not in others.

In both CV1 and CV2, a five-fold cross-validation scheme was used to generate the training (TRN) and testing (TST) sets and assess the prediction ability for each testing set. The data were randomly divided into five subsets, with 80% of the lines assigned to the training set and 20% assigned to the testing set. Four

subsets were combined to form the training set, and the remaining subset was used as the validation set. Permutation of five subsets led to five possible training and validation data sets. This procedure was repeated 20 times, and a total of 100 runs were performed in each population for each trait-environment combination.

Results and Discussion

WAMI trials

The grain yield data ranged from 2.2 t/ha in Bangladesh Joydebpur to 7.0 t/ha in Mexico under irrigated conditions (Table 1). High G×E was observed in the data.

Table 1. Descriptive statistics of the wheat association mapping initiative (WAMI) panel grown in several international environments.

Country	Location	Abbreviation	Grain yield (t/ha)
Bangladesh	Joydebpur	BGLD J10	2.2±0.3
		BGLD J11	3.4±0.5
India	Delhi	India D10	3.8±0.6
	Dharwad	India H10	3.1±0.4
	Indore	India I11	5.7±0.9
	Karnal	India K10	4.2±0.7
	Ludhiana	India L11	4.3±0.7
	Varanasi	India V10	3.2±0.6
Mexico	Drought*	Mex D10	3.7±0.4
	Heat*	Mex H10	4.0±0.4
	Heat drought*	Mex HD10	3.4±0.4
	Irrigated*	Mex I10	7.0±0.3
Nepal	Bhairahawa	Nepal B10	2.7±0.5
		Nepal B11	2.5±0.5
Pakistan	Islamabad	Pak I10	3.2±0.9
		Pak I11	6.9±2.0
Iran	Darab	Iran D10	5.3±0.9
Sudan	Wad Medani	Sudan W10	2.9±0.4

*Campo Experimental Norman E. Borlaug (CENEB), México, different environments.

Among the seven models used, the models incorporating the G×E term, models 6 and 7, were the best models in both CV1 and CV2 scenarios (Fig. 1). The prediction accuracy for grain yield in the CV1 scenario ranged from 0 to 0.6 and in the CV2 scenario ranged from 0.1 to 0.5. The mean prediction accuracy in the CV2 scenario was almost constant for different models but varied across environments. There was high genetic correlations between the Mexican environments and environments in South Asia (data not shown).

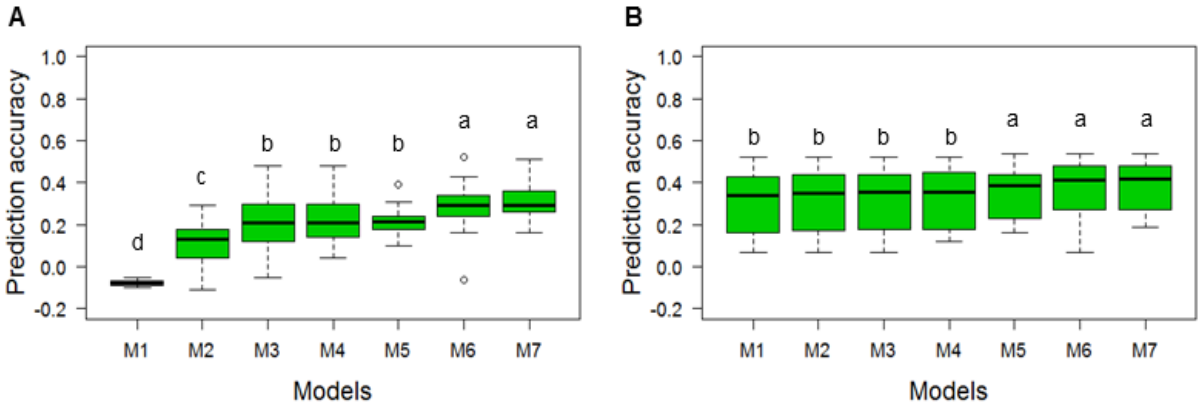

Fig. 1. Comparison of boxplot distributions of prediction accuracy (correlations) for each model (M1-M7) for trait grain yield using two prediction cross-validation scenarios: (**A**) CV1 and (**B**) CV2 for grain yield (GY). Different letters denote significant differences among groups (post hoc non-parametric Tukey's test, p <0.05). Models: M1 Y=E+L+e; M2 Y= E+L+A+e; M3 Y= E+L+G+e; M4 Y= E+L+A+AE+e; M5 Y= E+L+G+GE+e; M6 Y= E+L+G+A+e; M7 Y= E+L+G+A+GE+AE+e. G denotes the matrix from the marker data.

A comparison of the heritability values for grain yield in each environment with the prediction accuracy of the best and worst model indicated the best model's prediction accuracy was associated with heritability estimates, but not linearly (Fig. 2).

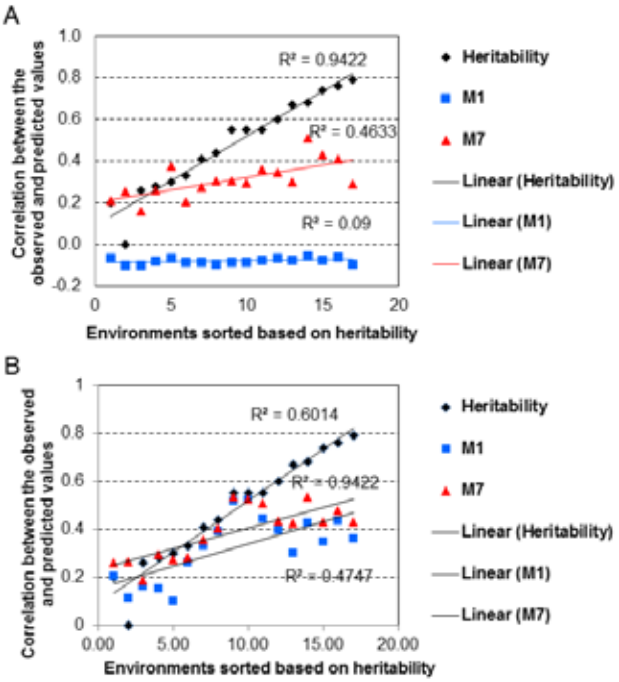

Fig. 2. Comparison between heritability values and the correlations between observed and predicted values for the best and worst models in predicting trait grain yield (GY) in different environments for two cross-validation scenarios: (**A**) CV1 (the best and worst models were M7 and M1, respectively) and (**B**) CV2 (the best and worst models were M7 and M1, respectively).

WYCYT and SATYN international nurseries

These analyses focused on 109 wheat lines from three Wheat Yield Collaboration Yield Trials (WYCYT) and 168 lines from four SATYN trials developed by CIMMYT and grown in a combination of 136

environments altogether. Among the trials, 2SATYN had the highest prediction accuracies, and the lowest prediction accuracy was observed for 1 SATYN. This variation is, among other causes, due to significant genotypic differences, large environmental differences, and large G×E. In these nurseries prediction accuracy was estimated only in the CV2 scenario and models 3, 6, and 7 had the highest prediction accuracy.

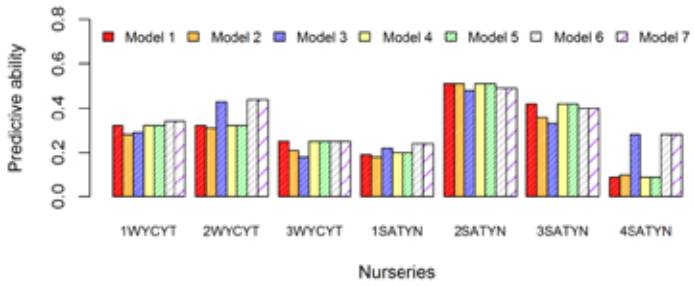

Fig. 3. Comparison of seven different pedigree-based prediction models (model 1 = E+L+e, model 2 = E+A+e, model 3= E+A+AE+e, model 4= E+L+A+e, model 5= E+L+A+LE+e, model 6 = E+L+A+AE+e, and model 7 = E+L+A+LE+AE+e) in seven international nursery data sets (1 to 3 wheat yield collaboration yield trials [WYCYT] and 1 to 4 stress adapted trait yield nurseries [SATYNs]).

Use of genomic prediction in a real breeding program

In normal genomic prediction, random cross-validation in the CV1 scenario uses 80% of the data to predict 20% of the data to develop the GS models and estimate its prediction accuracy. In CIMMYT's pre-breeding program, lines are routinely selected and distributed to national and international partners through the International Wheat Improvement Network based on phenotypic selection. Having developed GS models and tested them on diverse germplasm in multi-environmental trials, it will be worthwhile to pursue and apply them in a real breeding program.

One way to do this is to predict lines in a sparse testing scheme where markers are used to predict the breeding values of lines not evaluated in all the environments. This scenario (CV2) has shown high prediction accuracy in the present study of WYCYTs and SATYNs. An alternate way depends on rapid cycle breeding (3 to 4 generations per year), where multiple generations are advanced in the greenhouse and selections are done based on molecular marker-based predictions. The predictions are based entirely on molecular markers; this will avoid the field evaluation of progeny and therefore decrease the selection interval cycle. A third way is to complement phenotypic selection with GS and pedigree-based selection when screening and selecting $F_{4:5}$, F_6 and candidate lines for international trials. Since this includes phenotype selection and genomic selection, it is expected to exhibit the highest prediction accuracy and higher genetic gains. This will increase the selection intensity of breeding populations and will deliver higher genetic gains in spring wheat, as proposed in the diagram (Fig. 4).

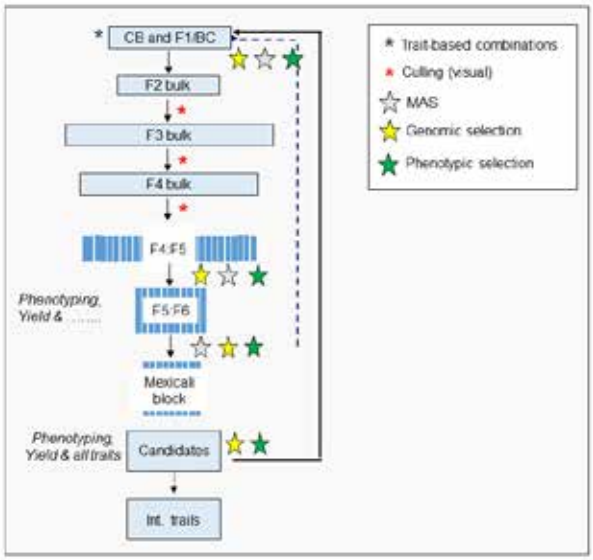

Fig. 4. Schematic diagram of physiological pre-breeding and proposed incorporation of genomic and pedigree-based selection.

Conclusions

Incorporation of G × E terms in prediction models of GS and pedigree-based selection can help to achieve better prediction accuracies and accelerate the breeding cycles for complex traits such as grain yield in multi-environmental trials. Traditionally breeders have depended on phenotypic selection for generation advancement. The present results show that the GS is a complementary method to phenotypic selection with medium to high prediction ability values. Genomic prediction ability of grain yield in spring wheat lines evaluated in a large number of diverse international environments indicated that sites in Mexico and India could be considered key sites for genomic-assisted breeding.

Acknowledgments

The authors acknowledge the financial support from International Wheat Yield Partnership (IWYP), Mexico's Secretariat of Agriculture, Livestock, Rural Development, Fisheries and Food (SAGARPA), and ARCADIA Biosciences. We also would like to acknowledge the staff at research stations where the field experiments were conducted.

References

Bernardo, R., and J. Yu. 2007. Prospects for genomewide selection for quantitative traits in maize. Crop Sci. 47(3): 1082–1090.

Burgueño, J., G. de los Campos, K. Weigel, and J. Crossa. 2012. Genomic prediction of breeding values when modeling genotype × environment interaction using pedigree and dense molecular markers. Crop Sci. 52(2): 707–719.

Crossa, J., G.D.L. Campos, P. Pérez, D. Gianola, J. Burgueño, J.L. Araus, D. Makumbi, R.P. Singh, S. Dreisigacker, J. Yan, V. Arief, M. Banziger, and H.-J. Braun. 2010. Prediction of Genetic Values of Quantitative Traits in Plant Breeding Using Pedigree and Molecular Markers. Genet. Soc. Am. 186(2): 713–724Available at http://www.pubmedcentral.nih.gov/articlerender.fcgi?artid=2954475&tool=pmcentrez&rendertype=abstract (verified 30 July 2013).

Heslot, N., J.-L. Jannink, and M.E. Sorrells. 2015. Perspectives for Genomic Selection Applications and Research in Plants. Crop Sci. 55(february): 1–12Available at https://dl.sciencesocieties.org/publications/cs/abstracts/55/1/1.

Jarquín, D., J. Crossa, X. Lacaze, P. Du Cheyron, J. Daucourt, J. Lorgeou, F. Piraux, L. Guerreiro, P. Pérez, M. Calus, J. Burgueño, and G. de los Campos. 2014. A reaction norm model for genomic selection using high-dimensional genomic and environmental data. Theor. Appl. Genet. 127(3): 595–607.

de los Campos, G., D. Gianola, and G.J.. Rosa. 2009. Reproducing kernel Hilbert spaces regression: a general framework for genetic evaluation. J. Anim. Sci. 87(6): 1883.

de los Campos, G., and P. Pérez. 2013. BGLR=Bayesian Generalized Linear Regression. R Package.

Meuwissen, T.H.E., B.J. Hayes, and M.E. Goddard. 2001. Prediction of Total Genetic Value Using Genome-Wide Dense Marker Maps. Genetics 157: 1819–1829.

Pérez-Rodríguez, P., J. Crossa, K. Bondalapati, G. De Meyer, F. Pita, and G. De Los Campos. 2015. A pedigree-based reaction norm model for prediction of cotton yield in multienvironment trials. Crop Sci. 55(3): 1143–1151.

Saint Pierre, C., J. Burgueño, J. Crossa, G. Fuentes Dávila, P. Figueroa López, E. Solís Moya, J. Ireta Moreno, V.M. Hernández Muela, V.M. Zamora Villa, P. Vikram, K. Mathews, C. Sansaloni, D. Sehgal, D. Jarquin, P. Wenzl, and S. Singh. 2016. Genomic prediction models for grain yield of spring bread wheat in diverse agro-ecological zones. Sci. Rep. 6: 27312Available at http://www.nature.com/articles/srep27312.

Poland, J., J. Endelman, J. Dawson, J. Rutkoski, S.Y. Wu, Y. Manes, S. Dreisigacker, J. Crossa, H. Sanchez-Villeda, M. Sorrells, J.-L.L. Jannink, H. Sánchez-Villeda, M. Sorrells, J.-L.L. Jannink, H. Sanchez-Villeda, M. Sorrells, J.-L.L. Jannink, H. Sánchez-Villeda, M. Sorrells, and J.-L.L. Jannink. 2012. Genomic Selection in Wheat Breeding using Genotyping-by-Sequencing. Plant Genome J. 5(3): 103Available at https://www.crops.org/publications/tpg/abstracts/5/3/103 (verified 4 March 2013).

Reynolds, MP. et al. 2017. Strategic crossing of biomass and harvest index -source and sink- achieves genetic yield gains in wheat (Submitted to Euphytica)

Sukumaran, S., J. Crossa, D. Jarquin, M. Lopes, and M.P. Reynolds. 2017. Genomic Prediction with Pedigree and Genotype 3 Environment Interaction in Spring Wheat Grown in. G3 Genes, Genomes, Genet. 7(February).

Sukumaran, S., M.S. Lopes, S. Dreisigacker, L.E. Dixon, M. Zikhali, S. Griffiths, B. Zheng, S. Chapman, and M.P. Reynolds. 2016. Identification of earliness per se flowering time locus in spring wheat through a genome-wide association study. Crop Sci. 56(6): 2962–2972.

Sukumaran, S., M.P. Reynolds, M.S. Lopes, J. Crossa, and J.C. Sivakumar Sukumaran, Matthew P. Reynolds,* Marta S. Lopes, S. Sukumaran, M.P. Reynolds, M.S. Lopes, and J. Crossa. 2015. Genome-Wide association study for adaptation to agronomic plant density: A component of high yield potential in spring wheat. Crop Sci. 55(6): 2609–2619.

Strategic research for developing improved wheat germplasm for Mexico

Francisco J. Piñera-Chavez[1], Enrique Autrique[1], Jorge L. Valenzuela-Antelo[1], Pawan K. Singh[1], Carlos Guzman[1], Xinyao He[1], Caixia Lan[1], Mandeep S. Randhawa[1], Julio Huerta[2], Ivan Ortiz-Monasterio[1] and Ravi P. Singh[1]

[1] CIMMYT, Mexico; [2] INIFAP, Mexico

Abstract

Current projections of tight global grain markets in the future, environmental risks to expand agricultural land, and falling of relative yield increase rates are worldwide challenges that food security is facing. As a wheat producing country, Mexico is not only facing these challenges but also a great deficit of bread wheat, which makes it necessary to import bread wheat to meet national demand. Thus, strategic research for developing improved wheat germplasm for Mexico will be crucial. The strategic breeding conducted by CIMMYT's Global Wheat Program (GWP) aims to obtain genetic gains through high and stable yields and resistance/tolerance to biotic and abiotic stresses while maintaining wheat quality. This study aimed to develop germplasm through the CIMMYT and Mexican NARS collaboration that can be suitable for national growing areas and end use markets of wheat in Mexico. Activities of this study were conducted during the 2015-2016 winter cycle at Ciudad Obregon and the 2016 summer cycles at Toluca and El Batan. Data were collected on grain and flour quality characteristics and the resistance to leaf (*Puccinia triticina* f. sp. *tritici*), yellow (*Puccinia striiformis* f. sp. *tritici*) and stem (*Puccinia graminis* f. sp. *tritici*) rusts, leaf blotch (*Septoria tritici*) and Fusarium head blight (*Fusarium graminearum*) of 1384 CIMMYT advanced lines was assessed. Another set of 1092 advanced lines (2015 selection) was evaluated for heat, drought and yield potential during 2015-2016. A total of 16 advanced lines with great potential for release were also evaluated in Yaqui Valley production fields. After screening 1384 advanced lines, a total of 1092 advanced lines with resistance or reasonable resistance to these diseases and desirable grain quality were selected in 2016 and included in grain yield trials that are currently being conducted (2016-2017 winter cycle, Ciudad Obregon) and will help to further select the best lines for high and stable grain yield in a number of environments (heat, drought, yield potential). Advanced lines were evaluated during the 2015-2016 winter cycle in Ciudad Obregon under heat, drought and irrigation, and results indicate that the grain yield rankings of the best lines are equal or superior to those of the checks (677 outstanding lines selected for national and international nurseries). Ongoing activities aimed at delivering materials for new variety release are showing promising results, due in part to fundamental collaboration with INIFAP, seed producers and wheat growers.

Introduction

Recently, three key challenges for global food security have been identified: a) projections of tight global grain markets in the future (climate change, rising energy prices, increasing global food, feed and fuel demands and limited land and water); b) environmental risks to expand agricultural land, and c) falling of relative yield increase rates (Fischer et al., 2014). Main crops such as rice, maize and wheat are all facing these challenges. Wheat is the most widely grown crop, with more than 220 million hectares worldwide; it is adapted to a wide range of latitudes, temperatures, and water and nutritional levels (Reynolds et al., 2012) and contributes 19% of the calories consumed by the world population (FAO, 2014). Thus, improving wheat germplasm through strategic breeding to address these global challenges will be paramount. It has been stated that genetic gains in wheat grain yield of 2-3% per year will be required to contribute to global food security under this scenario (Hawkesford et al., 2013). Breeding strategies to increase yield potential (stable yield), protect against biotic and abiotic stresses and increase resource use efficiency while maintaining desirable quality are the key (Hawkesford et al., 2013; Guzman et al. 2016; Crespo-Herrera et al. 2017). As a wheat producing country, Mexico is not only facing these challenges but also a great deficit of bread wheat, which makes it necessary to import bread wheat to meet national demand (UNCTAD, 2013). Mexico ranked in the top 10 wheat importing countries, with bread wheat imports above 4 million tons, while exporting more than 1 million tons of durum wheat (30% of total wheat production) in 2016, due to the surplus in durum wheat production that exceeds the demand of Mexican pasta manufacturers (USDA, 2017; FAO, 2017).

Strategic breeding by CIMMYT's Global Wheat Program (GWP) aims to obtain genetic gains through high and stable yields and resistance/tolerance to biotic and abiotic stresses while maintaining wheat quality. Over the years, the GWP has been able to deliver suitable germplasm to the wheat market in developing

countries (Lantican et al., 2016). This germplasm is usually delivered to national agricultural research systems (NARS) that release it directly as new varieties or use it to improve their own materials (Guzman et al., 2016). Strategic breeding at CIMMYT includes a shuttle breeding method with exchange and selection of segregating populations in contrasting environments, testing of experimental lines in key wheat growing areas and evaluation of germplasm under stressed and optimal conditions (Braun et al., 1996; Crespo-Herrera et al., 2017). The breeding method is based on single-backcross, selected bulk (Singh and Trethowan, 2007). Shuttle breeding includes evaluating spring wheat in environments with low rainfall (irrigated) (mega-environment 1, ME1), high rainfall (mega-environment 2, ME2), and drought (mega-environment 4, ME4) and heat (mega-environment 5, ME5) stresses.

Northwestern Mexico (Sonora, Baja California and Sinaloa) is the main wheat producing area, accounting for 72% of total national wheat production (SIAP, 2015). The Yaqui Valley, Sonora, is an ME1 location where ME4 and ME5 can be simulated easily. Toluca in central Mexico belongs to ME2. Therefore, Mexico is an attractive and versatile country where germplasm can be evaluated in different environments. Additionally, CIMMYT's shuttle breeding recently expanded internationally to include Njoro in Kenya (ME2) (Velu and Singh, 2013). According to Singh and Trethowan (2007), targeted traits in these environments are: high yield potential, lodging tolerance, water and nutrient use efficiency, resistance to leaf (*Puccinia triticina* f. sp. *tritici*), yellow (*Puccinia striiformis* f. sp. *tritici*) and stem (*Puccinia graminis* f. sp. *tritici*) rust for ME1 and ME2 (including stem rust Ug99 resistance at Njoro); leavened and flat bread quality (large white grain) for ME1 and ME4; resistance to leaf blotch (*Septoria tritici*) and Fusarium head blight (*Fusarium graminearum*) and leavened bread quality (large red grain) for ME2; drought tolerance, increased root development, adaptation to conservation agriculture, resistance to rust, leaf blotch, tan spot and root diseases for ME4; and high yield with early maturity, lodging tolerance, heat tolerance, resistance to rust and spot blotch for low rainfall areas; resistance to rust and fusarium head blight for high rainfall areas; and leavened and flat bread or noodle quality (large white or red grain) for ME5.

Through the years, CIMMYT and NARS such as INIFAP have worked to address Mexico's national wheat issues. Recently, these efforts have been also promoted through the MasAgro Initiative (SAGARPA-CIMMYT, 2011) (http://masagro.mx/) and a project named "System of Improvement to Produce Rust Resistant Varieties, High Yield and High Quality for a Sustainable Wheat Production in Mexico" (SAGARPA-CONACYT-CIMMYT-INIFAP-UACh-COLPOS) (Villaseñor-Mir, 2015).

Leaf and yellow rust, Septoria tritici blotch and Fusarium head blight are diseases that can be found in Mexico's wheat producing areas (Gilchrist-Saavedra, 2000; Rodriguez-Contreras et al., 2008; Rodriguez-Garcia et al., 2010; Solis-Moya et al., 2013) which include irrigated and rainfed environments where drought and heat stresses can be found. According to Autrique et al. (2016), a new yellow rust race (MEX03.37;219MEX0) overcame the resistance of varieties released in the last decade (e.g., Nana F2007, Luminaria F2012, Don Carlos M2015, etc.). This is an example that disease resistance can be broken by the adaptation of pathogens causing the disease. If the time of development and disease of new varieties takes at least eight years or longer in Mexico, seems challenging to place successful materials in the wheat growing areas of Mexico. However, thousands of advanced lines are evaluated every year by CIMMYT and Mexican NARS to identify potential lines to be released as suitable varieties for the different wheat growing areas and end use wheat markets of Mexico.

The main objective of this study was to develop germplasm through CIMMYT and Mexican NARS collaboration that are suitable for national wheat growing areas and end use markets in Mexico.

Methods

The breeding process at CIMMYT usually starts when new crosses are made in Ciudad Obregon, Sonora (winter season). After this, the process follows the scheme in Table 1. This method is explained in more detail in Velu and Singh (2013).

This paper describes the activities on advanced lines from years five and six in CIMMYT's breeding scheme (Table 1). A total of 9,506 advanced lines were grown in the 2015-2016 winter cycle at Ciudad Obregon, Sonora, and 1384 advanced lines (candidate lines for international nurseries) were selected based on yield potential compared with checks Reedling#1 and Kachu#1. The selected lines were then screened for leaf rust and Fusarium head blight at El Batan, yellow rust and Septoria tritici blotch at Toluca and stem rust at Njoro during the summer cycle of 2016. Additionally, grain (harvested in Ciudad Obregon) from these lines was used to perform quality analysis at the Quality Laboratory of CIMMYT at El Batan.

During the 2015-2016 winter cycle, 1092 candidate lines were evaluated at Ciudad Obregon under drought (180 and 280 mm of water), yield potential (irrigated) and heat (irrigated) trials. Checks Reedling#1 and Kachu#1 were used in irrigated trials (yield potential) and Reedling#1 and Baj#1 in drought and heat trials. These trials were the sixth year activities of the breeding scheme (Table 1) and helped to understand the yield performance of the candidate lines for international nurseries under yield potential, drought and heat conditions.

Table 1. Breeding scheme at CIMMYT (Velu and Singh, 2013).

Germplasm	Activities	Year
Crossing block	New crosses are made (Ciudad Obregon, Sonora)	1
F_1 (filial breeding generation 1)	Back and top crosses (BC_1 and F_1-Top, respectively) are done on selected F_1 (El Batan, Texcoco)	1
*BC_1, F_1-Top and F_2 (from simple crosses)	Plants from BC_1, F_1-Top and F_2 are selected for agronomic traits and leaf rust resistance and bulk harvested (Ciudad Obregon)	2
F_2 (BC_1, F_1-Top) and F_3 (from F_2 simple)	Plants from F_2 and F_3 are selected for agronomic traits, yellow rust and Septoria tritici blotch resistance and bulk harvested (Toluca, Estado de Mexico)	2
F_3 and F_4	F3 and F4 generations are grown under stem and yellow rust pressure and selected plants are bulk harvested in Njoro, Kenya (off season)	3
F_4 and F_5	F_4 and F_5 are grown again under stem and yellow rust pressures at the same location (main season) where selected resistant plants with short stature are bulk harvested	3
F_5 and F_6	F_5 and F_6 are grown in Ciudad Obregon and individual plants are selected for agronomic traits and resistance to leaf rust	4
Advanced lines	Advanced lines are grown in small plots and the best lines are selected for agronomic traits and resistance to yellow rust, Septoria tritici blotch in Toluca and leaf rust at El Batan. Selected lines are harvested in El Batan and those with plump grains are promoted to yield trials	4
Advanced lines	Advanced lines are grown as replicated trials in Ciudad Obregon and in small plots in Ciudad Obregon, Njoro and Santa Catalina, Ecuador. Lines are phenotyped for leaf (Ciudad Obregon), yellow (Santa Catalina) and stem rust (Njoro) and the best lines are retained	5
International nurseries candidate lines	Candidate lines for international nurseries are multiplied at El Batan an also grown and screened for leaf, yellow and stem rust, Septoria tritici blotch, Fusarium head blight, etc. (El Batan, Toluca and Njoro). Quality analysis is also performed with grain harvested at Ciudad Obregon	5
International nurseries candidate lines	Candidate lines for international nurseries are grown in a second yield trial in five environments at Ciudad Obregon; additionally, multiplication of lines is done in Mexicali, Mexico and phenotyping for stem rust resistance is done at Njoro	6
International nurseries	International yield trials and screening nurseries are prepared and distributed	6

* Lines with plump grains are retained from BC_1, F_1-Top and F_2 (from simple crosses) until F5 and F6.

During the 2016-2017 winter cycle, six trials were conducted in production fields at the Yaqui Valley. Trials under full irrigation and drought were located in blocks B1216, B1607, B1803 and B2212 scattered across the Yaqui Valley grid. Advanced lines evaluated in these trials included bread (8) and durum (8) wheat and local checks (8). The measured traits included grain yield, hectolitric weight, thousand-kernel weight, black point, yellow berry, lodging and grain quality. These trials are part of a multi-year evaluation

conducted by CIMMYT-INIFAP-wheat producers to identify advanced lines with potential to be released as new varieties for Mexico's wheat producing areas.

Evaluation of disease resistance

Evaluation of leaf rust and yellow rust resistance was conducted as follows: lines were planted in double rows 0.7 m long, with 0.3 m spacing between them. A mixture of Avocet+Yr24 and Avocet+Yr26 lines were used as leaf rust spreaders, whereas a mixture of six susceptible wheat lines derived from an Avocet × Attila cross, Morocco and Avocet near-isogeneic lines carrying genes *Yr31* and *Yr17* were used as yellow rust spreaders in field trials. Spreaders were planted around the experimental area and as hill plots in the middle of a 0.3 m pathway on one side of each experimental plot. A mixture of Mexican *P. triticina* races MBJ/SP and MCJ/SP (2-3 mg/ml) suspended in Soltrol® 170 was used to inoculate the leaf rust spreader, whereas a mixture of Mexican *P. striiformis* races (Mex96.11, Mex08.13 and Mex14.191) also suspended in Soltrol® 170 was sprayed onto stripe rust spreaders within and around the experimental areas. Both disease severity and reaction were recorded 2-3 times for each line based on the modified Cobb Scale. In the case of repeated notes, the first reading was recorded when the susceptible parent Avocet displayed approximately 70-80% severity and repeated about a week later when it reached 90-100%.

Evaluation of Fusarium head blight (FHB) resistance was conducted as follows: a mixture of five aggressive *Fusarium graminearum* isolates was inoculated in the field experiments in the FHB nursery (1384 advanced lines). Lines were planted in 1 m plots with double rows. The inoculum at a concentration of 55,000 spores/ml was applied to each line at anthesis stage, and a second inoculation was applied two days later. To enhance FHB disease development, the nursery was misted for 10 minutes each hour from 9 AM to 8 PM, from anthesis until early dough stage, to create humid conditions favorable for disease development. The nursery was also planted in fields where maize-wheat rotation under conservation agriculture practices was adopted to enhance FHB disease development. The total number of infected spikes and spikelets of each spike were counted to calculate the FHB index using the formula FHB index (%) = (Severity x Incidence) / 100, where severity is the average percentage of diseased spikelets and incidence is the percentage of symptomatic spikes.

Evaluation of Septoria tritici blotch (STB) resistance was conducted as follows: lines were sown in 0.75 m double rows and exposed to a mixture of six virulent isolates {St1 (B1), St2 (P8), St5 (OT), St6 (KK), 64 (St 81.1) and 86 (St133.4)} of *S. tritici*. The spore suspension applied was mixed and adjusted to $1x10^7$ spores/mml. The first inoculation was conducted 28 to 30 days after planting and continued every week for a total of three applications. The first measurement of disease severity was done approximately four weeks after the last inoculation by visually scoring each plot using the double-digit scale (00-99), where the first digit (D1) indicates disease progress in canopy height from ground level and the second digit (D2) refers to the severity measured based on diseased leaf area. Both D1 and D2 were scored on a scale of 1-9. Five disease evaluations were recorded during September and August 2016. For each evaluation, percentage disease severity was estimated based on the following formula: % severity = (D1/9) x (D2/9) x 100. The area under the disease progress curve (AUDPC) was subsequently calculated using the formula:

$$AUDPC = \sum_{i=1}^{n} [\{(Yi + Y_{(i+1)}) / 2\} x (t_{(i+1)} - t_i)$$

where Yi = STB severity at the time ti; $t_{(i+1)}$-ti= time interval (days) between two disease scores; and n = number of times STB was recorded.

Quality analysis

Wheat quality improvement is an important breeding aspect that CIMMYT's breeding scheme also takes into account. As shown in Table 1, advanced wheat lines that are candidates for international nurseries are assessed for diverse quality characteristics. In addition to the relevant quality data, wheat breeders receive an end-use quality classification that is intended to help them identify the distribution of wheat end-use quality types (Table 2) within their different breeding populations. Relevant quality data include analyses and traits such as grain image analysis (test weight and thousand-kernel weight), visual grain inspection (color), grain analysis by NIR (hardness, protein and moisture content), milling (flour yield), flour analysis by NIR (protein, ash and moisture content; water absorption for mixograph, alveograph and bread-making), SDS-sedimentation, dough rheology (mixograph for optimum mixing time and torque, and alveograph for

gluten strength and extensibility) and end-use product testing (baking pup loaf for volume and crumb structure) (Peña et al., 1990; American Association of Cereal Chemists, 2010; Guzmán et al., 2015; 2016).

Table 2. Wheat classification according to end-use type and grain protein content (Guzman et al., 2016).

End-use type	Type number*
Hard wheat	
Pan type breads (mechanized baking industry)	1a, 1b
Leavened breads in general (semi mechanized baking industry)	2a
Flat breads such as pocket bread	2a
Dry noodles: alkaline, white-salted, instant	2a
Steamed bread (Northern China style)	2b
Flat breads such as chapatti, roti, and flour tortillas	2b
Dense hearth breads, and some flour tortillas	3a, 3b
Soft wheat	
Steamed bread (Southern China style)	4a
White salted noodles	4a
Pastries, biscuits, cakes, and other steamed breads (Southeast Asia)	4b
Household (utility) use	5

* Based on grain hardness, grain color, dough mixing properties, and gluten strength and extensibility requirements achieved by CIMMYT germplasm under Mexican (Cd Obregon, Sonora, Northwest Mexico) growing conditions with experimental yield level between 6-9 ton/ha.
End-use class number followed by letter "a" has higher protein content than the same followed by the letter "b".
Type 1a should have grain protein above 12.5% (12.5% M. B.).
Types 2a and 3a should have grain protein above 11.5% (12.5% M. B.).
Type 4a should have grain protein above 11.0% (12.5% M. B.).

Results/Discussion

Screening 1384 advanced wheat lines for resistance to leaf and yellow rusts, Septoria tritici blotch and Fusarium head blight

The evaluation of leaf rust has indicated that 79% (1092 lines) of the advanced lines presented less than 5% disease severity, while 19% (266 lines) of the lines presented a disease severity below 20%. Only 1.2% (17 lines) of the lines presented a disease severity between 20 and 40%. A total of nine lines were extremely dry and not assessed (Fig. 1). Yellow rust assessment at El Batan (BV) showed that the infection level was below 5% in about 93% (1280 lines) of the advanced lines evaluated, while 7% showed disease severity between 5 to 20% (97 lines). Only seven advanced lines presented disease severity above 20%. Similarly, infections with Nana and Borlaug rust races indicated that 96% and 84%, respectively, of the lines had less than 5% disease severity (Fig. 2). Reactions to yellow rust were mainly recorded as resistant (R) and moderately resistant (MR).

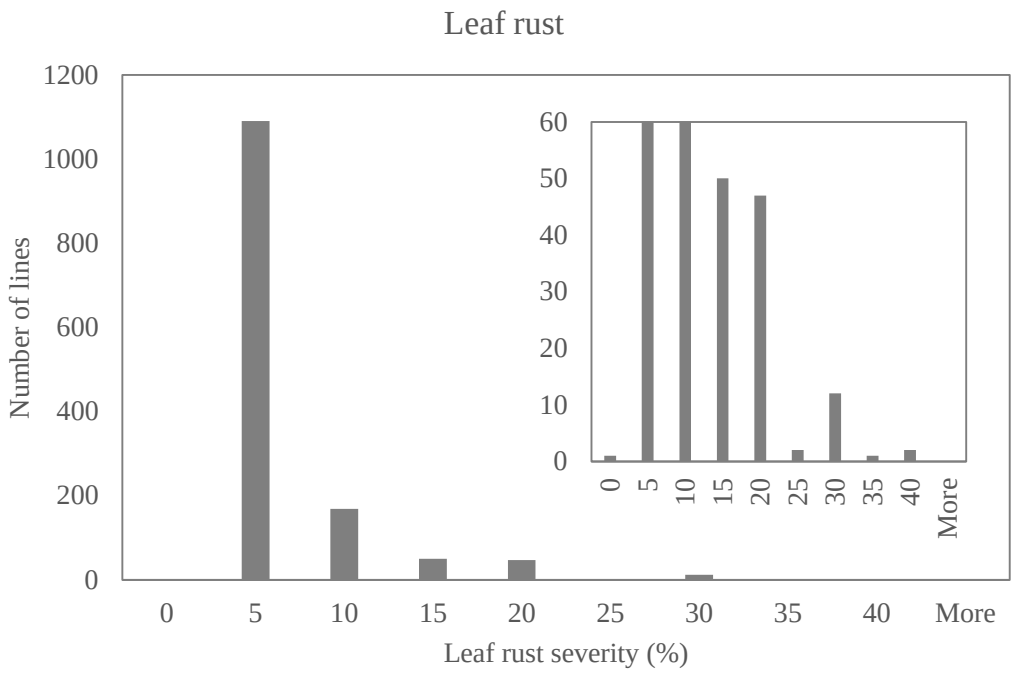

Fig. 1. Frequency distribution of field disease severity data for leaf rust of 1384 advanced lines grown in the 2016 summer cycle at El Batan.

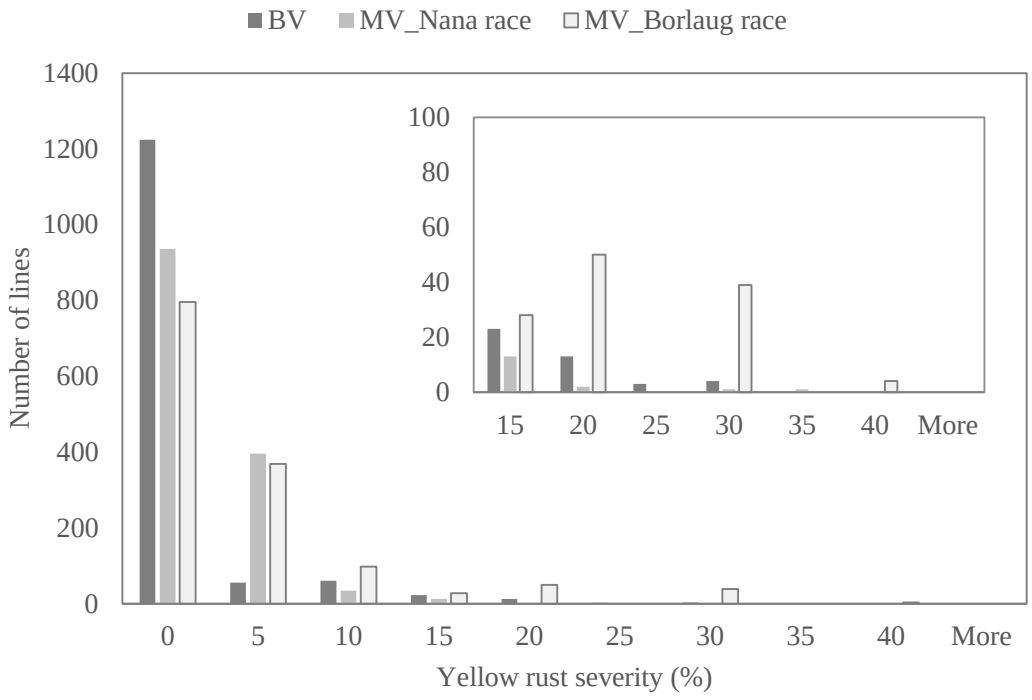

Fig. 2. Frequency distribution of field disease severity data for yellow rust of 1384 advanced lines grown in the 2016 summer cycle at Toluca (MV) and El Batan (BV).

The frequency distribution of the 1384 advanced lines evaluated indicated that most lines (957) were under 800 for the disease AUDPC, which indicates an intermediate to resistant reaction to Septoria tritici blotch infection. A total of 427 (31%) lines showed higher disease development with values above 800 for the disease AUDPC (Fig. 3). Normal values of susceptible checks such as Huirivis should be above 1000, while values of resistant checks such as Murga should be below 400 (Osman et al., 2016). It is important to mention that Septoria tritici blotch affects the grain filling process in high rainfall and rainfed areas, which are environments that are found in Mexico (e.g., Valles Altos, Estado de Mexico, highlands of Jalisco, etc.) (Rodriguez-Contreras et al., 2008).

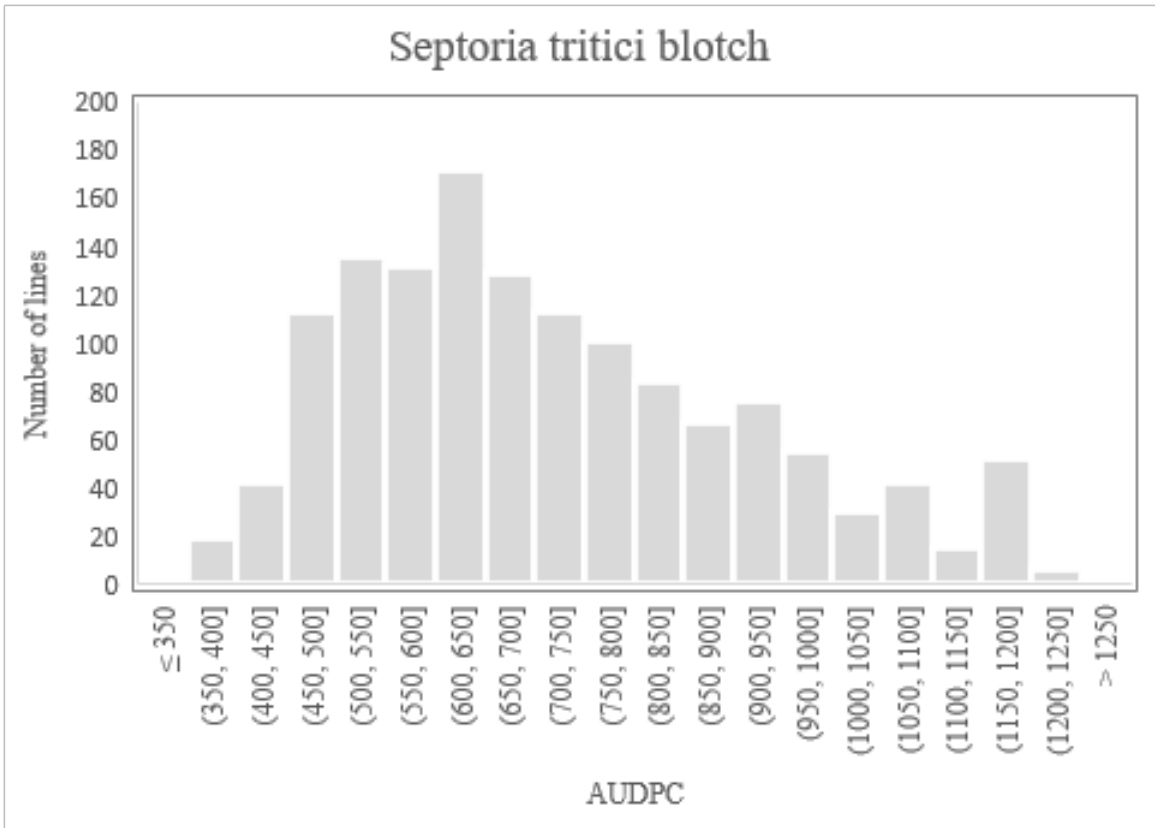

Fig. 3. Frequency distribution of field disease severity data (area under disease progress curve, AUDPC) for Septoria tritici blotch (STB) of 1384 advanced lines grown during the 2016 summer cycle in Toluca.

The frequency distribution of Fusarium head blight infection in the 1384 advanced lines indicated that 32% (444) were resistant (below 5% on the disease index), and 68% (944) were resistant to moderately resistant (between 10 and 35% on the disease index). Performance values of susceptible checks such as Gamenya were above 45% and below 2% for a resistant check such as Sumai#3 (Fig. 4). Fusarium head blight is an important fungal disease that infects wheat spikes and affects grain yield and quality (including mycotoxin contamination) (Osman et al., 2016). This disease can be found in Mexican wheat growing areas (e.g., Valles Altos, Estado de Mexico) and can become a costly issue due to the high demand of fungicides for disease control (Gilchrist-Saavedra, 2000).

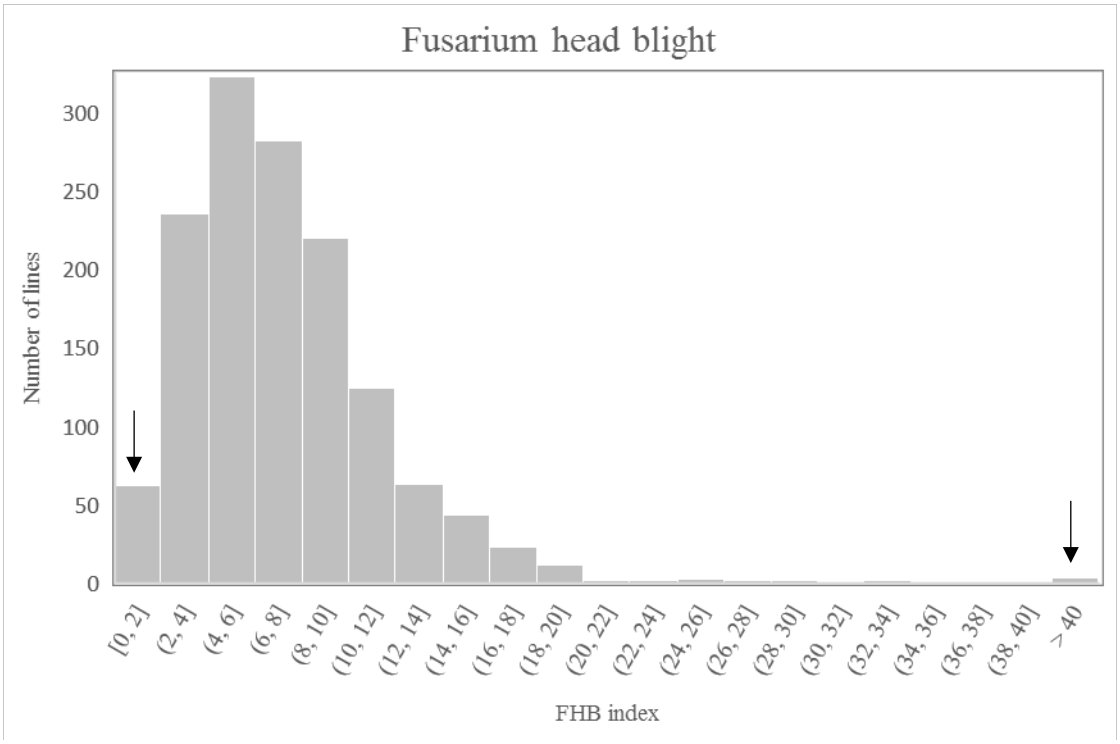

Fig. 4. Frequency distribution of field disease severity data for Fusarium head blight (FHB). Disease scores of resistant (Sumai#3, left arrow) and susceptible (Gamenya, right arrow) checks are indicated.

Screening advanced wheat lines for grain quality

As an integral component of the breeding scheme, grain quality has been an important aspect addressed by the CIMMYT Global Wheat Program over the years (Guzman et al., 2016). These same authors have stated that the CIMMYT's strategy has been to ensure proper gluten quality (diverse levels of gluten strength combined with good extensibility) at medium protein content levels, in semi-hard or hard grains. Under this strategy, every year thousands of advanced experimental lines are analyzed for key aspects. Evaluation of the 1384 advanced lines during 2016 indicated a wide range of end use types of wheat (Fig. 5). Guzman et al. (2016) stated that progress in the quality of CIMMYT germplasm has advanced by decreasing the percentage of end use type 5 genotypes (>50 to <10 from 2005 to 2015). However, during 2016 this percentage was around 29% (400 lines), as indicated in Fig. 5. Nevertheless, sufficient grain quality diversity was found in the advanced lines evaluated, which is desirable in end use types for the Mexican value chain. According to the grain quality assessment, the grain of these lines was found to be hard, soft and soft-hard, and its colour was white, red and red/white with gluten types that are strong, medium strong, weak, tenacious and weak/tenacious. CIMMYT's Wheat Chemistry and Quality Laboratory recommended classifying the advanced lines as follows: best strong and extensible (41 lines), best medium to strong and extensible (146 lines) and fair quality (medium, strong and overly strong) (129 lines) (Table 3).

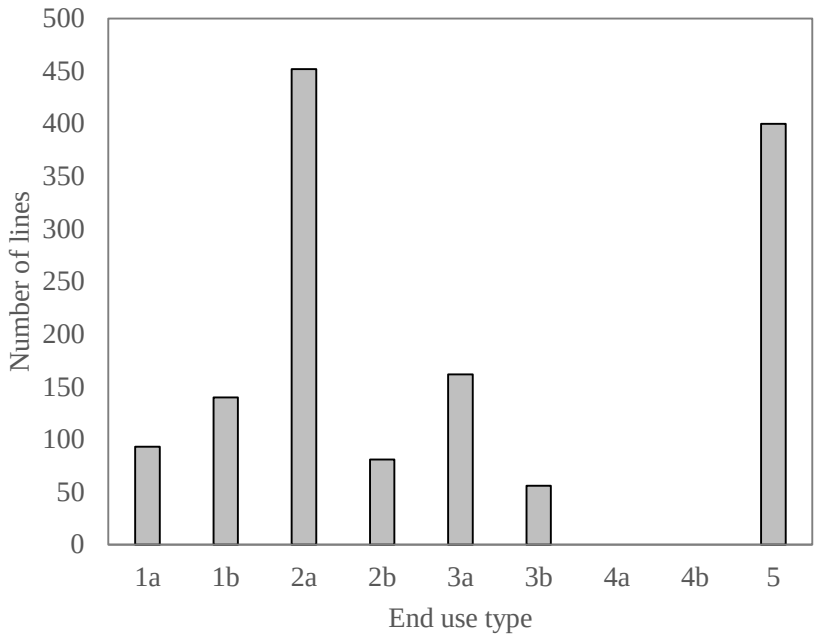

Fig. 5. Frequency distribution of advanced lines for end use types of wheat.

Table 3. Mean values of quality characteristics: best strong and extensible, best medium to strong and extensible, fair quality and rest of the lines.

Parameter	Best strong and extensible	Best medium to strong and extensible	Fair quality	Rest
TESTWT	82.58	82.83	82.83	82.76
TKW	47.06	47.83	48.03	48.25
GRNHRD	43.45	43.33	42.58	42.15
FLRYLD	71.57	72.55	71.84	71.53
GRNPRO	12.57	12.35	12.24	11.99
FLRPRO	10.78	10.62	10.51	10.26
FLRSDS	17.93	16.79	16.57	15.19
MIXTIM	3.500	3.065	3.176	2.987
MP	138.0	119.4	123.8	117.1
ALVW	343.0	262.0	283.6	260.0
ALVPL	0.790	0.730	0.906	1.204
LOFVOL	856.8	838.4	813.9	758.0

TESTWT, test weight (kg hL^{-1}); TKW, thousand-kernel weight (g); GRNHRD, grain hardness (PSI); FLRYLD, flour yield from milling (percentage recovered); GRNPRO, grain protein (based on 12.5% moisture); FLRPRO, flour protein (based on 14% moisture); FLRSDS, flour sodium dodecyl sulfate sedimentation volume (mL); MIXTIM, optimum mix time (min); MP, torque at the integral of the midline peak; ALVW, work value from Alveograph curve (J); ALVPL, Alveograph P (tenacity) divided by L (extensibility) (mm mm^{-1}); LOFVOL, pup loaf volume (cm^3).

Based on the performance of the 1384 advanced lines for disease resistance and quality, a total of 1092 were selected and sown in November-December 2016 for evaluation under drought (180 and 280 mm of water), yield potential (irrigated) and heat (irrigated), during the 2016-2017 winter cycle at Ciudad Obregon.

Evaluation of 1092 advanced wheat lines under yield potential, drought and heat conditions
Evaluation under drought, yield potential and heat conditions is another step in the breeding scheme (as mentioned in the previous section). A set of 1092 lines selected in the 2014-2015 summer cycle (El Batan and Toluca) were evaluated under drought (180 and 280 mm of water), yield potential (irrigated) and heat (irrigated) during the 2015-2016 winter cycle at Ciudad Obregon. Analyses of variance indicated statistically significant genetic differences for grain yield between the genotypes in all five environments (data not shown) with high heritability values (Table 4). Advanced lines were compared to suitable check for each environment (Reedling#1 and Kachu#1 for irrigation (yield potential) and Reedling#1 and Baj#1 for drought and heat). Ranges and ranking of lines indicated that the best lines performed the same as the checks and, in some cases, they were superior (e.g. irrigated/raised beds, 4% more than Reedling#1 and 20% more than Kachu#1).

Table 4. Grain yield of 1092 advanced lines under severe drought, heat and yield potential (irrigated) conditions during 2015-2016 in the Yaqui Valley.

Environment		**Range/Mean**	**CV%**	**LSD $_{(0.05)}$**	**Heritability**
Reduced irrigation (180 mm)	Advanced lines	0.12 - 3.33	10.2	0.33	0.90
(flat basins)	Reedling#1 (check)	2.06			
	Baj#1 (check)	2.14			
Reduced irrigation (280 mm)	Advanced lines	0.94 - 4.47	5.84	0.38	0.75
(raised beds)	Reedling#1 (check)	3.66			
	Baj#1 (check)	3.58			
Irrigated (raised beds)	Advanced lines	5.71 - 8.53	3.43	0.49	0.78
	Reedling#1 (check)	7.94			
	Kachu#1 (check)	7.12			
Irrigated (flat basins)	Advanced lines	4.71 - 8.99	5.36	0.75	0.66
	Reedling#1 (check)	7.94			
	Kachu#1 (check)	6.95			
Irrigated/heat (raised beds)	Advanced lines	1.98 - 5.39	6.95	0.51	0.77
	Reedling#1 (check)	4.16			
	Baj#1 (check)	3.90			

Based on the grain yield performance and comparison of 1092 candidate lines (2015-2016) with checks Reedling#1 and Kachu#1 for irrigated trials (yield potential) and checks Reedling#1 and Baj#1 for drought and heat trials, a total of 677 lines were further selected for international nurseries. The latter were also delivered to INIFAP (Mexican NARS) where they will be further evaluated in Mexican growing environments in 2017.

Evaluation of advanced wheat lines with potential to be released as new varieties in Mexico
Advanced lines that had already been tested in the production fields of the Yaqui Valley in Sonora showed great potential to be released as new varieties in the near future. Statistically significant differences were found for all traits assessed (Table 5). Best checks Cirno C2008 (check for durum wheat lines) and Borlaug 100 F2014 (Reedling#1, check for bread wheat lines) were outstanding and always ranked in the top ten genotypes in all environments. Three durum and one bread wheat lines showed great potential in terms of high yield and stability. However, the assessment of these lines is ongoing and more growing seasons are needed before the best lines can be selected.

These lines were also analysed for grain quality characteristics, as depicted in Table 6. According to the grain quality assessment, the grain of these lines was found to be hard, soft and soft-hard, and its colour was white, red and amber with gluten types such as strong, medium strong, weak, tenacious and weak/tenacious.

Table 5. Mean, range and LSD values for grain yield, black point, yellow berry and lodging index of seven bread wheat and nine durum genotypes grown in the Yaqui Valley under irrigation and drought conditions during 2015-2016 (bread and durum wheat checks included).

Trait	Trial*	Mean	Max	Min	LSD $_{(0.05)}$
Grain yield t/ha (12% moisture)	Irrigated (B1216)	5.97	6.98	4.01	0.98
	Irrigated (B2212)	8.05	9.87	6.21	0.99
	Irrigated (B1803)	6.60	7.78	5.03	1.63
	Irrigated (B1607)	6.67	7.57	6.20	0.78
	Drought (B1216)	6.41	7.36	5.20	1.17
	Drought (B2212)	8.95	10.19	7.78	1.54
Black point (%)	Irrigated (B1216)	7.48	0.33	17.58	4.51
	Irrigated (B2212)	9.22	0.33	35.25	8.11
	Irrigated (B1803)	14.06	4.08	42.33	13.86
	Irrigated (B1607)	5.52	0.17	19.00	5.64
	Drought (B1216)	1.97	0.00	6.92	3.49
	Drought (B2212)	10.48	0.75	22.58	8.60
Yellow berry (%)	Irrigated (B1216)	1.62	0.42	3.17	2.22
	Irrigated (B2212)	23.81	3.58	54.17	24.24
	Irrigated (B1803)	4.83	1.08	11.08	6.36
	Irrigated (B1607)	1.66	0.17	6.42	2.04
	Drought (B1216)	1.17	0.25	5.08	3.21
	Drought (B2212)	11.94	0.17	40.33	14.39
Lodging index (% lodged area x angle/10)	Irrigated (B1216)	-	-	-	-
	Irrigated (B2212)	4.18	0.10	33.83	-
	Irrigated (B1803)	25.94	1.03	50.50	-
	Irrigated (B1607)	0.09	0.00	2.17	-
	Drought (B1216)	-	-	-	-
	Drought (B2212)	6.04	0.47	21.37	-

* Irrigated: five irrigation events; drought: 3 irrigation events.

Table 6. Mean values for quality characteristics of seven bread wheat and nine durum genotypes grown in the Yaqui Valley under irrigation and drought conditions during 2015-2016 (bread and durum wheat checks included).

Parameter*	Wheat type	Irrigated (B1216)	Irrigated (B2212)	Irrigated (B1803)	Irrigated (B1607)	Drought (B1216)	Drought (B2212)
TESTWT**	durum	82.85	83.64	82.29	83.96	83.19	84.13
	bread	81.36	82.29	80.19	82.37	81.69	82.00
TKW	durum	53.05	50.79	46.36	49.53	47.84	52.03
	bread	46.63	49.78	44.56	47.12	45.03	50.28
GRNHRD	durum	-	-	-	-	-	-
	bread	45.67	45.49	46.20	44.19	45.53	44.48
FLRYDL	durum	-	-	-	-	-	-
	bread	68.77	70.32	72.74	72.69	69.73	69.94
GRNPRO	durum	13.59	10.76	12.77	11.87	13.29	11.14
	bread	12.78	11.19	12.60	12.11	12.62	11.45
FLRPRO	durum	11.13	8.36	10.42	9.68	10.85	8.85
	bread	11.17	9.51	10.94	10.55	11.00	9.82
FLRSDS	durum	12.17	8.79	11.67	10.47	12.78	9.72
	bread	16.81	13.01	15.46	15.92	17.40	13.18
MIXTIM	durum	2.96	4.22	3.40	3.20	3.23	3.78
	bread	2.86	3.84	2.81	2.99	3.20	3.62
MP	durum	123.59	-	143.89	119.57	131.89	116.42
	bread	116.89	151.18	118.21	122.57	132.14	143.58
ALVW	durum	-	-	-	-	-	-

	bread	292.00	344.75	246.53	299.06	348.00	320.28
ALVPL	durum	-	-	-	-	-	-
	bread	0.77	1.59	0.69	0.81	0.92	1.29
LOFVOL	durum	-	-	-	-	-	-
	bread	802.50	720.83	807.01	788.33	815.42	756.81

* Irrigated: five irrigation events; drought: 3 irrigation events.
** TESTWT, test weight (kg hL^{-1}); TKW, thousand-kernel weight (g); GRNHRD, grain hardness (PSI); FLRYLD, flour yield from milling (percentage recovered); GRNPRO, grain protein (at 12.5% MB bread, 12.5% BH durum); FLRPRO, flour protein (at 14% MB bread, 14% BH durum); FLRSDS, flour sodium dodecyl sulfate sedimentation volume (mL); MIXTIM, optimum mix time (min); MP, torque at the integral of the midline peak; ALVW, work value from Alveograph curve (J); ALVPL, Alveograph P (tenacity) divided by L (extensibility) (mm mm^{-1}); LOFVOL, pup loaf volume (cm^3).

Assessment of advanced lines under the cultural practices of wheat growers is a necessary strategy that CIMMYT is applying in collaboration with Mexican NARS, seed producers and wheat growers. This strategy has been implemented over the years and needs to evolve according to current needs. Varietal replacement needs to be accelerated to avoid having varieties that lose resistance or are susceptible to new disease races. Another aspect that is essential for varietal replacement is seed multiplication. Through the MasAgro initiative, CIMMYT has been collaborating with INIFAP in order to multiply, register and promote recently released varieties. In the past year, six new varieties developed through this collaboration were registered and multiplied on a low scale. A total of nine recently released varieties (including six registered varieties) are currently being multiplied on a larger scale by CIMMYT-INIFAP in collaboration with seed producers in the northwest (Sonora), north (Chihuahua), northeast (Nuevo Leon), El Bajio (Guanajuato) and Altiplano (Hidalgo) regions of Mexico.

Conclusions

- A total of 1092 advanced lines with reasonable resistance to disease were selected and promoted to second year yield trials that are currently being conducted (Ciudad Obregon) and will help to further select the best lines for high and stable grain yield in a number of environments.
- These 1092 lines showed resistance to leaf and yellow rust with disease severity below 5%. Most of them showed good resistance to Septoria tritici blotch (values under 800 AUDPC) and were resistant to moderately resistant to Fusarium head blight. Sufficient grain quality diversity was also found which is desirable for the end use types used by the Mexican value chain.
- Advanced lines evaluated during the 2015-2016 winter cycle in Ciudad Obregon under heat, drought and irrigation indicated that the grain yield rankings of the best lines were equal or superior to those of the checks. A total of 677 outstanding lines were selected for national and international nurseries.
- Ongoing activities to propose materials for release are showing promising results and are possible due in part to the collaboration with INIFAP, seed producers and wheat growers.

References

American Association of Cereal Chemists (2010) Approved Methods of the AACC. St. Paul, Minessota.

Autrique E, Guzman C, Singh PK, et al (2016) Wheat breeding in Mexico: Delivering newly developed advanced lines. In: Reynolds M, Molero G, Quilligan E (eds) Proceedings of the 2nd International TRIGO (Wheat) Yield Potential Workshop. CENEB, CIMMYT, Ciudad Obregon, Sonora, Mexico, 9-10 March 2016. Mexico, DF.:CIMMYT,

Braun H-J, Rajaram S, Ginkel M (1996) CIMMYT's approach to breeding for wide adaptation. Euphytica 92:175–183. doi: 10.1007/BF00022843

Crespo-Herrera LA, Crossa J, Huerta-Espino J, et al (2017) Genetic yield gains in CIMMYT's international Elite Spring Wheat Yield Trials by modeling the genotype × environment interaction. Crop Sci 56:1–13. doi: 10.2135/cropsci2016.06.0553

FAO (2017) FAO statistics. http://www.fao.org/faostat/en/#data. Accessed February 2016.

FAO (2014) FAO statistics. http://www.fao.org/resources/infographics/infographics-details/en/c/240943/. Accessed 7 Nov 2015

Fischer T, Byerlee D, Edmeades G (2014) Crop yields and global food security. Aust Cent Int Agric Res 660.

Gilchrist-Saavedra LI (2000) Problemas fitosanitarios de los cereales de grano pequeño en los Valles Altos de México. Rev Mex Fitopatol 18:132–137.

Guzmán C, Mondal S, Govindan V, et al (2016) Use of rapid tests to predict quality traits of CIMMYT bread wheat genotypes grown under different environments. LWT - Food Sci Technol 69:327–333. doi: 10.1016/j.lwt.2016.01.068

Guzman C, Peña RJ, Singh R, et al (2016) Wheat quality improvement at CIMMYT and the use of genomic selection on it. Appl Transl Genomics 11:3–8. doi: 10.1016/j.atg.2016.10.004

Guzmán C, Posadas-Romano G, Hernández-Espinosa N, et al (2015) A new standard water absorption criteria based on solvent retention capacity (SRC) to determine dough mixing properties, viscoelasticity, and bread-making quality. J Cereal Sci 66:59–65. doi: 10.1016/j.jcs.2015.10.009

Hawkesford MJ, Araus JL, Park R, et al (2013) Prospects of Doubling Global Wheat Yields. Food Energy Secur 2:34–48. doi: 10.1002/fes3.15

Lantican MA, Braun HJ, Payne TS, et al (2016) Impacts of international wheat improvement research, 1994-2014. Mexico, D. F.: CIMMYT

Osman M, He X, Benedettelli S, et al (2016) Identification of new sources of resistance to fungal leaf and head blight diseases of wheat. Eur J Plant Pathol 145:305–320. doi: 10.1007/s10658-015-0843-0

Peña RJ, Amaya A, Rajaram S, Mujeeb-Kazi A (1990) Variation in quality characteristics associated with some spring 1B/1R translocation wheats. J Cereal Sci 12:105–112. doi: http://dx.doi.org/10.1016/S0733-5210(09)80092-1

Reynolds M, Foulkes J, Furbank R, et al (2012) Achieving yield gains in wheat. 1799–1823. doi: 10.1111/j.1365-3040.2012.02588.x

Rodriguez-Contreras ME, Villaseñor-Mir HE, Leyva-Mir G, et al (2008) Efecto de Septoria tritici en el rendimiento de trigo de temporal en ambientes lluviosos de los Valles Altos Centrales de Mexico. Agrociencia 42:435–442.

Rodriguez-Garcia MF, Huerta-Espino J, Villaseñor-Mir HE, et al (2010) Análisis de virulencia de la roya amarilla (Puccinia striiformis f. sp. tritici) del trigo (Triticum aestivum L.) en los Valles Altos de Mexico. Agrociencia 44:491–502.

Singh RP, Trethowan R (2007) Breeding spring bread wheat for irrigated and rainfed production systems of developing world. In: Kang MS, Priyadarshan PM (eds) Breeding for Major Food Staples. Blackwell, Ames, Iowa, p 437

Solis-Moya E, Huerta-Espino J, Rodríguez-García MF, et al (2013) Resistencia a roya de la hoja en variedades de trigo (Triticum spp. L.) adaptadas a El Bajío, México. Agrociencia 47:457–469.

UNCTAD (2013) MEXICO ' S AGRICULTURE DEVELOPMENT : Perspectives and outlook. United Nations Conf Trade Dev 184.

USDA (2017) United states Department of Agriculture. http://www.usda.gov/. Accessed 17 Jan 2017

Velu G, Singh RP (2013) Phenotyping in Wheat Breeding. In: Panguluri SK, Kumar AA (eds) Phenotyping for Plant Breeding: Applications of Phenotyping Methods for Crop Improvement. Springer Science, New York, pp 1–211

Villaseñor-Mir HE (2015) Sistema de mejoramiento genético de trigo en México. Rev Mex Ciencias Agrícolas Pub. Esp.:2183–2189.

Evaluation of the 3rd Wheat Yield Consortium Yield trial under irrigated growing conditions in Mexico during the 2015-2016 cycle

Ernesto Solís-Moya[1], Miguel A. Camacho-Casas[1], Jorge I. Alvarado-Padilla[1], Javier Ireta Moreno[1], Alberto Borbón-Gracia[1], Gemma Molero[2] and Matthew Reynolds[2]
[1] INIFAP, Mexico; [2] CIMMYT, Mexico

Abstract
The 3rd Wheat Yield Consortium Yield Trial (WYCYT) was established at five locations in Mexico (Baja California, Guanajuato, Jalisco, Sinaloa and Sonora) during the 2015-2016 cycle. The trial included 42 genotypes derived from Physiology pre-breeding activities targeting high yield potential irrigated environments. Agronomic and phenotypic traits were evaluated at the five sites and the combined analysis detected highly significant differences among locations for all measured traits. The AMMI analysis showed that the Sonora and Jalisco locations recorded the highest and lowest grain yield estimates, respectively, and that these locations also classified the genotypes in a similar way. The Sonora and Baja California locations outyielded the average grain yield across locations. In general, genotype 23 (SERI / BAV92 // PUB94.15.1.12 / WBLL1) registered the highest grain yield among environments, followed by entry 21 (SERI / BAV92 // PUB94.15.1.12 / WBLL1).

Introduction
Grain crops are the staple foods worldwide, especially in developing countries (Fischer and Edmeades, 2010). Increasing populations and the negative effects of climate change create an unprecedented challenge to food security.

Wheat scientists and agricultural experts from various private and public institutions are coming together in a collaborative network to increase wheat yield potential by applying an international strategy aimed at boosting future wheat yields: International Wheat Yield Partnership (IWYP). IWYP activities in Mexico are coordinated by the International Maize and Wheat Improvement Center (CIMMYT) and are sponsored by the Mexican Secretariat of Agriculture (SAGARPA) through the MasAgro project. One of the main objectives of the project is to increase wheat production in Mexico. Wheat accounts for 40% of total cereal expenditure by Mexican households, providing 10% of total dietary calories. Domestic wheat consumption reached 6.1 million tons (MT) in 2012, 58% of which was imported (4.6 MT), while national production stood at 3.2 MT. This places Mexico among the 10 largest wheat importers worldwide, at a cost of 20 billion pesos per year. The projected demand for wheat in Mexico estimates an increase in total wheat consumption of 21% by 2015, 31% by 2020 and 55% by 2030. Given this scenario, it is important to unite international and national efforts to raise yield potential in order to further increase Mexico's wheat production. To this end, Mexico's National Institute of Forestry, Agriculture and Livestock (INIFAP) collaborates with CIMMYT in evaluating elite genotypes in different agro-climatic areas representative of wheat production in Mexico. The aim is to identify lines outstanding in yield and biomass with the objective of further incorporating them into national breeding programs and contribute to increasing wheat production in Mexico. During 2015-2016, CIMMYT lines derived from strategic crosses were evaluated at five Mexican (INIFAP) test sites.

A pre-breeding program for yield potential initiated by CIMMYT in 2008 has profited from many of these outputs in terms of parental and progeny selection, and resulted in the creation of the Wheat Yield Consortium Yield Trial (WYCYT). Results of the WYCYT trials provide a first proof of concept that yield potential can be improved through deterministic crosses based on physiological dissection of yield potential traits. This material consists of new genetically diverse germplasm that will be used to generate varieties with new alleles that can provide adaptive stress traits (Reynolds et al., 2015) or yield potential traits. This adaptation will be achieved by increasing physiological aspects of the plant, such as harvest index, biomass, number of effective tillers per plant, grains per spike and 1000-grain weight (Bolaños and Britto, 1991).

Materials and Methods

During the 2015-2016 wheat growing cycle, the 3rd WYCYT grain yield trial consisting of 42 genotypes with two replicates was evaluated at five different locations representing Mexico's wheat producing areas:

Guanajuato, Jalisco, Sinaloa, Sonora and Baja California. Table 1 shows planting dates, geographical coordinates and environmental growing conditions of the locations where the 3rd WYCYT was evaluated.

Table 1. Geographical locations and environmental growing conditions at five locations for evaluating 42 genotypes in Mexico. 2015-2016 autumn-winter season.

Location	Sowing date	Coord.	masl (m)	Fert. (N-P-K)	Irrigations	Rainfall	AT	t° Max.	t° Min	Harvest date
Baja California	26/12/2015	32°18'N 115°4W	8.6	280-80-00	0-40-60-50-90-105	0.10	17.1	26.4	7.5	03/06/2016
Guanajuato*	16/12/2015	105°29W 20°32'N 100°49W	1752	240-60-00	0-15-45-60-75-87-100-110	5.4	16.7	26.5	7.2	17/05/2016
Jalisco	7/01/2016	20°16'N 102°34W	1542	180-00-00	0-37-60-81-102	16.95	18.33	28.5	8.25	15/05/2016
Sinaloa	02/01/2016	25°45'N 108°48W	14	241-52-00	0-48-74-92	8.4	20.26	30.09	11.4	24/05/2016
Sonora	04/12/2015	32°18'N 115°4W	37	257-52-00	0-39-73-97-115	11.7	17.4	27.7	8.7	27/04/2016

The following phenotypic traits were measured: 1) plant height (PH); 2) days to heading (DH); 3) days to physiological maturity (DPM); 4) harvest index (HI); 5) grain yield (GY); 6) biomass (BIO); 7) spikes per square meter (SSM); 8) 1000.kernel weight (TKW); and 9) grains per square meter (GSM). The information obtained was subjected to a combined analysis of variance for each of the above mentioned variables. Mean comparisons were tested using Tukey's range test at the 0.05 level. An analysis of genotype by environment interaction using the AMMI1 method was also performed. All analyses were performed using the statistical software SAS version 9.3.

Results and Discussion

The combined analysis of variance (Table 2) showed that over 40% of the total variation was explained by locations for all traits, and statistically ($p<0.01$) highly significant differences among locations were detected among all evaluated traits. With the exception of biomass (BIO), highly significant ($p<0.01$) differences were observed among genotypes for the remaining traits. The location by genotype interaction showed statistical significance for six traits, but plant height (PH), biomass (BIO) and spikes per square meter (SSM).

Table 2. Mean squares for variables recorded on 42 genotypes evaluated at five locations in Mexico. 2015-2016 autumn-winter season.

S of V	DF	DH	PH	DPM	GY	TKW	HI	BIO	GSM	SSM
Loc	4	6469 **	4682 **	12620 **	44398610 **	2876 **	0.421 **	365 **	493236932 **	326984 **
Rep	1	2.3	45.3	6.7	177861	0.01	0.003	22.3	1272371	5997
Blo(Rep)	12	7.1	39.6	7.6	1604667	10.67	0.001	15.6	12722670	6495
Gen	41	33.8 **	125.9 **	23.1 **	1001627 **	80.0 **	0.002 **	6.00	8918797 **	7081 **
Loc*Gen	164	5.6 **	23.1	8.1 **	512984 *	22.5 **	0.002 **	5.19	5241466 *	4463
Error	197	2.9	23.2	4.8	393209	13.36	0.001	4.39	4048179	3718
Total	419									
CV		2.1	4.6	1.7	9.89	8.18	7.684	13.30	13.80	17.22

S of V = source of variation; DF = degrees of freedom; Loc = location; Gen = genotype; Rep = replication; Blo = block; DH = days to heading; PH= plant height; DPM = days to physiological maturity; GY = grain

yield (kg ha^{-1}); TKW = thousand-kernel weight; HI = harvest index; Bio = biomass (t ha^{-1}); GSM = grains per square meter; SSM = spikes per square meter.

The analysis of variance for grain yield (GY) showed that 44.4, 10.3 and 21.0% of the total variation was explained by location, genotype and genotype by environment interaction, respectively. Statistically significant differences ($p<0.01$) were detected among locations and genotypes, as well as for the interaction between locations and genotypes ($p<0.05$).

The AMMI1 programming routine used to explain the genotype by environment interaction showed high significance ($p <0.01$) for the first two axes of the principal component analysis, which explained 48.52% and 25.38% of variation due to genotype by environment interaction. The AMMI model retained 75.74% of variation due to environment, genotype, and genotype by environment interaction using 209 degrees of freedom.

The AMMI analysis also showed that the Sonora and Jalisco locations recorded the highest (7,450 kg ha^{-1}) and lowest (5,625 kg ha^{-1}) grain yield estimates across genotypes. Averaging 7,145 kg ha^{-1}, genotype 23 (SERI / BAV92 // PUB94.15.1.12 / WBLL1) expressed the highest average grain yield across locations, and ranked 1st, 2nd, 4th, 6th and 11th in Baja California, Sonora, Jalisco, Guanajuato and Sinaloa, respectively. Genotypes 21 (SERI / BAV92 // PUB94. 15.1.12 / WBLL1), 31 (MEX94.27.1.20 / 3 / SOKOLL // ATTILA / 3 * BCN / 4 / PUB94.15.1.12 / WBLL1) and 22 (SERI / BAV92 // PUB94.15.1.12 / WBLL1) were among the four highest yielding genotypes; while another check, genotype 39 (ROELFS F2007) averaged 5,219 kg ha^{-1}, the lowest yield (Fig. 1). In addition, the check from the breeding program, 42 (REEDLING # 1 = Borlaug 100), had high yield in most environments.

Sonora (7,450 kg ha^{-1}) and Baja California (6,637 kg ha^{-1}) were the only locations with yields above the overall average (6,339 kg ha^{-1}), while the most stable genotypes showing low or near zero CP1 values were genotypes 3, 34, 17, 36, 32, 12, 24, 19, 18, 30, 9, 10, 29, 35, 13, 23, 38 and 26. Locations showing estimated angles lower than 90 degrees, Sonora and Baja California, classified genotypes in a similar way. In contrast, locations showing angles close to 90 degrees between the vectors of Guanajuato and Sonora, and Guanajuato and Sinaloa indicate that these environments classified genotypes differently. Jalisco and Guanajuato were the locations that contributed the most to the first axis of the interaction (Fig. 1).

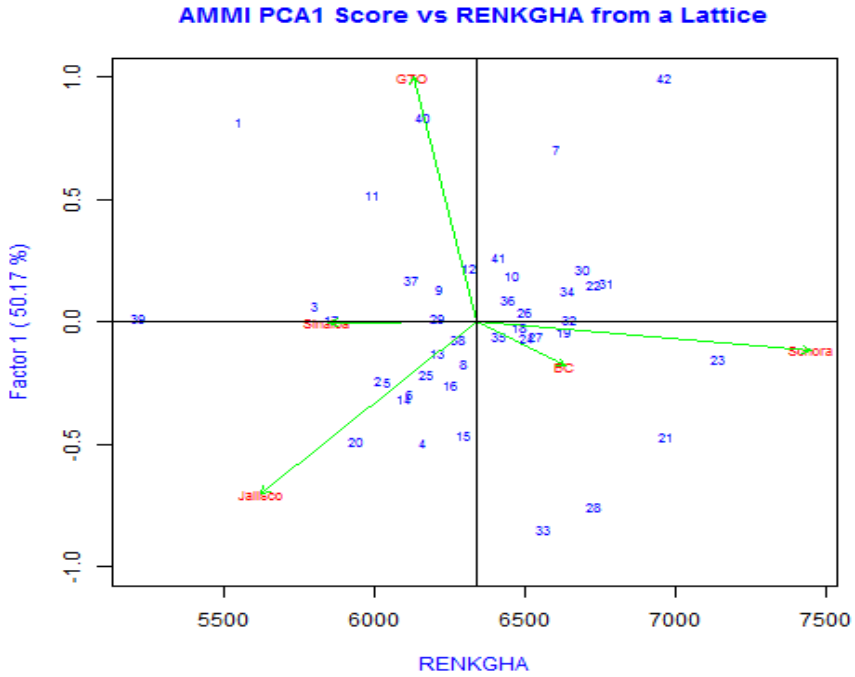

Fig. 1. Biplot of genotype by environment interaction from the AMMI model.

Correlation analysis across genotypes averaged over locations showed that in this particular set of genotypes, grain yield showed the highest positive correlation coefficient (0.82) with biomass, followed by those with thousand-kernel weight (0.42), plant height (0.37), grains per square meter (0.36) and spikes per square meter (0.25). Other interesting correlations were those computed for plant height with thousand-kernel weight (0.62) and biomass (0.49).

Conclusions

For this particular set of genotypes, a significantly greater amount of variation in grain yield was due to the growing conditions or locations used for their evaluation, followed by the genotype by environment interaction.

In general, SERI / BAV92 // PUB94.15.1.12 / WBLL1) was the highest yielding genotype, reaching 8,000 and 8,270 kg ha^{-1} in Baja California and Sonora. Other outstanding genotypes were 21 (SERI/BAV92//PUB94.15.1.12/WBLL1), 31 (MEX94.27.1.20/3/SOKOLL//ATTILA/3*BCN/4/ PUB94.15.1.12/WBLL1) and 22 (SERI/BAV92//PUB94.15.1.12/WBLL1). The highest grain yield in Guanajuato, Sinaloa and Jalisco was achieved by genotypes 42 (Borlaug 100, the check from the breeding program), 32 (MEX94.27.1.20/3/SOKOLL//ATTILA/3*BCN/4/PUB94.15.1.12/WBLL1) and 28 (C80.1/3*QT4118//KAUZ/RAYON/3/2*TRCH/4/BERKUT/KRICHAUFF).

The estimated correlation coefficients among yield and agronomic traits suggest that biomass, through plant height, continues to be an important trait for increasing grain yield potential in wheat.

References

Bolaños, A.A., and Britto R. M. 1991. Heredabilidad del Índice de Cosecha en Trigo (*Triticum aestivum* L.) y su Relación con Tres Componentes de Rendimiento. Agronomía Colombiana. 8(2):268-279.

Reynolds, M. P. Tattaris, M., Cossani, C.M., Ellis, M., Yamaguchi-Shinozaki, K., and Saint-Pierre, C. 2015. Exploring genetic resources to increase adaptation of wheat to climate change. In: Ogihara, Y., Takumi, S., and Handa, H. (Eds.). Advances in wheat genetics: From Genome to Field. Springer, Japan.

Evaluation of stress adaptive nurseries (1st SATYT and 5th SATYN) under irrigated growing conditions in Mexico during the 2015-2016 cycle

Ernesto Solís-Moya[1], Miguel A. Camacho-Casas[1], Jorge I. Alvarado-Padilla[1], Javier Ireta Moreno[1], Alberto Borbón-Gracia[1], Gemma Molero[2] and Matthew Reynolds[2]
[1] INIFAP, Mexico; [2] CIMMYT, Mexico

Abstract
Two international nurseries with stress adaptive traits —1st SATYT (1st Stress Adaptive Trait Yield Trial) and 5th SATYN (Stress Adaptive Trait Yield Nursery)— were evaluated in five locations of Mexico (Baja California, Guanajuato, Jalisco, Sinaloa and Sonora) during the 2015-2016 cycle under full irrigated conditions. These trials included 45 and 35 genotypes with two replicates. Agronomic traits, yield and yield components were measured. For 1st SATYT, the combined variance analysis showed highly significant differences for sites across all measured traits. The highest yields were observed in Sonora and Baja California with 6,615 and 6,367 kg ha^{-1}, respectively. The most productive genotype (45) was Reedling #1, the check provided by CIMMYT breeding programs, which had an average yield across locations of 6,999 kg ha^{-1}. The new genotypes selected for their high yield in this trial were lines 27 (SOKOLL/3/ PASTOR//HXL7573/2*BAU/4/ATTILA/PASTOR), 12 (SOKOLL/WBLL1), 8 (PUB94.15.1.12/ WBLL1) and 11 (SOKOLL/WBLL1). Line number 8 derives from a cross with a Mexican landrace. For 5th SATYN, the highest yield was observed in Sonora, while the lowest was recorded in Guanajuato. As with the previous nursery, line 45 (REEDLING #1) was the highest yielding genotype, followed by line 19 (205) // BORL95 / 3 / PRL / SARA // TSI / VEE # 5/4 / FRET2. The genotypes selected in this trial were 19 (WBLL4//OAX93.24.35/WBLL1/5/ CROC_1/ AE.SQUARROSA), 21 (PASTOR // HXL7573/2*BAU /3/WBLL1), 18 (WBLL4//OAX93.24.35/ WBLL1 /5/CROC_1/AE.SQUARROSA) and 20 (PASTOR // HXL7573/2*BAU/3/ WBLL1), which had the highest yields across locations. Although the overall performance of the PT lines in comparison with local checks was good, the fact that these lines were selected specifically for stress adaptive traits (such as heat and drought) and evaluated under yield potential conditions did not allow them to express their maximum advantage in comparison with check Reedling #1.

Introduction
It is predicted that by 2050 the world population will reach more than nine billion inhabitants, most of them in developing countries (UN, 2016). Unless global food production increases by 70%, the number of undernourished people will continue to increase. Mexico is 21st among the world's wheat producers, with an average of 3.7 MT produced in 2014. Wheat is the second most important caloric source from plants for Mexicans (after maize), with a total of 40% household expenditure in cereals, according to Mexico's National Millers Association (CANIMOLT). Wheat consumption in Mexico is likely to increase in the coming years due to the growth of Mexico's population and the increase in the popularity and convenience of wheat product consumption. Due to wheat's importance as a low-cost nutrient source, promoting national wheat production is necessary to ensure food security. To this end, the National Institute for Forestry, Agriculture and Livestock Research (INIFAP) collaborates with CIMMYT to evaluate elite wheat genotypes in different agro-climatic areas representative of wheat production in Mexico.

A pre-breeding program for stress adaptation initiated by CIMMYT has profited from many of these outputs in terms of parental and progeny selection and resulted in the delivery of the Stress Adaptive Trait Yield Nurseries (SATYNs). In general, odd numbers indicate nurseries with traits for adaptation to drought environments, while even numbers indicate nurseries with adaptive traits under heat conditions. The best lines resulting from the evaluation of previous SATYNs were selected and included in a new nursery: 1st Stress Adaptive Trait Yield Trial (SATYT). This material consists of new genetically diverse germplasm that will be used to generate varieties with new alleles that can provide stress adaptive traits (Reynolds et al., 2015). This adaptation will be achieved by increasing physiological aspects of the plant, such as harvest index, biomass, number of effective tillers per plant, grains per spike and 1000-grain weight (Bolaños and Britto, 1991).

Material and Methods
During the 2015-2016 cycle, the 1st SATYT (1st Stress Adaptive Trait Yield Trial) and 5th SATYN (Stress Adaptive Trait Yield Nursery) were evaluated under favorable conditions. These experiments included 45

and 35 genotypes with two replicates. These populations were evaluated at five different sites representing Mexico's wheat producing areas: Guanajuato, Jalisco, Sinaloa, Sonora and Baja California. Table 1 shows planting dates, agronomic management, geographical coordinates and growing conditions at the locations where the different trials were conducted.

Table 1. Geographical location and growing conditions at five locations where 1st SATYT and 5th SATYN were evaluated.

Location	Sowing date	Coord.	masl (m)	Fert. (N-P-K)	Irrigations	Rainfall	AT	t° Max.	t° Min	Harvest date
Baja California	26/12/2015	32°18'N 115°4W	8.6	280-80-00	0-40-60-50-90-105	0.10	17.1	26.4	7.5	03/06/2016
Guanajuato*	16/12/2015	105°29W 20°32'N 100°49W	1752	240-60-00	0-15-45-60-75-87-100-110	5.4	16.7	26.5	7.2	17/05/2016
Jalisco	7/01/2016	20°16'N 102°34W	1542	180-00-00	0-37-60-81-102	16.95	18.33	28.5	8.25	15/05/2016
Sinaloa	02/01/2016	25°45'N 108°48W	14	241-52-00	0-48-74-92	8.4	20.26	30.09	11.4	24/05/2016
Sonora	04/12/2015	32°18'N 115°4W	37	257-52-00	0-39-73-97-115	11.7	17.4	27.7	8.7	27/04/2016

The following phenotypic traits were measured: 1) plant height (PH); 2) days to heading (DH); 3) days to physiological maturity (DPM); 4) harvest index (HI); 5) grain yield (GY); 6) biomass (BIO); 7) spikes per square meter (SSM); 8) 1000-kernel weight (TKW); and 9) grains per square meter (GSM). The information obtained was subjected to a combined analysis of variance for each of the above mentioned variables. Mean comparisons were tested using Tukey's range test at the 0.05 level. An analysis of genotype by environment interaction using the AMMI1 method was also performed. All analyses were performed using the statistical software SAS version 9.3.

Results and Discussion

We divide the next section by the results of each nursery separately.

1st SATYT

In the combined analysis, we detected highly significant differences among the test sites. Among genotypes, highly significant differences were detected for all variables except HI. In the interaction between locations by genotypes, highly significant differences were detected for DH, DPM, grain yield, TKW, HI, BIO, GSM and SSM and significant for PH (Table 2).

Table 2. Mean squares across locations of the variables studied in 1st SATYT evaluated at five locations in the 2015-16 autumn-winter cycle.

SV	DF	DH	PH	DPM	GY	TKW	HI	BIO	GSM	SSM
LOC	4	11955**	4228**	14081**	31015552**	2745**	0.5**	376.7**	475383792**	236140**
GEN	44	41.8**	112**	37.7**	1287061**	76.5**	0.002	10.7**	9670747**	8703**
REP	1	0.6	0.05	44.8	138253	0.62	0.000	8.1	385578	16.0
BLO(REP)	16	3.9	43.5	4.5	413438	6.8	0.001	4.2	2132295	1851
LOC*GEN	176	5.4**	26.5*	8.4**	886737**	19.6**	0.003**	9.5**	6986853**	7708**
ERROR	208	2.8	20.5	5.2	451857	4.9	0.001	5.2	2509580	3670
TOTAL	449									
C.V		2.1	4.5	1.8	11.4	4.9	9.0	15.7	11.7	17.3

S of V = source of variation; DF = degrees of freedom; Loc = location; Gen = genotype; Rep = replication; Blo = block; DH = days to heading; PH= plant height; DPM = days to physiological maturity; GY = grain yield (kg ha^{-1}); TKW = thousand-kernel weight; HI = harvest index; Bio = biomass (t ha^{-1}); GSM = grains per square meter; SSM = spikes per square meter.

The analysis of variance showed a highly significant effect of the environment ($p < 0.01$) with 27.7% of the total sum of squares variation (SCT). The genotypic effect was highly significant ($p < 0.01$), accounting for 12.6% of SCT. The genotype by environment interaction was significant ($p < 0.05$), accounting for 34.8% of SCT. The AMMI model showed the first two axes of the ACP were highly significant ($p < 0.01$), explaining 40.6% and 30.5% of the SC of the interaction, respectively. The remaining three main components and the residue were not significant. The AMMI model retained 54% of SCT (environment + genotype + interaction) using 95 degrees of freedom (4 for environments, 44 for genotypes and 47 for the first major component).

The study of the interaction with the AMMI model was complemented with the representation of the biplot (Fig. 1). According to this information, line Reedling #1 (45) was the genotype with the highest yield, followed by line 27 SOKOLL / 3 / PASTOR // HXL7573 / 2 * BAU / 4 / ATTILA / PASTOR, while line 31 SOKOLL / 3 / PASTOR // HXL7573 / 2 * BAU / 4 / ASTREB had the lowest yields. The Sonora location had the highest yield and Sinaloa had the lowest yield. Only two locations (Sonora and Baja California) produced yields equal to or above the average and the rest had inferior yields. On the other hand, genotypes 45 (Reedling #1), 21 (CHEN/AE.SQ//2*OPATA/3/FINSI) and 34 (SOKOLL/3/PASTOR // HXL7573 /2*BAU/4/WBLL4//OAX93.24.35/WBLL1) were the most stable genotypes with CP1 values that were low or close to zero. Genotypes 1 (LOCAL CHECK) and 8 (PUB94.15.1.12/WBLL1), together with the Jalisco and Baja California locations, contributed the most to the first axis of the interaction, being more unstable. The Sinaloa and Guanajuato locations presented between them an angle of less than 90 degrees by which they classify to the genotypes of similar way reason why one can eliminate one of them without losing precision in the results. The same situation is inferred between the Sonora and Baja California locations. The length of the environmental vectors shows that Guanajuato presented less variation among genotypes.

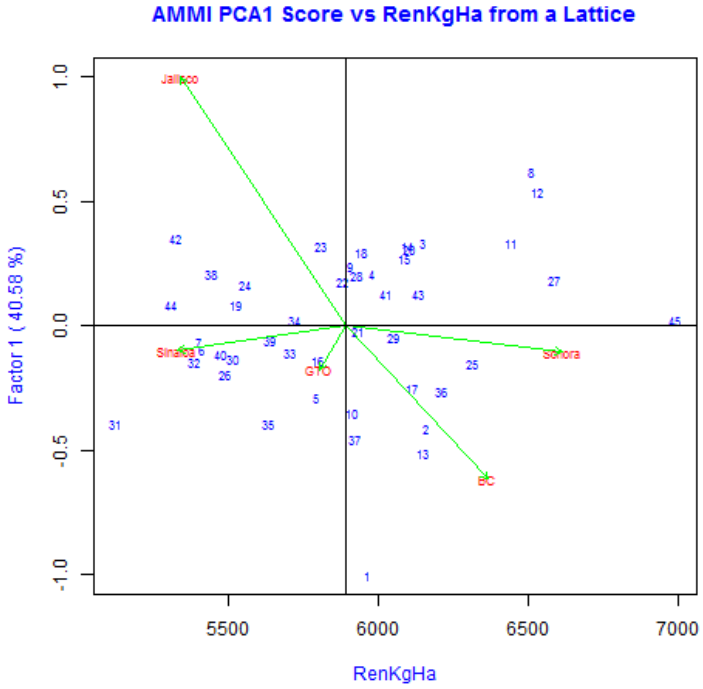

Fig. 1. Biplot of grain yield of 1st SATYT evaluated at five locations during the 2015-16 autumn-winter cycle.

5th SATYN

The analysis of variance across locations (Table 3) showed highly significant differences for locations across all measured traits. Genotypes had highly significant differences in all traits except SSM. In the genotype by environment interaction, there were highly significant differences in DH, Yield, TKW, HI, BIO, and GSM. In all cases, the highest proportion of the variation was observed in the locations factor.

Table 3. Mean squares across locations of the variables studied in the 5th SATYN evaluated at five locations in the 2015-16 autumn-winter cycle.

SV	DF	DH	PH	DPM	GY	TKW	HI	BIO	GSM	SSM
LOC	4	8718**	1704**	9007**	25259275**	2867**	0.37**	692.2**	179271293**	573631**
GEN	34	4.4**	92.5**	29.6**	659885**	79.1**	0.003**	7.6**	11081599**	13799
REP	1	11.7	128	96.7	2200798	4.1	0.000	10.7	31326059	8198
BLO(REP)	12	6.2	51	8.5	522941	15.0	0.001	5.7	4307922	13637
LOC*GEN	136	4.4**	30	8.0	547904**	13.9**	0.002**	6.5**	4526316**	12698
ERROR	162	2.1	22.9	6.5	380432	8.0	0.001	4.4	2848913	10300
TOTAL	349									
C.V		1.7	4.7	2.1	10.0	6.3	8.5	13.6	12.1	25.2

S of V = source of variation; DF = degrees of freedom; Loc = location; Gen = genotype; Rep = replication; Blo = block; DH = days to heading; PH= plant height; DPM = days to physiological maturity; GY = grain yield (kg ha^{-1}); TKW = thousand-kernel weight; HI = harvest index; Bio = biomass (t ha^{-1}); GSM = grains per square meter; SSM = spikes per square meter.

The analysis of variance of the genotype by environment interaction showed a highly significant effect of the environment ($p < 0.01$) with 36.8% of the total sum of squares variation (SCT). The genotypic factor was highly significant ($p < 0.01$), accounting for 8.2% of SCT. The genotype-environment interaction was significant ($p < 0.05$), explaining 27.1% of SCT. The AMMI model showed the first two axes of the ACP were highly significant ($p < 0.01$), explaining 47.3% and 32.9% of the SC of the interaction, respectively. The remaining three main components and the residue were not significant. The AMMI model retained 72% of SCT (environment + genotype + interaction) using 110 degrees of freedom (4 for environments, 34 for genotypes and 72 for interaction).

According to Figure 2, line Reedling #1 was the highest yielding genotype, followed by line 19 205) // BORL95 / 3 / PRL / SARA // TSI / VEE # 5/4 / FRET2, while line 11 (205) // BORL95 / 3 / PRL / SARA // TSI / VEE # 5/4 / FRET2 had the lowest yields. Sonora produced the highest yield and Guanajuato had the lowest. Only two environments produced yields equal to or above the average; the rest had inferior yields.

Genotypes with CP1> 0 values responded positively (fit well) to environments with CP1> 0 values (i.e., their interaction is positive), but they responded negatively to environments with CP1 values <0. The opposite is true of genotypes that had CP1 values <0 (Samonte et al., 2005). Genotypes 15, 30 and 32 were the most stable genotypes with CP1 values that were low or close to zero. Genotypes 4 and 20, together with the Jalisco, Sonora and Guanajuato locations, contributed the most to the first axis of the interaction, being more unstable.

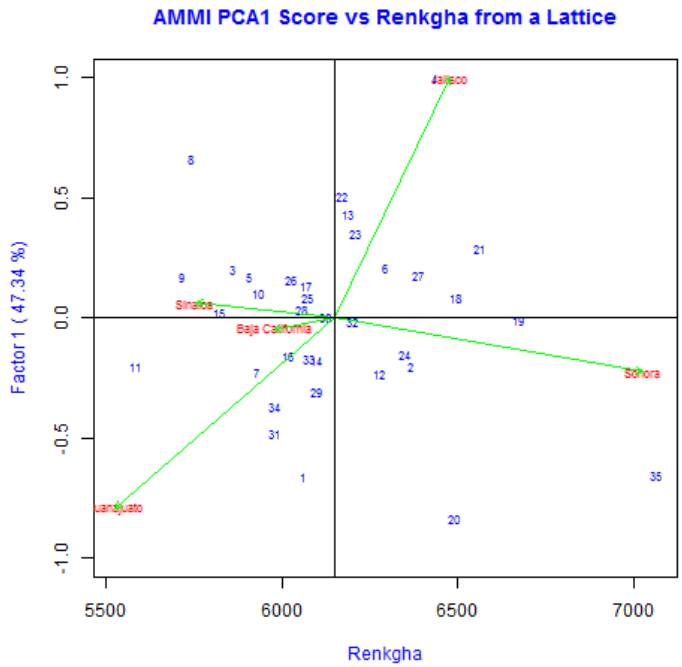

Fig. 2. Biplot of 5th SATYN evaluated at five locations in the 2015-16 autumn-winter cycle.

Conclusions

- The genotypes selected from 1st SATYT were lines 27 (SOKOLL/3/PASTOR//HXL7573/2* BAU/4/ATTILA/PASTOR), 12 (SOKOLL/WBLL1), 8 (PUB94.15.1.12/WBLL1), and 11 (SOKOLL/WBLL1), which recorded the highest yields across locations.
- The genotypes selected from 5th SATYN were lines 35, 19, 21, 18 and 20, which had the highest yields across locations.
- Although the overall performance of the PT lines in comparison with the local checks was good, the fact that these lines were selected specifically for stress adaptive traits (such as heat and drought) and evaluated under yield potential conditions did not allow them to express their maximum advantage in comparison with check Reedling #1.

References

Bolaños, A.A. y Britto R. M. 1991. Heredabilidad del Índice de Cosecha en Trigo (*Triticumaestivum* L.) y su Relación con Tres Componentes de Rendimiento. Agronomía Colombiana. 8(2):268-279.

Reynolds, M. P. Tattaris, M., Cossani, C.M., Ellis, M., Yamaguchi-Shinozaki, K., Saint-Pierre, C., 2015. Exploring genetic resources to increase adaptation of wheat to climate change. In Ogihara, Y., Takumi, S., and Handa, H. (Eds.), Advances in wheat genetics: From Genome toField. Springer, Japan.

Samonte. S. O., L. T. Wilson, A. M. McClung, and J. C. Medley. 2005. Targeting Cultivars onto Rice Growing Enviroments Using AMMI and SREG GGE Biplot Analyses. Crop Sci 45:2414-2424

UN.2016. World population projected to reach 9.6 billion by 2050. http://www.un.org/en/development/desa/news/population/un-report-world-population-dfg projected-to-reach-9-6-billion-by-2050.html

Phenotypic characterization of the International Wheat Yield Partnership-Hub (IWYP-HUB) panels

Gemma Molero[1], Francisco J. Piñera[1], Alma C Rivera-Amado[1], Francisco Pinto[1], Jacinta Gimeno[1], Sivakumar Sukumaran[1] and Matthew P. Reynolds[1]
[1] CIMMYT, Mexico

Abstract
Systematic screening of genetic resources from a number of different sources, including IWIN nurseries, materials from physiological traits (PT) crosses, mapping populations, exotic genetic resources including landraces, durums and primary synthetic hexaploids, enabled the selection of lines that were included in a set of different panels that represented the core material for research conducted at IWYP-HUB. Almost 1,500 accessions from the different panels were phenotyped to identify lines with "source" and "sink" complementary traits to be incorporated in the pre-breeding pipeline. In addition, these panels were the base of various IWYP research projects. These populations were grown at the IWYP-HUB in Cd. Obregon, NW Mexico, during 2015-2016 for physiological and agronomic characterization and additional genetic analyses were carried out (Sukumaran et al., 2017, these proceedings). The present study shows that between 73 to 93% of the lines were comprised in a phenological range of 10 days for anthesis date. This effect was taken into account and experimental designs were used to block lines of different phenology classes. High genetic variation in final biomass was observed in all the panels, and lines showing almost 50% more biomass than the check with the highest biomass (Sokoll) were identified. However, a trade-off with HI was observed in the panels with high BM. Wide genotypic variation was observed for all partitioning traits in the studied panels, highlighting the correlation between HI and YLD in all panels. As previously demonstrated in a set of elite lines, the investment in internodes 2 and 3 and stems+lamina was negatively correlated with yield and HI, while SPI was positively correlated in most panels, suggesting competition for resources during spike development and the impact on grain yield. Regarding source:sink balance, adaptation to density (ADi) was highly correlated with yield, biomass and number of grains per m^2, indicating that lines better adapted to density have higher yield potential.

Introduction
The ultimate frontier for raising yield potential of crops is to improve photosynthetic capacity and efficiency and translate these extra photoassimilates to the spikes (Reynolds et al., 2011). In recent studies conducted under MasAgro-Trigo using CIRNO C2008, the most cultivated durum wheat variety in the Yaqui Valley (NW-Mexico), well-balanced source:sink was the key to explaining CIRNO's high yield potential, as previously observed in lines with the *Lr19* translocation from *Agropyron elongatum* (Reynolds et al., 2001). We observed that CIRNO establishes a strong grain-sink (large grain number per spike, high grain weight potential and no infertile spikelets per spike) that results in drastically increased radiation use efficiency (RUE) during grain filling, high grain filling rate and, therefore, high yield (Molero et al., unpublished). These results highlight the importance of studying source- and sink-related traits in the same platform to boost yield potential. To do so, three near-term approaches are the main research focus in the IWYP-HUB:

1. Biomass: increase crop biomass by tapping into genetic resources that express favorable growth rate.
2. Harvest index: stabilize and increase expression of harvest index.
3. Source-sink: increase RUE by increasing sink demand for assimilates.

Exploring genetic diversity for biomass
While biomass of elite cultivars has increased modestly in recent years (Shearman et al., 2005; Aisawi et al., 2015), genetic resource screenings have identified biomass values well over those expressed in the best modern cultivars, including primary synthetic lines that under yield potential conditions in Mexico, showed up to 23% more biomass than the check (Reynolds et al., 2015). Under the MasAgro-Trigo project, detailed growth showed genetic diversity for LI and RUE at different phenological stages, suggesting discrete genetic control (Molero et al., 2016). These findings strongly support the case for significant underutilized photosynthetic capacity in existing wheat germplasm. The overarching goal of exploring genetic diversity for biomass is to introduce sources of alleles that can contribute to the expression of high final biomass and other contributing photosynthetic-related traits into a range of elite genetic backgrounds.

Exploring genetic diversity for harvest index and other partitioning traits

While HI still shows significant genetic variation, it is no longer generally associated with yield in the most recent cultivars (Aisawi et al., 2015), indicating that breeders have not been able to fix the trait. The main reason is that the physiological and genetic basis for assimilate partitioning among different plant organs is relatively poorly understood. Nonetheless, in recent studies of wheat yield potential under MasAgro-Trigo, large genetic ranges for dry matter partitioning among plant organs have been reported and some promising leads have been identified (Rivera-Amado, 2016). This variation in the ability to partition resources to grain represents significant untapped yield potential, especially given the generally negative association between HI and biomass in the most modern cultivars (Aisawi et al., 2015; Rivera-Amado et al., 2016). So far, two main phenotypic traits are associated with optimal expression of HI: reduced structural dry matter investment to stem internodes 2 and 3 to enhance spike growth during stem elongation and increased fruiting efficiency (FE) (Foulkes et al., 2015). Therefore, the main objective is to characterize different genotypes with a view to identifying genetic resources with promising expression of HI and related traits for use in pre-breeding, as well as perform physiological and genetic analyses.

Source:sink balance to tap photosynthetic potential

Evidence for genetic variation in source:sink balance (SSB) and its importance in boosting yield and RUE has been presented previously (Reynolds et al., 2001; Sukumaran et al., 2015). It is well established that there is a dynamic interaction in plants between source and sink. Previous experiments in cereals have shown that a high demand for assimilates — determined by sink strength of the grains — can stimulate the supply of photo-assimilates (Reynolds et al., 2005), and vice-versa (Calderini et al., 2001). These studies have demonstrated that wheat plants growing under yield potential conditions have excess photosynthetic capacity, a probable conservative response to the natural risk of losing leaf area or photosynthetic function. As a result, increasing photosynthetic potential does not necessarily optimize grain number (Sadras, 2007), as shown by the negative association observed between harvest index and biomass (Bustos et al., 2013). Therefore, to achieve full expression of yield potential, it will be necessary to optimize the source:sink dynamic by ensuring that expression of grain set matches the photosynthetic potential of current and future genotypes. The main objective of exploring different genetic materials is to select lines that, under high plant density, show both good grain set and good grain-filling characteristics as indicators of a favorable SSB.

All the above information was obtained by exploring traits related to biomass, SSB and HI with a view to combining the best sources in pre-breeding, thereby increasing the probability of pyramiding favorable alleles.

Methods

Germplasm material

Systematic screening of genetic resources from a number of different sources including IWIN nurseries, materials from Physiological Traits (PT) crosses, mapping populations, exotic genetic resources including landraces, durums and primary synthetic hexaploids enabled the selection of lines that were included in a set of different panels (**Fig. 1**) that represented the core material for research conducted at IWYP-HUB.

The High Biomass Association Mapping Panel (HiBAP, 150 lines) is the result of systematic screening of genetic resources from the World Wheat Collection that allowed identifying genotypes with favorable expression of biomass at different growth stages. The panel is composed of a total of 150 spring types, including elite high yield material, pre-breeding lines crossed and selected for high yield and biomass, synthetic derived lines, and appropriate checks. The material has a restricted range of maturity to avoid confounding effects associated with extreme phenology.

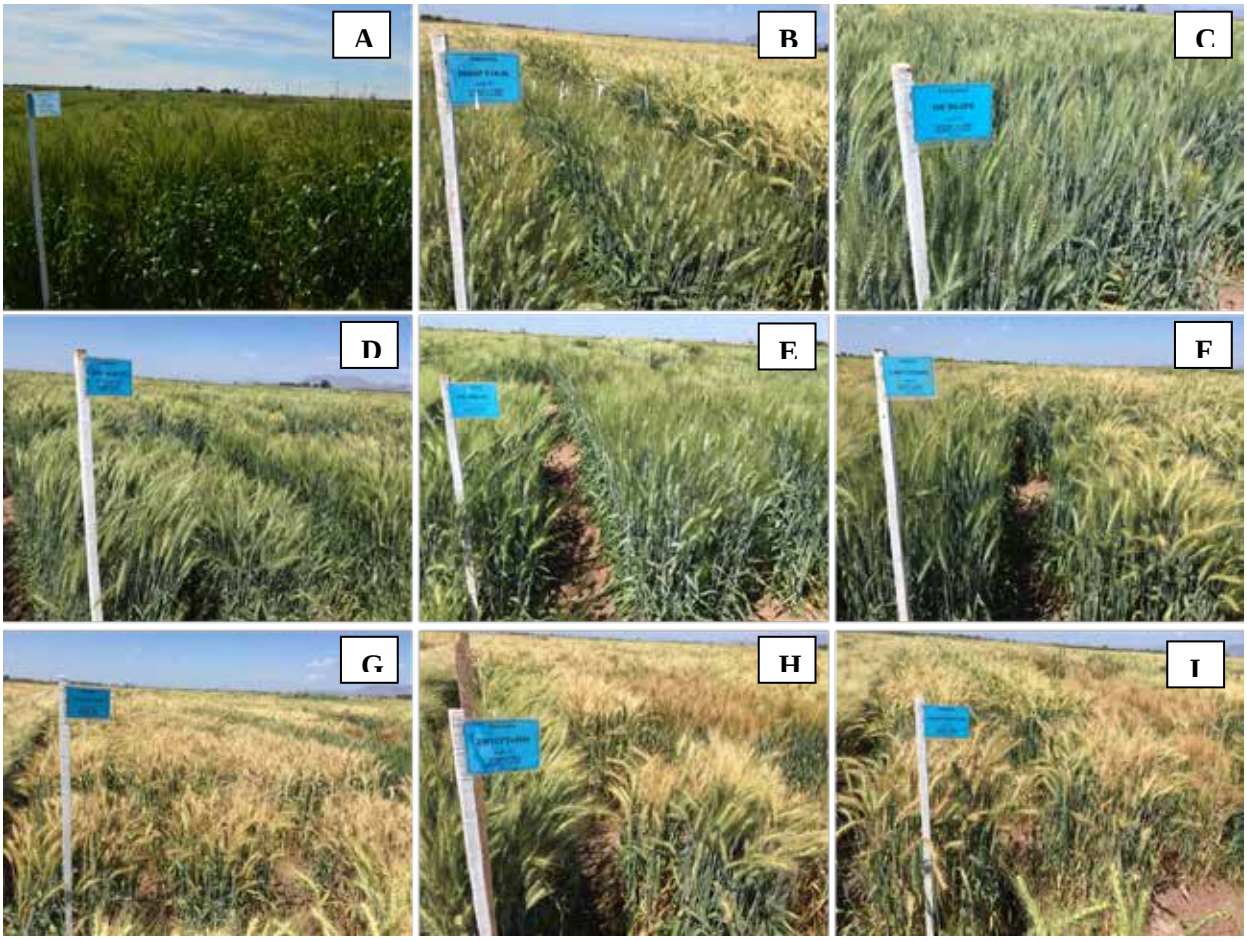

Fig. 1. Main panels that represent the core material for research conducted at IWYP-HUB. A) SynPan, B) HiBAP, C) DH_SNAPE(BCN/WBLL), D) BWDiv, E) DWDiv, F) Cand4WYCYT, G) 1stWYCYT, H) 2nd WYCYT, I) 3rd WYCYT.

Primary Synthetics Diversity Panel (SynPan, 200 lines). CIMMYT has generated 2,000 so-called 'synthetic wheat' genotypes using novel genetic variation in diploid and tetraploid wheat. Field studies have shown that synthetic-derived material can confer significant advantages in terms of yield and biomass under heat stress, a trait that may indicate superior Rubisco, for example (Cossani and Reynolds, 2015). Wheat Physiology recently screened all 2,000 lines under yield potential conditions as well as under heat and drought stress, and identified lines that expressed superior performance under each of these conditions as well as some in combination. A panel of 160 of the best primary synthetics showing high expression of biomass was assembled from screenings under high yield potential conditions.

Progeny of Physiological Trait Crosses + Parents (WYCYTs+Pads). CIMMYT has recently distributed — through the IWIN— a number of nurseries comprising novel elite germplasm designed to combine specific physiological traits associated with increased yield potential (1st to 3rd WYCYT and CAND4thWYCYT, Wheat Yield Collaboration Yield Trials). To plan the strategic crosses at least one parent was selected for favorable expression of biomass –source– and the other for sink traits related to grain yield components. International trials have identified lines with significant genetic gains over elite checks for both yield and biomass.

Bread and Durum Wheat diversity panels (BWDiv, DWDiv). Association panels of selected wheat genetic resources (370 bread wheat; 225 durum wheat) have been assembled from spring wheat sources after screening approximately 70,000 lines for heat and drought adaptation in NW Mexico. They were derived from: (1) international nurseries; (2) wheats with ancestral chromosomal introductions (e.g., 7Ag.7DL,

1B.1R, Lr34, Lr42); (3) landraces (~ 15,000 spring wheat landraces from the World Wheat Collection); and (4) the Focused Identification of Germplasm Strategy (FIGS), a landrace panel that has been selected based on their origin being in regions with abiotic stress (Sehgal et al., 2015).

Mapping populations and parents. Several populations (bi-parental, association mapping, genomic selection and NAM populations) are available at CIMMYT for the genetic dissection of complex traits. A number of suitable RIL populations are available whose parents are elite high yield/biomass lines, some of whose progeny express transgressive segregation for these traits while not expressing a large range of phenology. Among the extant populations, the most relevant include the BCN/Weebil double haploid population (DH-Snape) that combines yield potential traits to generate lines with exceptional yield potential compared to either parent, as recently shown in southern Chile (Bustos et al., 2013).

Phenotypic and agronomic evaluation

Biomass. Diverse sets of spring wheat lines selected as described above were subjected to final biomass (physiological maturity) analysis in representative high yield spring wheat growing environments at the IWYP platform in NW Mexico during 2015-2016. Promising subsets of lines will be selected for more detailed and precise growth analysis in subsequent cycles involving biomass harvests during the growth cycle as well as direct estimates of light extinction.

Harvest index. A wide range of elite genetic resources was screened to identify diversity for HI and related traits including fruiting efficiency (FE), spike partitioning index (SPI), length of stem internodes 2 and 3 (Int2, Int3), flowering time and phenological pattern including relative duration of rapid spike growth phase (RSGP, from initiation of booting to anthesis) and grain filling phase (GFP, from anthesis to physiological maturity).

Source:sink. Recent work focusing on genetic variation for adaptation to agronomic planting density (Sukumaran et al., 2015) has demonstrated a high-throughput alternative based on a planting system (4 rows per bed vs. the conventional 2 rows) that allows different rows of the same plot to be evaluated under distinct light regimes. Experiments for SSB were sown in a high density system. Adaptation to density index (*ADi*) was calculated as the ratio between yield from inner rows divided by yield from outer rows (Yld Inner/Yld outer).

Results and Discussion

Phenological range for days to anthesis

One of the concerns when measuring large populations is that they tend to encompass a large range of phenology which can confound phenotypic and genetic analysis (Pinto et al., 2010). To overcome this problem, a number of these panels and mapping populations were developed or selected to restrict the range of phenology (Fig. 1A, 1B, 1C). In the other panels, experimental designs are used to block lines of different phenology classes (Fig. 1D, 1E and 1F). In all the panels, most of the lines (73-93%) were comprised in a phenological range of 10 days for anthesis date. In the case of HiBAP, WYCYTs and DH_BCN/WBLL, the phenological ranges between the earliest and the latest line were 18, 24 and 16 respectively. In the case of the diversity panels, SynPan, BWDiv and DWDiv, the phenological range was much broader, being 34, 38 and 35 days, respectively, between the earliest and the latest line.

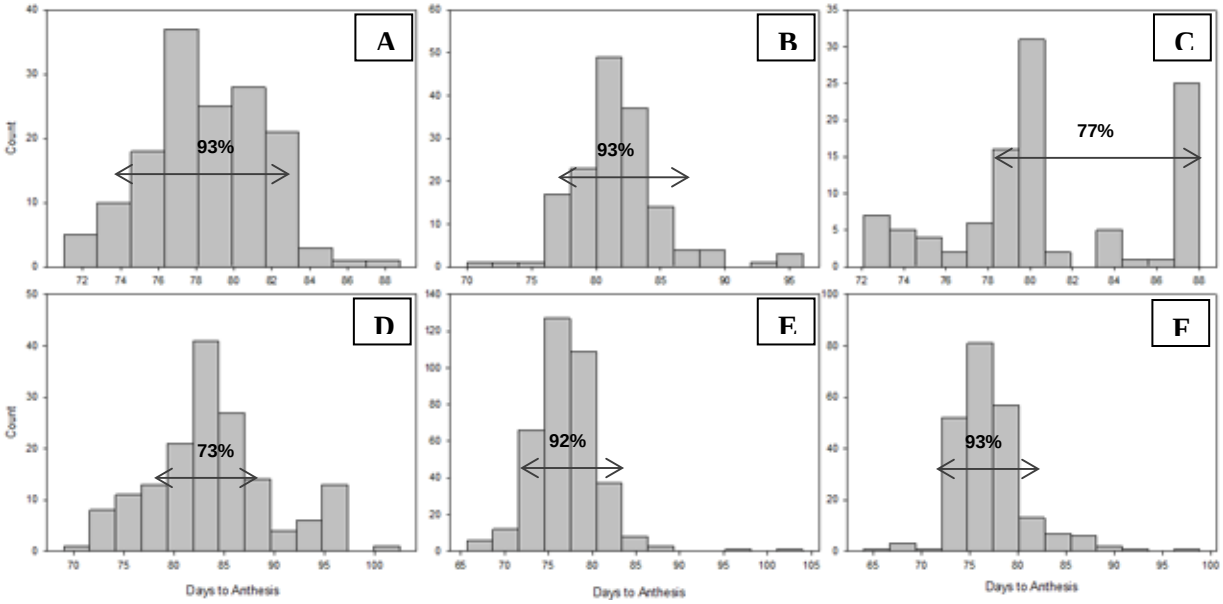

Fig. 1. Histogram representing days to anthesis from the lines in the different panels: A) HiBAP, B) WYCYTs, C) DH_BCN/WBLL, D) SynPan, E) BWDiv and F) DWDiv. The numbers in the graph indicate the percentage of lines comprised in a phenological range of 10 days.

Phenotypic variation for biomass

While theory suggests that radiation use efficiency (RUE) of wheat and other C3 crops can be improved by at least 50%, this will require considerable research focusing on cellular and sub-cellular processes (Zhu et al., 2010). In the meantime, identification of germplasm with high biomass expression can be used as a near-term approach to boost yield potential. In the IWYP-HUB, biomass at physiological maturity was measured in almost 1,300 lines showing genotypic variation among lines (P<0.001) in all the panels (**Fig. 2**).

Overall, SynPan presented lines with the highest biomass (Fig. 2), where 44% of the lines had higher biomass (up to 35% more) than the best check in biomass (Sokoll).

The progeny of Physiological Trait Crosses (1st to 3rd WYCYT and Cand4th WYCYT, Wheat Yield Collaboration Yield Trials) also included lines with high biomass at physiological maturity. In the combined analysis of the 1st to 3rd WYCYT, 23% of the lines had higher biomass than Sokoll, with the top line showing 47% more biomass. Among the candidate progeny for the new international nursery that was released during 2016 (Cand4th WYCYT), 50% of the lines had higher biomass than Sokoll, with the top lines having 20% more.

In the panel composed by lines showing higher biomass at different phenological stages (HiBAP), almost 40% of the lines had higher biomass than Sokoll, with lines showing 34% higher biomass. Panels BWDiv, DWDiv and DH_BCN/WBLL were sown later in the cycle, which may explain the lower absolute values for biomass. Compared with the best check in biomass, only 15% of the lines from BWDiv had higher biomass than Sokoll, with lines showing 20% more. In the case of DWDiv, 73% of the lines had higher biomass than Sokoll, with lines showing up to 50% more. However, HI of this line was 0.18, while in the other panels, lines with the highest biomass presented values between 0.31-0.49.

For HiBAP and SynPan, a negative correlation between HI and biomass was observed, as previously reported (Aisawi et al., 2015). This negative correlation was not observed in the WYCYTs, suggesting the success in the PT progeny combining lines with good source:sink balance (Reynolds et al., these proceedings).

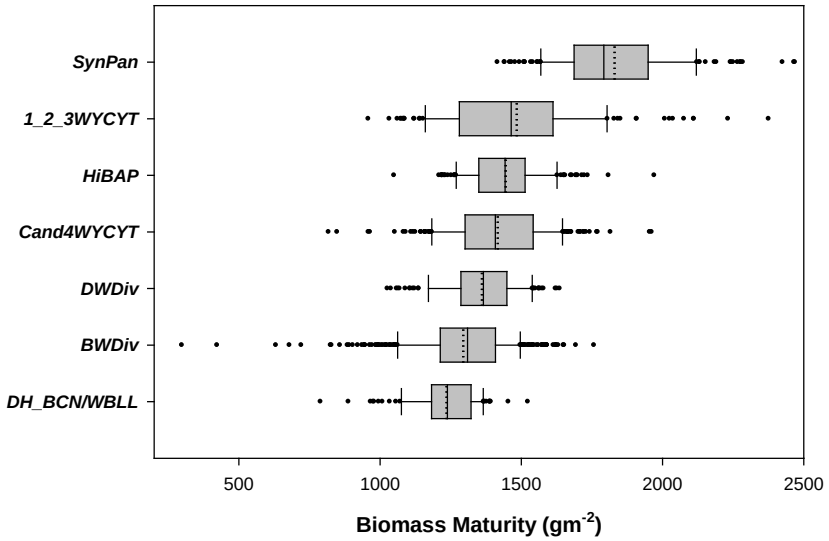

Fig. 2. Variation in biomass measured at physiological maturity in different panels at the IWYP-HUB evaluated during 2015-2016. The panels were organized from the one who presented the highest mean value (SynPan) until the one with the lowest (DH_BCN/WBLL). The box-whisker plots report the distribution of the data. The left and right part of the rectangles (box) give the estimated 25th and 75th percentile, the line in the middle indicates the median value, the dotted line shows the mean, the error bars (whisker) represent 10th and 90th percentiles and the black dots handle the outliers.

Exploring genetic diversity for harvest index and other partitioning traits

Partitioning-related traits were evaluated in almost 1,500 genotypes showing genotypic variation for all the panels studied. In the present report, only the most relevant panels are presented in Table 1 (HiBAP, SynPan, BWDiv, DWDiv and DH_BCN/WBLL).

Table 1. Broad-sense heritability (h^2), mean, significance of the genotype and coefficient of correlation (r) with yield (YLD) and final biomass (BM) with partitioning traits for different panels studied during 2015-2016 in IWYP-HUB. HI: Harvest Index; Int2: Length of internode 2; Int3: Length of internode 3; StLamPI: Stem+Lamina partitioning index (only stem partitioning index for HiBAP and SynPan); SPI: Spike partitioning index; FE: Fruiting Efficiency; RSGP: Rapid Spike Growth Phase; GFP: percentage of grain filling. Values highlighted in black are statistically significant.

		HI	Int2	Int3	StLamPI*	SPI	FE	RSGP	GFP
HiBAP (n=150)	h^2	0.80	0.77	0.79	0.80	0.69	0.60	0.81	0.86
	Mean	0.48	19.0	13.9	0.511	0.268	56.7	10.8	33.3
	P-Value (G)	**0.00**	**0.00**	**0.00**	**0.00**	**0.00**	**0.00**	**0.00**	**0.00**
	r (YLD)	**0.21**	0.08	-0.03	0.10	-0.04	**0.26**	0.08	0.03
	r (BM)	**-0.43**	0.02	**0.17**	**0.23**	-0.15	0.00	**0.20**	**-0.17**
SynPan (n=160)	h^2	0.96	0.84	0.91	0.88	0.59	0.90		0.94
	Mean	0.32	20.2	16.6	0.539	0.210	32.4		31.5
	P-Value (G)	**0.00**	**0.00**	**0.00**	**0.00**	**0.00**	**0.00**	-	**0.00**
	r (YLD)	**0.89**	**-0.36**	**-0.61**	**-0.63**	**0.23**	**0.81**		**0.18**
	r (BM)	**-0.33**	**0.24**	**0.27**	**0.19**	-0.15	**-0.27**		**0.16**
BWDiv (n=370)	h^2	0.91	0.89	0.91	0.78	0.78	0.81		0.77
	Mean	0.47	20.9	15.0	0.743	0.257	45.8		31.9
	P-Value (G)	**0.00**	**0.00**	**0.00**	**0.00**	**0.00**	**0.00**	-	**0.00**
	r (YLD)	**0.66**	**-0.32**	**-0.21**	**-0.32**	**0.32**	**-0.16**		**0.12**
	r (BM)	**0.30**	**-0.15**	-0.04	**-0.14**	**0.14**	**-0.13**		-0.03
DWDiv (n=225)	h^2	0.97	0.89	0.92	0.93	0.93	0.88		0.87
	Mean	0.45	17.4	13.2	0.735	0.265	38.6		31.9
	P-Value (G)	**0.00**	**0.00**	**0.00**	**0.00**	**0.00**	**0.00**	-	**0.00**
	r (YLD)	**0.75**	**-0.45**	**-0.35**	**-0.40**	**0.40**	**0.28**		**0.49**
	r (BM)	0.04	-0.05	0.01	0.01	-0.01	0.01		0.01
DH_BCN/WBLL (n=108)	h^2	0.85	0.85	0.67	0.74	0.74	0.68	0.80	0.89
	Mean	0.48	17.9	13.2	0.696	0.304	52.4	16.6	26.0
	P-Value (G)	**0.00**	**0.00**	**0.00**	**0.00**	**0.00**	**0.00**	**0.00**	**0.00**
	r (YLD)	**0.48**	-0.13	**0.54**	**0.51**	**-0.51**	**0.37**	**-0.20**	**0.28**
	r (BM)	-0.02	0.10	**0.45**	**0.25**	**-0.25**	0.14	-0.07	0.11

*for HiBAP, SynPan, stem partitioning index is presented, for the rest of panels is the sum of the stems+lamina

A step change in the expression of harvest index (HI) underpinned the dramatic yield gains of the Green Revolution, and steady genetic gains in HI were associated with yield improvements of semi-dwarf wheat until the late 1990s (Reynolds et al., 1999). Despite this, HI still expresses significant genetic variation in the most panels including in modern cultivars (HiBAP) –vary in the range of 0.39 to 0.53 while in the other panels wider variations were observed (i.e., BWDiv 0.18-0.56, DWDiv 0.16-0.53). This variation in the ability to partition resources to grain represents significant untapped yield potential, especially given the generally negative association between HI and biomass in panels with the highest biomass (Table 1), while both traits (BM and HI) were positively related with yield.

As previously demonstrated in a set of elite wheat lines (Rivera-Amado et al., 2016), the investment in internodes 2 and 3 and stems+lamina was negatively correlated with yield, while SPI was positively correlated in most panels (Table 1), suggesting competition for resources during spike development. HI was also negatively correlated with Int2, Int3 and StemPI suggesting that investing in these organs reduces the ability of the plant to partition assimilates to the grain.

In the case of FE, positive correlations with yield were observed in all panels except BWDiv, where there was a negative correlation (Table 1).

The positive correlation between GFP and yield in most of the panels indicates a positive effect on the duration of grain filling where GFP was positively associated with higher radiation use efficiency during grain filling ($P<0.01$) and higher HI ($P<0.001$).

Adaptation to the density of the IWYP-HUB panels

The hypothesis of studying adaptation to the density of the panels is based on earlier studies by the team (Reynolds et al., 1994; Sukumaran et al., 2015) and infers that low yield potential lines respond more to reduced competition for light under low planting density than high yield potential lines. Our results from the first year of evaluation indicated that high yield potential lines showed less variation in YLD between high and low plant densities (data not shown). The GNO also exhibited a similar trend, but TGW showed no response to plant density.

In the specific case of HiBAP, on average, inner rows yielded 21% less than outer rows, and the yield of inner rows ranged from 9.8 to 30% of the yield of outer rows. Inner rows had 18% less GNO, with a range of 13.6 to 28.6% of outer rows. For TGW, on average, the outer rows had an insignificantly 4% higher TGW than the inner rows (Table 2).

A comparison of inner and outer rows in the pre-breeding material evaluated during 2015-2016 (Wheat Yield Collaboration Yield trials, WYCYTs), showed that outer rows in general had 10% higher YLD and 6% higher GNO (Table 2). These estimates are lower than estimates previously observed in WAMI (Sukumaran et al., 2015), suggesting that new lines derived from strategic crosses for yield potential are in general better adapted to density; however, this result needs to be confirmed in a second year.

Table 2. Mean, min, max, repeatability, LSD test differences (P<0.05) and P-value G (genotypes) estimates in HiBAP and a combined analysis from the 1st, 2nd and 3rd WYCYT analyzed as RCBD and using mixed model for grain yield (YLD), 1000-grain weight (TGW), and grain number (GNO) studied in IWYP-HUB at Ciudad Obregon, Mexico, during 2015-2016 under four-row planting (I, inner two rows; O, outer two rows). Values for YLD and GNO are estimated per unit length (grams per meter).

	HiBAP (n=150)						**WYCYTs (n=141)**					
	YLD		**TGW**		**GNO**		**YLD**		**TGW**		**GNO**	
	——g m^{-1}——		—— g ——		— grains m^{-1}—		——g m^{-1}——		—— g ——		— grains m^{-1}—	
	I	*O*	*I*	*O*	*I*	*O*	*I*	*O*	*I*	*O*	*I*	*O*
Mean	242	308	44.5	46.4	5496	6706	264	294	42.5	44.3	6275	6662
Min	152	217	29.3	30.7	3416	4782	136	130	21.7	20.6	3491	3559
Max	371	411	54.9	57.6	8056	9320	615	448	54.3	54.4	15437	9874
Repeatability	0.806	0.734	0.953	0.961	0.83	0.775	0.602	0.454	0.938	0.942	0.646	0.425
LSD	64	61	3.7	3.7	1483	1499	130	116	3.8	3.6	3029	2542
P-value (G)	***0.00***	***0.00***	***0.00***	***0.00***	***0.00***	***0.00***	***0.00***	***0.00***	***0.00***	***0.00***	***0.00***	***0.001***

Adaptation to density index (ADi) was calculated as the ratio between YLD from inner rows divided by YLD from outer rows (YLD_{IN}/YLD_{OUT}). Good values for broad-sense heritability (h^2) were obtained for the ADi and statistical differences among genotypes were observed in HiBAP (P<0.001) and in the 1st, 2nd and 3rd WYCYT (P<0.001). The ADi was highly correlated with yield, biomass and number of grains per m^2 in both sets of materials (Table 3), indicating that lines better adapted to density have higher yield potential. The robustness of ADi will be achieved with 2 years of data, as previously reported (Sukumaran et al., 2015), and a combined analysis using data from the evaluation during 2016-2017 will be performed.

Table 3. Broad-sense heritability (h^2), phenotypic range, significance of the genotypes (P Gen) and correlations of with yield (YLD), biomass (BM) and number of grains per m^2 (GM2) for adaptation to density index (ADi) calculated as YLD_{IN}/YLD_{OUT} for the HiBAP experiments (consisting of 150 elite spring wheats) and a combined analysis of the 1st, 2nd and 3rd WYCYT (consisting of 141 lines).

	ADi (I/O)	
	HiBAP	WYCYTs
h^2	0.763	0.442
Phenotypic range Mean [Min-Max]	0.8 [0.45-1.55]	0.93 [0.43-1.7]
P(Gen)	**<0.001**	**<0.001**
Correl YLD	**0.001**	**<0.001**
Correl BM	**0.014**	**<0.001**
Correl GM2	**0.022**	**<0.001**

These studies will continue during 2016-2017 with the objective of identifying lines better adapted to high density through a combined analysis and incorporating them as parents in strategic crosses during 2018.

Conclusions

- The present study shows how, even the presence of extreme lines in phenology in diversity panels, most of the lines were comprised in a range of phenology of 10 days for anthesis date.
- High genetic variation in final biomass was observed in all the panels, and lines showing almost 50% more biomass than the check with the highest biomass (Sokoll) were identified. However, a trade-off with HI was observed for the panels with high BM.
- Wide genotypic variation was observed for all partitioning traits in the studied panels, highlighting the correlation between HI and YLD in all panels.
- As previously demonstrated in a set of elite lines, the investment in internodes 2 and 3 and stems+lamina was negatively correlated with yield, while SPI was positively correlated in most panels, suggesting competition for resources during spike development.
- ADi was highly correlated with yield, biomass and number of grains per m^2, indicating that lines better adapted to density have higher yield potential.

References

Aisawi KAB, Reynolds MP, Singh RP, Foulkes MJ. 2015. The Physiological Basis of the Genetic Progress in Yield Potential of CIMMYT Spring Wheat Cultivars from 1966 to 2009. Crop Science 55, 1749–1764.

Bustos D V., Hasan AK, Reynolds MP, Calderini DF. 2013. Combining high grain number and weight through a DH-population to improve grain yield potential of wheat in high-yielding environments. Field Crops Research 145, 106–115.

Calderini DF, Savin R, Abeledo LG, Reynolds MP, Slafer GA. 2001. The importance of the period immediately preceding anthesis for grain weight determination in wheat. Euphytica 119, 199–204.

Cossani CM, Reynolds MP. 2015. Heat stress adaptation in elite lines derived from synthetic hexaploid wheat. Crop Science 55, 2719–2735.

Foulkes M, Rivera-Amado A, Trujillo E, Sylvester-Bradley R, Reynolds MP. 2015. Achieving a Step-Change in Harvest Index in High Biomass Wheat Cultivars. In: Reynolds MP,, In: Molero G, In: Mollins J,, In: Braun HJ, eds. Proceedings of the International TRIGO (Wheat) Yield Potential Workshop 2015. CENEB, CIMMYT, Cd. Obregón, Sonora, Mexico, 24-26 March 2015. Mexico, D.F.: CIMMYT, 31–35.

Molero G, Slafer G, Rivera-Amado A, *et al.* 2016. Traits determining differences in yield potentialamong elite lines of a spring wheat panel with the view to accelerating genetic gains. In:Reynolds M,, In: Molero G,, In: Quilligan E, eds. Proceedings of the 2nd International TRIGO (Wheat) Yield

Potential Workshop 2016. CENEB, CIMMYT, Cd. Obregón, Sonora, Mexico, 9-10 March 2016. Mexico, D.F.: CIMMYT, 25–34.

Pinto RS, Reynolds MP, Mathews KL, McIntyre CL, Olivares-Villegas J-J, Chapman SC. 2010. Heat and drought adaptive QTL in a wheat population designed to minimize confounding agronomic effects. Theoretical and applied genetics. 121, 1001–21.

Reynolds MP, Acevedo E, Sayre KD, Fischer RA. 1994. Yield potential in modern wheat varieties: its association with a less competitive ideotype. Field Crops Research 37, 149–160.

Reynolds MP, Bonnett D, Chapman SC, Furbank RT, Manès Y, Mather DE, Parry M a J. 2011. Raising yield potential of wheat. I. Overview of a consortium approach and breeding strategies. Journal of experimental botany 62, 439–52.

Reynolds M, Calderini D, Condon A, Rajaram S. 2001. Physiological basis of yield gains in wheat associated with Lr19 translocation from Agropyron elongatum. Euphytica 119, 137–141.

Reynolds MP, Pask A, Torres A, *et al.* 2015. Pre-Breeding for Yield Potential: Summary of International Data from 2nd WYCYT and Performance of Pipeline Material. Proceedings of the International TRIGO (Wheat) Yield Potential Workshop. CENEB, CIMMYT, Cd. Obregón, Sonora, Mexico, 24-26 March 2015. Mexico, DF: CIMMYT, 17–22.

Reynolds MP, Pellegrineschi a, Skovmand B. 2005. Sink-limitation to yield and biomass: a summary of some investigations in spring wheat. Annals of Applied Biology 146, 39–49.

Reynolds MP, Rajaram S, Sayre KD. 1999. Physiological and Genetic Changes of Irrigated Wheat in the Post–Green Revolution Period and Approaches for Meeting Projected Global Demand. Crop Science 39, 1611–1621.

Rivera-Amado C. 2016. Optimizing assimilate partitioning in wheat for genetic enhancement of spike fertility and yield potential. PhD Thesis, University of Nottingham School of Biosciences, Sutton Bonnington Campus, Leistershire, UK.

Rivera-Amado A, Trujillo-Negrellos E, Sylvester-Bradley R, Molero G, Sierra-Gonzalez A, Reynolds M, Foulkes M. 2016. Achieving increases in spike growth, fruiting efficiency, and harvest index in high biomass wheat cultivars. In: Reynolds M,, In: Molero G,, In: Quilligan E, eds. Proceedings of the 2nd International TRIGO (Wheat) Yield Potential Workshop 2016. CENEB, CIMMYT, Cd. Obregón, Sonora, Mexico, 9-10 March 2016. Mexico, D.F.: CIMMYT, 70–76.

Sadras VO. 2007. Evolutionary Aspects of the Trade-off Between Seed Size and Number in Crops Field Crops Research 100, 125–138.

Sehgal D, Vikram P, Sansaloni CP, *et al.* 2015. Exploring and Mobilizing the Gene Bank Biodiversity for Wheat Improvement. Plos One 10, e0132112.

Shearman VJ, Scott RK, Foulkes MJ. 2005. Physiological Processes Associated with Wheat Yield Progress in the UK. Crop Science 45, 175–185.

Sukumaran S, Reynolds MP, Lopes MS, Crossa J. 2015. Genome-Wide Association Study for Adaptation to Agronomic Plant Density: A Component of High Yield Potential in Spring Wheat. Crop Science 55, 1–11.

Zhu X-G, Long SP, Ort DR. 2010. Improving photosynthetic efficiency for greater yield. Annual review of plant biology 61, 235–61.

Genetic gains in wheat under high yield and heat stressed conditions resulting from physiological breeding

Matthew P. Reynolds[1], Alistair J.D. Pask[1], Sivakumar Sukumaran[1], Gemma Molero[1], William J.E. Hoppitt[2], Kai Sonder[1], Carolina Saint Pierre[1], Thomas Payne[1], Ravi P. Singh[1], Hans J. Braun[1], Fernanda G. Gonzalez[3], Ignacio I. Terrile[3], Naresh C.D. Barma[4], Abdul Hakim[4], Zhonghu He[5], Zheru Fan[6], Dario Novoselovic[7], Maher Maghraby[8], Khaled I.M. Gad[9], ElHusseiny G. Galal[9], Adel Hagras[9], Mohamed M. Mohamed[9], Abdul Fatah A. Morad[9], Uttam Kumar[10], Gyanendra P. Singh[11], Rudra Naik[12], Ishwar K. Kalappanavar[12], Suma Biradar[12], Sakuru V.S. Prasad[13], Ravish Chatrath[14], Indu Sharma[14], Kishor Panchabhai[15], Virinder S. Sohu[16], Gurvinder S. Mavi[16], Vinod K. Mishra[17], Arun Balasubramaniam[17], Mohammad R. Jalal-Kamali[18], Manoochehr Khodarahmi[19], Manoochehr Dastfal[19], Seyed M. Tabib-Ghaffari[19], Jabbar Jafarby[19], Ahmad R. Nikzad[19], Hossein Akbari Moghaddam[19], Hassan Ghojogh[20], Asghar Mehraban[20], Ernesto Solís-Moya[21], Miguel A. Camacho-Casas[21], Pedro Figueroa-López[21], Javier Ireta Moreno[21], Jorge I. Alvarado-Padilla[21], Alberto Borbón-Gracia[21], Araceli Torres[22], Yei Nayeli Quiche[22], Shesh R. Upadhyay[23], Deepak Pandey[23], Muhammad Imtiaz[24], Monsif U. Rehman[24], Manzoor Hussain[25], Makhdoom. Hussain[26], Riaz Ud-Din[27], Maqsood Qamar[27], Sohail Kundi[27], Muhammad Y. Mujahid[27], Gulzar Ahmad[28], Abdul J. Khan[29], Mahboob A. Sial[30], Pompiliu Mustatea[31], Eben von Well[32], Moses Ncala[32], Stephan de Groot[33], Abdelraheem H.A. Hussein[34], Izzat S.A. Tahir[34], Amani A.M. Idris[34], Hala M.M. Elamein[34], Arun K. Joshi[35]

[1]CIMMYT, Mexico; [2]Leeds University, UK; [3]Instituto Nacional de Tecnología Agropecuaria, Pergamino, Argentina; [4]Bangladesh Agricultural Research Institute, Bangladesh; [5]CIMMYT, China; [6]Xinjiang Academy of Agricultural Science, Wulumuqi, China; [7]Agricultural Institute Osijek, Osijek, Croatia; [8]CIMMYT, Egypt; [9]Field Crops Research Institute, Egypt; [10]CIMMYT BISA, India; [11]Indian Agricultural Research Institute, New Delhi, India; [12]University of Agricultural Sciences, Dharwad, India; [13]Indian Agricultural Research Institute, Indore, India; [14]Indian Institute of Wheat and Barley Research, Karnal, India; [15]Syngenta India Ltd., Karnal, India; [16]Punjab Agricultural University, Ludhiana, India; [17]Banaras Hindu University, Varanasi, India; [18]CIMMYT, Iran; [19]Seed and Plant Improvement Institute, Iran; [20]Dryland Agricultural Research Institute, Iran; [21]Instituto Nacional de Investigaciones Forestales, Agrícolas y Pecuarias, Mexico; [22]CIMMYT CENEB, Mexico; [23]Nepal Agriculture Research Council, Bhairahawa, Nepal; [24]CIMMYT, Pakistan; [25]Regional Agricultural Research Institute, Bahawalpur, Pakistan; [26]Wheat Research Institute, Ayub Agricultural Research Institute Faisalabad, Pakistan; [27]Crop Sciences Research Institute, National Agricultural Research Council, Islamabad, Pakistan; [28]Cereal Crop Research Institute, Nowshera-Pirsabak, Pakistan; [29]Nuclear Institute for Food and Agriculture, Tarnab-Peshawar, Pakistan; [30]Nuclear Institute of Agriculture, Tando-Jam, Pakistan; [31]National Agricultural Research and Development Institute, Fundulea, Romania; [32]Small Grain Institute, Bethlehem, South Africa; [33]Sensako Pty Ltd., Bethlehem, South Africa; [34]Agricultural Research Corporation, Wad Medani, Sudan; [35]CIMMYT, Nepal.

Abstract

Physiological trait (PT) information of parents can be used to make strategic crosses, increasing the probability of pyramiding favorable alleles compared to crossing simply on the basis of yield. Here at least one parent was selected for favorable expression of biomass –source– and the other for sink traits related to grain yield components. Generally, female parents were selected from genetic resources –including landraces, introductions, and primary synthetic lines– that had been selected for high yield potential or under heat stress, while CIMMYT elite lines with disease resistance and wide adaptation were used as males based on testing at hundreds of international sites via the International Wheat Improvement Network (IWIN). Cross progenies were advanced to F_4, and populations ($F_{4:5}$) derived from single plants were yield tested for two generations ($F_{4:5}$ and $F_{4:6}$) in respective environments simulating target mega-environments to select lines for international nurseries, targeted to high yield and heat stressed environments, respectively. All of the nurseries were grown as multi-location yield trials at up to 32 international sites. Most new PT-derived lines expressed higher yield and biomass than local checks in almost all sites. A number of new PT lines expressed higher yield and biomass than CIMMYT elite checks. Results support –in a realistic breeding context– the hypothesis that yield and radiation use efficiency can be increased by crossing complementary physiological traits.

Introduction

Genetic yield gains in spring wheat are currently around 0.5-1% annually (Crespo et al., 2017), resulting from unspecified recombination of minor genes among elite germplasm, as well as the introduction of novel genetic diversity typically associated with disease resistance and grain quality. Physiological breeding complements this approach by using well-characterized genetic resources to make strategic trait-based crosses, increasing the probability of accumulating favorable genes compared to using physiologically uncharacterized parents (Reynolds and Langridge, 2016). Since the genetic bases explaining cultivar-level differences in yield are generally not available for wheat, physiological breeding relies heavily on phenotypic data. The advent of affordable high-throughput phenotyping tools provides a means to screen a larger genepool for selecting parents (Tattaris et al., 2016). In this study, crossing schemes were implemented to complement "source" with "sink" traits, with one parent being selected for favorable expression of biomass (source) and the other for favorable expression of sink-related traits including grain yield components. A principal objective was to test, in a realistic breeding context, the hypothesis that combining source with sink traits can accelerate genetic gains in wheat.

Materials and Methods

Germplasm

Parents for trait-based crossing came from a number of different sources including IWIN nurseries (Braun et al., 2010), and more exotic genetic resources including landraces, introductions (FIGS), and primary synthetic hexaploids. In this study, two types of nurseries were developed using almost the same breeding methodology; one targeting high yield potential irrigated environments (Wheat Yield Collaboration Yield Trial, WYCYT) and the other targeting heat stressed, irrigated environments (Stress Adaptive Trait Yield Nursery, SATYN). In both cases, crosses were designed so that at least one parent was selected for favorable expression of biomass (source) and the other for favorable expression of sink-related traits – including harvest index (HI), grain number per m^2 (GNO), thousand-grain weight (TGW), spike density (SPM2), and grains per spike (GSP)–, under their respective yield potential and irrigated heat stress environments. Two classes of check were used in this study: (1) local checks (LCH) selected by national program collaborators –when they sow the trial– that represent their best available advanced lines adapted to local conditions; and (2) elite CIMMYT advanced lines (ECH), selected based either on their superior performance in experiments at the breeding site or on recent international performance data.

Breeding methodology

Physiological trait crosses are designed to combine source and sink traits in a 5-year time frame. Growing conditions at the CIMMYT Obregon breeding station (27° 20' N; 109° 54' W; 38 m above sea level) are that of an irrigated, spring wheat growing environment. Most selection was done at this site, namely: crossing; selection for traits (plant type, phenology and leaf rust resistance which were made in F_2 and F_4 bulks of 3000-4000 plants/cross), yield measured in small F_5 yield plots derived from the seed of selected individual F_4 plants (augmented designs); and yield and yield components at F_6 in replicated trials. The F_1, F_3 generations were selected at CIMMYT El Batán experiment station (19° 31' N; 98° 50' W; 2,249 m above sea level), a rainfed, temperate, spring wheat growing environment with high disease pressure. Crossing and selection were performed in the field without fungicide in order to incorporate an acceptable level of disease resistance which would otherwise confound yield data in international trials. In the case of the SATYN, segregating generations up to F_3 were sown in the same environment as the WYCYT, but selections in F_4 and beyond were made under heat stress by delayed sowing.

Evaluation of performance at international sites

The trials were grown at multiple sites located across the main wheat growing regions worldwide, providing contrasting spring wheat production environments (Table 1). At most sites, SATYN trials were planted later than WYCYT trials to increase exposure to heat stress. Trials were grown under well managed conditions; at all sites appropriate fertilization was applied to avoid yield limitations, while weed, disease, and pest control measures were applied according to local best practices. Irrigation was applied by gravity-fed flood irrigation, and both trials were grown under fully irrigated conditions. The 2nd and 3rd WYCYT were grown in the 2013/14 and 2015/16 wheat cycles, respectively, both with 42 lines; and the 2nd and 4th SATYN were grown in the 2012/13 and 2014/15 wheat cycles, respectively, consisting of 50 and 28 lines, respectively. The experimental design at each location was a randomized alpha-lattice with two replications per entry.

Table 1. Details of sites growing pre-breeding nurseries during spring wheat seasons 2012/13 to 2015/16.

Country	Site	Institution	T max	T min	2WYCYT	3WYCYT	2SATYN	4SATYN
Argentina	Pergamino	Instituto Nacional de Tecnología Agropecuaria (INTA-EEA)	24.0	11.7	Aug-14	ns	ns	ns
Bangladesh	Dinajpur	Bangladesh Agricultural Research Institute	26.2	13.7	Dec-13	*	ns	Dec-14
Bangladesh	Joydebpur	Bangladesh Agricultural Research Institute	27.0	15.6	Nov-13	*	Dec-12	Dec-14
Bangladesh	Rajshahi	Bangladesh Agricultural Research Institute	27.9	14.6	Nov-13	ns	ns	*
China	Urumqi	Junhu Wheat Experiment Station of Changji	21.6	9.3	*	Apr-16	ns	*
Croatia	Osijek	Agricultural Institute Osijek	9.0	1.1	ns	Oct-15	ns	ns
Egypt	Assiute	Field Crops Research Institute	25.0	8.4	Dec-13	ns	ns	ns
Egypt	Nubaria	Field Crops Research Institute	21.4	10.7	ns	*	ns	Dec-14
Egypt	Sakha	Field Crops Research Institute	21.1	11.4	ns	Dec-15	ns	ns
Egypt	Sids	Field Crops Research Institute	23.0	10.1	ns	Dec-15	ns	ns
Egypt	Sohag	Field Crops Research Institute, Shandaweel	25.4	8.8	ns	Dec-15	Dec-12	ns
Egypt	Tanta	Field Crops Research Institute, Gemmeiza	25.4	8.8	ns	Dec-15	ns	ns
India	Dharwad	University of Agricultural Sciences	31.8	18.6	Nov-13	ns	*	Dec-14
India	Indore	Indian Agricultural Research Institute	29.4	12.6	Nov-13	*	Nov-12	Dec-14
India	Jabalpur	Borlaug Institute for South Asia, Jabalpur	28.0	12.4	Nov-13	ns	ns	Nov-14
India	Karnal	Indian Institute for Wheat and Barley Research	24.4	10.1	Nov-13	Nov-15	Nov-12	Dec-14
India	Karnal_Syngenta	Syngenta Rice farm	24.8	10.3	ns	Nov-15	ns	ns
India	Ladhowal	Borlaug Institute for South Asia, Ludhiana	24.0	9.8	Nov-13	ns	ns	Nov-14
India	Ludhiana	Punjab Agricultural University	24.0	9.8	Nov-13	Nov-15	Nov-12	Dec-14
India	New Delhi	Indian Agricultural Research Institute	25.2	10.8	Nov-13	Nov-15	*	Dec-14
India	Pusa	Borlaug Institute for South Asia, Samastipur	26.8	13.4	ns	ns	ns	Nov-14
India	Ugar_Khurd	University of Agricultural Sciences, Dharwad	32.7	18.4	*	Nov-15	Nov-12	Dec-14
India	Varanasi	Banaras Hindu university	29.3	14.0	Dec-13	Nov-15	Dec-12	Dec-14
Iran	Darab	Seed and Plant Improvement Institute, Hasan Abad	18.0	3.8	Dec-13	Dec-15	ns	*
Iran	Dezfoul	Seed and Plant Improvement Institute, Safiabad	23.0	9.6	Dec-13	Dec-15	Dec-12	Nov-14
Iran	Gonbad	Seed and Plant Improvement Institute, Gonbad	13.0	3.5	ns	Nov-15	ns	ns
Iran	Gonbad	Dryland Agricultural Research Institute, Gonbad	14.6	4.2	ns	Nov-15	ns	ns
Iran	Karaj	Seed and Plant Improvement Institute, Karaj	11.9	2.6	Nov-13	ns	Oct-12	ns
Iran	Parsabad	Dryland Agricultural Research Institute, Parsabad	9.2	0.4	ns	Nov-15	ns	ns
Iran	Shiraz	Seed and Plant Improvement Institute, Zarghan	15.5	1.6	Nov-13	Nov-15	ns	Nov-14
Iran	Zabol	Seed and Plant Improvement Institute, Zahak	21.7	6.7	ns	ns	ns	Nov-14
Mexico	Celaya	Instituto Nacional de Investigaciones Forestales, Agrícolas y Pecuarias	26.2	9.0	*	*	ns	Dec-14
Mexico	Los Mochis	Instituto Nacional de Investigaciones Forestales, Agrícolas y Pecuarias	31.0	12.2	*	Dec-15	ns	*
Mexico	Obregon	Instituto Nacional de Investigaciones Forestales, Agrícolas y Pecuarias	29.3	12.9	*	Dec-15	ns	*
Mexico	Mexicali	Instituto Nacional de Investigaciones Forestales, Agrícolas y Pecuarias	28.3	10.9	Dec-13	Dec-15	ns	Jan-15
Mexico	Tepatitlan	Instituto Nacional de Investigaciones Forestales, Agrícolas y Pecuarias	29.0	8.6	Dec-13	Dec-15	ns	Jan-15
Mexico	Obregon	Campo Experimental Norman E. Borlaug (CENEB CIMMYT)	29.3	12.9	Dec-12	2x Dec-15	Dec-11	Dec-14
Nepal	Bhairahawa	Nepal Agricultural Research Council	25.8	11.6	Dec-13	Dec-15	*	Nov-14
Pakistan	Bahawalpur	Regional Agricultural Research Institute	26.8	10.8	Nov-13	Nov-15	Dec-12	*
Pakistan	Faisalabad	Ayub Agricultural Research Institute	21.4	7.0	Nov-13	Nov-15	*	*
Pakistan	Islamabad	National Agricultural Research Centre	19.3	5.9	Nov-13	Dec-15	Nov-12	*
Pakistan	Nowshera-Pirsabak	Cereal Crops Research Institute	20.3	6.5	Nov-13	Nov-15	ns	Nov-14
Pakistan	Peshawar	Nuclear Institute for Food and Agriculture	20.5	6.8	ns	Nov-15	ns	ns
Pakistan	Tando-Jam	Nuclear Institute for Agriculture	34.6	18.1	ns	ns	ns	Dec-14
Romania	Fundulea	National Agricultural Research and Development Institute	8.7	0.5	ns	Oct-15	ns	ns
South Africa	Bethlehem	Small Grain Institute	20.4	2.6	Jun-14	ns	ns	Jun-15
South Africa	Lichtenburg	Sensako (PTY) Ltd.	24.2	5.7	Jun-14	ns	ns	ns
Sudan	Dongola	Agricultural Research Corporation	33.0	13.9	Dec-13	ns	ns	ns
Sudan	Wad Medani	Agricultural Research Corporation	37.2	18.8	ns	Dec-15	Dec-12	*

Mean temperatures during the growing season (5-month period, 5-year mean 2010/11 to 2014/15). Sowing dates for yield trials are shown (month/year) or ns (not shown). * Data not included in the analysis.

Results and Discussion

The strategic crosses in this study generated progeny (PT) with significant yield gains across most target environments (Table 2; Figs. 1-2). Most new PT lines outyielded local checks in the majority of cases. Given the high frequency of landraces and synthetics in the pedigree of PT lines (Table 2), this further supports the approach of broadening the genepool to accelerate yield gains (Reynolds et al., 2015), while providing new sources of genetic variation in good agronomic backgrounds to national collaborators. Some PT lines showed superior performance over elite CIMMYT checks, and while statistical significance was marginal in some cases, the trend across nurseries was the same, with genetic gains being realized in both temperate and hot, irrigated environments (Figs. 1 and 2). The new PT material was also adapted in terms of agronomic type. While lines in WYCYT and SATYN nurseries expressed a broader range of height and maturity than the checks, the best material was generally similar for these traits to checks (Table 2). Leaf and yellow rust screening indicated that most material had acceptable resistance.

Table 2. Agronomic traits of the 9 best yielding PT lines and all checks of the 3rd WYCYT across 32 international target environments, 2016.*

Lines (in reverse order of above ground biomass)	PT or CH	Yield g m^{-2}	Biomass g m^{-2}	Heading days	Height cm
BORLAUG100 F2014	ECH	593	1037	94	98
ROELFS F2007	ECH	446	1082	97	95
KACHU #1	ECH	538	1085	95	95
LOCAL CHECK	LCH	534	1115	95	97
BAJ #1	ECH	539	1118	91	98
SOKOLL/3/PASTOR//HXL7573/2*BAU/4/PARUS/PASTOR	PT	594	1151	96	102
MEX94.27.1.20/3/SOKOLL//ATTILA/3*BCN/4/PUB94.15.1.12/WBLL1	PT	603	1167	98	104
SERI/BAV92//PUB94.15.1.12/WBLL1	PT	595	1176	97	102
SOKOLL/3/PASTOR//HXL7573/2*BAU/4/PARUS/PASTOR	PT	600	1212	96	101
SUP152//PUB94.15.1.12/WBLL1	PT	533	1247	98	106
MEX94.27.1.20/3/SOKOLL//ATTILA/3*BCN/4/PUB94.15.1.12/WBLL1	PT	**617**	1272	96	105
SERI/BAV92//PUB94.15.1.12/WBLL1	PT	600	1284	97	104
BCN/WBLL1//PUB94.15.1.12/WBLL1	PT	483	1294	98	102
WBLL4//OAX93.24.35/WBLL1/5/CROC_1/AE.SQUARROSA (205)//BORL95/3/PRL/SARA//TSI/VEE#5/4/FRET2	PT	605	**1296**	95	100
P value Top PT line v local check (LCH)		<0.01	0.010	<0.01	<0.01
P value: Top 3 PT lines v Top 3 checks		0.19	0.12	0.44	0.55
SE mean		25.0	99.7	3.0	1.3
Coefficient of variation		0.35	0.31	0.25	0.10

* Abbreviations: PT: Physiological trait selected line. LCH: local check; ECH: elite CIMMYT check.

The study provides, for the first time, proof of concept that crossing strategies based on combining source and sink can accelerate genetic gains in wheat. This is to be expected since biomass drives yield potential, while sinks influence both harvest index and demand-driven assimilation rate, so their strategic combination is likely to result in the accumulation of complementary alleles. Physiological breeding can also make use of markers, especially those associated with genes of major effect (Eagles et al., 2014), as well as genomic and pedigree selection of progeny in combination with high-throughput screening of phenotypic traits (Rutkoski et al., 2016; Sukumaran et al., 2017).

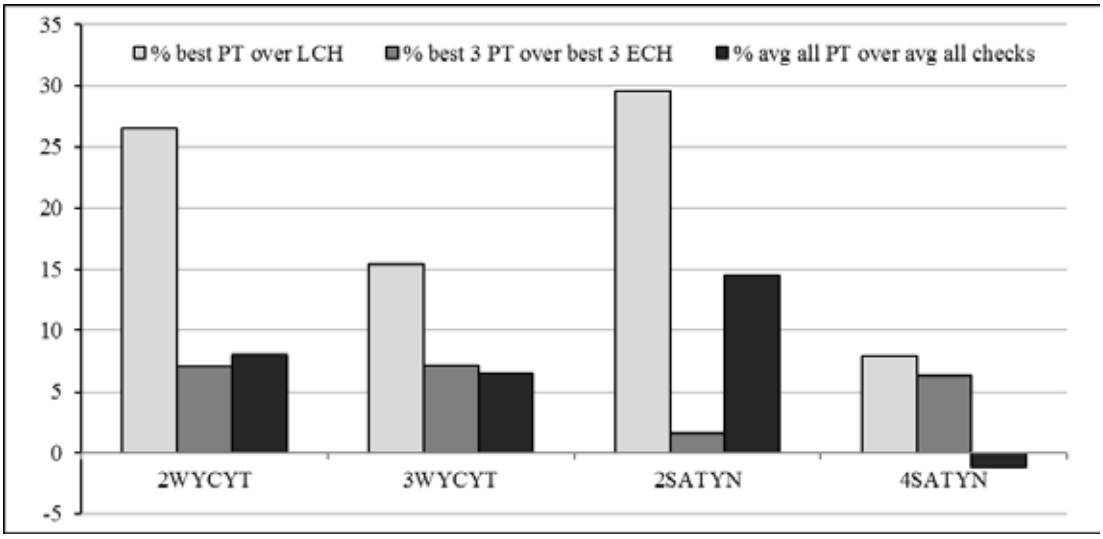

Fig 1. Percent genetic gains expressed for: (i) the best PT line over the local check (LCH); (ii) the best 3 PT lines over the best 3 elite checks (ECH); and (iii) the average of all PT lines over the average of all checks; for all 27, 32, 13 and 24 international sites of the 2nd WYCYT, 3rd WYCYT, 2nd SATYN, and 4th SATYN, respectively.

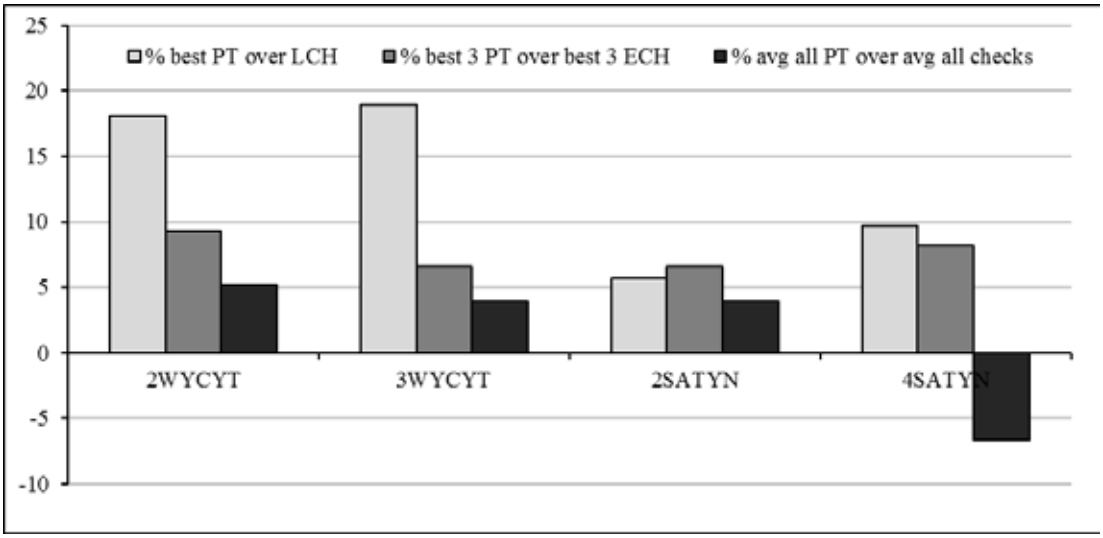

Fig 2. Percent genetic gains expressed for: (i) the best PT line over the local check (LCH); (ii) the best 3 PT lines over the best 3 elite checks (ECH); and (iii) the average of all PT lines over the average of all checks; for 7 sites in Mexico of the 2nd WYCYT, 3rd WYCYT, 2nd SATYN, and 4th SATYN, respectively.

Conclusions

By making crosses and testing progeny in target environments, this study confirmed the hypothesis –in a realistic breeding context– that physiological approaches can accelerate genetic gains in wheat under both yield potential and heat stressed environments. New PT lines have been selected as candidates for national release in several countries and two PT lines have been released in Pakistan for heat stressed conditions. These results also support the use of exotic material –like landraces and products of wide crossing– to widen the wheat genepool.

References

Crespo-Herrera LA, Crossa J, Huerta-Espino J, Autrique E, Mondal S, Velu G, Vargas M, Braun HJ, Singh RP (2017) Genetic yield gains in CIMMYT's international elite spring wheat yield trials by modeling the genotype x environment interaction. Crop Sci. (in press)

Eagles HA, Cane K, Trevaskis B, Vallance N, Eastwood RF, Gororo NN, Kuchel H, Martin PJ (2014) Ppd1, Vrn1, ALMT1 and Rht genes and their effects on grain yield in lower rainfall environments in southern Australia. Crop Pasture Sci. 65: 159-170

Reynolds M, Langridge P (2016) Physiological Breeding. Current Opinion in Plant Biology 31: 162-171

Reynolds MP, Tattaris M, Cossani CM, Ellis M, Yamaguchi-Shinozaki K, Saint Pierre C (2015) Exploring genetic resources to increase adaptation of wheat to climate change. In: Ogihara Y, Takumi S, Handa H. (eds) Advances in Wheat Genetics: From Genome to Field. Springer, Japan

Rutkoski J, Poland JP, Mondal S, Autrique E, González Pérez L, Crossa J, Reynolds M, Singh R (2016) Canopy temperature and vegetation indices from high-throughput phenotyping improve accuracy of pedigree and genomic selection for grain yield in wheat. G3 Genes|Genomes|Genetics 6: 2799-2808

Sukumaran S, Crossa J, Jarquin D, Reynolds M (2017) Genomic Prediction with Pedigree and Genotype × Environment Interaction in Spring Wheat Grown in South and West Asia, North Africa, and Mexico. G3: Genes, Genomes, Genetics 7: 481–495

Tattaris M, Reynolds MP, Chapman SC (2016) A direct comparison of remote sensing approaches for high-throughput phenotyping in plant breeding. Front. Plant Sci. 7: 1131

PARTITIONING TO YIELD

Physiological traits to increase grain partitioning in high biomass cultivars in wheat

Aleyda Sierra-Gonzalez[1,2], Carolina Rivera-Amado[2], Gemma Molero[2], Matthew Reynolds[2] and John Foulkes[1]

[1] University of Nottingham, UK, [2]CIMMYT, Mexico

Abstract

To meet global wheat demands, it is important to expand our current understanding of how physiological traits are associated with genetic gains and to identify phonemic and genomic approaches to improve yield potential. Yield is directly related to both biological yield (above-ground dry-matter per unit area; AGDM) and harvest index (grain yield/AGDM; HI), but in recent years the rate of genetic progress in HI has not increased; indeed, there is evidence for decreases in modern CIMMYT spring wheat cultivars as a result of a trade-off with increasing biomass. Therefore, it is important to identify new avenues for optimal dry matter (DM) partitioning of assimilates in order to improve grain sink strength – grain number – and HI in high biomass backgrounds as well as further identify genetic markers for these traits for application in marker-assisted selection. A summary of the main DM partitioning data collected during 2015-16 in the CIMMYT high biomass spring wheat panel ***HiBAP*** (High Biomass Association Panel, 150 genotypes) is presented and discussed. The general aim is to identify combinations of novel DM partitioning traits to increase HI. Results showed a strong association among genotypes between grain yield and AGDM (R^2=0.49, P< 0.001), a trade-off between AGDM and HI (R^2=0.23, P< 0.001) and an association between enhanced HI and reduced length of internode 3 (peduncle -2) (P< 0.05) at anthesis (GS65 +7d).

Introduction

Grain yield was historically increased with the introduction of the semi-dwarf *Rht* genes during the Green Revolution, by increasing assimilate availability to the developing spike favoring grain number per m^2 (GN) and harvest index (HI) (González et al., 2011; Lázaro and Abbate, 2012). Therefore, optimizing source-sink relationships before grain filling is critical for determining GN and grain yield. Increasing the amount of assimilate partitioning to the spike during the stem-elongation phase, in which the peduncle and other internodes are extending, is one opportunity to raise GN, by reducing the competition between the spike and alternative sink organs during this phase (Rivera-Amado, 2015). To achieve this, spike partitioning index (spike dry weight /AGDM at anthesis; SPI) has been identified as a trait that offers scope to enhance GN by making more of the total assimilates available to reproductive structures (Gaju et al., 2009; 2014). An alternative trait to increase GN is the fruiting efficiency (ratio of GN to spike dry weight at anthesis; FE) which is potentially additive to SPI (Ferrante et al., 2015; Foulkes et al., 2011; Lázaro and Abbate, 2012). This has been demonstrated in recent field investigations where genotypes combining high SPI with high FE were identified (Lázaro and Abbate 2012; Rivera-Amado, 2015).

Since the Green Revolution, HI values have increased to ca. 0.45-0.50 in spring wheat and 0.50-0.55 in winter wheat (Foulkes et al., 2011) with a hypothetical limit of approximately 0.65 (Austin et al., 1980; Foulkes et al., 2011). A recent analysis of advanced CIMMYT spring wheat lines (Rivera-Amado et al., 2016) in the CIMCOG (México Core Germplasm) panel showed that an HI > 0.60 can theoretically be achieved given the ideal combination of traits including: (1) increased spike partitioning index through reduced stem structural dry matter, (2) increased fruiting efficiency, and (3) improved spike morphology (through decreased rachis specific weight and increased lemma partitioning). While stable expression of HI at values of 0.55 and above (Aisawi et al., 2015; Rivera-Amado, 2015; Shearman et al., 2005) would represent a step change in yield (given that the average expression in spring wheat is closer to 0.45), the ability to improve HI is currently restricted by a limited understanding of its genetic basis.

The aim of this project was to identify physiological traits associated with enhanced grain partitioning in high biomass backgrounds and to identify genetic markers for these traits through Genome Wide Association Study (GWAS) for application in marker-assisted selection.

Methods

A high biomass association panel (***HiBAP***) of 150 CIMMYT spring wheat genotypes was grown during the 2015-16 cycle at CIMMYT's experiment station near Ciudad Obregón in NW México. The panel was grown on raised beds under full irrigation, using an alpha-lattice design with four replications. The experiment was sown on the 24th November 2015 and harvested during the second week of May 2016.

Physiological traits were measured at different stages during the whole cycle, with emphasis at seven days after anthesis (GS65+7d), when a full DM partitioning analysis was carried out for the 150 genotypes (spike, leaf lamina and stem and leaf sheath DM proportions) including stem morphological related traits, such as internode lengths: internode 2 and 3 (peduncle -1 and -2, respectively). At physiological maturity, AGDM, grain yield and yield components were evaluated within a plot area of 4 m^2.

A similar but more detailed analysis of true-stem and leaf-sheath internode DM partitioning (peduncle, internode 2, internode 3 and internode 4+) was done on 30 genotypes (subset 1) at GS65+7d. The subset was selected to represent the full range found among the 150 genotypes for internode 2 and 3 length, spike, stem and lamina DM with a restricted range of anthesis dates. From subset 1, a non-grain spike DM partitioning analysis (glume, palea, lemma, awns and rachis) was done at GS65+7d on 15 genotypes (subset 2). The rationale for selecting subset 2 was having a full range of dry matter partitioning for stem and leaf lamina components at GS65+7d and spike partitioning index (SPI).

Results/Discussion

DM partitioning traits at GS65+7d, fruiting efficiency and associations with key yield components traits

Wide genetic variation was found at GS65+7d for DM per shoot for each plant component: spike = 0.52-1.09 g per shoot ($P< 0.001$), stem+leaf sheath = 0.92-2.00 g per shoot ($P< 0.001$) and green lamina = 0.46-0.91 g per shoot ($P< 0.05$). Genetic variation was also found for DM partitioning indices (plant component DM as a proportion of total plant DM) calculated for each plant component: spike partitioning index (SPI) = 0.19-0.36 ($P< 0.001$), stem and leaf sheath partitioning index (StemPI) = 0.46-0.56 ($P< 0.001$) and lamina partitioning index (LamPI) = 0.18-0.28 ($P< 0.05$) (Fig. 1).

Results showed a negative linear association between SPI and StemPI, indicating that a high DM partitioning to the spike was strongly associated with reduced DM partitioning to the stem at GS65+7d;

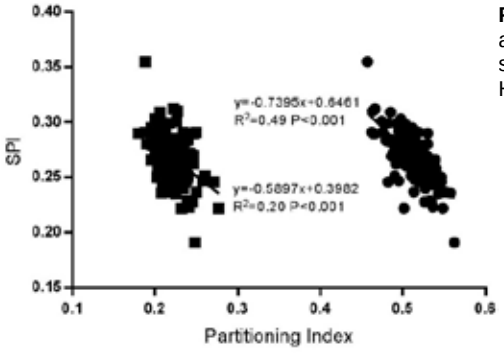

Fig. 1. Regression between spike PI (SPI) and lamina PI (LamPI) and stem+leaf sheath PI (Stem PI) at GS65+7d stage in HiBAP during 2015-16.

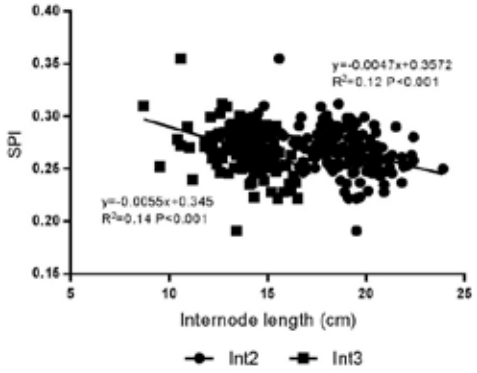

Fig. 2. Regression between Spike Partitioning Index (SPI) and internode lengths in HiBAP at GS65+7d in 2015-16.

there was also a weaker but significant negative relationship between SPI and LamPI. Stem morphological traits showed that internode 3 length at GS65+7d ranged from 8.7-17.3 cm ($P< 0.001$) and internode 2 length ranged from 14.2-23.9 cm ($P< 0.001$). A negative linear association was found between SPI and internode 2 length (R^2=0.12, $P< 0.001$) and internode 3 length (R^2 = 0.14, $P< 0.001$; Fig, 2). These preliminary results suggest that genotypes with a longer internode 2 and 3 compete more with the spike for assimilate at GS65+7d and could be related to reduced GN and HI within HiBAP genotypes.

A more detailed internode DM partitioning analysis was done on 30 genotypes (subset 1). Genetic variation among genotypes was found for true stem (TS) and leaf sheath (LS) DM partitioning indices at each internode (internode PI) with a positive association between GN and true-stem internode 2 PI (R^2 = 0.20, $P< 0.05$: Fig. 3).

For the 15 genotypes of HiBAP (subset 2), the DM partitioned to the different spike structural components was determined at GS65+7d showing that dry matter was allocated according to the following pattern: lemma > awns > glumes > rachis > palea. Genetic variation was found for all spike component partitioning indices (spike component DM/total spike DM excluding grain) and there was a positive association between DM per spike and each rachis PI (R^2=0.176, $P<0.01$) and palea PI (R^2=0.113, $P<0.05$). However, there were no statistically significant associations between spike DM partitioned to each component (glumes, lemma, palea, awns, rachis PIs) and FE (data not shown).

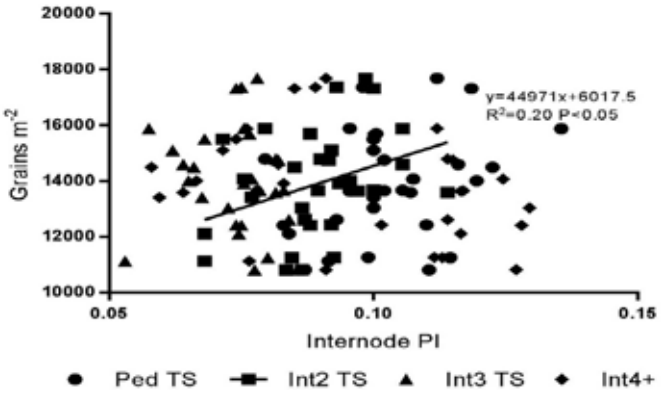

Figure 3. Regression of grains m^{-2} vs true stem internode PIs at GS65+7 days in HiBAP experiment 2015-6.

Physiological maturity traits: grain yield and its components

Overall, grain yield among HiBAP genotypes ranged from 487 to 797 g m^{-2} ($P< 0.001$) and GN from 10,815-17,689 ($P< 0.001$). A positive linear association was found between grain yield and GN (R^2=0.21, $P< 0.001$; Fig. 4a), as well as a weaker association between grain yield and HI (R^2=0.05, $P< 0.05$; Fig 4b). There was a strong association between grain yield and AGDM (R^2=0.49, $P< 0.001$; Fig 4c), but also a trade-off between AGDM and HI (R^2=0.23, $P< 0.001$; Fig 4d). Moreover, a trend for a trade-off was found between FE and SPI (R^2=0.10, $P< 0.05$), indicating higher SPI was associated with more chaff per grain.

Overall summary: spring wheat HiBAP field cycle 2015-16

Table 2 shows a summary of the genetic ranges for key traits measured at GS65+7d and physiological maturity, as well as correlations with grain yield, harvest index and grain number per meter square. Results showed that fruiting efficiency was positvely correlated with HI (r= 0.37, *P*< 0.001) and GN (r= 0.41, *P*< 0.001). Spike partitioning inde was also positively correlated with HI (r= 0.22, *P*< 0.01) and with GN (r= 0.17, *P*< 0.05). There were also negative correlations between internode 3 length and HI (r= -0.22, *P*< 0.01) and GN (r= 0.27, *P*< 0.001).

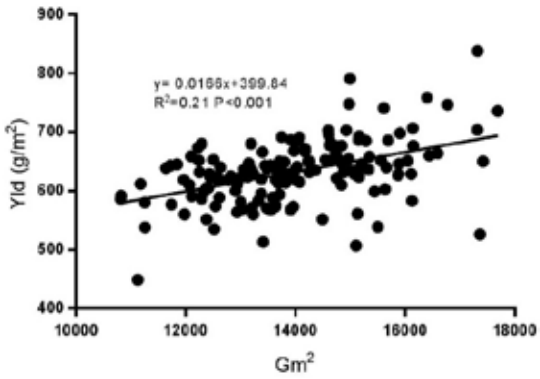

Fig. 4a. Regression between grain yield and grains per meter square at PM in HiBAP 2015-6.

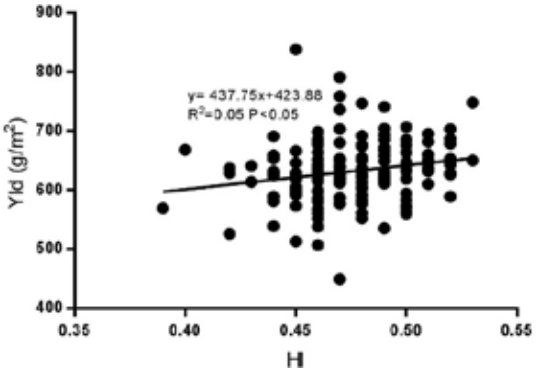

Fig. 4b. Regression between grain yield and HI at physiological maturity in HiBAP 2015-6.

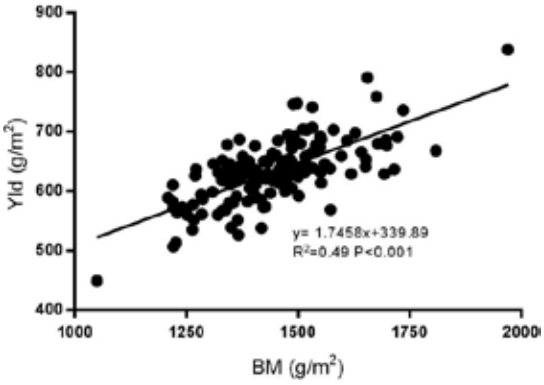

Fig. 4c. Regression between yield and biomass at physiological maturity in HiBAP 2015-6.

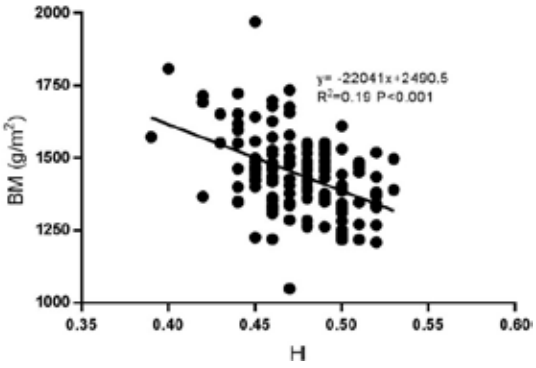

Fig. 4d. Regression between biomass (AGDM) and.HI at physiological maturity in HiBAP 2015-6.

Table 2. Genetic ranges for DM partitioning traits at GS65+7d and correlations with grain yield (GY), harvest index (HI) and grain number per meter square (GN) for HiBAP in 2015-16.

Traits		Range (Min-Ma)	Prob.	Correlation (r)		
				GY	HI	GN
Yield (g m^{-2})		449.3-837.8	***	-	0.20*	0.46***
Harvest Inde		0.39-0.53	***	0.20*	-	0.14ns
Grains m^{-2}		10,815-17,689	***	0.46***	0.14ns	-
Fruiting Eff. (grains g^{-1})		41.0-97.6	***	-0.03ns	0.37***	0.41***
Le ngt h (c m)	**GS65 + 7 d**	604.78	***	0.08ns	-0.21**	0.02ns
	Physiol. mat.	1049-1971	***	0.70***	-0.44***	0.26***
	Internode 2	14.2-23.9	***	0.07ns	0.06ns	-0.11ns

Part. Inde GS65+7d DM g shoot^{-1}	**Internode 3**	8.7-17.3	***	-0.03ns	-0.22**	-0.27***
	Stem	0.92-2.00	***	0.20*	-0.34***	-0.26***
	Spike	0.52-1.09	***	0.17*	-0.18*	-0.14ns
	Lamina	0.46-0.91	**	0.18*	-0.35***	-0.24**
	Stem	0.46-0.56	***	0.10ns	-0.19*	-0.15ns
	Spike	0.19-0.36	***	-0.04ns	0.22**	0.17*
	Lamina	0.18-0.28	*	-0.07ns	-0.05ns	-0.03ns

Next steps:

- Data from a second year of the HiBAP experiment are needed to confirm results obtained in the 2015-16 cycle, as well as to run a more detailed analysis to test specific hypotheses within subsets of genotypes 1 and 2 in 2016-17.
- Using SNPs (Single Nucleotide Polymorphisms) a Genome Wide Association Study (GWAS) will be done in the HiBAP experiment to identify marker-trait associations for the key DM partitioning traits determining SPI and FE to increase HI in high biomass backgrounds.
- For a winter wheat Savannah Rialto DH population, a DM partitioning data set has been collected in a field experiment in 2015-16 at Nottingham, UK (data not shown in this paper). The experiment will be repeated in 2016-17 and a QTL (Quantitative Trait Loci) analysis will be run to determine the chromosomal locations for DM partitioning traits.
- Associations between phenotypic and genomic data will be quantified in the spring and winter panel/population to review the possibility of having common selection criteria for raising HI in high biomass backgrounds in spring and winter wheat breeding programs.

Acknowledgments

We thank CONACYT, MasAgro and the University of Nottingham for funding the PhD studentship of Aleyda Sierra-Gonzalez. We are grateful to Dr. Francisco Piñera-Chavez for his advice and the CIMMYT Wheat Physiology team for their help with the collection of field data in the HiBAP eperiment.

References

Aisawi, K. A. B., Reynolds, M. P., Singh, R. P., & Foulkes, M. J. (2015a). The physiological basis of the genetic progress in yield potential of CIMMYT spring wheat cultivars from 1966 to 2009. *Crop Science*, *55*(4), 1749–1764. http://doi.org/10.2135/cropsci2014.09.0601

Aisawi, K. A. B., Reynolds, M. P., Singh, R. P., & Foulkes, M. J. (2015b). The Physiological Basis of the Genetic Progress in Yield Potential of CIMMYT Spring Wheat Cultivars from 1966 to 2009. *Crop Science*, *55*(4), 1749. http://doi.org/10.2135/cropsci2014.09.0601

Austin, R. B., Bingham, J., Blackwell, R. D., Evans, L. T., Ford, M. A., Morgan, C. L., & Taylor, M. (1980). Genetic improvements in winter wheat yields since 1900 and associated physiological changes. *The Journal of Agricultural Science*, *94*, 675. http://doi.org/10.1017/S0021859600028665

Ferrante, A., Savin, R., & Slafer, G. A. (2015). Relationship between fruiting efficiency and grain weight in durum wheat. *Field Crops Research*, *177*, 109–116. http://doi.org/10.1016/j.fcr.2015.03.009

Foulkes, M. J., Slafer, G. a., Davies, W. J., Berry, P. M., Sylvester-Bradley, R., Martre, P., Reynolds, M. P. (2011). Raising yield potential of wheat. III. Optimizing partitioning to grain while maintaining lodging resistance. *Journal of Eperimental Botany*, *62*(2), 469–486. http://doi.org/10.1093/jb/erq300

Gaju, O., Allard, V., Martre, P., Le Gouis, J., Moreau, D., Bogard, M., Foulkes, M. J. (2014). Nitrogen partitioning and remobilization in relation to leaf senescence, grain yield and grain nitrogen concentration in wheat cultivars. *Field Crops Research*, *155*, 213–223. http://doi.org/10.1016/j.fcr.2013.09.003

Gaju, O., Reynolds, M. P., Sparkes, D. L., & Foulkes, M. J. (2009). Relationships between large-spike phenotype, grain number, and yield potential in spring wheat. *Crop Science*, *49*(3), 961–973. http://doi.org/10.2135/cropsci2008.05.0285

González, F. G., Miralles, D. J., & Slafer, G. a. (2011). Wheat floret survival as related to pre-anthesis spike growth. *Journal of Eperimental Botany*, *62*, 4889–4901. http://doi.org/10.1093/jb/err182

Lázaro, L., & Abbate, P. E. (2012). Cultivar effects on relationship between grain number and photothermal quotient or spike dry weight in wheat. *The Journal of Agricultural Science*, *150*(4), 442–459. http://doi.org/10.1017/S0021859611000736

Rivera-Amado, C., Trujillo-Negrellos, E., Sylvester-Bradley, R., , Molero,, G., Sierra-Gonzalez, A., Reynolds, M.P., Foulkes, M. J. (2016). Achieving increases in spike growth, fruiting efficiency and harvest inde in high biomass wheat cultivars. *Conference Paper: 2nd International TRIGO (Wheat) Yield Potential*, (Workshop March 2016).

Rivera-Amado, A. C. (2015). Identifying physiological traits to optimize assimilate partitioning and spike fertility for yield potential in wheat (Triticum aestivum L.) genotypes. *PhD Thesis, University of Nottingham School of Biosciences, Sutton Bonnington Campus, Leistershire, UK*, (September).

Shearman, V. J., Scott, R. K., & Foulkes, M. J. (2005). Crop Physiology and Metabolism. Physiological Processes Associated with Wheat Yield Progress in the UK. *Crop Science*, *185*, 175–185. http://doi.org/10.2135/cropsci2005.0175

Identifying avenues for increasing harvest index in high biomass wheat cultivars while maintaining post-anthesis photosynthetic capacity

Carolina Rivera-Amado[1,2], Eliseo Trujillo-Negrellos[1], Roger Sylvester-Bradley[3], Gemma Molero[2], Matthew Reynolds[2] and John Foulkes[1]

[1] University of Nottingham, UK; [2] CIMMYT, Mexico; [3] ADAS, Cambridge, UK

Abstract

When optimizing pre-anthesis dry matter (DM) partitioning among plant organs to enhance grains per m2 and harvest index, the consequences for post-anthesis photosynthetic capacity should be considered. Key processes to consider are: i) leaf lamina and leaf sheath DM partitioning in relation to light interception and photosynthetic rate; ii) non-structural (water soluble carbohydrates; WSC) stem DM partitioning in relation to utilization of stored assimilate for grain filling; and iii) the spike's potential capacity for up-regulation of photosynthesis in relation to decreases in the source:sink balance. In this study, for a set of 26 CIMMYT spring wheat genotypes, grain source:sink balance was estimated by comparing grain weight (GW) responses to several source:sink manipulation treatments. The objectives were to quantify variation in source:sink balance and associations with DM partitioning with photosynthetic traits and grain yield. Results showed responses of cultivars to a de-graining treatment ranged from 1% to 27.9% increases in individual GW in 2011, 2012 and 2013 ($P < 0.001$). The overall decreases in GW in response to a leaf lamina defoliation treatment ranged from -6.5 to -16% ($P < 0.05$) in 2012 and 2013, and in response to a leaf sheath covering treatment from -9.3 to -11.2% ($P < 0.01$) in 2014. Our results indicated that the grain yield of high yielding lines was co-limited by source and sink and that the leaf sheath's contribution to grain filling is important in the studied genotypes and should be taken into account when optimizing partitioning pre-anthesis to enhance HI in high biomass backgrounds.

Introduction

To exploit potential genetic gains in biomass for yield potential derived from current strategies to improve photosynthetic capacity (Evans, 2013; Parry et al., 2011; Reynolds et al., 2012), it will be crucial to identify traits enabling breeders to discriminate 'useful' and 'non useful' biomass in new high biomass cultivars to maximize partitioning to grain. The physiological processes determining growth of each organ overlap in their development, resulting in competition for assimilate among plant organs, which in turn relates to the trade-off observed between biomass and harvest index (HI) in elite high biomass spring wheat cultivars (Rivera-Amado et al., 2016). Therefore, increases in spike growth pre-anthesis through decreasing dry matter (DM) partitioning to alternative organs, (stems, lamina and sheaths) can have a positive effect on grains m-2 and HI (Foulkes et al., 2011). On the other hand, grain yield of modern wheat cultivars may be limited by the sink size (grain storage capacity) or source size (photosynthetic capacity of the crop to supply assimilate to grains). Although evidence in the last decades suggests wheat cultivars are still generally more sink- than source-limited during grain filling under favorable conditions (Miralles and Slafer, 2007; Sayre et al., 1997; Shearman et al., 2005; Fischer, 2009), recent investigations in CIMMYT spring wheat suggest that yield progress has occurred through increased grain size through enhanced potential grain weight matched to some extent by increases in photosynthetic capacity through improved post-anthesis green area duration (Aisawi et al., 2015; Lopes et al., 2012).

The extent to which post-anthesis source may be limiting the grain yield of wheat cultivars can be estimated from source:sink manipulation experiments. Co-limitation of grain growth can be present when grain growth is limited by grain sink size in the earlier stage of grain filling and by photosynthetic capacity in the latter stage, on the basis that grain weight response to de-graining is >10% (Acreche and Slafer, 2009). Therefore, it is important to quantify source:sink balance in the wheat germplasm currently used by breeders and the extent of source limitation of yield to help inform on physiological strategies to optimize DM partitioning for increases in HI and yield. In summary, when optimizing pre-anthesis DM partitioning among plant organs, the consequences for post-anthesis photosynthetic capacity should be considered. Some key processes to consider are lamina DM partitioning in relation to light interception and photosynthetic rate, leaf sheath DM partitioning in relation to the same processes during the latter stages of grain filling when leaf lamina senesce is advanced, and stem WSC in relation to the utilization of stem soluble carbohydrate during grain filling. It will also be important to assess any potential capacity of the spike for up-regulation of photosynthesis in relation to decreases in the source.

In this study, for a set of 26 CIMMYT spring wheat genotypes, grain source:sink balance was estimated by comparing grain weight (GW) responses to several source:sink manipulation treatments. The objectives were to quantify variation in the extent of source limitation of grain yield in the latest CIMMYT spring wheat germplasm with an emphasis on estimating the contribution of leaf lamina and leaf sheath photosynthesis post-anthesis to grain filling and the capacity for upregulation of leaf lamina and spike photosynthesis in response to decreases in source sink balance.

Materials and Methods

The CIMCOG panel (CIMMYT Mexico Core Germplasm) comprising a set of 26 CIMMYT elite spring wheat (Triticum aestivum L.) genotypes (Rivera-Amado et al., 2014) was grown during three seasons (2011, 2012 and 2013) at the CIMMYT experimental station near Ciudad Obregon, NW Mexico. The experimental design was an alpha-lattice with two replications in 2011 and three in 2012 and 2013. The 26 CIMCOG cultivars were evaluated for DM partitioning-related traits at seven days after anthesis (GS65+7d) and for harvest traits (grain yield, harvest index and yield components), as described previously by Foulkes et al. (2015). Furthermore, source:sink manipulation treatments were applied as described below, in 12 randomly selected shoots per treatment per plot across a defined area of approximately 1.5 m x 1.6 m (Fig. 1a). In each experiment, plots were irrigated using a gravity-based system with flood irrigations 4–6 times during the crop cycle, abiotic stress was controlled and a full fertilization scheme was followed.

Spikelet removal (de-graining) treatment

First, grain source:sink balance was estimated in the 26 genotypes by comparing individual grain weight (GW) in control and de-grained (removal of half spikelets at GS65+10 days, referred as GS65+10d) spikes (12 randomly selected spikes per treatment; Fig. 1-b), aiming to quantify variation in source:sink balance and the extent of source limitation of grain yield. Flag-leaf green area duration was measured in the un-manipulated crop by weekly SPAD assessment post-anthesis and by fitting a linear relationship with thermal time (base temperature 0 °C) post-anthesis (GS65).

Leaf lamina defoliation and leaf sheath covering treatments

Additionally, the relative contribution to grain filling of the top three leaf laminae and the leaf sheath was separately estimated in subsets of the 26 cultivars by imposing the following source:sink treatments at GS65+10 days: i) lamina defoliation (2012 and 2013; 10 cultivars – subset 1) and ii) leaf lamina defoliation and leaf sheath covering (2014; 4 cultivars – subset 2). Final grain growth was compared to a treatment control for both defoliation and sheath covering (Fig. 1-c and Fig. 1-d, respectively). Flag leaf and spike photosynthesis rates were measured using the Li-6400XT Photosynthesis System (Licor Inc. NE, USA) at GS65+15 d in 2014. Spike photosynthetic rate was measured as described in Molero et al. (2013).

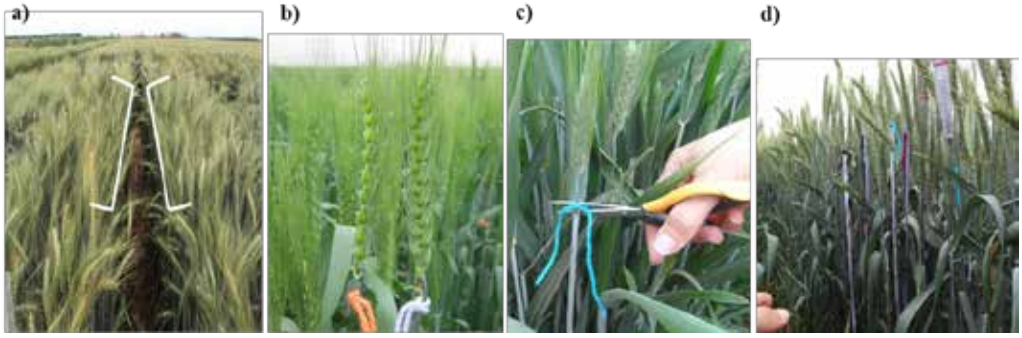

Fig. 1. **Source:sink manipulation treatments: a) plot indicating the area designated for manipulation treatments; b) de-grained spike at GS65+10d and control spike; c) defoliation at GS65+10d; and d) sheath covering with fabric at GS65+10d.**

Results and Discussion

Results from previous years on DM partitioning analyses at GS65+7 and associations with harvest traits showed that HI >0.6 can be achieved by combining the best expression for 'useful' biomass traits (Rivera-Amado et al., 2016). Subsets of germplasm with the highest expression of favorable traits (while minimizing trade-offs) for increases in spike DM partitioning were identified for strategic crosses in pre-breeding at CIMMYT. Among these, the most promising traits were reduced stem structural DM, particularly to internodes 2 and 3. No changes in leaf lamina DM partitioning were considered due to

concerns about photosynthetic capacity and no association with spike DM partitioning. Although leaf sheath DM partitioning showed some negative associations with spike DM partitioning (Foulkes et al., 2013), considerations for trade-off with photosynthesis contribution should also be taken into account, among support aspects, when considering decreasing DM partitioning to this plant organ.

Source:sink balance during grain filling

Averaging across the three years (2011, 2012 and 2013) and the 26 cultivars, there was a trend for a positive linear association between individual grain weight (GW) response to de-graining and grain yield (r = 0.40, P <0.05; Fig. 2-a), indicating that cultivars with higher yields were more responsive to increases in extra source availability. There was also a trend in the de-graining treatment data for a linear increase in individual GW response to de-graining with year of release (YoR) among the 26 cultivars (r = 0.38, P <0.05; data not shown).

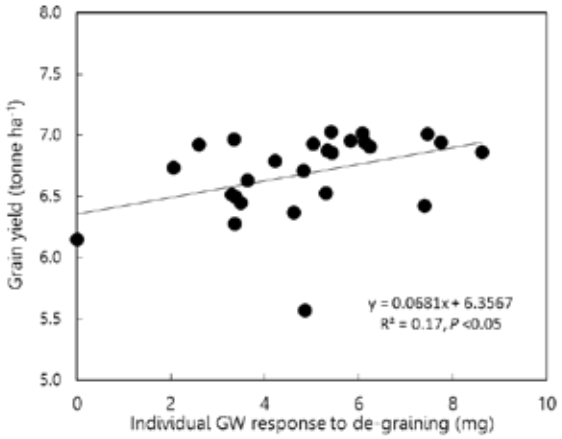

Fig. 2**. Linear relationship between grain yield (ton ha^{-1}) and individual GW response to de-graining (mg grain^{-1}) for the 26 CIMCOG cultivars in 2011, 2012 and 2013.**

Regarding the source:sink balance estimations during grain filling, individual GW increased in response to de-graining by 5.19 mg (11.4%) (P <0.001; Fig. 3-a). The response ranged among cultivars from 0 mg (Siete Cerros) to 8.61 mg (27.9%) (Bcn/Rialto) (P <0.001; Fig. 3-a). There was no association between individual GW response to flag-leaf SPAD senescence rate or SPAD at physiological maturity (PM), or between flag leaf SPAD senescence parameters and YoR. These results overall indicated that in high yield potential modern CIMMYT spring cultivars there is evidence for co-limitation of source and sink of grain yield. Individual GW responses to de-graining indicated co-limitation of grain growth for 18 cultivars (>10% increase in individual GW with de-graining) and sink limitation for eight cultivars. Individual GW in control and de-grained spikes averaged just for 2012 and 2013 among the 26 cultivars also showed similar responses, increasing in response to de-graining from 0 to 7.43 mg (23.3%) (P <0.001; Fig. 3-b). There was also a positive linear association between GW in the de-grained treatment (an indicator of potential grain weight) and YoR (R^2 0.36, P <0.001; data not shown).

Estimations of contribution of leaf lamina and leaf sheath photosynthesis to grain filling

Results for individual GW comparing control and defoliated shoots are shown in Figs. 3-c and 3-d, respectively, for 2012 and 2013 (*subset 1*) and 2014 (*subset 2*). Overall, there were significant differences among cultivars in the individual GW response to defoliation in both subsets (P <0.05 and P <0.001, respectively, for *subset 1* and *subset 2*). In *subset 1* (10 cultivars in 2012 and 2013), the overall decreases in GW in response to defoliation averaging -10.2% and ranging from -6.5 (Seri M82) to -16% (Becard/Kachu) were smaller than expected in comparison to the strong defoliation (top three leaves). The cultivars that showed the greatest and the smallest response to de-graining treatment in 2012 and 2013 (highest and lowest source limitation, respectively) showed similar responses to defoliation, 8.9 (Babax/LR42) and 7.1% (CMH79A.955).

Individual GW decreases in response to defoliation in 2014 in *subset 2* were higher than in 2012-2013, averaging -18.7% and ranging from -12.9 (Seri M82) to -24.0% (CMH79A.955). Individual GW responses to the sheath covering treatment showed less variation among the four cultivars (9.3 to 11.2%; P <0.05),

averaging 10.4%. The DM partitioned to the leaf sheath at physiological maturity (PM) was relatively high (25% on average) for the four cultivars, as a proportion of shoot (i.e., lamina, stem and sheath) (Table 1). Based on these results, we consider the leaf sheath represents an important assimilate investment pre-anthesis, and has a very important role in photosynthesis during the entire wheat cycle, especially during the latter stages of grain filling when most of the lamina tissue is senesced. Therefore, these aspects of leaf sheath photosynthesis should be considered in a similar way as aspects of leaf lamina photosynthesis when optimizing leaf DM partitioning during pre-anthesis.

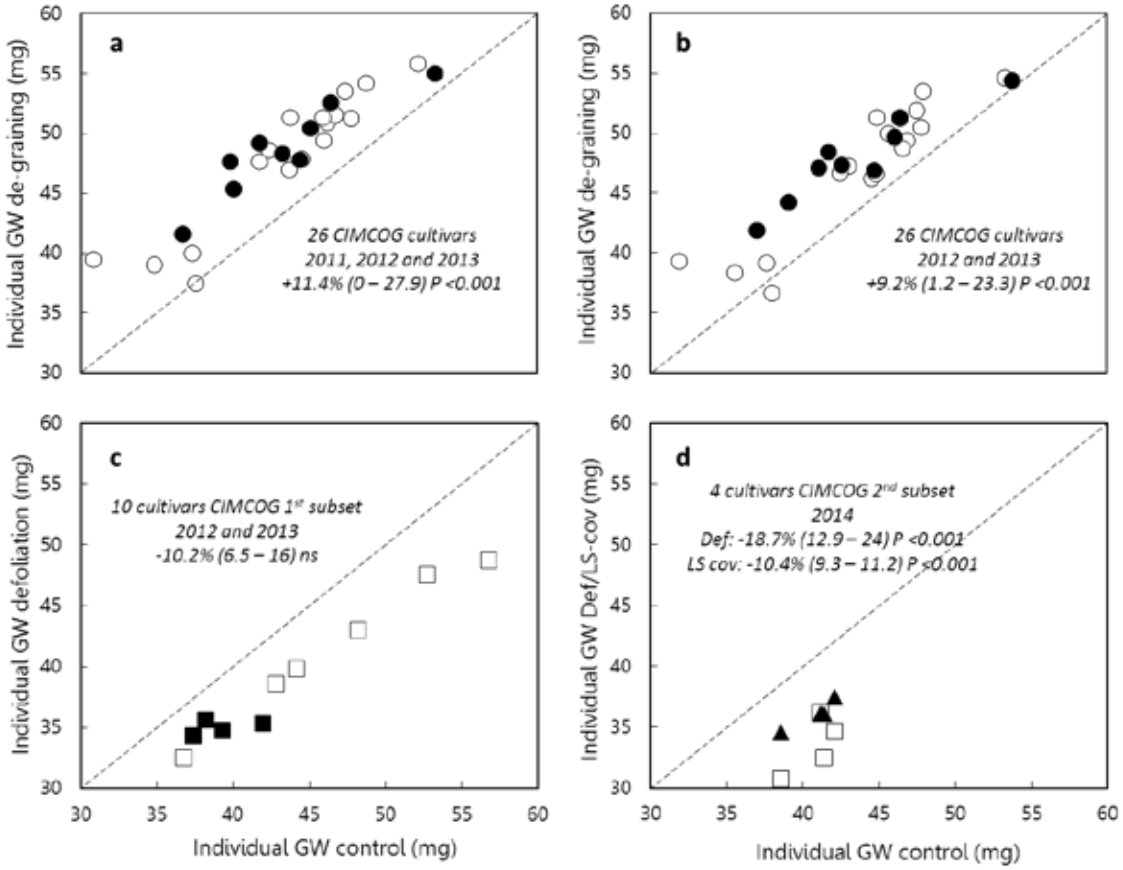

Fig. 3. Individual grain weight (GW) in control shoots versus a) DEG shoots for 26 CIMCOG cultivars in 2011, 2012 and 2013; b) in 2012 and 2013; c) individual GW in control shoots versus DEF shoots for 10 CIMCOG cultivars (*subset 1*) in 2012 and 2013; and d) individual GW in control shoots versus DEF shoots (□) and LSCOV shoots (▲) for 4 CIMCOG cultivars (*subset 2*) in 2014. Dashed line represents the 1:1 ratio and bold symbols represent *subset 1* in a and b and *subset 2* in c and d.

Table 1. Plant components DM per shoot at physiological maturity in 2014 *for subset 2*.

Entry	Cultivar	Stem DM per shoot (g) PM	Sheath DM per shoot (g) PM	Lam DM per shoot (g) PM	Sheath % to straw PM
1	BECARD/KACHU	1.035	0.460	0.432	0.24
2	CMH79A.955	1.173	0.611	0.516	0.27
3	SERI M 82	1.039	0.497	0.447	0.25
4	UP2338*2/4/SNI	1.099	0.426	0.325	0.23

Flag leaf and spike photosynthesis responses to source:sink manipulation treatments

The estimated contribution of organ photosynthesis to grain yield showed variation according to the different treatments applied and as reflected by GW response (Fig. 3c and d). However, even when the

treatments reduced light interception by photosynthetic organs by large amounts, no compensations of unaffected photosynthetic organs were observed in contrast with other studies (Aggarwal et al., 1990; Zhu et al., 2004). It was predicted that removal of leaf laminae may enhance the photosynthetic capacity of other green parts, as these mechanisms can avoid the restriction of grain filling in such a manner that often no source limitation occurs (Cruz-Aguado et al., 1999). In contrast with these and additional studies by Serrago et al. (2013), where the entire canopy was shaded below the spike, no consistent statistically significant up-regulation of spike photosynthesis or flag leaf was observed for the different source:sink treatments applied in the present study. This suggested that even though source limitation was confirmed by grain weight reduction, no signaling mechanism was involved in inducing gas exchange responses (or these could not be detected), and the only compensation involved was through increasing DM translocation from pre-anthesis assimilates (data not shown).

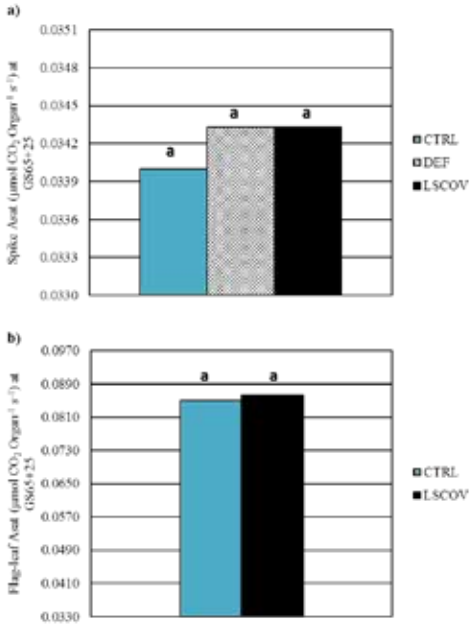

Fig. 4. Summary of a) spike light-saturated photosynthesis rate (A_{sat}) in control, defoliated and leaf-sheath covering shoots; and b) flag-leaf A_{sat} per organ in control and leaf-sheath covering shoots. Values represent means for the four cultivars in 2014.

Conclusions

Results from post-anthesis de-graining treatments showed that in some cultivars, grain yield was co-limited during grain filling (individual GW increases in de-grained spikes up to 27.9% among the 26 cultivars) and post-anthesis defoliation treatments showed that removal of the top three leaves reduces individual GW by *ca*. 10.2% on average within a subset of 10 cultivars from the CIMCOG panel. Even when all photosynthetically active laminae were removed at GS65+10d, the extent of source limitation was moderate, supporting previous estimates that flag leaf photosynthesis contributed an average of 5 to 10% of final grain yield under irrigated conditions (Aggarwal et al., 1990; Carr and Wardlaw, 1965; Evans et al., 1975; Evans and Rawson, 1970; Merah and Monneveux, 2015), while the top three leaves contributed approximately 20% of assimilates partitioned to grains (Kruk et al., 1997; Thorne, 1982). Sanchez-Bragado et al. (2014) reported that the specific contribution of the flag leaf blade to grain filling (as assessed by comparing the $\delta^{13}C$ of grains with the $\delta^{13}C$ of the water-soluble fraction of the flag leaf and the awns) was relatively minor under irrigated conditions, ranging between 3 and 18% in CIMMYT elite spring wheat cultivars. In contrast, in our experiments leaf sheath photosynthesis contribution to grain yield was more than expected, reaching a maximum value of 11.2% among a second subset of 4 cultivars from the CIMCOG panel. Araus and Tapia (1987) concluded that, although the rate of net CO_2 assimilation was basically similar in flag leaf blades and leaf sheaths, the leaf sheaths' role of storing and later transporting assimilates to the developing grains seemed to be more important than their photosynthetic function after the onset of senescence. However, our results in the leaf sheath covering treatment indicated that photosynthetic function of the leaf sheath is important in modern spring wheat CIMMYT cultivars.

Moreover, if potential grain weight continues to increase with breeding with no changes in leaf lamina stay-green traits, it seems that the importance of leaf sheath photosynthesis in maintaining source:sink balance post-anthesis is likely to increase. Similarly, enhanced capacity for up-regulation of spike photosynthesis post-anthesis seems likely to be an important trait for minimizing source limitation post-anthesis and enhancing HI in high biomass backgrounds and grain yield.

These results highlight the importance of accounting for the effects on source during grain filling in optimizing partitioning in the pre-anthesis phase. Increases in GW of up to 27% in the de-graining treatment indicated co-limitation of grain growth in the highest yielding cultivars. Overall grain growth co-limitation could be balanced by up-regulating photosynthesis in response to increasing grains m^{-2} (sink strength) during pre-anthesis, as suggested by Reynolds et al. (2005), who showed improvements in post-anthesis crop growth and higher radiation use efficiency (RUE) to increased sink demand by increased radiation interception during booting stage.

Acknowledgments
We thank the Mexican government (MasAgro), CONACYT and the University of Nottingham for funding the PhD studentships of Carolina Rivera-Amado and Eliseo Trujillo-Negrellos.

References

Acreche, M.M. & G.A. Slafer, 2009. Grain weight, radiation interception and use efficiency as affectedby sink-strength in Mediterranean wheats released from 1940 to 2005, Field Crops Research 110(2), 98–105.

Aggarwal, P.K., R.A. Fischer & S.P. Liboon, 1990. Source–sink relations and effects of post-anthesiscanopy defoliation in wheat at low latitudes, The Journal of Agricultural Science 114(1), 93–99.

Aisawi, K.A.B., M.P. Reynolds, R.P. Singh & M.J. Foulkes, 2015. The Physiological Basis of the Genetic Progress in Yield Potential of CIMMYT Spring Wheat Cultivars from 1966 to 2009, Crop Science 55(4), 1749.

Araus, J.L. & L. Tapia, 1987. Photosynthetic Gas Exchange Characteristics of Wheat Flag Leaf Blades and Sheaths during Grain Filling: The Case of a Spring Crop Grown under Mediterranean Climate Conditions, PLANT PHYSIOLOGY 85(3), 667–73.

Brancourt-Hulmel, M., G. Doussinault, C. Lecomte, P. Bérard, B. Le Buanec & M. Trottet, 2003. Genetic improvement of agronomic traits of winter wheat cultivars released in France from 1946 to 1992, Crop Science 43(1), 37–45.

Carr, D.J. & I.F. Wardlaw, 1965. Supply of photosynthetic assimilates to grain from flag leaf and ear of wheat, Australian Journal of Biological Sciences 18(4), 711.

Cruz-Aguado, J.A., F. Reyes, R. Rodes, I. Perez & M. Dorado, 1999. Effect of Source-to-sink Ratio on Partitioning of Dry Matter and14C-photoassimilates in Wheat during Grain Filling, Annals of Botany 83(6), 655–65.

Evans, J.R., 2013. Improving Photosynthesis, Plant Physiology 162(4), 1780–93.

Evans, L.T. & H.M. Rawson, 1970. Photosynthesis and Respiration by the Flag Leaf and Components of the Ear During Grain Development In Wheat, Australian Journal of Biological Sciences 23(2), 245–54.

Evans, L.T., I.F. Wardlaw & R.A. Fischer, 1975. Wheat, in Crop Physiology: Some Case Histories., ed. L.T. Evans. Cambridge, UK: Cambridge University Press, 101–49.

Foulkes, J., C. Rivera, E. Trujillo, R. Sylvester-Bradley & M. Reynolds, 2015. Achieving a Step-Change in Harvest Index in High Biomass Wheat Cultivars, in Proceedings of the International TRIGO (Wheat) Yield Potential Workshop 2015, eds. M. Reynolds, G. Molero, J. Mollins & H. Braun. Obregon, Sonora, Mexico.: CIMMYT.

Foulkes, J., C. Rivera, E. Trujillo, R. Sylvester-Bradley, G. Slafer & M. Reynolds, 2013. Optimizing harvest index through increasing partitioning to spike growth and maximizing grain number, in Proceedings of the 3rd International Workshop of the Wheat Yield Consortium, eds. M. Reynolds & B. Hans. Obregon, Sonora, Mexico.: CIMMYT.

Foulkes, M.J., G.A. Slafer, W.J. Davies, P.M. Berry, R. Sylvester-Bradley, P. Martre, D.F. Calderini, S. Griffiths & M.P. Reynolds, 2011. Raising yield potential of wheat. III. Optimizing partitioning to grain while maintaining lodging resistance, Journal of Experimental Botany.

Kruk, B.C., D.F. Calderini & G.A. Slafer, 1997. Grain weight in wheat cultivars released from 1920 to 1990 as affected by post-anthesis defoliation, The Journal of Agricultural Science 128(3), 273–81.

Lopes, M.S., M.P. Reynolds, Y. Manes, R.P. Singh, J. Crossa & H.J. Braun, 2012. Genetic Yield Gains and Changes in Associated Traits of CIMMYT Spring Bread Wheat in a 'Historic' Set Representing 30 Years of Breeding, Crop Science 52(3), 1123.

Merah, O. & P. Monneveux, 2015. Contribution of Different Organs to Grain Filling in Durum Wheat under Mediterranean Conditions I. Contribution of Post-Anthesis Photosynthesis and Remobilization, Journal of Agronomy and Crop Science 201(5), 344–52.

Miralles, D.J. & G.A. Slafer, 2007. Sink limitations to yield in wheat: how could it be reduced?, The Journal of Agricultural Science 145(2), 139–49.

Molero, G., R. Sanchez-Bragado, J.L. Araus & M.P. Reynolds, 2013. Phenotypic selection for spike photosynthesis, in Proceedings of the 3rd International Workshop of the Wheat Yield Consortium, eds. M. Reynolds & H. Braun. Obregon, Sonora, Mexico.: CIMMYT.

Parry, M.A.J., M. Reynolds, M.E. Salvucci, C. Raines, P.J. Andralojc, X.-G. Zhu, G.D. Price, A.G. Condon & R.T. Furbank, 2011. Raising yield potential of wheat. II. Increasing photosynthetic capacity and efficiency, Journal of Experimental Botany 62(2), 453–67.

Peltonen-Sainio, P., A. Kangas, Y. Salo & L. Jauhiainen, 2007. Grain number dominates grain weight in temperate cereal yield determination: Evidence based on 30 years of multi-location trials, Field Crops Research 100(2–3), 179–88.

Reynolds, M., J. Foulkes, R. Furbank, S. Griffiths, J. King, E. Murchie, M. Parry & G. Slafer, 2012. Achieving yield gains in wheat, Plant, Cell & Environment 35(10), 1799–1823.

Reynolds, M.P., A. Pellegrineschi & B. Skovmand, 2005. Sink-limitation to yield and biomass: a summary of some investigations in spring wheat, Annals of Applied Biology 146(1), 39–49.

Rivera-Amado, C., E. Trujillo-Negrellos, M. Reynolds, R. Sylvester-Bradley, G. Molero & J. Foulkes, 2014. Genetic variation in total, soluble and structural DM partitioning among plant organs and association with harvest index in elite spring wheat lines, in Proceedings of the 4th International Workshop of the Wheat Yield Consortium, eds. M. Reynolds, G. Molero, E. Quilligan, M. Listman & H. Braun. : CIMMYT.

Rivera-Amado, C., E. Trujillo-Negrellos, R. Sylvester-Bradley, G. Molero, A. Sierra-Gonzalez, M. Reynolds & J. Foulkes, 2016. Achieving increases in spike growth, fruiting efficiency, and harvest index in high biomass wheat cultivars, in Proceedings of the 2nd International TRIGO (Wheat) Yield Potential Workshop 2016, eds. M. Reynolds, G. Molero & E. Quilligan. Obregon, Sonora, Mexico.: CIMMYT.

Sanchez-Bragado, R., G. Molero, M.P. Reynolds & J.L. Araus, 2014. Relative contribution of shoot and ear photosynthesis to grain filling in wheat under good agronomical conditions assessed by differential organ 13C, Journal of Experimental Botany 65(18), 5401–13.

Sayre, K.D., S. Rajaram & R.A. Fischer, 1997. Yield Potential Progress in Short Bread Wheats in Northwest Mexico, Crop Sci. 37(1), 36–42.

Serrago, R.A., I. Alzueta, R. Savin & G.A. Slafer, 2013. Understanding grain yield responses to source–sink ratios during grain filling in wheat and barley under contrasting environments, Field Crops Research 150, 42–51.

Shearman, V.J., R. Sylvester-Bradley, R.K. Scott & M.J. Foulkes, 2005. Physiological Processes Associated with Wheat Yield Progress in the UK, Crop Sci. 45(1), 175–85.

Thorne, G.N., 1982. Distribution between parts of the main shoot and the tillers of photosynthate produced before and after anthesis in the top three leaves of main shoots of Hobbit and Maris Huntsman winter wheat, Annals of Applied Biology 101(3), 553–59.

Zhu, G.X., D.J. Midmore, B.J. Radford & D.F. Yule, 2004. Effect of timing of defoliation on wheat (Triticum aestivum) in central Queensland, Field Crops Research 88(2–3), 211–26.

The trade-off between grain weight and grain number is affected by environmental conditioning: Wheat breeding strategies to increase yield potential

Alejandro Quintero[1, 2], Paola Montecinos[1], Gemma Molero[2], Matthew Reynolds[2] and Daniel F. Calderini[1]
[1] Universidad Austral de Chile, Chile; [2] CIMMYT, México.

Abstract
Identifying the mechanisms that are functionally linked to grain yield (GY) and its components —i.e., grain number (GN) and grain weight (GW)— is necessary for boosting GY potential of wheat. The objectives of the current study were to: (i) analyze the trade-off between GW and GN in 27 elite wheat genotypes grown in two contrasting locations with different yield potential; (ii) assess its causes; and (iii) evaluate the performance of transformed lines (T2) developed to overexpress the expansion gene *TaExpA6* in grain tissues. A set of 27 elite wheat genotypes was evaluated during three years in Ciudad Obregón, Mexico (CO), and two years in Valdivia, Chile (Val); an experiment assessing 24 T2 lines plus the parental wheat cultivar was also carried out in Valdivia. GY was higher in Val than CO. Also, individual grain weight (IGW) of most categories was higher in Val than in CO. Remarkably, the relationships between GY and GN showed contrasting responses between locations despite the similar GN.

A few transformed lines evaluated in Val showed higher grain weight across grain positions (g1, G2, G3 and G4) in the central spikelets of the spike, reaching up to 15.8% over the parental cultivar.

Introduction
Wheat breeding is challenged by the need to increase both potential and actual grain yield to feed a growing human population. In the past, wheat yield potential was increased by improving biomass partitioning to allow more grains per area to be set. However, the trade-off between thousand-grain weight (TGW) and grain number (GN) generally reported in the literature, could decrease genetic yield gains if GN is further strengthened. Asymptotic associations between grain yield and GN have already been reported in doubled haploid lines of wheat (Bustos et al., 2013; García et al., 2013). In addition, a preliminary evaluation of elite wheat genotypes from the CIMMYT Core Germplasm (CIMCOG) panel supports this trade-off, which could be due to: (i) source limitation during grain filling (Sinclair and Jamieson, 2006); (ii) the setting of smaller grains in distal position of the spikes, with lower weight potential (Acreche and Slafer, 2006; Fischer, 2008); or (iii) a combination of both. However, little is known about the causes behind this trade-off and the extent of the negative association between TGW and GN in elite wheat germplasm and their impact on grain yield.

Even less known is the effect of environmental conditions on the trade-off between the two major yield components. GN and grain weight (GW) are determined along an extended period of the wheat cycle; however, the determination of both yield components overlaps around anthesis (approximately between booting and 10 days after anthesis). Therefore, environmental conditions when flowers are growing could modify the interaction between GW and GN, taking into account that the size of the flowers has been associated with both final GW (Calderini and Reynolds, 2000; Hasan et al., 2011) and the likelihood of grain setting (Guo et al., 2016). Therefore, 27 CIMCOG genotypes were evaluated in Ciudad Obregón (Mexico) and Valdivia (Chile) in the present study.

To counteract the negative association between TGW and GN, the increase in GW potential is a prerequisite to avoid unsuccessful improvements of GN. However, key mechanisms controlling GW potential and traits associated to this yield component are still only partially understood. Therefore, the search for physiological mechanisms and genes associated with GW is important for increasing the efficiency of breeding programs aimed at improving the grain yield of wheat. Previous findings showed that maternal tissues of wheat grains (Hasan et al., 2011), grain length (Lizana et al., 2010), pericarp cell growth (Muñoz and Calderini, 2015) and the expression of expansin genes (Lizana et al., 2010) are associated with GW, among other factors. Taking into account this background, transformed lines overexpressing the *TaExpA6* gene in grains of wheat have been developed by the NIAB Project (UK). Evaluation of T2 transformed lines and their parental cultivar was also performed as part of the present study.

The present study aimed to: (i) account for the trade-off between TGW and GN in CIMMYT elite wheat germplasm (CIMCOG) and its effect on grain yield under high but different grain yield environments in Mexico and Chile; and (ii) assess the impact of the overexpression of gene *TaExpA6* in 24 T2 transformed lines respect to the parental cultivar.

Methods

A set of 27 elite wheat genotypes (26 *Triticum aestivum* and 1 *T. turgidum* var. *durum*) from the CIMMYT Core Germplasm (CIMCOG) panel were provided by CIMMYT's breeding programs. The 27 genotypes represent historical genetic gains and are derived from CIMMYT selections since 1999. Field trials to evaluate the CIMCOG panel were carried out at two contrasting locations (Cd. Obregón, Mexico, and Valdivia, Chile). At Ciudad Obregón (CO), the elite wheat genotypes were evaluated at CIMMYT's experiment station (CENEB) (27°23'N, 109°55'W) in Sonora, Mexico, for three consecutive growing seasons (CO_{y11}, CO_{y12} and CO_{y13}), under fully irrigated conditions. The seed rates were 101 kg ha^{-1} in CO_{y11}, 108 kg ha^{-1} in CO_{y12} and 110 kg ha^{-1} in CO_{y13}. During CO_{y13}, a source-sink ratio treatment was applied to 20 plants in each plot 10 days after anthesis by halving the spikes along the rachis to compare them with a control without manipulation. Sowing dates were December 6, 8 and November 23 for CO_{y11}, CO_{y12} and CO_{y13}, respectively. In Valdivia (Val), the same genotypes were assessed at the Estación Experimental Agropecuaria Austral (EEAA) (39° 47' 18"S, 73° 14' 5"O), of the Universidad Austral de Chile (UACh), during two growing seasons (Val_{y13} and Val_{y14}). The source-sink ratio treatment was applied to 5 plants in each plot 10 days after anthesis by halving the spikes along the rachis to compare them to a non-manipulated control. Sowing dates were September 10 and 14 in Val_{y13} and Val_{y14}, respectively, and seed rate was 333 seeds m^{-2} in both growing seasons.

At both locations, the phenological stages of plants were recorded at both locations using the Zadoks scale (Zadoks et al., 1974). At harvest, grain yield (GY), aboveground biomass (BM), harvest index (HI), grain number (GN), spike number (SPK), grain number per spike (GNSPK), thousand-grain weight (TGW) and individual grain weight of proximal (G2) and distal (G4) grain positions were estimated. In two contrasting genotypes, the individual grain weight (IGW) of grains in position two (G2, proximal grain) and four (G4, distal grain) on two spikelets in the middle of the spike was measured from anthesis up to 60 days after anthesis (A+60).

At each location (CO and Val), best linear unbiased predictors (BLUPs) were estimated for each elite wheat genotype and trait, and analyses of variance were performed using the linear mixed model and the GLM procedure from META-R 5.0 (Alvarado et al., 2015). A second analysis using BLUPs and consisting of a descriptive statistic (i.e., mean, min, max values, LSD, coefficient of variation, genetic correlation with yield, and significance of interactions among experimental factors) was carried out to evaluate the behavior of the 27 CIMCOG wheat genotypes at each location; linear and nonlinear regression analyses were carried out to determine the relationships between GY and its main components.

An experiment was carried out in Valdivia to assess the performance of transformed lines designed to overexpress the gene *TaExpa6* and the parental cultivar. These genotypes were developed in the Project "Wheat transformation to increase grain yield …" (Community Resource for Wheat Transformation UK), led by Simon McQueen-Mason and Daniel Calderini. The experiment was carried out in the EEAA of the Universidad Austral de Chile (UACh) in the 2016-2017 cropping season using a complete randomized design with three replicates. The seed rate was 45 seeds m^{-2} and the sowing date was September 2, 2016. Plots were fertilized and irrigated, weeds were removed, and pests and diseases were prevented or controlled.

At harvest, 7 spikes per plot were sampled and the weight of individual grains set at each position on the central spikelets of the spikes was measured.

Results

Similar GN was found between CO and Val averaged across genotypes and years (Tables 1 and 2). In CO, 15,850 grains m^{-2} were harvested, while 15,197 grains m^{-2} were harvested in Val. Despite the similar GN between both locations, GN showed statistical differences ($P<0.01$) through the years, since GN values in CO were 15,130, 16,315 and 16,104 grains m^{-2} for CO_{y11}, CO_{y12} and CO_{y13}, respectively, while in Val they were 16,441 and 13,939 grains m^{-2} for Val_{y13} and Val_{y14}, respectively.

Table 1. The average best linear unbiased predictors (BLUPs) of grain yield (GY), above-ground biomass (BM), harvest index (HI), grain number m^{-2} (GN), spikes number m^{-2} (SPK), grain number per spike (GNSPK), thousand-grain weight (TGW), individual grain weight of grain G2 (G2), individual grain weight of grain G4 (G4). The data are the BLUP of each genotype grown in Ciudad Obregón (CO) during three growing years.

Ciudad Obregon									
GENOTYPE	**YLD (g m^{-2})**	**BM (g m^{-2})**	**HI**	**GN (# m^{-2})**	**SPK (# m^{-2})**	**GNSPK (# spk^{-1})**	**TGW (g)**	**G2 (mg)**	**G4 (mg)**
BLUP	664.6	1414	0.47	15850	303	53	42.5	54.1	32.06
Max	731	1457	0.52	22348	384	68	52	65.51	44.19
Min	570.1	1363	0.42	13316	245	46	29.9	38.99	24.92
LSD	45.8	88.4	0.02	1511	33	6	2.4	3.51	6.52
CV	5	7.2	4.1	6.5	7.9	8.5	4.4	3.8	12.5
Pvalue G	***	Ns	***	***	***	***	***	***	***
Pvalue Y	***	***	***	***	***	***	***	***	***
Pvalue GxY	***	***	ns	***	***	***	***	**	**

BLUP, maximum and minimum value across the genotypes. Value of LSD test differences (P<0.05) across the genotypes. Coefficient of variation (CV). P-value G (genotypes), P-values Y (years) and P-value GxY (genotype for year); ns means non-significant effects between genotypes, * Significant difference at P < 0.05, ** Significant difference at P < 0.01, *** Significant difference at P < 0.001.

Table 2. The best linear unbiased predictors (BLUPs) of grain yield (GY), above-ground biomass (BM), harvest index (HI), grain number m^{-2} (GN), spikes number m^{-2} (SPK), grain number per spike (GNSPK), thousand-grain weight (TGW), individual grain weight of grain G2 (G2), individual grain weight of grain G4 (G4). The data are the BLUP value of each genotype grown in Valdivia (Val) during two growing years.

Valdivia									
GENOTYPE	**YLD (g m^{-2})**	**BM (g m^{-2})**	**HI**	**GN (# m^{-2})**	**SPK (# m^{-2})**	**GNSPK (# spk^{-1})**	**TGW (g)**	**G2 (mg)**	**G4 (mg)**
BLUP	783.3	1507.6	0.52	15197	473	32	52.2	65.66	42.35
Max	1021.8	1775.1	0.57	24482	595	48	60.5	74.53	52.92
Min	542.5	1223.6	0.4	9544	380	25	41.5	54.8	33.7
LSD	172.3	278.3	0.03	3432	94	5	4.4	5.56	5.87
CV	21.2	18.1	3.7	20	14.9	12.7	3.9	4.5	10.8
P-value G	***	***	***	***	***	***	***	***	***
P-value Y	***	***	***	***	ns	***	***	***	***
P-value GxY	ns	Ns	**	ns	ns	ns	***	***	ns

BLUP, maximum and minimum value across the genotypes. Value of LSD test differences (P<0.05) across the genotypes. Coefficient of variation (CV). P-value G (genotypes), P-values Y (Years) and P-value GxY (genotype for year); ns means not significant effects between genotypes, * Significant difference at P < 0.05, ** Significant difference at P < 0.01, *** Significant difference at P < 0.001.

Interestingly, the relationship between GY and GN showed contrasting responses between locations despite the similar GN. A very low relationship was found in CO, while a positive and linear relationship was

plotted in Val (Fig. 1a and 1b). The virtual lack of association in CO was due to a clear trade-off between TGW and GN (Fig. 1c). This negative relationship was consistent across years (data not shown). On the other hand, the positive association found in Val (Fig. 1b) was the result of a low trade-off between the two main yield components (Fig. 1d). In CO, the IGW of G2 presented a highly negative association with GN (Fig. 1e), proving that the trade-off between TGW and GN also affected individual grains, even proximal grains. On the other hand, in Val, the individual grain weight of G2 was also associated with GN; however, it had a lower determination coefficient than in CO (Fig. 1f).

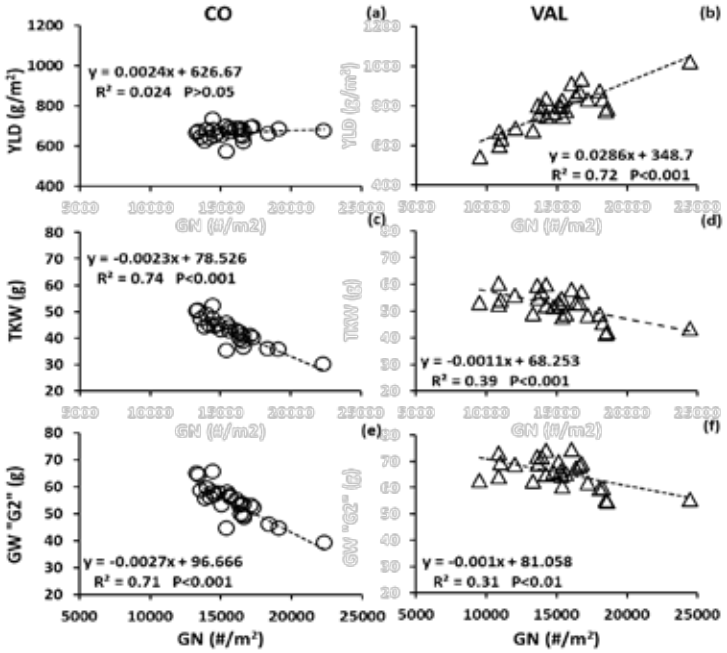

Fig. 1. Relationships of grain yield (GY) (a, b), thousand-grain weight (TGW) (c, d) and individual grain weight (IGW) of grain G2 (e and f) with grain number (GN) in the 27 wheat elite genotypes grown in CO (a, c, e) and Val (b, d, f).

The grain filling rates (GFR) were higher in Val than in CO. On the other hand, GFR across the years showed that genotype 11 had a higher GFR in grain positions G2 and G4 than genotype 15 (Fig. 2). The physiological maturity (PM) of grain both in positions G2 and G4 was shorter in Val than in CO. These results highlight the Valdivia location as a high potential environment, where the GFR is enormously benefited; therefore, in Val it is possible to obtain grains of greater weight than in CO.

To gain a better understanding of the contrasting trade-off found in CO and Val, the response of individual GW to the source-sink treatments (control and halved spikes at A+10) was analyzed at both locations (CO_{y13}, Val_{y13} and Val_{y14}). In CO_{y13}, the increased source-sink ratio had a positive effect ($P<0.001$) on final IGW, since G2 showed an average increase of 7.7% across genotypes and G4 improved by 16%. On the other hand, in Val, G2 increased 15% and 6.5% each year, i.e., Val_{y13} and Val_{y14}, respectively, while G4 increased 5.1% and 9.6% during Val_{y13} and Val_{y14}, respectively. The increases in IGW recorded at both locations across genotypes, years and different grain positions were always much lower than the enhancement of the source-sink ratio (approximately 100%); however, GW was more sensitive to the increase in the source-sink ratio in CO, contributing to the contrasting trade-off between locations.

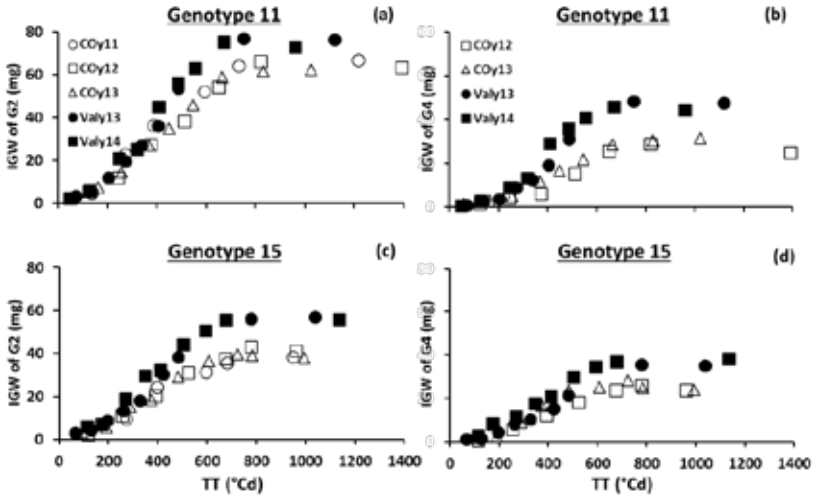

Fig. 2. Dynamics of individual grain weight of grains in positions G2 (a and c) and G4 (b and d) in genotypes 11 (a and b) and 15 (c and d) during grain filling.

The evaluation of the transformed lines and the parental cultivar showed different ($P<0.001$) final GW at each measured grain position (Table 3), where the highest ranked T2 line (52.16) outyielded the parental cultivar by 12.8%, 10.5%, 13.6% and 26.5% in grain positions G1, G2, G3 and G4.

Table 3. Grain weight of 24 transformed wheat lines overexpressing the *TaExpA6* gene and the parental cultivar.

GENOTYPE	**Grain weight (mg)**			
	G1	**G2**	**G3**	**G4**
52.16	62.9	66.5	60.6	49.9
52.4	59.6	64.4	60.3	46.4
51.1	60.3	64.4	58.5	44.7
51.18	59.4	62.7	55.6	42.5
52.1	55.7	62.3	55.6	39.0
52.11	58.6	62.3	57.9	43.7
52.3	56.0	62.1	56.4	41.5
51.10	58.2	62.1	58.7	46.5
51.21	57.2	62.0	56.6	42.0
52.12	56.3	61.9	61.0	38.5
51.20	56.7	61.7	55.3	39.6
52.14	57.6	61.4	56.6	41.7
52.7	56.5	60.7	56.2	41.0
51.14	55.3	60.4	53.8	40.6
52.2	55.6	60.0	57.6	43.2
52.8	53.2	59.9	53.1	36.9
52.15	54.3	59.9	52.3	38.4
51.9	58.6	59.1	55.5	43.3
51.6	54.6	59.1	53.9	41.6
51.15	53.2	58.9	55.2	40.1
51.12	57.8	58.7	53.7	39.3
52.17	52.9	58.7	53.2	38.1
52.10	53.1	58.2	53.0	38.0
52.13	53.4	57.1	50.4	37.1
Parental	**55.8**	**60.2**	**53.4**	**39.5**
P-value	***	***	***	***

Conclusions

This study confirms the lack of a linear association between GY and GN reported previously in evaluations of a wheat DH population (Bustos et al., 2013; García et al., 2013), which was due to the trade-off between the two main yield components (GW and GN). Therefore, the need to increase GW is clearly shown by the trade-off between TGW and GN recorded in CO in each of the three growing years. On the other hand, no trade-off between GW and GN was found in Val across the 27 elite wheat genotypes, given that the final GW of both proximal and distal grains in the spike were higher in Val than CO. In other words, grains in distal positions of the spikes do not power the negative association between GW and GN at this location.

These results reinforce the need to increase grain weight potential to improve grain yield of wheat. Transformed lines overexpressing the expansin gene *TaExpa6* show promise for producing heavier wheat grains which, in turn, will counteract the trade-off between grain weight and grain number found in environments like Ciudad Obregón.

References

Acreche, M., Slafer, G.A., 2006. Grain weight response to increases in number of grains in wheat in a Mediterranean area. F. Crop. Res. 98, 52–59.

Bustos, D. V., Hasan, A.K., Reynolds, M.P., Calderini, D.F., 2013. Combining high grain number and weight through a DH-population to improve grain yield potential of wheat in high-yielding environments. F. Crop. Res. 145, 106–115.

Calderini, D.F. and Reynolds, M.P., 2000. Changes in grain weight as a consequence of de-graining treatments at pre- and post-anthesis in synthetic hexaploid lines of wheat (Triticum durum x T. tauschii). Australian Journal of Plant Physiology 27: 183-191.

Fischer, R.A., 2008. The importance of grain or kernel number in wheat: A reply to Sinclair and Jamieson. F. Crop. Res. 105, 15–21.

García, G.A., Hasan, A.K., Puhl, L.E., Reynolds, M.P., Calderini, D.F., Miralles, D.J., 2013. Grain yield potential strategies in an elite wheat double-haploid population grown in contrasting environments. Crop Sci. 53, 2577–2587.

Guo, Z., Slafer, G.A., Schnurbusch, T., 2017. Genotypic variation in spike fertility traits and ovary size as determinants of floret and grain survival rate in wheat. J. Exp. Bot. 67: 4221-4230.

Hasan, A. K., Herrera, J., Lizana, C., and Calderini, D. F., 2011. Carpel weight, grain length and stabilized grain water content are physiological drivers of grain weight determination of wheat. Field Crops Research 123(3): 241–247. http://doi.org/10.1016/j.fcr.2011.05.019

Lizana, X. C., Riegel, R., Gomez, L. D., Herrera, J., Isla, A., McQueen-Mason, S. J., and Calderini, D. F., 2010. Expansins expression is associated with grain size dynamics in wheat (Triticumaestivum L.). Journal of Experimental Botany 61(4): 1147–1157. http://doi.org/10.1093/jxb/erp380

Muñoz, M. and Calderini, D. F., 2015. Volume, water content, epidermal cell area, and XTH5 expression in growing grains of wheat across ploidy levels. Field Crops Research 173: 30–40.

Quintero, A., Molero, G., Reynolds, M. P., Le Gouis, J., and Calderini, D. F., 2014. Trade-off between grain weight and grain number and key traits for increasing potential grain weight in CIMCOG population. In: Reynolds, M.P., Molero, G., Quilligan, E., Listman, M., and Braun, H.J. (Eds.), Proceedings of the 4th International Workshop of the Wheat Yield Consortium. CENEB, CIMMYT, Cd. Obregón, Sonora, México, pp. 114-121.

Sinclair, T., Jamieson, P., 2006. Grain number, wheat yield, and bottling beer: An analysis. F. Crop. Res. 98, 60–67.

Lignin, structural and non-structural carbohydrates and their association with stem strength components of irrigated spring wheat

Francisco J. Piñera-Chavez[1,2], Peter M. Berry[3], Michael J. Foulkes[1], Gemma Molero[2] and Matthew P. Reynolds[2]
[1]University of Nottingham, UK; [2]CIMMYT, Mexico; [3]ADAS, UK

Abstract
Wheat stem biomass is composed of three major components: lignin, cellulose and hemicellulose. Previous studies have shown that each of these components confer mechanical strength to the stems. However, assumptions about which is the key component might be complex. Most of the literature indicates that lignin is more related to stem strength, although cellulose and hemicellulose are also mentioned in some studies. In this study, the objective was to compare cultivars with low, intermediate and high stem strength. Fractions of biomass components (lignin, cellulose and hemicellulose) and water soluble carbohydrates (WSC) and key stem strength traits were estimated for 10 cultivars during 2012, 2013 and 2014. Significant differences were identified between experiments and cultivars for cellulose, hemicellulose, lignin and WSC. Genotype × environment (G×E) interaction was significant ($P < 0.01 – 0.001$) for lignin and cellulose but not for WSC and hemicellulose. Analyses of variance indicated no significant differences between means of low, intermediate and high stem strength cultivars. Additionally, regression analysis suggested that there was no individual effect of the three major components of the structural biomass (lignin, cellulose and hemicellulose) on the stem strength and stem material strength.

Introduction
Lodging is a complicated phenomenon described as the permanent displacement of cereal stems from the vertical, which can result from either failure of the stem base (stem lodging) or failure of the anchorage system (root lodging) (Berry et al., 2004). Lodging can reduce grain yield, quality and speed of harvest and increase drying costs (Berry, 1998; Berry et al., 2004). It has been stated that to improve lodging resistance, attention must be paid to the biophysical properties of the stem base (stem strength) and anchorage system (anchorage strength) (lodging traits) (Baker et al., 1998; Berry et al., 2003). Biomass of stem and crown roots has been found to be strongly and positively correlated to stem and anchorage strength, respectively. Thus, an investment of biomass in stems and roots will be required if improved lodging resistance is to be realized (Berry et al., 2007; Piñera-Chavez et al., 2016a).

This paper focuses on the chemical composition of stem biomass and its relationship with stem strength. This biomass can be broken down into non-structural (water soluble carbohydrates, WSC) and structural (lignin, cellulose and hemicellulose) carbohydrates. Several studies have described different associations of these components with lodging traits. For instance, Knapp et al. (1987) concluded that the arrangement and inter-relationships of the lignin and structural carbohydrates in wheat cell walls may be more important than their simple concentrations. Most recent investigations have reported findings where lignin or cellulose contents were more related to stem strength and lodging resistance. For instance, Ma (2009) found that the wheat gene *TaCM* (involved in lignin biosynthesis) is associated with stem strength and lodging index. It has also been reported that growth regulators alter lignin accumulation and the strength of basal internodes (Peng et al., 2014). Wiersma et al. (2011) found a positive association between lodging resistance and acid detergent lignin (ADL). On the other hand, Wang et al. (2012) proposed that cellulose plays a more important role in the ability of wheat stems to resist lodging. None of these studies indicated any contribution of hemicellulose or WSC to stem strength. For this study, cultivars with contrasting overall stem strength from the CIMMYT Mexico Core Germplasm Panel (CIMCOG) were selected (Table 1). The main goal was to investigate the contributions of structural biomass components (lignin, cellulose and hemicellulose) and WSC to stem strength.

Methods
Field experiments established during the field seasons 2011-2012, 2012-2013 and 2013-2014 (hereafter referred to as 2012, 2013 and 2014, respectively) were used for this study. Ten cultivars from the CIMCOG panel were selected to integrate a wide range of stem strength dimensions on internode 2 and were separated into high, intermediate and low stem strength cultivars (Table 1). Detailed information about

experiments, lodging trait measurements and calculations were given in two complementary papers of this investigation (Piñera-Chavez et al., 2016a,b).

WSC content (dry weight basis) was determined in CIMMYT's Maize Nutrition Quality and Plant Tissue Analysis Laboratory (El Batan, Mexico) using the Anthrone method (Galicia et al., 2008) and lignin, cellulose and hemicellulose concentrations (dry weight basis) were determined in the Bioenergy and Brewing Science Building laboratories of the University of Nottingham (Sutton Bonington, UK). For lignin concentration, the Acetyl Bromide Spectrophotometric Method (Fukushima and Hatfield, 2001) was used. Cellulose and hemicellulose fractions were estimated according to the method described by Fang et al. (1999). A combined analysis of variance across experiments 2012, 2013 and 2014 was carried out by using an unbalanced treatment structure for lignin concentration and WSC and using a general treatment structure with data of two replicates from experiments 2012 and 2013 for cellulose and hemicellulose. These analyses were implemented on GENSTAT 16th Edition.

Table 1. Cultivars from CIMCOG with contrasting stem strength (SS) performance.

No.	Name	SS classification	SS (N mm)*
1	BACANORA T 88	Low	127
2	BCN/RIALTO	Low	146
3	PFAU/SERI.1B//AMAD/3/WAXWING (=Super 152)	Low	154
4	CMH79A.955/4/AGA/3/4*SN64/CNO67//INIA66/5/NAC/6/RIALTO	Intermediate	196
5	CROC_1/AE.SQUARROSA (205)//BORL95/3/PRL/SARA//TSI/VEE#5/4/FRET2	Intermediate	162
6	SIETE CERROS T66 (Hist 1)	Intermediate	186
7	TACUPETOF2001/BRAMBLING*2/5/KAUZ//ALTAR84/AOS/3/MILAN/KAUZ/4/HUITES	Intermediate	183
8	WBLL1*2/KURUKU*2/5/REH/HARE//2*BCN/3/CROC_1/AE.SQUARROSA(213)//PGO/4/HUITES	High	208
9	YAV_3/SCO//JO69/CRA/3/YAV79/4/AE.SQUARROSA(498)/5/LINE 1073/6/KAUZ*2/4/CAR//KAL/BB/3/NAC/5/KAUZ/7/KRONSTAD F2004/8/KAUZ/PASTOR//PBW343	High	204
10	CNO79//PF70354/MUS/3/PASTOR/4/BAV92*2/5/FH6-1-7	High	229

* Means from cross-year analysis for SS of internode 2 (Piñera-Chavez et al., 2016b).

Results/Discussion

Individual cultivar means for each experiment, standard error of differences (SED) and significance for main effects (experiment and cultivar) and the interaction are given in Table 2. Significant differences ($P < 0.001$) were identified between experiments and cultivars for all traits. Genotype by environment interaction was significant ($P < 0.01 – 0.001$) for lignin and cellulose but not for WSC and hemicellulose. It is important to mention that cultivars selected for these analyses were chosen with a wide range of stem strength, providing enough of a testbed for testing the relationships between stem strength and stem biomass components. These analyses have shown that the simple proportion of WSC, lignin, cellulose and hemicellulose to overall stem dry weight showed significant differences among cultivars. However, cellulose and lignin cultivar ranks from one experiment were different when compared with the rest of the experiments, meaning that environment or genotype are not just simple main effects but depend on each other. This indicated that the best cultivar would not be stable across environments. A general analysis of variance indicated no significant differences between means of low, intermediate and high stem strength grouped cultivars (Figure 1), indicating no individual effect of lignin, cellulose, hemicellulose or WSC content on stem strength.

Table 2. Mean values of stem strength (SS) of internode 2, overall stem water-soluble carbohydrate content (WSC) and internode 2 lignin, cellulose and hemicellulose fractions for 10 cultivars from CIMCOG panel across experiments 2012, 2013 and 2014. All the percentages are on a dry weight basis.

Group	**Cultivar**	**WSC (%)**			**Lignin (%)**			**Cellulose† (%)**		**Hemicellulose† (%)**	
		2012	2013	2014	2012	2013	2014	2012	2013	2012	2013
Low	7	23.0	25.7	19.6	22.3	34.7	33.3	38.2	26.8	24.9	21.5
	9	26.8	26.1	–	26.1	38.4	–	41.5	23.1	27.2	23.1
	39	25.7	29.5	22.4	26.8	34.5	31.0	42.9	32.8	32.2	24.0
	Mean	25.2	27.1	21.0	25.1	35.9	32.2	40.9	27.6	28.1	22.9
Intermediate	19	18.3	22.4	–	27.4	33.8	–	46.7	22.5	32.1	24.9
	24	23.6	24.2	15.2	25.2	34.3	32.5	46.2	24.0	33.1	24.7
	45	28.3	34.8	–	29.1	37.7	–	41.2	20.9	37.5	24.4
	49	22.2	27.2	–	24.4	33.1	–	43.0	20.8	28.8	25.6
	Mean	23.1	27.2	15.2	26.5	34.7	32.5	44.3	22.1	32.9	24.9
High	23	30.0	29.1	–	29.2	37.4	–	34.0	16.5	27.3	25.5
	57	27.9	28.9	20.3	30.0	35.6	30.4	36.0	27.5	27.5	20.5
	60	25.7	26.1	22.0	27.4	32.6	27.3	35.6	19.4	33.8	25.7
	Mean	27.9	28.0	21.2	28.9	35.2	28.9	35.2	21.1	29.5	23.9
	Grand Mean	25.1	27.4	19.9	26.8	35.2	30.9	40.5	23.4	30.4	24.0
	Experiment (SED)	0.87***(2)			0.62***(2)			1.24***(1)		1.40***(1)	
	Cultivar (SED)	1.56***(9)			1.11***(9)			1.96***(9)		2.21*(9)	
	Interaction (SED)	2.19ns(13)			1.55**(13)			2.90**(9)		3.28ns(9)	

***, P < 0.001; **, P < 0.01; *, P < 0.05; ns, not significant

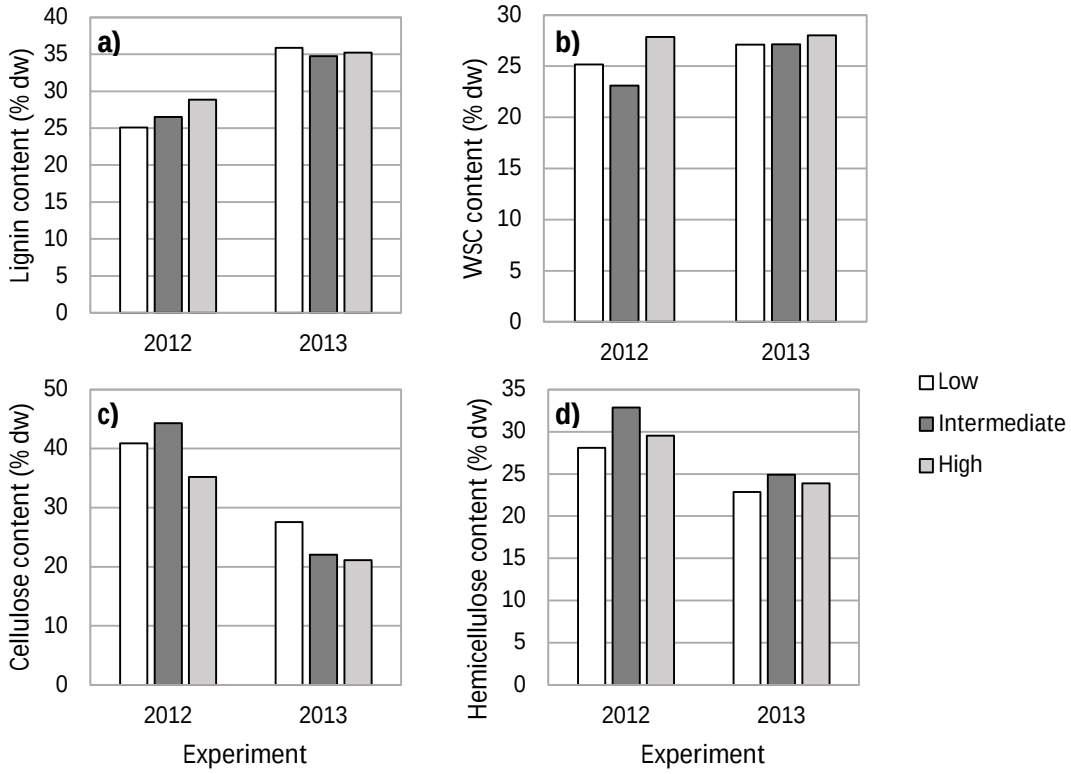

Fig. 1. Mean values for lignin (a), water-soluble carbohydrate (WSC) (b), cellulose (c) and hemicellulose (d) content of cultivars with low, intermediate and high stem strength scores from experiments in 2012 and 2013.

The secondary plant cell wall is the main component of the structural biomass and is composed mainly of cellulose, hemicellulose and lignin. However, the primary plant cell wall is also predominantly composed of cellulose and hemicellulose (CCRC 2007). Within the many functions of both primary and secondary plant cell walls are the mechanical properties that were of interest for this paper (Taiz, 1984; CCRC, 2007). If we consider that the structural and chemical composition of the plant cell wall is extremely complex, it seems logical that this mechanical support would not be explained by a single component. It has been suggested that the mechanical strength of the stem base of wheat plants is conferred by biophysical properties such as diameter, wall width and material strength (Berry et al., 2004). However, it is obvious that the components of the structural biomass (lignin, cellulose and hemicellulose) and their interactions combined with the biophysical dimensions of stems will influence stem strength.

The structural biomass composition of wheat cell walls has been described previously. For instance, Collins et al. (2014) and Ibbett et al. (2014) indicated lignin content ranged 13-23% on a dry weight basis, while cellulose and hemicellulose have been estimated from 39-40% and 28-29%, respectively (Ibbett et al., 2011, 2014). For wheat stems, percentages of lignin were estimated in the range of 9-14% (Qingxiang, 2002; Fukushima and Hatfield, 2004), cellulose at 46% and hemicellulose at 32% (Qingxiang, 2002). In the specific case of the lowest basal internodes (affected by lodging), lignin has been quantified from 10-30% (Knapp et al., 1987; Ma, 2009; Kong et al., 2013), cellulose from 36-50% (Knapp et al., 1987; Kong et al., 2013) and hemicellulose from 35-36 % (Knapp et al., 1987). The CIMCOG panel subgroup used in this study has shown particularly high lignin (28-33%) concentrations compared with the ranges mentioned before, while cellulose (28-35%) and hemicellulose (23-31%) concentrations were lower than these ranges. These variations can be due to differences in the methods used to quantify the component content or that in some cases this content was estimated on a whole stem dry weight basis instead of a particular internode. Moreover, some ranges were done on genetic variation basis and others included environment effects.

The summary of the regression analysis for each individual year and for the cross-experiment means indicated that there was no clear or no relationship between stem strength and stem material strength with dry weight components (lignin, cellulose, hemicellulose and water-soluble carbohydrates) (Table 3). For instance, stem strength was negative and significantly related to lignin only for the experiment in 2014 with a similar trend in the experiment in 2012 but there was no relationship for the experiment in 2013 or the cross-year mean. Cellulose content also showed a strong positive association with stem material strength during 2012 but no relationship for 2013. Data for the regression lines are plotted in Figures 2 and 3.

Table 3. Linear regression equations for relationships between stem strength (SS) and stem material strength with lignin, cellulose, hemicellulose and water-soluble carbohydrate content from each individual experiment. Significance indicated in brackets when needed.

		Stem strength		Stem material strength	
		Equation	R^2	Equation	R^2
Lignin					
	2012	y = 9.21x-36.1	0.21	y = -1.08x+58.7	0.11
	2013	y = -3.45x+315	0.05	y = -1.64x+99.9	0.06
	2014	y = -9.78x+486	$0.86_{(P < 0.05)}$	y = 2.45x-44.6	0.33
	Mean	**y = -2.99x+292**	**0.02**	**y = -1.40x+79.0**	**0.05**
WSC					
	2012	y = -1.15x+240	0.007	y = -1.07x+56.6	0.22
	2013	y = 0.87x+1.68	0.008	y = 0.82x+19.9	0.04
	2014	y = 2.96x+125	0.12	y = -2.38x+78.3	0.46
	Mean	**y = -1.61x+241**	**0.03**	**y = -0.36x+44.7**	**0.02**
Cellulose					
	2012	y = -1.98x+289	0.03	y = 1.49x-28.9	$0.71_{(P < 0.01)}$
	2013	y = -1.89x+239	0.07	y = 0.009x+42.1	0.00
	Mean	**y = -0.71x+222**	**0.006**	**y = 1.54x-13.7**	$\mathbf{0.30}_{(P = 0.10)}$
Hemicellulose					
	2012	y = -0.68x+233	0.03	y = 0.72x+6.93	0.13
	2013	y = 8.14x+9.21	0.19	y = 2.99x-24.9	0.15
	Mean	**y = 3.53x+103**	**0.08**	**y = 1.84x-14.6**	**0.21**

2012, N = 10; 2013, N = 10; 2014, N = 5; Mean, N = 10

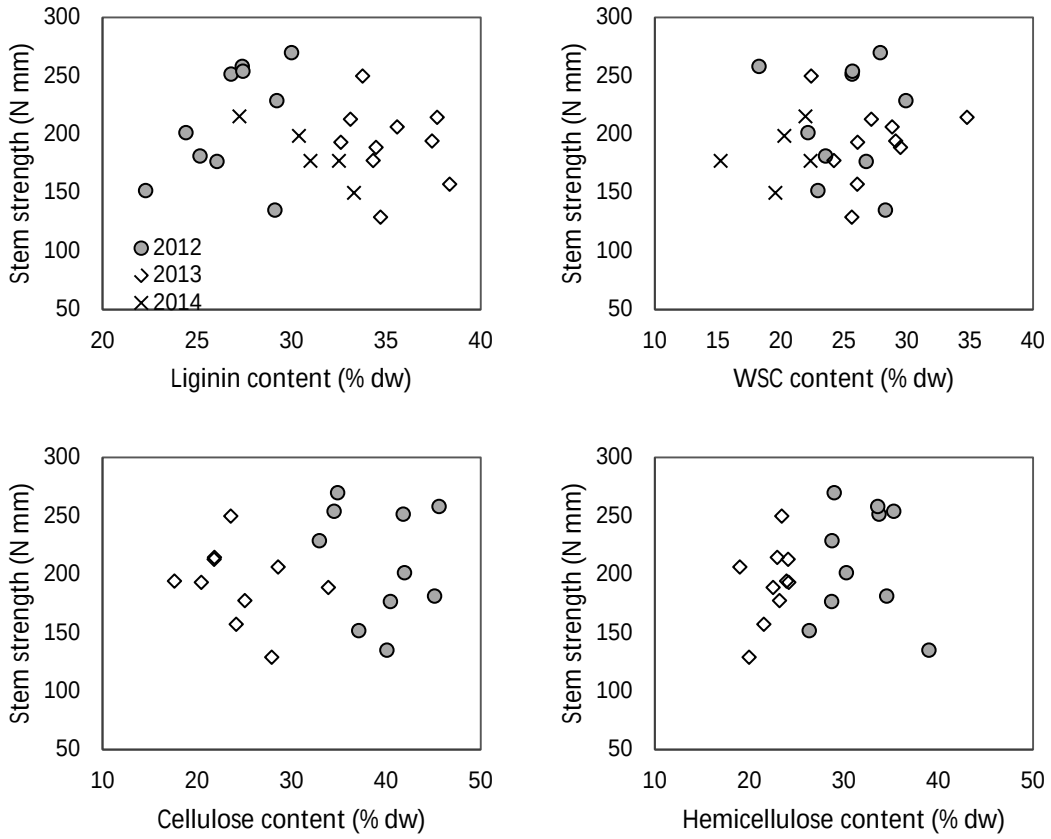

Fig. 2. Stem strength plotted against water-soluble carbohydrate (WSC), lignin, cellulose and hemicellulose. All the values were in terms of percentage of dry weight of internode 2, except for WSC (whole stem).

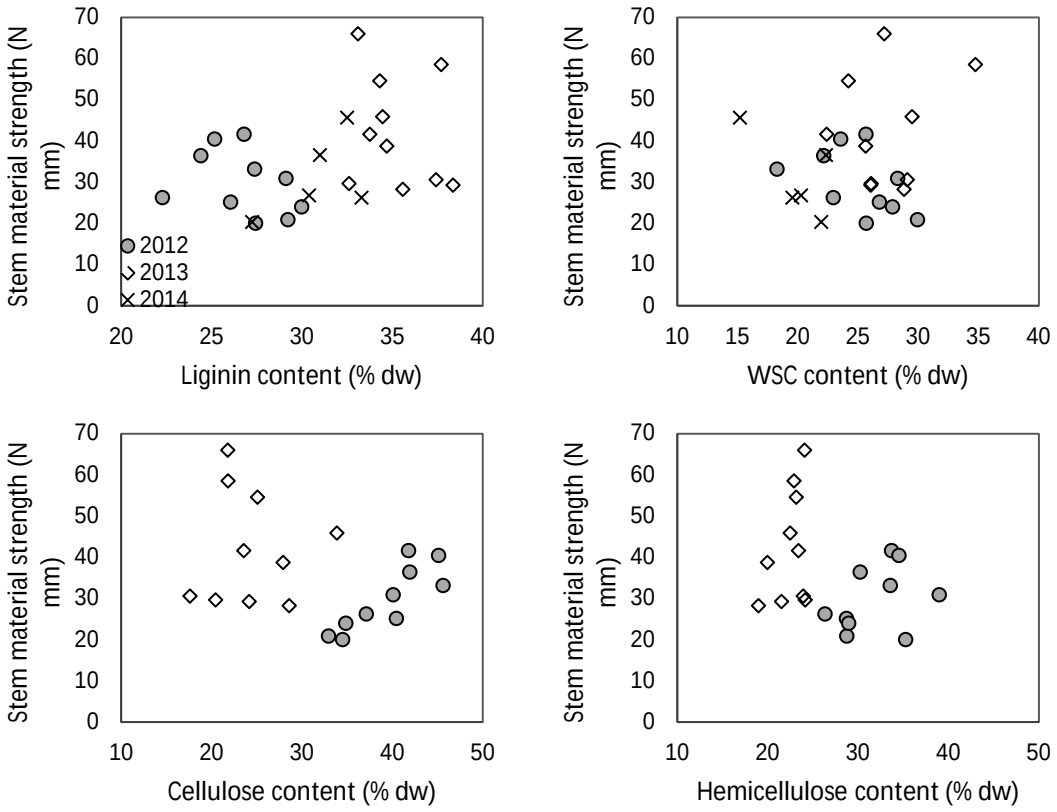

Fig. 3. Stem material strength plotted against water-soluble carbohydrate (WSC), lignin, cellulose and hemicellulose. All the values were in terms of percentage of dry weight of internode 2, except for WSC (whole stem).

A review of several studies suggested that there is no consensus regarding which key component of the cell wall confers strength to the stems of wheat (Knapp et al., 1987; Ma, 2009; Wiersma et al., 2011; Wang et al., 2012; Kong et al., 2013; Peng et al., 2014). Lignin has been long proposed to be associated with stem strength. Greater *TaCM* protein levels and *TaCM* activity in a lodging-resistant wheat cultivar than a lodging-susceptible cultivar and association with stem strength suggest that lignin synthesis plays an important role in lodging resistance (Ma, 2009). Interestingly, Peng et al. (2014) indicated that growth regulators paclobutrazol and gibberellic acid not only reduced lodging risk by reducing plant height but also increased the physical strength of basal internodes particularly by increasing lignin accumulation and lignin related enzymatic activity. Wiersma et al. (2011) identified an increment in acid detergent lignin (ADL) when growth regulator trinexapac-ethyl rates increased. This last study also identified positive correlations between lodging resistance and acid detergent lignin. Nevertheless, a histochemical evaluation of different wheat stems differing in lodging resistance performance identified the cellulose component as the main factor conferring these differences in lodging resistance (Wang et al., 2012).

Our study indicated that individually none of the cell wall components (% of stem dry weight) affects the stem strength or stem material strength of spring wheat. However, some individual associations by experiment suggest that there could be interesting interrelationships to follow up in further investigations. These results should be considered together with the strong relationship identified between stem dry weight per unit length with stem strength (Piñera-Chavez et al., 2016a) and between stem material strength and stem wall density (Berry et al., 2007). Thus, it can be inferred that all three major components of the plant cell walls of spring wheat have positive effects on strengthening the base of the stem, with special importance of the interactions between them (Knapp et al., 1987). Pinthus (1973) stated that plants with high cellulose, hemicellulose and lignin were more resistant to lodging. Thus, it can be

considered that biomass as a complex has major effects on stem strength. Interestingly, when WSC content was discarded from this biomass, the relationship with stem strength identified by Piñera-Chavez et al. (2016a) improved. This was consistent with Knapp et al. (1987) who also found that lodging was not associated with WSC content in wheat.

Conclusions

Significant differences were found between experiments and cultivars for cellulose, hemicellulose, lignin and WSC. G×E interaction was significant for lignin and cellulose but not for WSC and hemicellulose. Analysis of variance indicated no significant differences between means of low, intermediate and high stem strength cultivars. Regression analysis suggested that there was no individual effect of the three major components of the structural biomass (lignin, cellulose and hemicellulose) on stem strength and stem material strength. The complexity of the plant cell wall architecture should be considered when assumptions about which key component of the cell wall confers the mechanical strength of the stem base of wheat plants. Our results suggested that there is no individual effect of the three major components of the structural biomass (lignin, cellulose and hemicellulose) on stem strength and stem material strength.

References

Baker CJ, Berry PM, Spink JH, et al (1998) A method for the assessment of the risk of wheat lodging. J Theor Biol 194:587–603. doi: 10.1006/jtbi.1998.0778

Berry PM (1998) Predicting lodging in wheat. Ph. D. Thesis. The University of Nottingham, UK, 210 pp.

Berry PM, Sterling M, Baker CJ, et al (2003) A calibrated model of wheat lodging compared with field measurements. Agric For Meteorol 119:167–180. doi: 10.1016/S0168-1923(03)00139-4

Berry PM, Sterling M, Spink JH, et al (2004) Understanding and reducing lodging in cereals. Adv Agron 84:217–271. doi: 10.1016/S0065-2113(04)84005-7

Berry PM, Sylvester-Bradley R, Berry S (2007) Ideotype design for lodging-resistant wheat. Euphytica 154:165–179. doi: 10.1007/s10681-006-9284-3

CCRC (2007) Plant cell walls. Complex Carbohydrate Research Center, BioEnergy Science Center, University of Georgia, Athens GA, USA. http://www.ccrc.uga.edu/~mao/intro/ouline.htm. Accessed 7 Dec 2015

Collins SR, Wellner N, Martinez Bordonado I, et al (2014) Variation in the chemical composition of wheat straw: the role of tissue ratio and composition. Biotechnol Biofuels 7:121. doi: 10.1186/s13068-014-0121-y

Fang JM, Sun R, Fowler P, et al (1999) Esterification of wheat straw hemicelluloses in theN,N-dimethylformamide/lithium chloride homogeneous system. J Appl Polym Sci 74:2301–2311. doi: 10.1002/(SICI)1097-4628(19991128)74:9<2301::AID-APP20>3.0.CO;2-7

Fukushima RS, Hatfield RD (2001) Extraction and isolation of lignin for utilization as a standard to determine lignin concentration using the acetyl bromide spectrophotometric method. J Agric Food Chem 49:3133–3139. doi: 10.1021/jf010449r

Fukushima RS, Hatfield RD (2004) Comparison of the acetyl bromide spectrophotometric method with other analytical lignin methods for determining lignin concentration in forage samples. J Agric Food Chem 52:3713–3720. doi: 10.1021/jf035497l

Galicia L, Nurit E, Rosales A, Palacios-Rojas N (2008) Laboratory protocols 2009: Maize nutrition quality and plant tissue analysis laboratory. CIMMYT, Mexico, D. F.

Ibbett R, Gaddipati S, Davies S, et al (2011) The mechanisms of hydrothermal deconstruction of lignocellulose: New insights from thermal–analytical and complementary studies. Bioresour Technol 102:9272–9278. doi: 10.1016/j.biortech.2011.06.044

Ibbett R, Gaddipati S, Greetham D, et al (2014) The kinetics of inhibitor production resulting from hydrothermal deconstruction of wheat straw studied using a pressurised microwave reactor. Biotechnol Biofuels 7:45. doi: 10.1186/1754-6834-7-45

Knapp JS, Harms CL, Volenec JJ (1987) Growth regulator effects on wheat culm nonstructural and structural carbohydrates and lignin. Crop Sci 27:1201–1205.

Kong E, Liu D, Guo X, et al (2013) Anatomical and chemical characteristics associated with lodging resistance in wheat. Crop J 1:43–49. doi: 10.1016/j.cj.2013.07.012

Ma Q-H (2009) The expression of caffeic acid 3-O-methyltransferase in two wheat genotypes differing in lodging resistance. J Exp Bot 60:2763–71. doi: 10.1093/jxb/erp132

Peng D, Chen X, Yin Y, et al (2014) Lodging resistance of winter wheat (Triticum aestivum L.): Lignin accumulation and its related enzymes activities due to the application of paclobutrazol or gibberellin acid. F Crop Res 157:1–7. doi: 10.1016/j.fcr.2013.11.015

Piñera-Chavez FJ, Berry PM, Foulkes MJ, et al (2016a) Avoiding lodging in irrigated spring wheat. I. Stem and root structural requirements. F Crop Res 196:325–336. doi: 10.1016/j.fcr.2016.06.009

Piñera-Chavez FJ, Berry PM, Foulkes MJ, et al (2016b) Avoiding lodging in irrigated spring wheat. II. Genetic variation of stem and root structural properties. F Crop Res 196:64–74. doi: 10.1016/j.fcr.2016.06.007

Pinthus MJ (1974) Lodging in wheat, barley, and oats: the phenomenon, its causes, and preventive measures. Adv Agron 25:209–263.

Qingxiang M (2002) Composition , nutritive value and upgrading of crop residues. In: Tingshuang G, Sanchez M, Pei Yu G (eds) Animal Production Based on Crop Residues - Chinese Experiences. FAO, Rome, Italy, pp 24–52

Taiz L (1984) Plant cell wall expansion: Regulation of Cell Wall Mechanical Properties. Annu Rev Plant Physiol 35:585–657.

Wang J, Zhu J, Huang R, Yang Y (2012) Investigation of cell wall composition related to stem lodging resistance in wheat (Triticum aestivum L.) by FTIR spectroscopy. Plant Signal Behav 7:856–863.

Wiersma JJ, Dai J, Durgan BR (2011) Optimum timing and rate of trinexapac-ethyl to reduce lodging in spring wheat. Agron J 103:864–870. doi: 10.2134/agronj2010.0398

Uncoupling time to terminal spikelet and heading date in bread wheat (*Triticum aestivum* L.)

*Oscar E. Gonzalez-Navarro[1], Luzie U. Wingen[1], Claire West[1], Sarah A. Collier[1], Michelle Leverington-Waite[1], Joerg Plieske[2], Simon T. Berry[3], Fernanda G. Gonzalez[4], Gustavo A. Slafer[5] and Simon Griffiths[1]**

[1] John Innes Centre, UK;[2] TraitGenetics, Germany;[3] Limagrain, Woolpit, UK;[4] Consejo Nacional de Investigaciones Científicas y Técnicas (CONICET), Argentina;[5] ICREA (Catalonian Institution for Research and Advanced Studies), Spain

Abstract

A segregating doubled haploid population derived from UK winter wheat parents Buster and Charger was grown in four environments. Phenology traits were recorded and QTL identified with a particular focus on heading date and terminal spikelet. QTL for heading date were identified on chromosomes 2D and 4A in all environments. Coincident QTL for time to terminal spikelet were not detected. A single QTL for terminal spikelet was identified on chromosome 7A. The independent genetic control of these traits provides an opportunity for marker-based manipulation of the rapid stem extension phase.

Key words: heading time, QTL, stem elongation, terminal spikelet, *Triticum aestivum* L.

Introduction

Efforts to understand the genetic variation controlling crop adaptation have been ongoing for almost 100 years and have resulted in a vast accumulation of knowledge of flowering time and flowering time-related genes (Milec et al., 2014). Three key groups of genes are responsible for controlling crop adaptation by its responsiveness to: (i) the period of time it receives daylight (photoperiod genes, *Ppd*); (ii) the period of cold (vernalization, *Vrn*); and (iii) developmental rates after vernalization and photoperiod are fully satisfied (Eps) (Snape et al., 2001). This last group is involved in a more specialized adaptation known as fine-tuning (Griffiths et al., 2009).

The adaptation of hexaploid wheat by insensitive alleles of *Ppd-1* resulted in cultivars that performed well from Canada to Argentina (Borlaug, 1983). Insensitivity is a result of promoter deletion or copy number expansion in *Ppd-1* (Beales et al., 2007). On the other hand, vernalization is controlled by three homoeologous copies of *Vrn-1* (Loukoianov et al., 2005). A dominant *Vrn* gene in any of these locations will provide spring phenological growth (Stelmakh, 1987). The positional cloning of these genes was expedited by their strong effects on ear emergence.

Embracing the task of matching crop production with demand requires a deeper understanding of the association of yield component traits with their genes. Thus, an understanding of complex traits in wheat enables an accurate and effective search in a well-designed mapping population. Doubled haploid (DH) lines (homozygous offspring of haploid individuals that have undergone chromosome doubling) allows direct fixation of the genetic content. Once heterozygosity is taken from the equation, it becomes relatively easier to identify genomic loci that explain quantitative variation of a trait that segregates throughout the lines derived from distinct parental cultivars.

The aim of the present study was to identify the genetic controls responsible for developmental timing in a DH population derived from two elite winter wheat cultivars, Buster and Charger. These varieties differ very little in their heading date. They carry the same alleles for vernalization response and photoperiod sensitivity. Therefore, the population is very well-suited for the genetic dissection of components of heading date, the duration and timing of which constitute an importnant series of developmental events prior to ear emergence.

Materials and Methods

Plant material and growing conditions

The mapping population of 109 DH lines was derived from Buster x Charger, two elite winter wheat lines well adapted to UK's environment. Both Buster (Brimstone x Parade, developed by Nickerson Seeds Ltd.) and Charger (Fresco Sib x Mandate developed by Plant Breeding International Cambridge Ltd.) share a common background and a similar set of major genes having an effect on developmental phases (i.e., *Ppd-1* and *Vrn-1*). Both Buster and Charger are day-length sensitive winter wheat varieties.

Field trials were conducted at three locations: Norwich, Norfolk, UK, and Woolpit, Suffolk, UK. The lines were grown following standard agronomic practices. Trial locations and meteorological data are shown below.

Location	Coordinates	Plot size (m)	Harvest year	Total rainfall (mm)	Avg. daily temperature (°C)	Avg. daily radiation (MJ m^{-2} d^{-1})	Environment
Norwich	52°63 N, 01°30 E, 14 m a.s.l.	1x1	2012	414	7.6	13.7	CF12
		1.5x4	2013	501	6.1	12.8	CF13
		1.5x4	2014	434	8.1	14.2	CF14
Woolpit	52°11 N, 00°51 E, 80 m a.s.l.	1.2x4.5	2013	497	6.1	12.8	WP13

Phenology

Developmental traits were determined as the time when 50% of the plot presented the respective trait (e.g., time to heading, when half of the spike emerged from the flag leaf sheath). Terminal spikelet phase, on the other hand, was determined for environment CF12 by selecting individual plants randomly twice or thrice a week and dissecting the main tiller. The developing spike was then observed under the microscope to determine if the terminal spikelet phase had been reached (Gardner et al., 1985).

Accurate determination of terminal spikelet phase

Terminal spikelet phase determination is a laborious task; thus, for the purpose of acquiring more accurate data, a novel approach was used in environments CF13 and CF14. The method consisted of sampling the entire field trial at one moment in time, estimating when most of the plots seemed to be at terminal spikelet phase. Five main tillers from each plot were sampled and dissected in the laboratory. Then the developing spike was fixed and stored for 24 hours in FAA (water 50%, ethanol 35%, acetic acid 10%, and formaldehyde 5%, v/v) (Bancal, 2008). The samples were then analyzed under the microscope where the development of the terminal spikelet was determined by: (i) time to terminal spikelet phase using a back-scoring template (Supplementary Fig. S2); (ii) number of lemma primordia present in the terminal spikelet (>W3.25), and (iii) number of floret primordia present in the terminal spikelet (>W3.5) following the scale of Waddington et al. (1983) (see below).

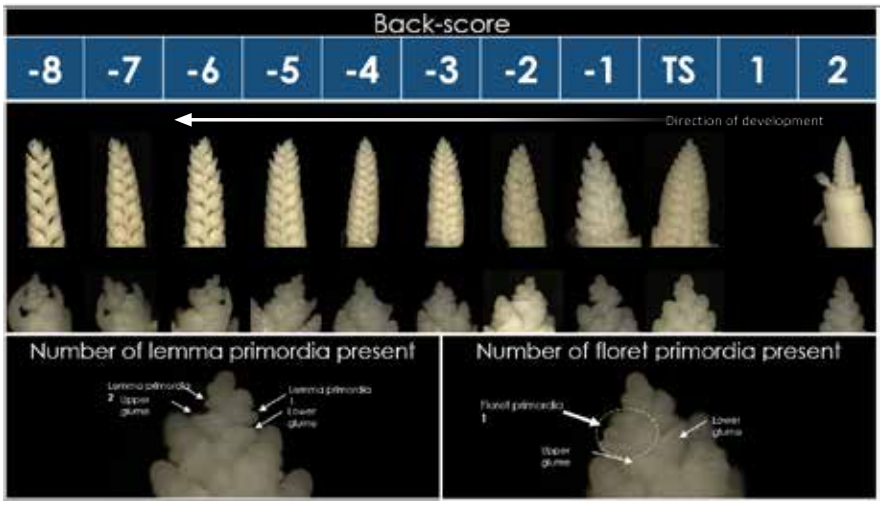

Top; images of developmental range surrounding terminal spikelet phase used for the back-scoring method. There is no photograph available for 1 in the back-score scale.

All other traits measured are shown in the table below.

Code	Trait	Unit	CF12	WP12	CF13	CF14
yield	Grain yield	t / ha		X	X	X
tgw	Thousand-grain weight	g			X	X
gm2	Grains per m^2	No. of grains / m^2			X	X
gps	Grains per spike	No. of grains / spike			X	X
sm2	Spikes per m^2	No. of spike / m^2			X	X
spks	Spikelets per spike	No. of spikelet / spike			X	X
gspk	Grains per spikelet	No. of grains / spikelet			X	X
dy_ts	Days from sowing to terminal spikelet	Days	X		X	X
dy_b	Days from sowing to booting	Days				X
dy_ib	Days from sowing to initiation of booting	Days				X
dy_ee	Days from sowing to heading	Days	X		X	X
dy_se	Days of stem elongation period (TS to EE)	Days	X		X	X
tt_ts	Thermal time to terminal spikelet	°C d	X		X	X
tt_b	Thermal time to booting	°C d				X
tt_ib	Thermal time to initiation of booting	°C d				X
tt_ee	Thermal time to heading	°C d	X		X	X
tt_se	Thermal time of stem elongation period	°C d	X		X	X
floretp	Floret primordia present (W3.5)	No. of primordia			X	X
lemmap	Lemma primordia present (W3.25)	No. of primordia			X	X

DNA extraction

Four seeds of each line of the population were positioned in a petri dish, on top of water-soaked filter paper. Of those seeds which emerged, one of the resulting plants was sown in a plastic tray approximately 1.5 cm deep. Between one and two weeks later in the glasshouse, the plants had developed 3-5 leaves from which the samples were taken. A 1-inch segment was dissected with clean scissors and collected in a Qiagen 96 well box (Collection microtube, cat. No. 19560), placed on ice and stored at -80°C prior to extraction. The DNA was then extracted following the protocol of Qiagen DNeasy 96 plant kit (cat. No. 69181). The extracted DNA was quantified using a Nanodrop spectrophotometer, measuring absorbance at 260 nm and 280 nm for quality (absorbance ratio) and concentration (compared to a standard curve), normalized to 50 ng/ul and sent on dry ice to TraitGenetics (Am Schwabeplan 1b, Stadt Seeland OT Gatersleben, D-06466, Germany) to be analyzed with the 90K iSelect chip (Wang et al., 2014).

Genetic map construction

The population was subjected to Illumina infinium 90k wheat chip array genotyping. This chip analyzed 81,587 single nucleotide polymorphisms (SNP) on an infinium ultra HD chip with 24 samples each. The genetic map was generated using three different software packages (JoinMap 4.0, Map Manager QTXb20, and MapChart 2.2). As a result, 5,665 SNP markers formed 21 linkage groups, 7 per genome (A, B, and D). The three genomes were well covered with markers. A total of 695 loci were mapped with an average distance between them of 7.3 cM with a combined map length of 3740.3 cM. The features of the Buster x Charger genetic map are shown below.

Linkage group	Length (cM)	Number of marker loci	Number of map loci	Mean distance between loci (cM)	Max. distance between loci (cM)
1A	99.1	286	22	4.7	25.6
1B	176.7	367	45	4.0	28.6
1D	90.3	131	19	5.0	25.6
2A	209.1	475	65	3.3	20.1
2B	318.7	847	48	6.8	101.7
2D	147.2	75	25	6.1	35.2
3A	235.5	341	38	6.4	45.3
3B	267.0	373	58	4.7	28.6
3D	127.2	29	12	11.6	37.0
4A	102.9	123	19	5.7	18.8
4B	92.7	153	20	4.9	20.1
4D	117.5	5	5	29.4	101.7
5A	298.9	320	59	5.2	35.2
5B	221.7	528	43	5.3	40.9
5D	179.9	180	22	8.6	47.7
6A	139.5	250	26	5.5	43.0
6B	115.5	226	24	5.0	17.5
6D	180.3	87	21	9.0	68.0
7A	286.3	499	74	3.9	35.2
7B	171.8	328	36	4.9	24.2
7D	162.5	42	14	12.5	45.3
Total	3740.3	5665	695	7.3	

Linkage between genetic markers on chromosomes 5B and 7B confirmed the segregation of this translocation in the population, as shown in the figure below. If no translocation was present, only the single red (strong linkage) diagonal linkage within single chromosomes would be seen. In this case, note the hot spots at the 5B/7B intersection.

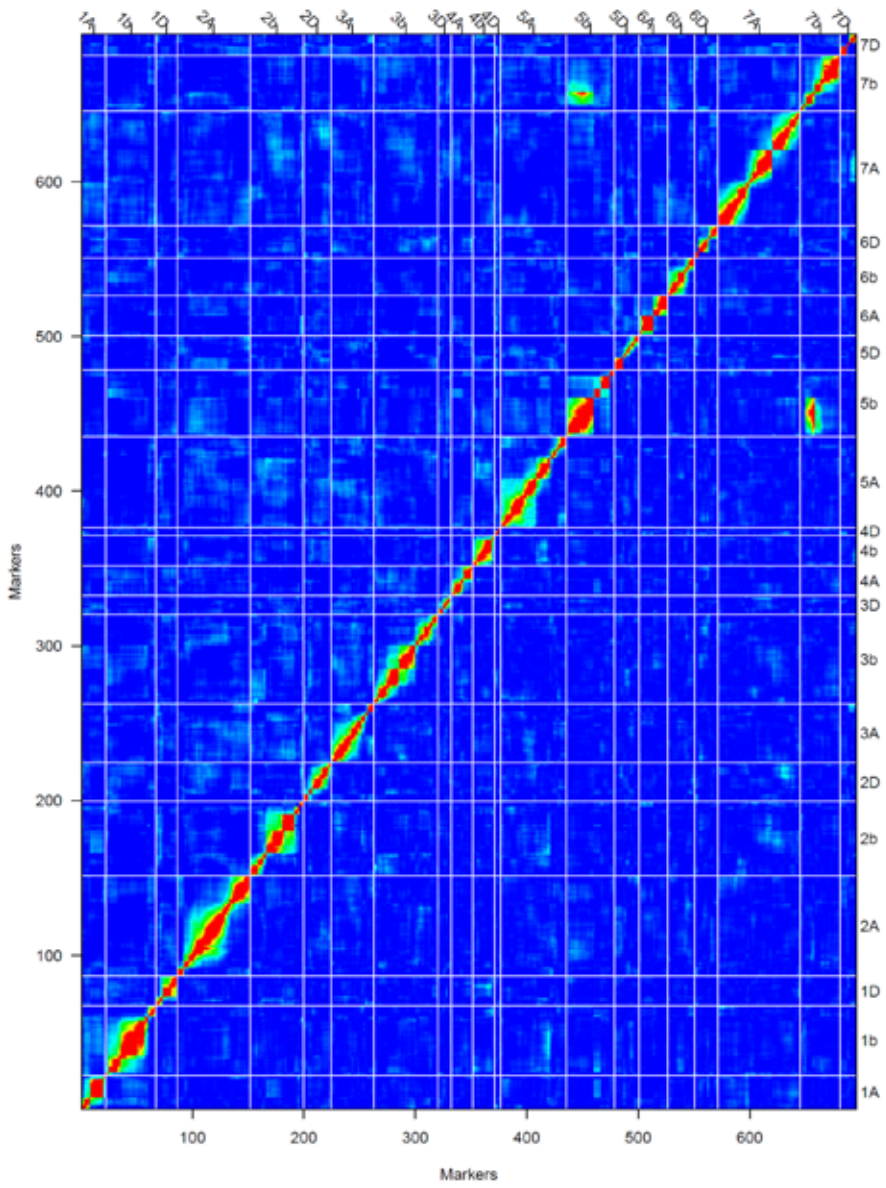

Heatmap of pairwise recombination fractions of BxC DH genetic map. Red stands for 1, and blue for 0.

Statistical and QTL analyses

Statistical analysis was performed using a combination of Genstat 17th (for heritability) and R software (for the rest of analysis). The significance of differences in traits between lines was assessed using a one-way analysis of variance.

In order to obtain a good indication of the different genomic regions contributing to the variations in phasic development, QTL mapping was done with R statistical software and R/qtl package (Broman et al., 2003), where in a first step a single-QTL genome scan was performed with a normal model calculated on QTL genotype probabilities. In a second step, all QTLs for one trait above a significance threshold in step one were statistically tested in a multi-QTL model. This second step detected ghost QTL, as they did not reach statistical significance, and detected the true LOD scores for each QTL.

The QTL is considered when the logarithm of the odds (LOD) score exceeds the threshold calculated using a permutation level of 1000 and a significance level of 0.2. Interval mapping was calculated using the Haley-Knott regression method.

Heritability

Heritability was estimated using a mixed model where environment, replicates within environment and checks (parents) within environment are considered as fixed factors; rows of plots within environment, column within environment, genotype, and genotype x environment interaction are set as random factors. The formula used is:

$$h^2 = \sigma^2_g / [\sigma^2_g + (\sigma^2_{ge} / e) + (\sigma^2_r / re)]$$

where σ^2_g is the variance of the genotype, σ^2_{ge} is the variance of the genotype x environment interaction, σ^2_r is the residual, e is the number of environments, and r is the number of replicates.

The figures were produced using GraphPad Prism 5 (2007), except for the principal component analysis, which was done with ggbiplot package with R statistical software.

Results

Phenotypic variation and heritability

The overall behavior of the population parents, Buster and Charger, and the segregating populations in the environments sampled are shown below. The parents show similar high yield potential and the populations are confined to a narrow window of segregation equivalent to a typical UK elite wheat breeding program at the stage of phenotypic fine-tuning for traits that include phenology.

Environment	Trait	Parents				DH population		
		Buster	SD	Charger	SD	Mean	Range	SD
WP12	yield	9.9	0.5	9.9	0.8	9.7	8.3 - 11.2	0.5
CF12	dy_ts	197	-	187	-	193.1	187 - 203	4.0
	dy_ee	245	-	239	-	241.9	236 - 247	2.5
	dy_se	48	-	52	-	48.8	37 - 55	3.8
CF13	yield	9.1	1.1	9.8	1.1	9.2	7.5 - 10.7	0.6
	tgw	45.4	3.1	45.1	3.1	44.6	40 - 49.7	1.9
	gm2	20494	2832	21970	2435	20830	15859 - 24498	1618
	gps	52.6	3.6	47.9	6.6	50.5	41.8 - 61.4	3.8
	sm2	389.6	43.3	466.2	83.7	412.5	335.8 - 597.8	42.9
	spks	20.5	1.2	20.6	1.3	20.2	18.3 - 22.1	0.8
	gspk	2.6	0.3	2.3	0.4	2.5	2.0 - 2.9	0.2
	dy_ts	203.9	1.1	203.6	-	203.7	200.4 - 207.2	1.3
	dy_ee	246.6	0.5	244.8	1.2	245.1	241.3 - 249.0	1.8
	dy_se	42.4	0.6	40.4	-	41.5	37.9 - 44.3	1.4
	floretp	1.9	0.3	1.8	-	1.9	0.1 - 3.3	0.8
	lemmap	4.4	0.9	4.4	-	4.3	2.2 - 6.4	0.9
CF14	yield	10.4	0.4	11.1	0.6	9.8	7.5 - 11.4	0.7
	tgw	48.6	2.9	47.1	2.7	48.2	39.5 - 54.2	2.6
	gm2	20202	1062	22692	1262	20462	13868 - 23807	1591.7
	gps	63	5.0	62.9	3.8	67.0	52.7 - 85.8	6.1
	sm2	322.3	30.8	361.8	29.7	309.2	226.3 - 428.0	32.1
	spks	19.7	0.7	19.5	0.9	20.7	18.0 - 24.0	1.3
	gspk	3.2	0.2	3.2	0.2	3.3	2.6 - 3.9	0.3
	dy_ts	172	0.7	171.3	0.8	172	170.0 - 174.7	0.9
	dy_ib	211.1	1.5	209.4	0.9	210.5	207.3 - 213.0	1.3
	dy_ee	217.7	0.5	215.2	1.0	216.4	213.0 - 219.0	1.5
	dy_se	45.7	0.8	43.9	1.2	44.4	40.9 - 46.5	1.2
	floretp	0	0.0	0	0.0	0.01	0.0 - 0.1	0.0
	lemmap	1.3	0.7	1.8	0.7	1.4	0.0 - 2.9	0.7

QTL analysis for phenology

Many of the yield components described in the table above are strongly influenced by developmental events occurring between the time the crop reached terminal spikelet up to heading date. For this study we were interested in the extent to which these two stages are controlled independently. We found two major QTL for heading date on chromosomes 2D and 4A. The QTL plots for these two effects are shown below.

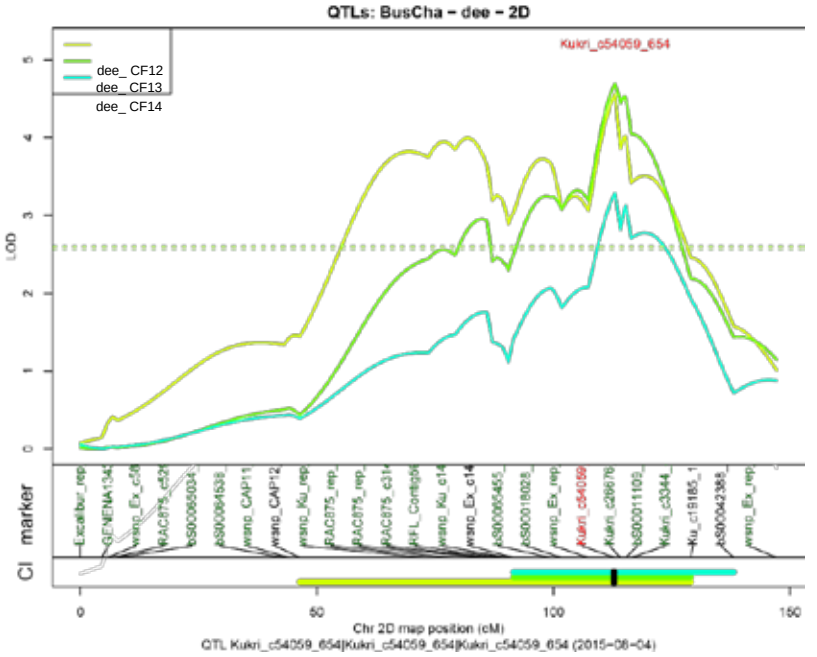

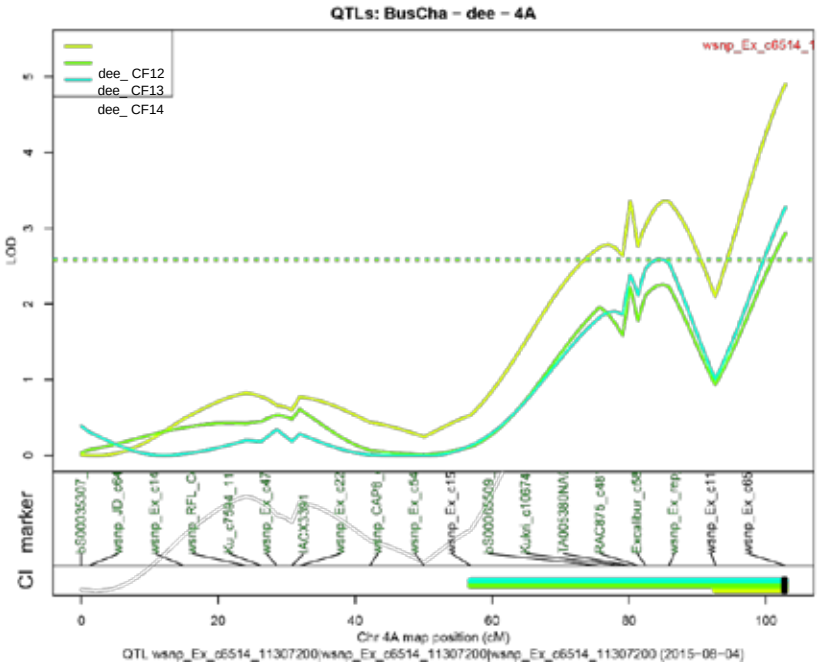

No QTL for time to terminal spikelet were identified at these loci, even when the LOD threshold was reduced to an arbitrary level of 1.5.

However, one QTL for time to terminal spikelet was identified on chromosome 7A. This is shown in the QTL plot below. No heading date QTL were identified at the 7A locus.

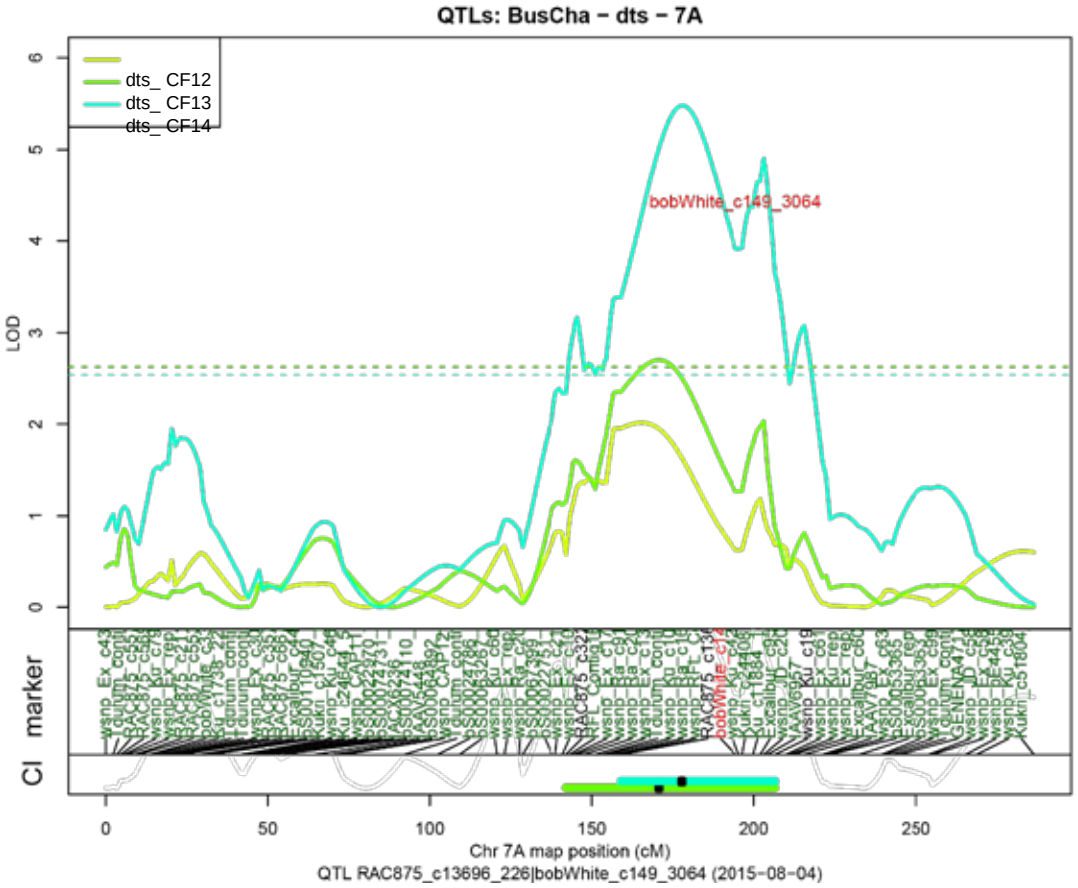

Discussion

The study identified independent genetic control of time to terminal spikelet and time to heading between elite UK winter wheat parents. By identifying the QTL controlling these traits, we provide breeders with new tools for their selection. This is particularly useful with regard to terminal spikelet, as manual scoring of the trait is not usually viable in a breeding program. The high quality of the Buster Charger genetic map allows good alignment with the wheat whole genome assembly. This work is still underway. The success of the approach using UK material was encouraging. Equivalent populations were developed in a collaboration between the UK's Wheat Improvement Strategic Programme (BBSRC) and MasAgro under the umbrella of the Wheat Yield Consortium.These populations are now being scrutinized in the International Wheat Yield Partnership project: A Genetic Diversity Toolkit to Maximize Harvest Index by Controlling the Duration of Developmental Phases.

References

Bancal P (2008) Positive contribution of stem growth to grain number per spike in wheat. Field Crops Research 105 (1-2):27-39. doi:10.1016/j.fcr.2007.06.008

Beales J, Turner A, Griffiths S, Snape JW, Laurie Da (2007) A pseudo-response regulator is misexpressed in the photoperiod insensitive Ppd-D1a mutant of wheat (Triticum aestivum L.). TAG Theoretical and applied genetics Theoretische und angewandte Genetik 115 (5):721-733. doi:10.1007/s00122-007-0603-4

Borlaug NE (1983) Contributions of conventional plant breeding to food production. Science 219 (4585):689-693

Broman KW, Wu H, Sen S, Churchill Ga (2003) R/qtl: QTL mapping in experimental crosses. Bioinformatics 19 (7):889-890. doi:10.1093/bioinformatics/btg112

Gardner JS, Hess W, Trione E (1985) Development of the young wheat spike: a SEM study of Chinese spring wheat. American Journal of Botany:548-559

Griffiths S, Simmonds J, Leverington M, Wang Y, Fish L, Sayers L, Alibert L, Orford S, Wingen L, Herry L, Faure S, Laurie D, Bilham L, Snape J (2009) Meta-QTL analysis of the genetic control of ear emergence in elite European winter wheat germplasm. Tag Theoretical And Applied Genetics Theoretische Und Angewandte Genetik 119 (3):383-395. doi:10.1007/s11032-010-9534-x

Kirby EM, Appleyard M (1984) Cereal development guide. Cereal development guide. 2nd Edition. Cereal Unit, National Agricultural Centre, Stoneleigh, Keniworth, Warwickshire CV8 2LZ, England

Loukoianov A, Yan L, Blechl A, Sanchez A, Dubcovsky J (2005) Regulation of VRN-1 vernalization genes in normal and transgenic polyploid wheat. Plant Physiology 138 (4):2364-2373

Milec Z, Valárik M, Bartoš J, Šafář J (2014) Can a late bloomer become an early bird? Tools for flowering time adjustment. Biotechnology advances 32 (1):200-214

Snape JW, Butterworth K, Whitechurch E, Worland AJ (2001) Waiting for fine times: genetics of flowering time in wheat. Euphytica 119 (1):185-190

Stelmakh A (1987) Growth habit in common wheat (Triticum aestivum L. EM. Thell.). Euphytica 36 (2):513-519

Waddington SR, Cartwright PM, Wall PC (1983) A quantitative scale of spike initial and pistil development in barley and wheat. Annals of Botany 51:119-130

Wang S, Wong D, Forrest K, Allen A, Chao S, Huang BE, Maccaferri M, Salvi S, Milner SG, Cattivelli L (2014) Characterization of polyploid wheat genomic diversity using a high-density 90 000 single nucleotide polymorphism array. Plant biotechnology journal 12 (6):787-796

Natural variation and genetic analysis of wheat spike ethylene under heat stress conditions

Ravi Valluru[1,], Matthew P. Reynolds[1], William J. Davies[2] and Sivakumar Sukumaran[1]*
[1] CIMMYT, Mexico; [2] Lancaster Environment Center, UK

Abstract
Plants produce ethylene in response to numerous environmental conditions. Ethylene has been shown to negatively affect crop yields. However, the genotypic variation and the genomic regions governing spike ethylene production under long-term heat stress have been elusive. Two treatment conditions —heat stress without silver nitrate spray (HT) and heat stress with silver nitrate spray (HSN)— were imposed on diverse wheat genotypes grown under heat stressed field conditions. This study found substantial genotypic variation for spike ethylene production under heat stress conditions. In response to HSN, spike ethylene decreased noticeably among genotypes, that is, an average *c*. 18% lower than without HSN. Spike ethylene had a broad-sense heritability of 25%. The genome-wide association analysis (GWAS) uncovered 5 and 32 significant SNPs for spike ethylene in the glasshouse and under field conditions, respectively. Phenotypic and genetic elucidation of spike ethylene supports future efforts toward gene discovery and will contribute to breeding wheat cultivars with reduced ethylene effects on yield under heat stress.

Introduction
Many plants produce extra ethylene under heat stress; this has been linked to a yield penalty in various crops (Hays et al., 2007). The main effects attributed to ethylene are reductions in spike fertility and final grain weight and accelerated senescence (Yang et al., 2004). Previous studies have used various approaches such as inhibitors of ethylene biosynthesis or sensitivity of response (Hays et al., 2007) and/or down-regulation of ethylene signaling components (Habben et al., 2014) to reduce the negative effects of ethylene on crop yields. However, the natural variation in ethylene production to reduce the negative effects of ethylene on crop yield has been less explored. In addition, genome-wide association analysis (GWAS) offers the high-resolution genetic capacity to capture the genetic architecture of complex traits such as spike ethylene. In this study, we explored natural variation and the genetic analysis of spike ethylene in diverse wheat genotypes grown under heat stress conditions.

Materials and methods
A diverse set of spring wheat (*Triticum aestivum* L.) genotypes (130) consisting of elite materials and landraces were grown under heat stressed field conditions during 2013-2015. In addition, a separate diverse set of the spring wheat elite WAMI panel (190 genotypes) was grown under heat stressed field and glasshouse conditions for genetic studies. The plots were arranged in a randomized lattice design with two replications. Two treatment conditions were maintained: heat stress without silver nitrate spray (control, HT) and heat stress with silver nitrate spray (HSN). Silver nitrate was dissolved in water (0.05 mM) containing 0.01% (v/v) Tween 20 (Sigma-Aldrich) and ethanol (0.1%), and the solution was foliar-sprayed onto the leaves of whole plants at the early booting stage. The control plots were sprayed with water. Both treatments were applied on a 1-m plot.

Spike ethylene was measured at the anthesis stage. Spikes were randomly sampled, incubated in glass tubes under a constant temperature (35 ^{o}C) for around 2 h. Using a 5-ml syringe, 4 ml of gas was extracted and used to measure ethylene using a laser-based ethylene detector (ETD-300; Sensor Sense) (Valluru et al., 2017). Ethylene production was corrected for spike dry weight and incubation period. Ethylene data were subjected to one-way and two-way ANOVA.

We performed genome-wide association analysis (GWAS) on the spike ethylene data using TASSEL algorithms (Zhang et al., 2010) using Illumina iSelect 90K genotyping data. We incorporated kinship matrix as the random component and the principal components (PCs) as fixed effects. The threshold for defining an SNP as significant was 10^{-03}, considering the number of SNPs and the deviation of the observed F-test statistics from the expected F-test distribution in the quantile–quantile (QQ) plots.

Results and Discussion
Genotypic variation for spike ethylene at anthesis among 130 genotypes
Spike ethylene (SET) under HT conditions (Fig.1a) ranged from 0.017 to 0.155 nl g DW^{-1} h^{-1}, with a mean of 0.077 nl g DW^{-1} h^{-1}, and a broad-sense heritability of 25%. In response to HSN, SET decreased noticeably among genotypes, ranging from 0.01 to 0.145 nl g DW^{-1} h^{-1}, with a mean of 0.063 nl g DW^{-1} h^{-1}, that is, an average *c*. 18% lower than without HSN (Fig. 1b). There were significant main effects of genotype ($P < 0.001$), treatment ($P < 0.001$), and their interaction ($P < 0.001$) on SET. In response to HSN, both elite materials (EM) and landraces (LR)

exhibited a reduction in SET, by 18% and 17%, respectively (Fig. 1c,d). Across both HT and HSN conditions, EM genotypes had significantly lower SET (13%; P < 0.001; Fig. 2c) compared with LR. Overall, these findings suggest that there is large genotypic variation for SET among the wheat genotypes studied and spike ethylene decreased significantly in response to HSN.

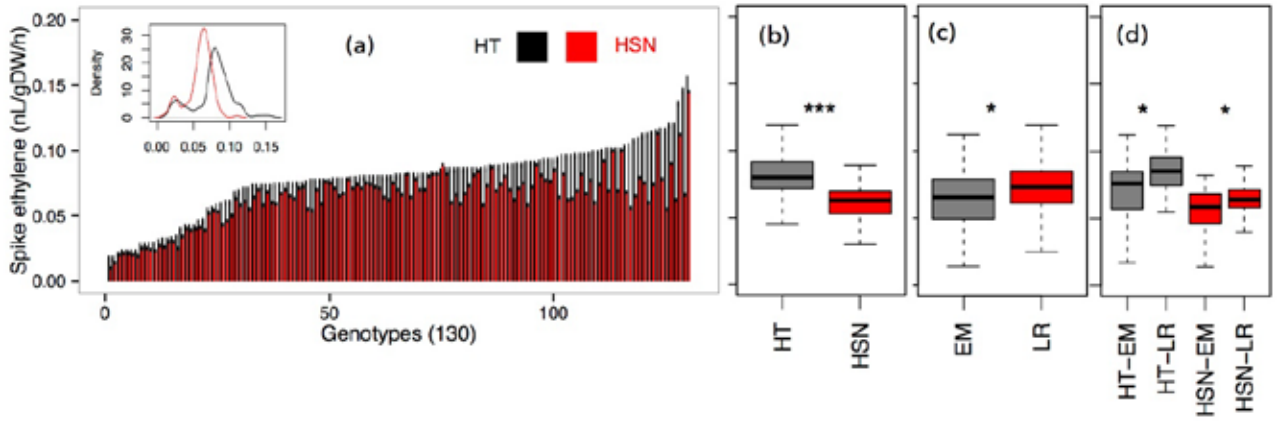

Fig. 1. Spike ethylene (SET) of 130 wheat genotypes grown under heat stress (HT) or HT plus ethylene (ET) response inhibitor silver nitrate spray (HSN) conditions. (a) Natural variation in SET in two treatments (HT and HSN). SET under HT was arranged in ascending order. (b, c, d) Average mean values of SET in (b) two treatments (HT and HSN), (c) two genotype categories (EM, elite material; LR, landraces), and (d) their combination. The inset in (a) is a density plot of SET. The vertical bars represent ` SE. *, P = 0.05; ***, P = 0.001.

Genome-wide association analysis for spike ethylene

GWAS was performed using 18,704 SNPs. We identified a number of candidate SNPs (5 and 32 SNPs in the glasshouse and field, respectively), suggesting that some are environment-specific. These SNPs are located on chromosomes 1A, 1B, 1D, 3B, 5B and 7B (Fig. 2) and explained 5.7–10.5% of the variation in spike ethylene. A major SNP (kukri-c15603-1116) at 69cM on chromosome 3B explained 10.5%, while a major SNP (wsnp-JD-c38123-27754848) located at 40 cM on chromosome 5B explained 8.8% of total spike ethylene variation under field conditions.

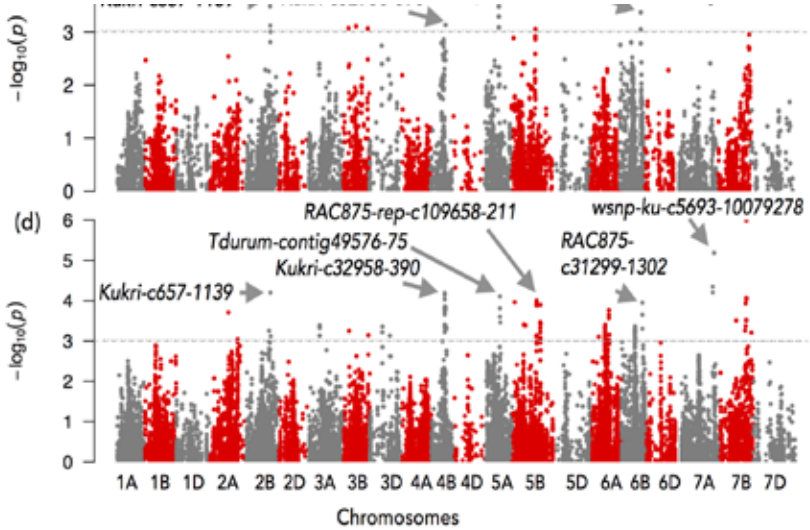

Fig. 2. Manhattan plots of genome-wide association (GWA) mapping results for spike ethylene production at the anthesis stage. GWA mapping was performed for spike ethylene production of 163 lines from the wheat association mapping initiative panel grown in (a) the glasshouse or (b) under field conditions.

Limited SNP overlap and lower heritability (25%) suggest that spike ethylene may indeed be governed by a large number of genes of small effect that may not be possible to detect consistently across environments. Interestingly, two distinct SNPs (kukri-c29668-338 and BS00009866-51 in glasshouse and field conditions, respectively) are located at the same position at 70 cM on chromosome 1A (Fig. 2), indicating that this genomic region may be an important regulator of spike ethylene. Further, many SNPs are located close to previously detected markers controlling several agronomic traits such as peduncle length, maturity and plant density adaptation (Sukumaran et al., 2015), indicating close associations between these agronomic traits and spike ethylene.

Conclusions

There was substantial genotypic variation for spike ethylene at the anthesis stage among diverse genotypes. Further, spike ethylene appears to have been inadvertently selected against in elite lines. Such wide genetic diversity provides an excellent base for uncovering the physiological and genetic underpinning of ethylene insensitivity. These findings would be useful for breeding wheat cultivars with reduced ethylene effects on yield under heat stress.

References

Hays DB, Do JH, Mason RE, Morgan G, Finlayson SA. 2007. Heat stress induced ethylene production in developing wheat grains induces kernel abortion and increased maturation in a susceptible cultivar. Plant Science 172: 1113–1123.

Yang JC, Zhang JH, Ye YX, Wang ZQ, Zhu QS, Liu LJ. 2004. Involvement of abscisic acid and ethylene in the responses of rice grains to water stress during filling. Plant, Cell & Environment 27: 1055–1064.

Habben JE, Bao X, Bate NJ, DeBruin JL, Dolan D, Hasegawa D, Helentjaris TG, Lafitte RH, Lovan N, Mo H et al. 2014. Transgenic alteration of ethylene biosynthesis increases grain yield in maize under field drought-stress conditions. Plant Biotechnology Journal 12: 685–693.

Zhang Z, Ersoz E, Lai C-Q, Todhunter RJ, Tiwari HK, Gore MA, Bradbury PJ, Yu J, Arnett DK, Ordovas JM et al. 2010. Mixed linear model approach adapted for genome-wide association studies. Nature Genetics 42: 355–360.

Sukumaran S, Dreisigacker S, Lopes M, Chavez P, Reynolds MP. 2015a. Genome-wide association study for grain yield and related traits in an elite spring wheat population grown in temperate irrigated environments. Theoretical and Applied Genetics 128: 353–363.

Valluru R, Reynolds MP, Davies WJ, Sukumaran S. 2017. Phenotypic and genome wide association analysis of spike ethylene in diverse wheat genotypes under heat stress. New Phytologist, 10.1111/nph.14367.

Acknowledgments

This work was financially supported by the Consultative Group for International Agricultural Research (CGIAR) Research Program for Wheat (CRP-Wheat, SI6: Heat and Drought) through CIMMYT.

ABA and ethylene hormone balance and its diurnal variation as indicators of plant resilience to drought stress

Arnauld A. Thiry[1,2], Matthew P. Reynolds[1] and William J. Davies[2]
[1] CIMMYT, Mexico; [2] The Lancaster Environment Centre,UK

Abstract
Four elite wheat genotypes from a CIMMYT Core Germplasm (CIMCOG) ROOT trial were selected for a study of plant hormone balance, spike fertility and grain yield under drought stress. Abscisic acid (ABA) and ethylene (ETH) accumulations were measured at two different times of day (at 01:00 pm when the maximum temperature stress is experienced by the plant and at 05:30 pm when the temperature stress is reduced). Results showed that the time of the day is an important variable impacting hormonal accumulation, which may in turn influence spike fertility. Preliminary results suggest that at 01:00 pm, high ABA/ETH concentration may reduce spike sterility, while at 05:30 pm, high ABA/ETH is associated to the maintenance of fertile tillers. This work suggests that high-throughput measurements of hormone balance may provide information on abiotic stress resistance that is useful to crop breeders.

Introduction
The changing climate, a growing population and food demand combine to provide an impetus for more rapid selection of productive and adaptive crop plants for stress environments. Wheat is one of the world's major food sources and one of the most cultivated cereal crops with more than 220 million ha sown per year (Araus et al., 2008; Shiferaw et al., 2013).

Wheat yield is one of the main traits used by breeders for genotype selection (Slafer, 2005). However, yield is a complex trait, as it is the final outcome of a range of crop growth and development processes during the whole growing cycle (Slafer, 2003). This trait can be subdivided into numerical components; the two major yield components are grain number (GN) per unit of area and individual grain weight (GW) (Slafer, 2005). Grain number per m^2 has been identified as an influential trait, with more grain delivering higher grain yields under yield potential conditions (Sayre et al., 1997; Shearman et al., 2005; Peltonen-Sainio et al., 2007; Dolferus et al., 2011). Under drought stress, grain number per m^2 is significantly reduced when the stress occurs during the spike growth period (Hochman, 1982) from booting stage to anthesis.

In wheat, the meiosis process starts at the booting stage; the embryo sac originates in the carpel and the pollen in the anthers, first in the middle of the spike and continuing in the basal and apical parts (Zadoks et al., 1974). Meiosis is very sensitive to drought stress with a yield reduction commonly observed. From the booting stage to anthesis, floret abortion coincides with the maximum growth rate of the peduncle and stem (Siddique et al., 1989) and is associated with carbon competition between peduncle and stem elongation (Kirby, 1988) and also with reduced nitrogen availability (Acevedo et al., 2006). Also, the number of spikelets per spike of fertile tillers can be reduced during the spike-growing stage (Hochman, 1982). Under drought stress, plant hormones —mainly ABA and ethylene— have been shown to play important roles in regulating growth rate during plant development but also in controlling the reproductive processes (Wilkinson and Davies, 2002, 2010; Davies, 2010).

Ethylene is produced by almost all parts of the plant and is involved in an extensive range of effects on developmental processes along the plant cycle, such as breaking of dormancy, regulation of stem swelling, root hair development and adventitious root formation. High levels of this hormone also retard stem elongation and promote kernel abortion in wheat, as well as ripening of fruit, senescence, and abscission (Yang and Hoffman, 1984; Chang and Bleecker, 2004; Sisler et al., 2006; Hays et al., 2007; Acharya and Assmann, 2009; Davies, 2010; Abeles et al., 2012). Due to the huge range of effects on plant development, ETH production is a tightly regulated process controlled by developmental signals and the response to biotic or abiotic factors (Davies, 2004; Cristescu et al., 2013). Its production can vary quickly and induce effective biological responses at very low concentrations (nanomolar) and the lag time for ethylene responses can vary from minutes (10-15 minutes, case inhibition of seedling) to days (promoting leaf senescence) (Bleecker and Kende, 2000; Guo and Ecker, 2004; Davies, 2010; Abeles et al., 2012). Moreover, ethylene emissions from plant tissue vary depending on the plant species, plant tissue (e.g., root, leaf and flower) and developmental stage of the plant (Cristescu et al., 2013). Ethylene is usually considered a growth inhibitor mainly associated with a triple response in seedlings, which is probably the most well-known effect of ethylene on plant growth: 1) inhibition of stem elongation; 2) thickening of the stem; and 3) the formation of an apical hook (Guzmán and Ecker, 1990; Pierik et al., 2007; Abeles et al., 2012). Elucidating the basis of the impact of ethylene on plant growth is now an active research area (Pierik et al., 2006, 2007). It has also been

demonstrated that when plants are under abiotic stress, ethylene can promote growth at low concentrations. Additionally, high ethylene has been associated with some negative effect on pollen fertility and inhibiting anther dehiscence (Campbell et al., 2001).

ABA is usually considered a plant growth inhibitor, a conclusion largely based on research where exogenous hormone (ABA) is applied to plants under non-stress conditions (Sharp et al., 1994; Sharp and LeNoble, 2002). However, other research has shown that at low water potential, a reduced level of endogenous ABA generated by applying fluridone (a carotenoid inhibitor which reduces ABA production) was associated with the inhibition of root elongation and promotion of shoot elongation in maize (Saab et al., 1990).

Additionally, under drought stress, shoot growth is usually more restricted than root growth, which can benefit the plant by maintaining an adjusted water supply from the soil to the shoot (Sharp, 2002). Saab et al. (1990) concluded that at low water potentials, root ABA accumulation plays an important role in both the maintenance of primary root elongation and the inhibition of shoot elongation, although Guo et al. (2009) found that exogenous application of ABA decreases the number of lateral roots. Under drought stress, ABA is a key hormone for controlling stomatal aperture, root growth and plant water status (Sharp and LeNoble, 2002; Lee and Luan, 2012). Via the promotion of stomatal closure and promotion of primary root growth, ABA confers on the plant some avoidance or tolerance of drought stress (Sharp and LeNoble, 2002; Claeys and Inzé, 2013). This may be, for example, via partial stomatal closure in response to increased ABA accumulation, which increases water use efficiency (Davies et al., 2002) while allowing the entry of sufficient CO_2 for a rate of photosynthesis that may be optimal for the amount of water available to the plant (Acharya and Assmann, 2009).

ABA concentration in plant tissue is determined by the balance between its production and its degradation (Cutler and Krochko, 1999). Biosynthesis and degradation are influenced by the plant developmental stage, environmental factors and also other growth regulators (Cutler and Krochko, 1999; Finkelstein, 2013). Environmental factors such as reduced water availability often enhance ABA concentrations in roots, xylem sap and leaves (Davies and Zhang, 1991; Puértolas et al., 2013; Hu et al., 2016). Additionally, in maize under drought stress in the field, stomatal conductance is often tightly related to [ABA] in xylem sap (where higher ABA closes the stomata), but not with the current leaf water status or with ABA concentration in the bulk leaf (Tardieu et al., 1992). There is no doubt about the importance of precisely defining the tissue in which the hormones under consideration should be quantified. The importance of tissue and time of sampling has been highlighted by the research of Hu et al. (2016), who showed that ABA biosynthesis can be first promoted either in the leaf or in the root, depending on which tissue is stressed first; therefore the ABA concentration is enhanced first in the stressed tissue before being recirculated in the plant.

The importance of all of these responses notwithstanding, the study of plant growth regulators can present complications such as the induction of ethylene accumulation by a wide range of external stress factors such as pest damage, flooding, disease, chemicals, heat, drought and mechanical wounding; this extra hormone is usually called stress-ethylene (Davies, 2004; Abeles et al., 2012; Cristescu et al., 2013). Other complications may arise from internal factors, such as circadian regulation of synthesis of plant growth regulators (PGR) (Mcclung, 2000). The diurnal periodicity of ethylene production has been recorded in barley, wheat and rice (Ievinsh and Kreicbergs, 1992; Kobayashi and Saka, 2000), but also in other crops such as cotton (Abeles et al., 2012) and *Vicia faba* (faba bean) (El-Beltagy and Hall, 1974). Most studies report a peak of ethylene at the mid-photoperiod (Thain et al., 2004). Some reports have shown that the regulation of abscisic acid (ABA) is also under circadian control, e.g., in *Arabidopsis thaliana* (Lee et al., 2006). An appreciation of this kind of diurnal variation is certainly important if we hope to quantify genetic variation in ethylene and/or ABA accumulation and use these assessments to identify genetic variations in stress adaptation.
Due to the complexity of spatial and temporal variation in accumulation of individual hormones and their different effects on plant development, many questions are raised about when (in terms of phenological stage and time of day) and where (in terms of tissue such as leaf, spike) hormone quantification should take place. Our goal is to identify genetic variation in sensitivity to environmental cues and propose how this could be assessed using high-throughput methodology for breeding selection during early plant development stages.

The aim of this experiment is to investigate the importance of diurnal variation of leaf hormone balance (ethylene and ABA). Two principal (leaf and spike) tissues were selected to assess potential new traits, i.e., ethylene emission rate and ABA, as indicators of drought stress resilience. Leaf and spike were selected for sampling based on two hypotheses of hormone impact on yield under drought stress during the pre-anthesis period: 1) the reduction of grain number per spike during meiosis could be due to competition for carbon driven by the leaf (source tissue) hormone concentration and the photosynthetic rate or 2) the reduction in pollen fertility and spikelet fertility could be

associated with hormone concentration in the spike (sink and reproductive tissue). These questions have been fully addressed in another work (Thiry, 2017, PhD thesis in preparation).

Meiosis was selected as an appropriate period for studying genotypic drought stress adaptation, with particular focus on spike fertility, and the association with hormone (ethylene and ABA) quantification. The stage selected for studying the effect on diurnal variation was the mid-meiosis period between booting and heading when the leaf sheath is close to opening (GS47) (Zadoks et al., 1974).

Materials and Methods

Four genotypes from a CIMCOG-ROOT trial presenting contrasting responses to drought stress were selected based on the index method described in Thiry et al. (2016). Accordingly, two drought resilient genotypes (T1 and T2) and two drought sensitive genotypes (S1 and S2), in terms of yield under field conditions, were selected during the 2013-2014 crop cycle.

Seeds were initially germinated in Petri dishes on saturated filter paper and covered with absorbent paper saturated with water under dark conditions. When coleoptiles reached 3 cm in length (around 1 week), the germinated seeds were planted in pots (volume = 3.73 L; height = 21 cm; diameter: top = 17 cm and bottom = 13 cm), initially filled with the same soil substrate (John Innes nº2). Four seeds per pot and 6 pots per genotype were planted for this experiment. Then plants were placed under drought stress conditions (see below), in a controlled environment room (CE Room) at the Lancaster Environment Centre, under a 12-hour photoperiod (550 µmol photons m^{-2} s^{-1}). The experiment was a randomized complete block (RCB) design with 6 replications for hormone measurement. The plants were watered at the bottom of the pot in order to represent the field conditions as much as possible by keeping the soil surface dry, as occurs in the field through the different phenological stages. For this, the pots were placed on horizontal trays and water was added to the trays and never directly to the soil. The amount of water per tray was calculated based on the field capacity of the substrate and the number of pots per tray. For the well-watered treatment, 600 ml of water (full field capacity) per pot was added to the tray and 45% of the field capacity was applied for the water stress treatment. Irrigation was applied every six days. Irrigation was stopped when the plants reached physiological maturity (Zadoks et al., 1974; Pask et al., 2012).
Flag leaf tissues for ethylene and ABA analysis were sampled at GS 47 (flag leaf sheath opening) at two different times (01:00 pm and 05:30 pm). The last irrigation was applied four days before sampling.

ABA sampling and radioimmunoassay (RIA)

The leaf samples were placed into pre-labelled Eppendorf tubes (2 ml) and immediately frozen in liquid nitrogen contained in a cool box. The samples were kept in a -80 ºC ultra-freezer for three days. After this time, the samples were transferred to a -20 ºC freezer before being freeze-dried during 48 hours. Afterwards, the dry leaf tissues (in the 2ml Eppendorf tubes) were ground using a ball mill (MM400 Retsch GmbH, Germany) allowing 4 minutes for each cycle.

The ABA analysis was carried out at Lancaster LEC laboratories using the adapted radioimmunoassay (RIA) method described by Quarrie et al. (1988). To extract the ABA from the ground tissue, +/- 20 mg of ground material was mixed with deionized water at a 1:40 (mg:µl) ratio in a 1.5 ml Eppendorf tube and shaken at 4°C during 13 hours (overnight). Afterwards, the Eppendorf tube was centrifuged at maximum speed (1500 RPM) during 4 minutes and 50 µl of the supernatant was added to a tube containing 200 µl of phosphate-buffered saline (PBS). Then 100 µl of diluted [3H]-ABA was added first and then 100 µl of diluted antibody MAC 252. To homogenize the mixture, the tubes were sealed and centrifuged (1500 RPM) for one minute and then kept in the refrigerator for 45 minutes. After that, 500 µl of saturated ammonium sulfate was added and mixed by hand, and the mixture was left at room temperature for 30 minutes in the dark. Afterwards, the tubes were centrifuged (1500 RPM) for 4 min to precipitate the ABA-antibody complex at the bottom of the tube. The supernatant was removed into a sink. To remove the possible excess of unbound radioactivity, a washing process consisting of re-suspending the pellet in 1.0 ml of 50% saturated ammonium sulfate and then centrifuging (1500 RPM) for 5 minutes to form a new pellet was carried out. The new supernatant was removed into a sink. Finally, 100 µl deionized water was added to each tube and the pellets were re-suspended; then 1.5 ml of Econsint H was added to each tube. The radioactivity was measured with a liquid scintillation counter (Packard TriCARB 1600TR liquid scintillation analyzer, Canberra, CT, USA). To interpret the result and calculate the concentration, a standard curve is necessary. During the process, 8 ABA standards were used to determine the optimum for maximum and minimum binding, Bmax and Bmin, respectively: 0 (Bmax), 62.5, 125, 250, 500, 1000, 2000 and 2×106 pg 50 µl-1 (+)-ABA (Bmin). These ABA standards were prepared from (±)-ABA (A1049, Sigma-Aldrich). ABA quantification in the standards followed the same process used with the samples. The tubes (standards and samples) were placed on a foam rack with 50 free

spaces; 8 spaces were used for the standards and a maximum of 40 could be used for the samples. The analysis of each experiment for each tissue and environment was performed on the same foam rack. In general, two foam racks were run simultaneously (time necessary for one person to run two foams rack is around 3 hours 20 minutes to 4 hours, plus 6 min per sample to analyze it using the liquid scintillation counter).

Ethylene sampling and quantification

The method for quantifying the ethylene emission rate was adapted from the method described in Wilkinson and Davies (2009), Iqbal et al. (2011) and Chen et al. (2013) for field and laboratory conditions.

Fresh tissues (leaf at the ligule level and spike at the node level) were cleanly cut and then quickly and gently inserted into 25 ml glass test tubes containing fully moistened (deionized water) filter paper and sealed with rubber stoppers (Suba-Seal, SLS, Nottingham, UK), for incubation under the same light environmental conditions, on the bench inside the CE-room (500 µmol photons. m^{-2} s^{-1}) or greenhouse (550 µmol photons. m^{-2} s^{-1}) or Snijder cabinet (350 µmol photons. m^{-2} s^{-1}) for controlled environmental experiments during 1 hour and 20 minutes. After the incubation time, 1 ml of gas was extracted at once with a 1 ml syringe and immediately injected into a pre-labelled hermetic 6 ml vial with a rubber lid and previously crimped with an aluminum seal.

During the measurement process, the vials were kept out of the direct light in a cool box at all times. Once the gas was taken from the incubation tube, vials and tubes were kept out of direct light and temperature in a cool box. The fresh weight was determined by the tube-weighing method, which consists of estimating the fresh weight by the difference between a pre-prepared tube with fully humidified filter paper and the weight of the same tube containing the fresh material (not published). This method was developed to measure fresh weight at the field level.

The gas contained in the individual vials (6 ml) was measured using a laser-based ethylene detector system ETD-300 (Sensor Sense B.V., Nijmegen, The Netherlands). These vials were connected to inlet and outlet cuvettes in the VC-6 system, which allow six vials at one time, and continuously flushed with air at a constant flow of 4.5 L h^{-1}. The ETD-300 was set up in sample-mode for 5 minutes to alternatively monitor the ethylene emission from each vial. To remove any traces of external ethylene or other hydrocarbons, the airflow was passed through a platinum-based catalyzer before entering the vials. A scrubber with KOH and CaCl2 was placed before the ethylene detector to reduce the CO2 and water content from the gas sample, respectively. The ETD-300 was set up in sampling mode for 5 minutes with air flow at 4.5 l/h, meaning that after 5 minutes the sensor automatically switched to the next sample. The EDT gives the volume of ethylene contained in the samples (nl). All the data were corrected to determine ethylene emission rate, for incubation time, tube volume, and tissue fresh weight, and expressed in nL gFW^{-1} h^{-1} or nmol gFW^{-1} h^{-1}. The ETD-300 allows analyzing around 100 samples per day.

Results and Discussion

Fig. 1 A shows that under water stress (WS), higher rates of ethylene emission were generally observed at 01:00 pm. Tolerant genotypes, in terms of yield under drought stress, showed a significant decrease in ethylene emission rate between 01:00 pm and 05:30 pm at GS47, while sensitive genotypes did not. Fig. 1 B shows that one tolerant genotype (T2) showed a significant increase in ABA production between 01:00 pm and 05:30 pm under drought. Figure 1 C shows that both tolerant genotypes significantly increased the ABA/ethylene ratio between 01:00 pm and 05:30 pm under drought, while sensitive genotypes did not.

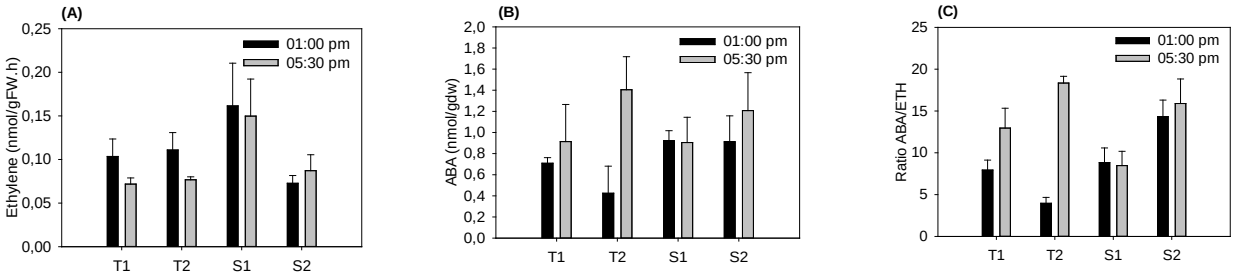

Fig. 1. Wheat leaf hormone diurnal variation at two different times (01:00 pm and 05:30 pm): a) ethylene emission; b) ABA accumulation; and c) the ABA/ETH ratio under drought stress at GS47 of four contrasting genotypes. T1 and T2 are tolerant genotypes and S1 and S2 are sensitive to drought stress. Columns and bars are means ± standard error.

The high levels of ethylene evolution observed at midday under water stress conditions (Fig. 1 A) in this experiment were also observed in cotton and rice (Abeles et al., 2012) and in *Arabidopsis* (Thain et al., 2004). In sorghum, Finlayson et al. (1999) demonstrated that the rhythmic production of ethylene is regulated by the rhythm in mRNA abundance for ACC oxidase (ACO) and ACC oxidase activity. Additionally, Thain et al. (2004) found that the circadian clock and the peak of ethylene at midday is driven by the expression of multiple ACC synthase (ACS) genes, which results in peak RNA levels at that time. It was initially thought that ACS was the rate limiting-step of ethylene biosynthesis in plants (Yang and Hoffman, 1984), but recent research has shown some examples where, in fact, the ACO is also a rate limiting-step, for example, during post-climacteric ripening of tomato fruit (Van de Poel et al., 2012). Consequently, both enzymes are highly important in the regulation of ethylene synthesis (Van de Poel and Van Der Straeten, 2014). Other research on rice leaves has associated the ethylene dynamic with sucrose concentration in the leaf, although its dynamic during the day could not be associated with carbohydrate consumption in that research (Kobayashi and Saka, 2000). It has also been observed that the absence of a functional ethylene receptor on ethylene insensitive tobacco and *Arabidopsis* sp. leads to a reduction in photosynthetic capacity and rubisco content (Tholen et al., 2007, 2008). In wheat, Ievinsh and Kreicbergs (1992) have shown a peak of ethylene coincided with periods of minimum growth. In the same study, a certain asynchronism in the oscillations in ethylene evolution of the individual seedlings was observed, which has been hypothesized to be associated with differences in the physiological or phenological stages where sampling took place. This suggests that tolerant and sensitive genotypes studied at different phenological stages could show very different responses to hormones. The significance of this needs to be considered further.

Diurnal variation in hormone accumulation and in hormone ratio suggests a possible resilience mechanism for wheat plants under drought. The ability to more rapidly reduce ethylene emission rate in interaction with ABA accumulation could be associated with a faster recovery process after maximum stress experienced (midday temperature stress). High ethylene concentrations could limit shoot growth, allowing more carbon availability for reproductive development during higher stress, resulting in more yield production. Additionally, the promoting or inhibiting effects of ethylene on shoot growth seem to depend on concentration, where low ethylene concentrations tend to promote shoot growth while high concentrations are inhibitory, although these concentration effects are apparently dependent on plant species and environment (Pierik et al., 2006). In the present study, tolerant genotypes showed a reduction in ethylene emission between 01:00 pm and 05:30 pm; this could be associated with promotion of shoot growth after the maximum stress experienced (temperature stress at 01:00 pm). Additionally, tolerant genotypes showed a high ABA/ethylene ratio after maximum stress experienced which could be related to a resilience mechanism used to recover shoot growth based on the research of Sharp and LeNoble (2002) where higher ABA concentration in the shoot was identified to reduce the inhibitory effect of ethylene on shoot growth. Based on the same research (Sharp and LeNoble, 2002), it would be interesting to determine whether similar variation in the ratio between 01:00 pm and 05:30 pm happened in the root, which would be associated with another mechanism of resilience, where a tolerant genotype enhanced the development of primary roots after having suffered maximum stress at 01:00 pm (temperature stress). Enhanced root growth may allow enhanced access to soil water, which can consequently enhance yield.

Yield is a complex trait and Slafer (2003) and others have suggested that it should be studied as the result of the action and interaction of different, more simple traits (yield components), and not used as a trait itself. Two major yield components are thousand grain weight and grain per m^2 (Slafer, 2005). It is usually considered that grain number per m^2 can be affected by stress from emergence to anthesis, while TGW is usually considered to be affected from a few days before anthesis until maturity (Slafer, 2005). Determining the grain number per square meter (G#/m^2) is more complex than determining thousand grain weight (TGW), as it is the result of the expression of many sub-components which can be influenced for long periods during plant development, from sowing to the beginning of grain filling (Slafer and Rawson, 1994).

The different sub-components of grain number per spike (G#/m^2) are spikes per square meter (Spk#/m^2) and grain number per spike (G#/spk), and the latter (G#/spk) can be sub-divided into number of grains per spikelet (G#/spklt) and spikelets per spike (Spklt/spk). Spikelets per spike is usually affected during the early reproductive phase — from floret initiation (FI) to terminal spikelet (TS)— and grains per spikelet (G#/spklt) during the late reproductive phase, from terminal spikelet (TS) to anthesis (At). The number of spike/m^2, a strong function of tillering and sowing density, is not associated with a specific development stage (from floret initiation to anthesis) and can influenced by environmental (such as plant density, abiotic stress, nutrient availability (nitrogen), etc.) and genetic factors (e.g., potential number of tillers) (Longnecker et al., 1993; Acevedo et al., 2006). Therefore, genotypic sensitivity to stress is not constant and can vary between the different yield components determined at different stages of plant development. For example, Table 1 shows that tolerant and sensitive genotypes in terms of yield do

not show similar strength or weakness in terms of yield components under drought stress in the field. In fact, sensitive genotype S1 had lower thousand grain weight (TGW) compared to the other three genotypes, while S2 had the highest TGW compared to the other three genotypes. However, S2 had one of the lowest values in terms of grain per spike and spike per m^2 and, consequently, lower yield. This means that genotype S1 seems to be sensitive to drought stress especially from anthesis to maturity, as TGW is mostly affected between yield potential and drought stress (Tables 1 and 2) but also from floret initiation to anthesis as it shows the highest reduction in terms of spike per m^2 between drought stress and irrigation (Tables 1 and 2) compared with the other three genotypes. S2 shows more sensitivity in terms of grain per spike under drought stress and therefore is more susceptible during the pre-anthesis period but less sensitive during the post-anthesis period.

Table 1. Mean values of yield, biomass and yield components under drought stress of four contrasting genotypes, in terms of yield under drought stress, where T1 and T2 represent the tolerant genotypes and S1 and S2 are sensitive genotypes. Yield under drought stress (Y_D), thousand grain weight (TGW), grain number per square meter (G#/m^2), spike number per square meter (Spk#/m^2) and grain number per spike (G#/Spk). Data from field experiment under yield potential conditions during the 2013-2014 crop season.

Genotypes	Y_D (T/Ha)	Biomass (g)	TGW (g)	G#/m^2	G#/spk	Spk/m^2
S1	2,21	601,5	24,79	8474,05	50,9	164,86
S2	2,44	744,47	36,44	6389,46	41,28	152,88
T1	2,86	772,9	36,04	7570,61	39,3	190,64
T2	2,92	735,11	32,64	8518,22	49,31	172,09

Table 2. Mean values of yield, biomass and yield components, under yield potential, of four contrasting genotypes, in terms of yield under drought stress, where T1 and T2 are tolerant genotypes and S1 and S2 are sensitive genotypes. Yield under drought stress (Y_D), thousand grain weight (TGW), grain number per square meter (G#/m^2), spike number per square meter (Spk#/m^2) and grain number per spike (G#/Spk). Data from field experiment under yield potential conditions during the 2013-2014 crop season.

Genotypes	Y (T/Ha)	Biomass (g)	TGW (g)	G#/m^2	G#/spk	Spk/m^2
S1	7,04	1410,44	36,31	18525,23	52,62	347,64
S2	7,89	1807,55	50,41	14990,44	55,56	264,46
T1	7,09	1831,81	53,75	12632,17	46,41	267,81
T2	7,48	1642,81	48,64	14723,14	49,91	291,33

Similarly, between tolerant genotypes T1 and T2 under drought stress, T1 shows a higher TGW compared with T2 but T1 show the lowest value in term of grain per spike compared with the other three genotypes but this is compensated by a higher number of fertile tillers resulting in high yielding under drought stress. This means that T1 compensates for sensitivity to drought stress in terms of grain per spike by maintaining high numbers of tillers per m^2. Genotype T2 shows a high grain number per spike and grain number per m^2 and an intermediate value in terms of spike per m^2 and TGW. Table 1 also shows that S1 and S2 had the lowest value in terms of spike per m^2 compared to T1 and T2 which had the highest values, which seem to be associated with the ratio values observed at 05:30 pm. Fig. 2 shows the relationship between the log (ABA/ETH) ratio at 05:30 pm and the reduction of spike number per m^2 between yield potential and drought stress. It is observed that a possible optimum log (ABA/ETH) ratio (around 1.20) could be associated with the maintenance of spike per m^2 when data are compared between yield potential and drought stress.

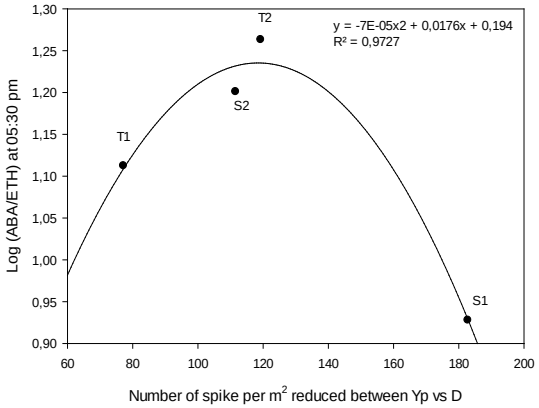

Fig. 2. Polynomial regression between the log (ABA/ETH) quantified at 05:30 pm and the number of spike per m^2 reduced under drought stress compared with yield potential (difference between spike per m^2 under yield potential and drought stress (under field conditions)) of four contrasting genotypes in terms of yield under drought. Selection was based on the data obtained under field conditions during the 2013-2014 crop season. The data on spike per m^2 came from the same field experiment.

Data in Figure 2 and Table 2 also show that using yield as a trait in itself for selection of contrast to understand or identify the action or interactive effect of hormones (in this case ABA and ethylene) on plant resilience, is not helpful and yield components seem to be a better approach to identify specific resilience mechanisms. In this case, T2 and S2 show a similar ABA/ETH ratio (Figure 2) and similar reduction of spike per m^2 (-119 and -111, respectively) but their tillering potential is different (Table 2). In fact, T2 showed higher tillering potential under yield potential conditions (Table 2) compared with S2 (291 vs 265, respectively).

In addition, Figure 3 shows a positive relationship between the (ABA/ETH) log ratio at 01:00 pm and the reduction of grain per spike between yield potential and drought stress. High ABA/ETH ratios seem to induce a higher reduction of grain per spike under drought stress, identifying more sensitive genotypes in these terms. High ABA/ETH ratios associated with drought tolerance (Figure 1) must therefore be associated with another positive effect, i.e., the positive effect of the ratio on vegetative growth (see Sharp and LeNoble, 2002).

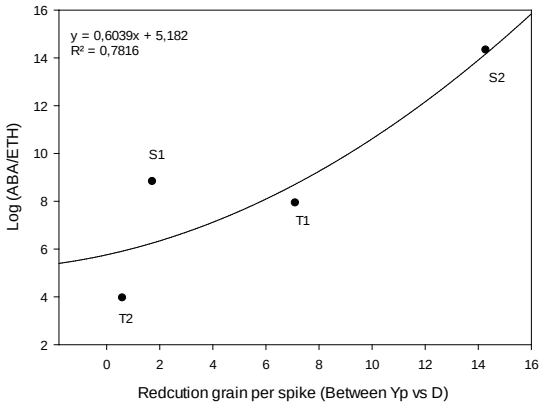

Fig. 3. Polynomial regression between the (ABA/ETH) log quantified at 01:00 pm and the number of grains per spike reduced under drought stress compared with yield potential (difference between grain per spike under yield potential and drought stress (under field conditions)) of four contrasting genotypes in terms of yield under drought. Selection was based on the data obtained under field conditions during the 2013-2014 crop season. The data on grain per spike came from the same field experiment.

Acknowledgments
We are grateful for the financial support provided by CIMMYT WHEAT CRP, to Elizabeth Morales Eliosa for her help in collecting field data and to Ascensión Martínez Pérez for taking care of the experiment before the plants reached analysis stage.

References

Abeles FB, Morgan PW, Saltveit Jr ME. 2012. Ethylene in Plant Biology. New York.

Acevedo E, Silva P, Silva H. 2006. Growth and wheat physiology, development. Laboratory of Soil-Plant-Water Relations. Faculty of Agronomy and Forestry Sciences. University of Chile. Casilla, 1004, 1–47.

Acharya BR, Assmann SM. 2009. Hormone interactions in stomatal function. Plant molecular biology 69, 451–62.

Araus JL, Slafer G a., Royo C, Serret MD. 2008. Breeding for Yield Potential and Stress Adaptation in Cereals. Critical Reviews in Plant Sciences 27, 377–412.

Bleecker AB, Kende H. 2000. Ethylene: a gaseous signal molecule in plants. Annual review of cell and developmental biology 16, 1–18.

Campbell WF, Salisbury FB, Bugbee B, et al. 2001. Comparative floral development of Mir-grown and ethylene-treated, earth-grown Super Dwarf wheat. Journal of plant physiology 158, 1051–60.

Chang C, Bleecker AB. 2004. Ethylene biology. More than a gas. Plant physiology 136, 2895–2899.

Chen L, Dodd IC, Davies WJ, Wilkinson S. 2013. Ethylene limits abscisic acid- or soil drying-induced stomatal closure in aged wheat leaves. Plant, cell & environment 36, 1850–1859.

Claeys H, Inzé D. 2013. The agony of choice: How plants balance growth and survival under water-limiting conditions. Plant Physiology 162, 1768–1779.

Cristescu SM, Mandon J, Arslanov D, De Pessemier J, Hermans C, Harren FJ. 2013. Current methods for detecting ethylene in plants. Annals of botany 111, 347–360.

Cutler AJ, Krochko JE. 1999. Formation and breakdown of ABA. Trends in Plant Science 4, 472–478.

Davies PJ. 2004. Plant hormones: biosynthesis, signal transduction, action! (PJ Davies, Ed.). Dordrecht: Kluwer Academic Publishers.

Davies PJ. 2010. The plant hormones: their nature, occurrence, and functions. In: Davies PJ, ed. Plant hormones: biosynthesis, signal transduction, action! Netherlands: Springer, 1–15.

Davies WJ, Wilkinson S, Loveys B. 2002. Stomatal control by chemical signalling and the exploitation of this mechanism to increase water use efficiency in agriculture. New Phytologist 153, 449–460.

Davies WJ, Zhang J. 1991. Root Signals and the Regulation of Growth and Development of Plants in Drying Soil. Annual Review of Plant Physiology and Plant Molecular Biology 42, 55–76.

Dolferus R, Ji X, Richards RA. 2011. Abiotic stress and control of grain number in cereals. Plant science 181, 331–41.

El-Beltagy AS, Hall MA. 1974. Effect of Water Stress Upon Endogenous Ethylene Levels in Vicia Faba. New Phytologist 73, 47–60.

Finkelstein R. 2013. Abscisic Acid synthesis and response. The Arabidopsis book / American Society of Plant Biologists 11, e0166.

Finlayson SA, Lee IJ, Mullet JE, Morgan PW. 1999. The mechanism of rhythmic ethylene production in sorghum. The role of phytochrome B and simulated shading. Plant physiology 119, 1083–9.

Guo H, Ecker JR. 2004. The ethylene signaling pathway: New insights. Current Opinion in Plant Biology 7, 40–49.

Guo D, Liang J, Li L. 2009. Abscisic acid (ABA) inhibition of lateral root formation involves endogenous ABA biosynthesis in Arachis hypogaea L. Plant Growth Regulation 58, 173–179.

Guzmán P, Ecker JR. 1990. Exploiting the triple response of Arabidopsis to identify ethylene-related mutants. The Plant Cell Online 2, 513–523.

Hays DB, Do JH, Mason RE, Morgan G, Finlayson S a. 2007. Heat stress induced ethylene production in developing wheat grains induces kernel abortion and increased maturation in a susceptible cultivar. Plant Science 172, 1113–1123.

Hochman Z. 1982. Effect of water stress with phasic development on yield of wheat grown in a semi-arid environment. Field Crops Research 5, 55–67.

Hu B, Cao J, Ge K, Li L. 2016. The site of water stress governs the pattern of ABA synthesis and transport in peanut. Scientific Reports 6, 32143.

Ievinsh G, Kreicbergs O. 1992. Endogenous rhythmicity of ethylene production in growing intact cereal seedlings. Plant physiology 100, 1389–91.

Iqbal N, Nazar R, Syeed S, Masood A, Khan NA. 2011. Exogenously-sourced ethylene increases stomatal conductance, photosynthesis, and growth under optimal and deficient nitrogen fertilization in mustard. Journal of Experimental Botany 62, 4955–4963.

Khan S, Rowe SC, Harmon FG. 2010. Coordination of the maize transcriptome by a conserved circadian clock. BMC Plant Biology 10, 126.

Kirby EJM. 1988. Analysis of Leaf, Stem and Ear Growth in Wheat from Terminal Spikelet Stage to Anthesis. Field Crops Research Elsevier Science Publishers B.V 18, 127–140.

Kobayashi H, Saka H. 2000. Relationship between Ethylene Evolution and Sucrose Content in Excised Leaf Blades of Rice. Plant Prod. Sci 3, 398–403.

Lee SC, Luan S. 2012. ABA signal transduction at the crossroad of biotic and abiotic stress responses. Plant, Cell and Environment 35, 53–60.

Lee KH, Piao HL, Kim HY, Choi SM, Jiang F, Hartung W, Hwang I, Kwak JM, Lee IJ, Hwang I. 2006. Activation of Glucosidase via Stress-Induced Polymerization Rapidly Increases Active Pools of Abscisic Acid. Cell 126, 1109–1120.

Longnecker N, Kirby EJM, Robson A. 1993. Leaf Emergence, Tiller Growth, and Apical Development of Nitrogen-Deficient Spring Wheat. Crop Science 33, 154.

Mcclung CR. 2000. Circadian rhythms in plants : a millennial view. Physiologia Plantarum 109, 359–371.

Pask A, Pietragalla J, Mullan D, Reynolds MP. 2012. Physiological Breeding II: A Field Guide to Wheat Phenotyping.

Peltonen-Sainio P, Kangas A, Salo Y, Jauhiainen L. 2007. Grain number dominates grain weight in temperate cereal yield determination: Evidence based on 30 years of multi-location trials. Field Crops Research 100, 179–188.

Pierik R, Sasidharan R, Voesenek LACJ. 2007. Growth Control by Ethylene: Adjusting Phenotypes to the Environment. Journal of Plant Growth Regulation 26, 188–200.

Pierik R, Tholen D, Poorter H, Visser EJW, Voesenek LACJ. 2006. The Janus face of ethylene: growth inhibition and stimulation. Trends in Plant Science 11, 176–183.

Van de Poel B, Bulens I, Markoula A, et al. 2012. Targeted systems biology profiling of tomato fruit reveals coordination of the Yang cycle and a distinct regulation of ethylene biosynthesis during postclimacteric ripening. Plant physiology 160, 1498–514.

Van de Poel B, Van Der Straeten D. 2014. 1-aminocyclopropane-1-carboxylic acid (ACC) in plants: more than just the precursor of ethylene! Frontiers in plant science 5, 640.

Puértolas J, Alcobendas R, Alarcón JJ, Doddian C. 2013. Long-distance abscisic acid signalling under different vertical soil moisture gradients depends on bulk root water potential and average soil water content in the root zone. Plant, Cell and Environment 36, 1465–1475.

Quarrie SA, Whitford PN, Appleford NEJ, Wang TL, Cook SK, Henson IE, Loveys BR. 1988. A monoclonal antibody to (S)-abscisic acid: its characterisation and use in a radioimmunoassay for measuring abscisic acid in crude extracts of cereal and lupin leaves. Planta 173, 330–339.

Saab IN, Sharp RE, Pritchard J, Voetberg GS. 1990. Increased endogenous abscisic acid maintains primary root growth and inhibits shoot growth of maize seedlings at low water potentials. Plant physiology 93, 1329–1336.

Sayre KD, Rajaram S, Fischer RA. 1997. Yield potential progress in short bread wheats in northwest Mexico. Crop Science 7, 36–42.

Sharp R. 2002. Interaction with ethylene: changing views on the role of abscisic acid in root and shoot growth responses to water stress. Plant, Cell & Environment, 211–222.

Sharp RE, LeNoble ME. 2002. ABA, ethylene and the control of shoot and root growth under water stress. Journal of experimental botany 53, 33–7.

Sharp RE, Wu Y, Voetberg GS, Saab IN, LeNoble ME. 1994. Confirmation that abscisic acid accumulation is required for maize primary root elongation at low water potentials. Journal of Experimental Botany 45, 1743–1751.

Shearman VJ, Sylvester-Bradley R, Scott RK, Foulkes MJ. 2005. Physiological processes associated with Wheat Yield Progress in the UK. 45, 175–185.

Shiferaw B, Smale M, Braun HJ, Duveiller E, Reynolds M, Muricho G. 2013. Crops that feed the world 10. Past successes and future challenges to the role played by wheat in global food security. Food Security 5, 291–317.

Siddique KHM, Kirby EJM, Perry MW. 1989. Ear:Stem Ratio in Old and Modern Wheat Varieties; Relationship with Improvement in Number of Grains per Ear and Yield. Field Crops Research Elsevier Science Publishers B.V 21, 59–78.

Sisler EC, Grichko V, Serek M. 2006. 1 Interaction of Ethylene and Other Compounds with the Ethylene Receptor : Agonists and Antagonists. Ethylene Action in plants.

Slafer GA. 2003. Genetic Basis of Yield as Viewed From a Crop Physiologist's Perspective. Annals of Applied Biology 142, 117–128.

Slafer GA. 2005. Physiology of determination of major wheat yield components. In: Buck, H.T., Nisi, J.E., Salomón N, ed. Environments Proceedings of the 7th International Wheat Conference, 27 November - 2 December 2005, Mar del Plata, Argentina (Developments in Plant Breeding). Springer, 557–565.

Slafer GA, Rawson HM. 1994. Sensitivity of Wheat Phasic Development to Major Environmental Factors: a Re-Examination of Some Assumptions Made by Physiologists and Modellers. Australian Journal of Plant Physiology 21, 393.

Tardieu F, Zhang J, Katerji N, Bethenod O, Palmer S, Davies WJ. 1992. Xylem ABA controls the stomatal conductance of field-grown maize subjected to soil compaction or soil drying. Plant, Cell & Environment 15, 193–197.

Thain SC, Vandenbussche F, Laarhoven LJJ, Dowson-Day MJ, Wang Z-Y, Tobin EM, Harren FJM, Millar AJ, Van Der Straeten D. 2004. Circadian Rhythms of Ethylene Emission in Arabidopsis. Plant Physiology 136, 3751–3761.

Thiry AA, Chavez Dulanto PN, Reynolds MP, Davies WJ. 2016. How can we improve crop genotypes to increase stress resilience and productivity in a future climate? A new crop screening method based on productivity and resistance to abiotic stress. Journal of Experimental Botany 67, 5593–5603.

Tholen D, Pons TL, Voesenek LACJ, Poorter H. 2007. Ethylene insensitivity results in down-regulation of rubisco expression and photosynthetic capacity in tobacco. Plant Physiology 144, 1305–15.

Tholen D, Pons TL, Voesenek LACJ, Poorter H. 2008. The role of ethylene perception in the control of photosynthesis. 3, 108–109.

Wang Z, Mambelli S, Setter TL. 2002. Abscisic Acid Catabolism in Maize Kernels in Response to Water Deficit at Early Endosperm Development. Annals of Botany 90, 623–630.

Wilkinson S, Davies WJ. 2002. ABA-based chemical signalling : the co-ordination of. Plant, Cell & Environment 25, 195–210.

Wilkinson S, Davies WJ. 2009. Ozone suppresses soil drying- and abscisic acid (ABA)-induced stomatal closure via an ethylene-dependent mechanism. Plant, Cell & Environment 32, 949–59.

Wilkinson S, Davies WJ. 2010. Drought, ozone, ABA and ethylene: new insights from cell to plant to community. Plant, Cell & Environment 33, 510–25.

Yang SF, Hoffman NE. 1984. Ethylene Biosynthesis and its Regulation in Higher Plants. Annual Review of Plant Physiology 35, 155–189.

Yang J, Zhang J, Liu K, Wang Z, Liu L. 2006. Abscisic acid and ethylene interact in wheat grains in response to soil drying during grain filling. The New Phytologist 171, 293–303.

Yang J, Zhang J, Liu K, Wang Z, Liu L. 2007. Abscisic Acid and Ethylene Interact in Rice Spikelets in Response to Water Stress During Meiosis. Journal of Plant Growth Regulation 26, 318–328.

Zadoks JC, Chang TT, Konzak CF. 1974. A decimal code for the growth stages of cereals. Weed Research 14, 415–421.

PHOTOSYNTHESIS

Overexpression of a putative carbon uptake facilitation mechanism in wheat

Luis Robledo-Arratia[1,2], Elizabete Carmo-Silva[2,4], Pippa Madgwick[2], Matthew Reynolds[3], Martin Parry[2,4] and Howard Griffiths[1]

[1] University of Cambridge, UK; [2] Rothamsted Research, UK; [3] CIMMYT, Mexico; [4] Lancaster University, UK.

Abstract

Mesophyll conductance (g_m) describes how CO_2 travels from the substomatal cavity to the inside of the chloroplast. This step, together with stomatal conductance (g_s) and the biochemical capacity of Rubisco, regulates the fixation of CO_2 to generate biomass. These processes cannot be considered in isolation and this carbon demand at leaf level should be integrated with leaf hydric status. Water and CO_2 share common pathways in their travel in and out of plants. It has been suggested that aquaporins, a group of proteins well known for their role as water transporters, could possibly act as uptake facilitators of CO_2. In this work, two aquaporin genes were overexpressed in wheat and the photosynthetic traits and yield components of the plants were analyzed. Assimilation, g_s and water use efficiency (WUE) increased in the transgenic lines but not g_m. There was no correlation between the concentration of aquaporins and these photosynthetic traits or yield. These results confirm the role of aquaporins as water transporters but no indication of CO_2 facilitation was confirmed.

Introduction

Diffusion of water and CO_2

Gas exchange in plants is possible due to the fine regulation of stomata, which mediate the trade-off with the atmosphere, allowing uptake of CO_2 and releasing H_2O by transpiration (Maurel et al., 2015). Inside the plants, water travels long distances through the vascular system, and the xylem vessels in particular, with relatively low hydraulic resistance. At the cellular level, membranes and cell walls are used to promote turgor and support, but represent a barrier that needs to be overcome in order to achieve hydric homeostasis (Chaumont and Tyerman, 2014; Maurel et al., 2015). The movement of water through veins and mesophyll cells contributes to overall leaf hydraulic conductance (K_{leaf}) and correlates with leaf CO_2 conductance or mesophyll conductance (Flexas et al., 2013). CO_2 and water travel in opposite directions, with CO_2 diffusing from the substomatal cavity across cell walls, plasma membrane, cytosol, and chloroplast envelop to the chloroplast interior, where carboxylation takes place. g_m describes this path, and from this trait it is possible to calculate the final CO_2 concentration inside the chloroplast (C_c; Evans et al., 2009).

Aquaporins

It is well known that aquaporins are a diverse family of channel proteins present in all organisms (Abascal et al., 2014) that help water molecules to flow across membranes, equilibrating hydraulic gradients and generating particular hydrostatic pressures, as well as the movement through bundle sheath and mesophyll cells to the substomatal cavities en route to the atmosphere (Prado and Maurel, 2013; Shatil-Cohen et al., 2011). Most are plasma membrane proteins, but in animals they are also located in mitochondria and in plants they are present in chloroplast membranes (Maurel et al., 2015). The folding patterns and membrane topology of aquaporins are conserved among subfamilies (Abascal et al., 2014). These proteins are comprised of four monomers with a central individual pore, with the subunits being assembled as homo- or heterotetramers (Bienert et al., 2012) that display a gating system with two conformations, closed and open, responsible for the high specificity of the pore, which allows water to pass through the inner space created by each monomer (Chaumont and Tyerman, 2014).

It has been proposed that CO_2 travels from cell to cell through a diffusion facilitation mechanism or mechanisms (Maurel et al., 2015). Aquaporins can transport other solutes such as glycerol, different nutrients, reactive oxygen species, urea and metalloids (Moshelion et al., 2015) and some studies suggest that aquaporins also facilitate the transport of CO_2 across plasma and chloroplast membranes (Kaldenhoff, 2012) and across artificial membranes (Uehlein et al., 2012). These facilitators would be most important in mesophytic annual herb species (Tomas et al., 2013) and they would be responsible for the observed changes in g_m in response to the environment (Tholen and Zhu, 2011).

The aim of the current study was to establish the physiological role of aquaporins in wheat; to do that, a couple of aquaporin genes were overexpressed and the photosynthetic and yield traits of the transformants were measured.

Methods

Cadenza wheat genotype was transformed with one of two different plasmids. Each of these plasmids contained a construct that includes a sequence that encodes an aquaporin. Plasmid p302AtPIP1;2 had the aquaporin gene from *Arabidopsis thaliana* (AtPIP1;2) and p302NtAQP1 contained the aquaporin gene from *Nicotiana tabacum* (NtAQP1). Both genes included their own transit peptide sequence at the amino terminal end. This directs them towards the chloroplast. Wheat was transformed with a biolistic method (Sparks and Jones, 2009). Plants were tested by PCR to confirm the presence of the transgene and those that gave a positive signal were later tested by Western blot using an antibody against aquaporins to prove the presence of the protein. These steps were repeated for the T_0, T_1 and T_2 generations.

When T_2 plants reached the early booting stage (4.3 according to Zadoks et al., 1974), photosynthetic assimilation, stomatal conductance and mesophyll conductance were measured using gas exchange and fluorescence analysis simultaneously using a portable leaf gas exchange and fluorescence system (LI-6400XT; LI-COR, Lincoln, NE, USA) as described by Driever et al. (2014). CO_2 response curves were measured at a leaf temperature of 25°C and a saturating quantum flux density of 1500 µmol m^{-2} s^{-1}. The CO_2 concentration in the cuvette (Ca) was lowered stepwise from 400 to 100 µmol CO_2 mol air^{-1}, then raised again to 400 µmol CO_2 mol air^{-1} and then raised stepwise to 1200 µmol CO_2 mol air^{-1}. After a first CO_2 response curve at ambient oxygen concentration (21%), a tank containing 2% of oxygen was connected to the air inlet of the LI-COR system and a second CO_2 response curve was measured. Mesophyll conductance was calculated as described by Bellasio and Griffiths (2013) and Bellasio et al. (2016). After these measurements were finished, flag leaves were cut and immediately scanned to calculate the leaf area, and thickness and length were measured. Leaves were oven-dried for 48 h and then weighed. After reaching physiological maturity, plants were harvested, spikes were weighed, threshed and grains were weighed and counted.

Results and Discussion

Control lines expressed the endogenous wheat aquaporins and the assay used here was unable to discriminate between those and foreign proteins. However, transgenic wheat lines were successfully obtained with the protocol used in this study; three lines expressing p302AtPIP1;2 (L1 to L3) and four lines with p302NtAQP (L4 to L7) had higher levels of aquaporin protein compared with the corresponding controls (Fig. 1; Robledo-Arratia, 2017).

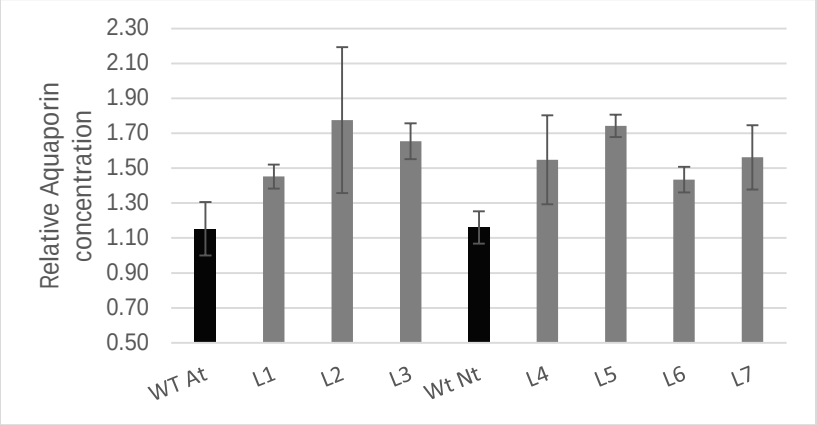

Fig. 1. Relative aquaporin concentration of wheat lines. Plants were transformed with *Arabidopsis* aquaporin (L1-3) or with tobacco aquaporin (L4-7) and controls were transformed with empty plasmids (Wt At and Wt Nt). Protein was detected with a specific antibody on a Western blot. Values are the mean of three plants and five independent loading signals for each plant; SED are shown.

Photosynthetic assimilation (A), stomatal conductance (g_s), instantaneous water use efficiency (WUE) and mesophyll conductance (g_m) were obtained from the A/Ci curves. There were no significant differences between the lines for any of these traits. A strong positive correlation was found between A and g_s when the lines were plotted ($r=0.43$, $p=0.003$, data not shown) and when independent plants were considered ($r=0.40$, $p=0.001$, Fig. 2A). Values for g_m did not correlate with A (Fig. 2B) or with g_s (Fig. 2C) (Robledo-Arratia, 2017). These results show that an increase in aquaporin concentration does not necessarily correlate with more efficient CO_2 transport into the chloroplast, which is ultimately linked to higher photosynthetic capacity and grain yield. The correlation between A and g_s was, however, very clear (Fig. 2A) and in agreement with several studies that have compared transgenic and non-transgenic plants (Robledo-Arratia, 2017).

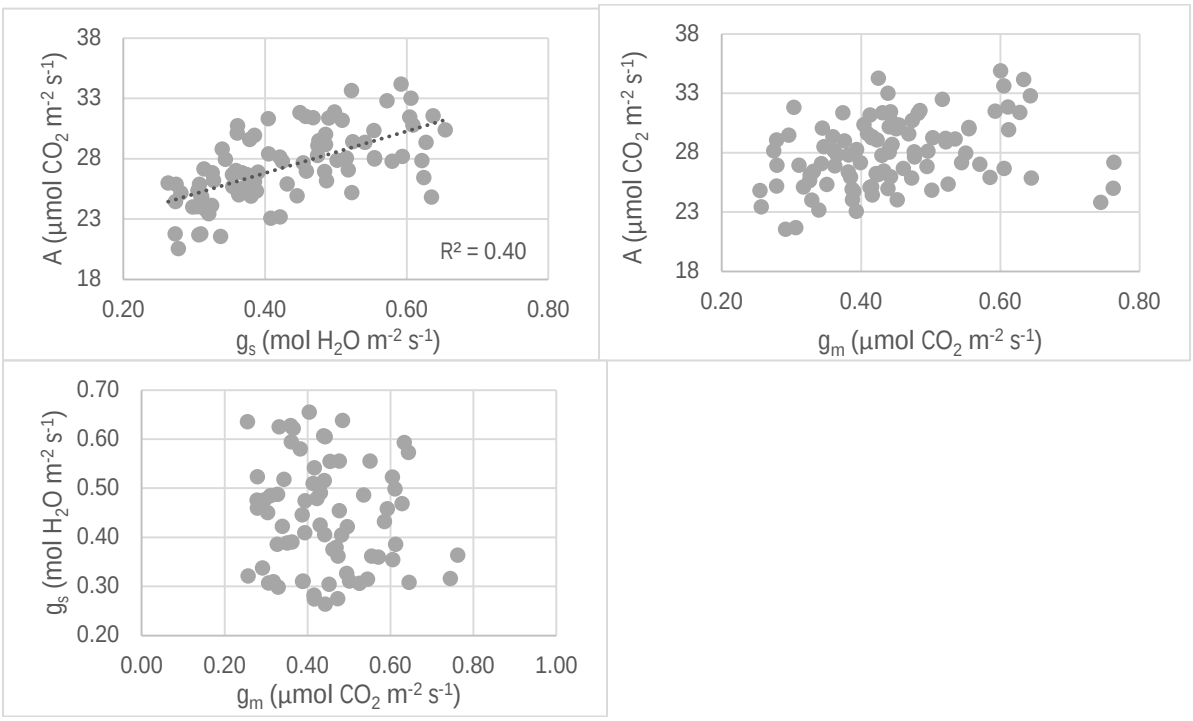

Fig. 2. Correlation between photosynthetic traits. All measurements were done at early booting stage in well-watered plants.

The values for WUE per line were positively correlated with A (r=0.2, p=0.03), with g_s (r=0.67, p=0.01), and with leaf area (r=0.17, p=0.03, data not shown), and negatively correlated with yield as grain weight per plant (r=0.55, p=0.02, Fig. 3). WUE was, however, not related with g_m (Fig. 3), with the relative aquaporin concentration or with yield (data not shown). Flexas et al. (2013) found that an increase in WUE necessarily requires a decrease in the g_s value, and that this is true for different species. In my study, however, WUE values had coincidences with g_s, so that the lines that had higher WUE than the controls had also higher g_s and these two traits were overall positively correlated (Fig. 5). This suggests that the presence of a higher concentration of aquaporins influences water utilization through elements like stomatal aperture, transpiration rate and, consequently, g_s. The observed WUE, g_s and g_m values in my work were different to the predicted trends in the literature; this indicates, on one hand, that these values are species-specific and, on the other hand, that the modification of the conductance ratios could confer physiological advantages to the plants (Robledo-Arratia, 2017).

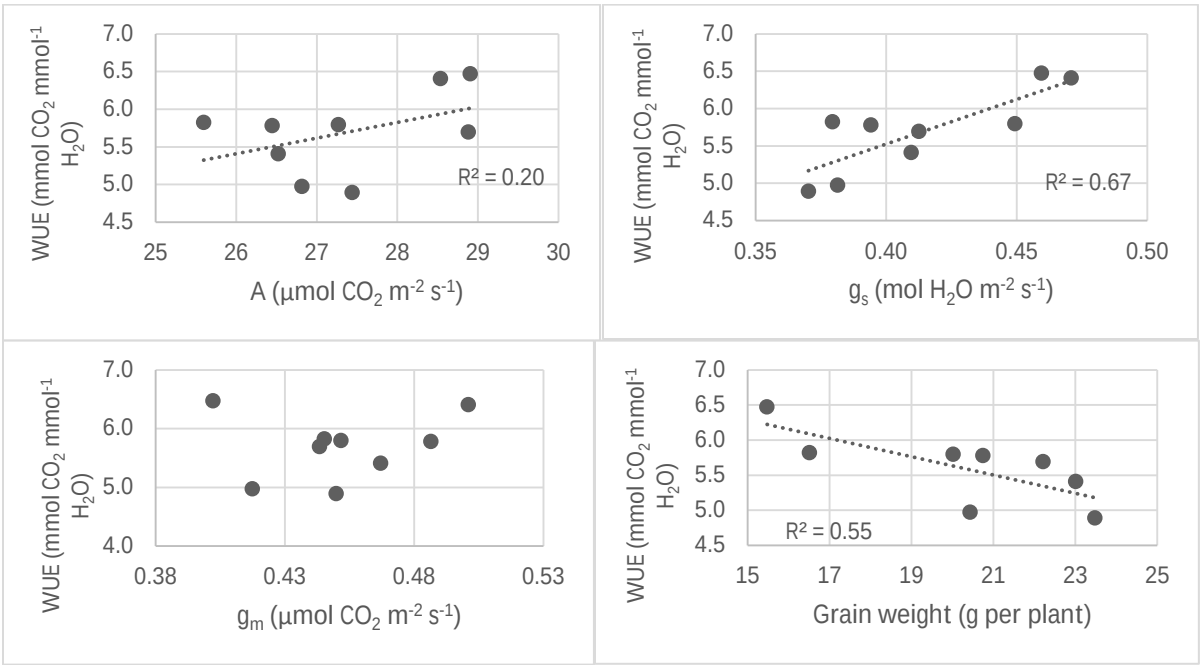

Fig. 3. Relation between WUE and photosynthetic and yield traits.

Grain weight and grain number per plant, there were significant differences between the transgenic and control lines (Fig. 4). A slight negative correlation between aquaporin concentration in the leaves and grain weight per plant (data not shown) can indicate that the increase in productivity is due to other factors like more efficient hydric use, less investment of resources in above-ground biomass or increase in A values.

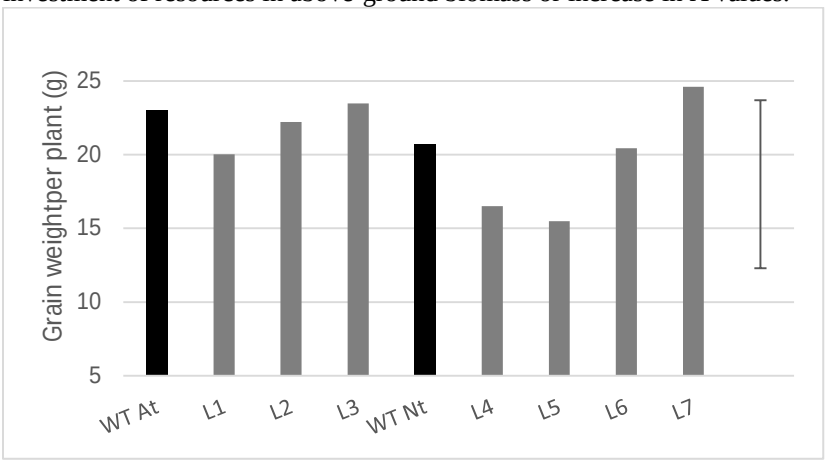

Fig. 4. Total grain weight per plant (g). Control lines are shown in black and bars are the average of 10 transgenic plants or 5 control plants. LSD (5%, 75 df, p=0.03) is shown.

Conclusions

- The transgenic lines generated in this study did show an overexpression of aquaporins and, in most cases, an increase in assimilation, stomatal conductance and WUE. However, there was no increase in mesophyll conductance.
- There was no link between specific levels of overexpressed aquaporin and the increase in these photosynthetic traits, so no causal relationship could be established.
- These results confirm the role of aquaporins as facilitators of hydraulic conductance under well-watered conditions. However, their suggested role as CO_2 transporters was not confirmed.
- There was no correlation between final grain yield and the expression of aquaporins.

References

Abascal F, Irisarri I, Zardoya R. 2014. Diversity and evolution of membrane intrinsic proteins. Biochimica Et Biophysica Acta-General Subjects 1840, 1468-1481.

Bellasio C, Griffiths H. 2013. Acclimation to low light by C4 maize: implications for bundle sheath leakiness. Plant, Cell and Environment 36, 1046-1058.

Bellasio C, Beerling D, Griffiths H. 2016. Deriving C_4 photosynthetic parameters from combined gas exchange and chlorophyll fluorescence using

Bienert G, Cavez D, Besserer A, Berny M, Gilis D, Rooman M, Chaumont F. 2012. A conserved cysteine residue is involved in disulphide bond formation between plant plasma membrane aquaporin monomers. Biochemistry Journal 445, 101–111.

Chaumont F, Tyerman S. 2014. Aquaporins: highly regulated channels controlling plant water relations. Plant Physiology 164, 1600-1618.

Driever S, Lawson T, Andralojc P, Raines C and Parry M. 2014. Natural variation in photosynthetic capacity, growth and yield in 64 field-grown wheat genotypes. Journal of Experimental Botany 65, 4959-4973.

Evans J, Kaldenhoff R, Genty B, Terashima I. 2009. Resistances along the CO_2 diffusion pathway inside leaves. Journal of Experimental Botany 60, 2235–2248.

Flexas J, Scoffoni C, Gago J, Sack L. 2013. Leaf mesophyll conductance and leaf hydraulic conductance: an introduction to their measurement and coordination. Journal of Experimental Botany 64, 3965–3981.

Kaldenhoff R. 2012. Mechanisms underlying CO_2 diffusion in leaves. Current Opinion in Structural Biology 15, 276–281.

Maurel C, Boursiac Y, Luu D, Santoni V, Shahzad Z, Verdoucq L. 2015. Aquaporins in plants. Physiology Review 95, 1321-1358.

Moshelion M, Halperin O, Wallach R, Oren R, Way D. 2015. Role of aquaporins in determining transpiration and photosynthesis in water-stressed plants: crop water-use efficiency, growth and yield. Plant, Cell and Environment, 38, 1785-1793.

Prado K and Maurel C. 2013. Regulation of leaf hydraulics: from molecular to whole plant levels. Frontiers in Plant Science 4, 255.

Robledo-Arratia, L. 2017. Improving photosynthesis and yield in wheat. PhD thesis. University of Cambridge.

Shatil-Cohen A, Attia Z, Moshelion M. 2011. Bundle-sheath cell regulation of xylem-mesophyll water transport via aquaporins under drought stress: a target of xylem-borne ABA? Plant Journal 67, 72–80.

Sparks C and Jones H. 2009. Biolistic transformation of wheat (in: Jones H and Shewry P (Eds.). Methods in molecular biology, transgenic wheat, barley and oats. Vol 478:71-91).

Tholen D, Zhu X. 2011. The mechanistic basis of internal conductance: a theoretical analysis of mesophyll cell photosynthesis and CO2 diffusion. Plant Physiology 156, 90–105.

Tomás M, Flexas J, Copolovici L, Galmés J, Hallik L, Medrano H, Ribas-Carbó M, Tosens T, Vislap V, Niinemets Ü. 2013. Importance of leaf anatomy in determining mesophyll diffusion conductance to CO2 across species: quantitative limitations and scaling up by models. Journal of Experimental Botany 64**,** 2269–2281.

Uehlein N, Otto B, Eilingsfeld A, Itel F, Meier W, Kaldenhoff R. 2012a. Gas-tight triblock-copolymer membranes are converted to CO_2 permeable by insertion of plant aquaporins. Scientific Reports 2:538.

Zadoks J, Chang T, Konzak C. 1974. A decimal code for the growth stages of cereals. Weed Research 14, 415–421.

Phenotypic variation for radiation use efficiency in a panel selected for high biomass (HiBAP) at different growth stages

Gemma Molero[1], Francisco J. Piñera, Alma C Rivera-Amado, and Matthew P. Reynolds[1]
[1] CIMMYT, Mexico

Abstract

It is predicted that future increases in yield potential will rely largely on improved radiation use efficiency (RUE) through improved photosynthesis. Genetic variation associated with RUE traits has been widely reported in wheat; however, less attention has been paid to the interaction between RUE at different growth stages. In the present study, a High Biomass Association Mapping Panel (HiBAP) consisting of a total of 150 spring wheat types, including elite high yield material, pre-breeding lines crossed and selected for high yield and biomass, synthetic-derived lines, and appropriate checks was assembled by selecting lines that presented high biomass at different growth stages. Genetic diversity for RUE at different phenological stages was found, suggesting discrete genetic control. These findings strongly support that significant underutilized photosynthetic capacity in existing wheat germplasm could come from increasing RUE at all growth stages. Unfortunately, negative correlations were observed among different RUE, highlighting the importance of understanding these trade-offs in more detail. In addition, lines that are better adapted to density had higher RUE in later stages, suggesting a better use of light resources that compensated for the competition among plants growing at high agronomic density.

Introduction

Yield potential (YP) can be expressed as a function of light intercepted (LI) and radiation use efficiency (RUE), whose product is biomass, and the partitioning of biomass to yield, i.e., harvest index (HI). It is predicted that future increases in yield potential will rely largely on improved radiation use efficiency (RUE) through improved photosynthesis. Genetic variation of RUE traits has been widely reported in wheat (Calderini et al., 1997; Miralles and Slafer, 1997). Although physiological traits related to RUE are generally more challenging to measure, the potential to increase RUE is supported by theory (Zhu et al., 2010), as well as the observed increase in biomass in recent cultivars (Shearman et al., 2005), which in some cases, stems from the introgression of exotic germplasm (Reynolds et al., 1998).

The main approaches for increasing RUE will most likely focus on overcoming constraints to increase biomass production. The overarching goal of exploring genetic diversity for biomass is to introduce sources of alleles that can contribute to the expression of high final biomass and other contributing photosynthetic related traits in a range of elite genetic backgrounds. To this end, systematic screening of genetic resources from the World Wheat Collection was conducted to identify genotypes with favorable expression of biomass at different growth stages. The High Biomass Association Mapping Panel (HiBAP) consists of a total of 150 spring wheat types, including elite high yielding material, pre-breeding lines crossed and selected for high yield and biomass, synthetic derived lines, and appropriate checks. The material has a restricted range of maturity to avoid confounding effects associated with extreme phenology. During 2015-2016, the first year of evaluation of HiBAP was carried out to determine biomass patterns across the lines and RUE at different phenological stages.

Methods

Growth analysis

150 HiBAP lines were subjected to growth analysis under yield potential growing conditions at the IWYP platform in NW Mexico during 2015-2016. The growth analyses were conducted at the following growth stages: (i) crop establishment (emergence to canopy closure); (ii) spike development (canopy closure until initiation of booting), (iii) rapid spike growth (initiation of booting until seven days after anthesis); and (iv) grain filling (anthesis until physiological maturity). To do so, biomass (BM) in the plots was harvested at different times: BME40: biomass measured at canopy closure; BMInB: BM at initiation of booting; BMA7: BM seven days after anthesis; BM: biomass at physiological maturity. Using the biomass and the Megajoules of radiation intercepted, radiation use efficiency (RUE) was calculated during the different growth stages: RUE_E40InB: from canopy closure to initiation of booting; RUE_InBA7: from initiation of booting to seven days after anthesis; RUE_GF: RUE from seven days after anthesis until physiological maturity; RUET: RUE from canopy closure to physiological maturity.

Yield and yield components

Yield (YLD) and yield components were calculated following the protocols outlined in Pask et al. (2012) from an area of approximately 4 m^2. GM2: grains per square meter, GSP: grain number per spike, HI: harvest index,

InfSPKL SP^{-1}: number of infertile spikelets per spike, SM2: spikes per square meter, TGW: thousand-grain weight, Height: height of the plant from the base to the tip of the spike. Adaptation to density index (*ADi*) was calculated as the ratio between yield from inner rows divided by outer rows (Yld Inner/Yld outer).

Results and Discussion

Future increases in yield potential must include improvements in structural and reproductive aspects of the crop together with increased RUE (Reynolds et al., 2011). According to the data (Fig. 1), there was genetic diversity for RUE at different phenological stages, suggesting discrete genetic control. These findings strongly support the case for significant underutilized photosynthetic capacity in existing wheat germplasm that could come from increasing RUE at all growth stages.

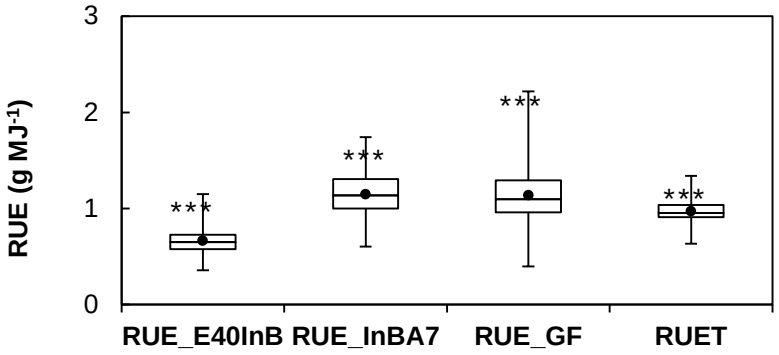

Fig. 1. Variation in Radiation Use Efficiency (RUE) measured at different growth stages in the HiBAP panel (150 lines) at the IWYP-HUB evaluated during 2015-2016. The box-whisker plots indicate the distribution of the data. The up and down part of the rectangles (box) give the estimated 25th and 75th percentile, the line in the middle indicates the median value, the black dot indicates the mean, the error bars (whisker) represent the 10th and 90th percentiles. RUE during spike development (canopy closure until initiation of booting, RUE_E40InB), RUE during rapid spike growth phase (initiation of booting until seven days after anthesis, RUE_InBA7) and RUE during grain filling (anthesis until physiological maturity, RUE_GF). Significance of the genotypes is indicated above the box plots, ***P<0.001.

This is even more evident as a negative trade-off is observed between RUE during rapid spike growth phase (initiation of booting until seven days after anthesis, RUE_InBA7) with RUE during spike development (canopy closure until initiation of booting, RUE_E40InB) and RUE during grain filling (anthesis until physiological maturity, RUE_GF) (Fig. 2). No trade-off was observed between RUE_E40InB and RUE_GF.

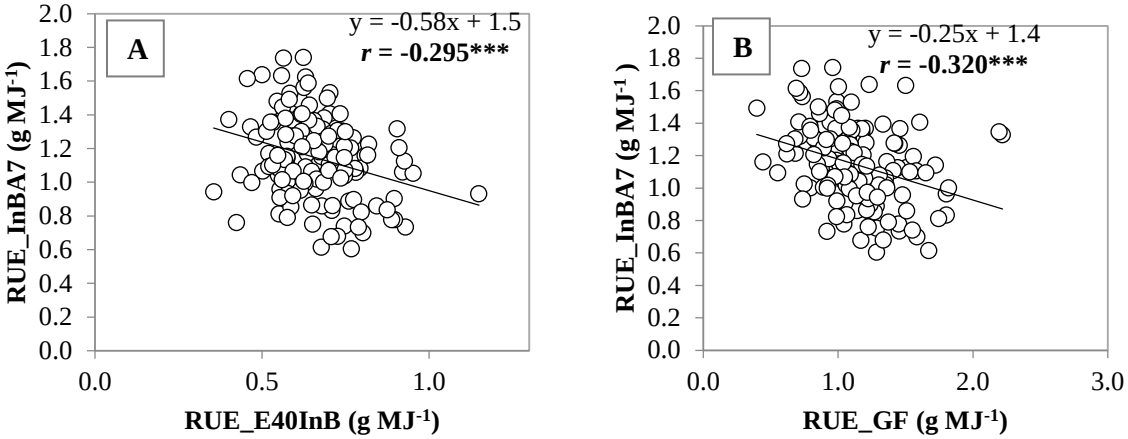

Fig. 2. Trade-off between radiation use efficiency during rapid spike growth phase (RUE_InBA7) and (A) RUE during spike development (RUE_E40InB) and (B) RUE during grain filling (RUE_GF). ***P<0.001.

In order to study in more detail variations in RUE profiles measured at different growth stages in the 150 lines evaluated from HiBAP, hierarchically clustered ‘heatmaps’ were created using the software MEV 4. All the 150 lines were analyzed together and two main clusters were identified that were negatively correlated among them (data not shown). Cluster 1 presents mainly lines with high RUE at early stages and low RUE at later stages, while cluster 2 presents mainly lines with low RUE at early stages and higher RUE at later ones (Fig. 3). The first cluster included 77 lines, while the second cluster included 73 lines. The analysis was repeated for the two clusters separately. As can be observed in Fig. 3, in general, lines with RUE_InBA7 values above the average (green color) presented low values (red) early in the cycle (RUE_EInB) and during grain filling (RUE_GF) (Fig. 3, Cluster 1, left). On the other side, lines presenting RUE_GF values above the mean showed low RUE_InBA7 (Fig. 3, Cluster 2, right), as shown in Fig. 2. Despite this general trend, in Fig. 3 some lines with no trade-off between RUE at different growth stages can be identified and this can be used to link the genetic background of the lines with enhanced RUE traits.

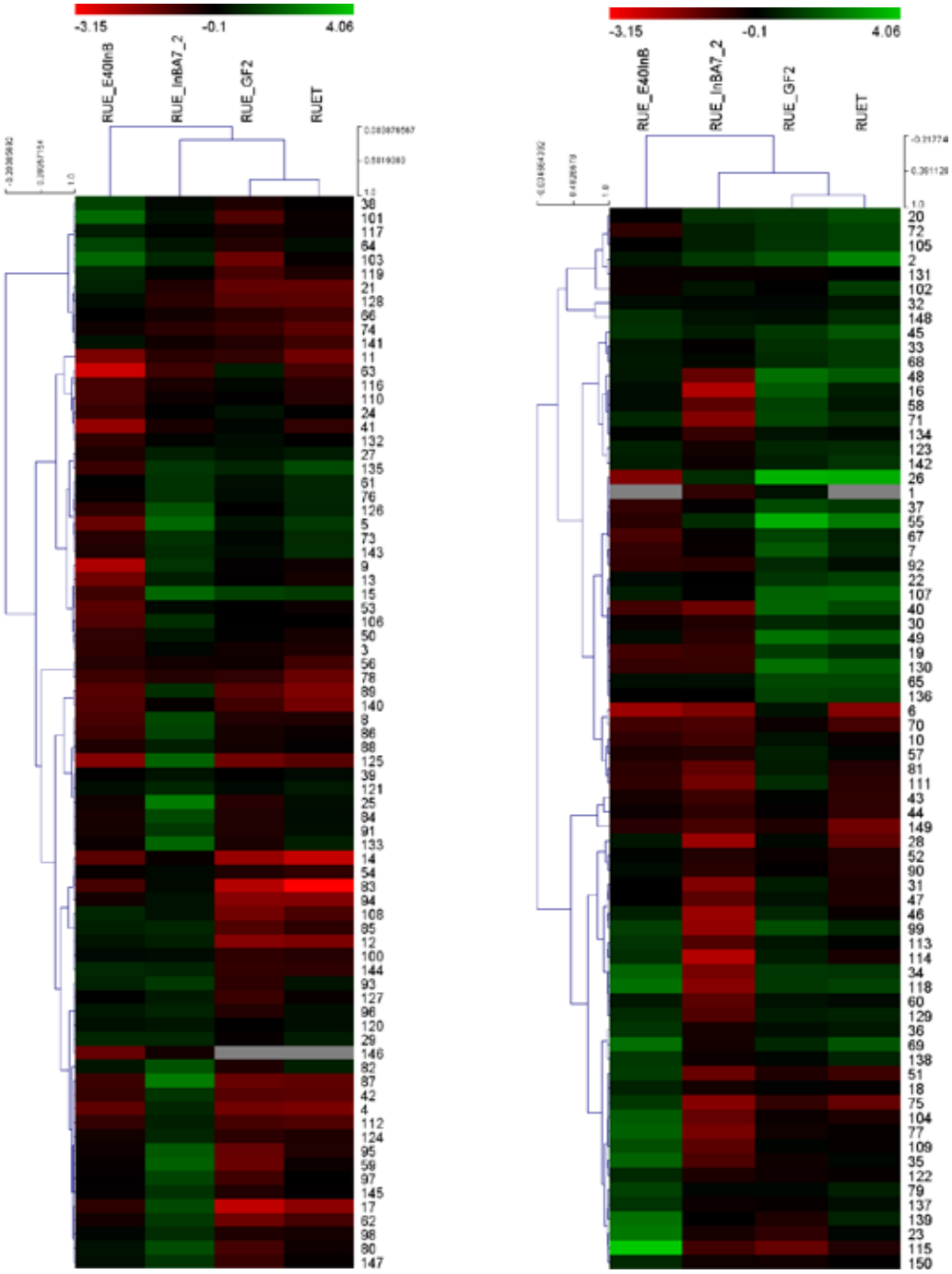

Fig. 3. Variations in RUE profiles measured at different growth stages. Hierarchically clustered 'heatmaps' of the mean centered-reduced RUE values separated in two main groups resulting from a preliminary analysis where cluster 1 presents mainly lines with high RUE at early stages and low RUE at later stages (left) and cluster 2 presents mainly lines with low RUE at early stages and higher RUE at later stages (right). Intense red and green indicate lower and higher RUE values relative to the mean (dark color), according to the color scale shown at the top of the figure.

Increasing RUE along the whole crop cycle has a positive effect on yield components such as TGW, while a negative correlation was observed between RUE at early stages and GM2 (Table 1), probably due to the competition for assimilates between the investment in aerial biomass and spike development. However, this negative correlation disappeared in later stages.

The negative correlation observed between RUE_GF and HI can be explained by the negative correlation also observed between HI and final biomass (data not shown), as previously reported in the most modern cultivars (Aisawi et al., 2015; Rivera-Amado et al., 2016).

Table 1. Phenotypic correlations between RUE at different growth stages with yield, yield components, biomass at different growth stages and adaptation to density index (ADi).

Traits	**RUE_E40InB**	**RUE_InBA7**	**RUE_GF**	**RUET**
YLD	0.00	0.12	**0.59**	**0.70**
HI	-0.13	0.15	**-0.32**	**-0.30**
TGW	**0.30**	-0.06	**0.25**	**0.38**
GM2	**-0.27**	0.16	**0.23**	**0.20**
SM2	**-0.21**	**0.19**	**0.28**	**0.26**
GSP	**0.19**	-0.09	**0.17**	**0.27**
InfSPKLSP	0.07	-0.04	0.13	0.11
Height	**0.20**	0.00	**0.18**	**0.30**
BME40	0.08	-0.11	-0.12	-0.13
BMInB	**0.79**	**-0.34**	-0.08	0.03
BMA7	**0.22**	**0.58**	**-0.23**	**0.17**
BM	0.08	0.04	**0.80**	**0.92**
ADi	**-0.25**	**0.20**	**0.20**	**0.19**

Taller plants presented higher RUE values probably associated with their ability to increase photosynthesis due to better light distribution (Song et al., 2013). This may explain why recent material derived from strategic crosses with high biomass have increased plant height in comparison with conventional checks.

Adaptation to density (ADi) was calculated in HiBAP lines grown in a high spring density experiment (4 rows per bed in spite of 2 rows). Previous studies conducted by the team (Reynolds et al., 1994; Sukumaran et al., 2015) infer that low-yield potential lines respond more to reduced competition for light under low planting density than high yield potential lines. In addition, improvement in yield potential has been associated with improvements in adaptation to plant density (Sukumaran et al., 2015). In the present study, lines that are better adapted to density have higher RUE in later stages (Table 1), suggesting better use of light resources, which compensated for the competition among plants growing under high agronomic density.

Conclusions

- Genetic diversity for RUE at different phenological stages was found, suggesting discrete genetic control. These findings strongly support the case for significant underutilized photosynthetic capacity in existing wheat germplasm that could come from increased RUE at all growth stages.

- Negative correlations among RUE at different growth stages were observed, highlighting the importance of understanding these trade-offs in more detail.

- Lines that are better adapted to density presented higher RUE in later stages, suggesting a better use of light resources, which compensated for the competition among plants growing under high agronomic density.

References

Aisawi KAB, Reynolds MP, Singh RP, Foulkes MJ. 2015. The Physiological Basis of the Genetic Progress in Yield Potential of CIMMYT Spring Wheat Cultivars from 1966 to 2009. Crop Science 55, 1749–1764.

Calderini DF, Dreccer MF, Slafer GA. 1997. Consequences of breeding on biomass, radiation interception and radiation-use efficiency in wheat. Field Crops Research 52, 271–281.

Miralles DJ, Slafer G a. 1997. Radiation interception and radiation use efficiency of near-isogenic wheat lines with different height. Euphytica 97, 201–208.

Pask A, Pietragalla J, Mullan DM, Reynolds MP. 2012. Physiological Breeding II: A Field Guide to Wheat Phenotyping. Mexico, D.F.: CIMMYT.

Reynolds MP, Acevedo E, Sayre KD, Fischer RA. 1994. Yield potential in modern wheat varieties: its association with a less competitive ideotype. Field Crops Research 37, 149–160.

Reynolds MP, Singh RP, Ibrahim A, Ageeb OAA, Larque A. 1998. Evaluating physiological traits to complement empirical selection for wheat., 85–94.

Rivera-Amado A, Trujillo-Negrellos E, Sylvester-Bradley R, Molero G, Sierra-Gonzalez A, Reynolds M, Foulkes M. 2016. Achieving increases in spike growth, fruiting efficiency, and harvest index in high biomass wheat cultivars. In: Reynolds M, In: Molero G, In: Quilligan E, eds. Proceedings of the 2nd International TRIGO (Wheat) Yield Potential Workshop 2016. CENEB, CIMMYT, Cd. Obregón, Sonora, Mexico, 9-10 March 2016. Mexico, D.F.: CIMMYT, 70–76.

Shearman VJ, Scott RK, Foulkes MJ. 2005. Physiological Processes Associated with Wheat Yield Progress in the UK. Crop Science 45, 175–185.

Song Q, Zhang G, Zhu X-G. 2013. Optimal crop canopy architecture to maximise canopy photosynthetic CO2 uptake under elevated CO2: a theoretical study using a mechanistic model of canopy photosynthesis. Functional Plant Biology 40, 108.

Sukumaran S, Reynolds MP, Lopes MS, Crossa J. 2015. Genome-Wide Association Study for Adaptation to Agronomic Plant Density: A Component of High Yield Potential in Spring Wheat. Crop Science 55, 1–11.
Zhu X-G, Long SP, Ort DR. 2010. Improving photosynthetic efficiency for greater yield. Annual review of plant biology 61, 235–61.

Notes:

Notes:

Proceedings of the 3rd International

TRIGO (Wheat) Yield Potential

WORKSHOP 2017

USAID
FROM THE AMERICAN PEOPLE

CIMMYT
International Maize and Wheat Improvement Center

MasAgro
Modernización Sustentable de la Agricultura Tradicional

SAGARPA
SECRETARÍA DE AGRICULTURA, GANADERÍA, DESARROLLO RURAL, PESCA Y ALIMENTACIÓN

CONACYT